THE UNIVERSITY
of EDINBURGH

Magnetic Resonance Elastography Studies of the Musculoskeletal System

Michael Perrins

A thesis submitted in partial satisfaction
of the requirements for the degree:

Doctor of Philosophy (Ph.D.)

School of Clinical Sciences
Edinburgh Medical School
College of Medicine and Veterinary Medicine
University of Edinburgh
2018

Declaration of Originality

I hereby declare that the research in this thesis, and the thesis itself, was composed and originated entirely by myself, except where specifically stated otherwise, in the Centre for Inflammation Research at the University of Edinburgh and has not been submitted for any degree or professional qualification.

Michael Perrins

Abstract

Manual palpation is a clinical methodology to determine tissue mechanical properties, such as viscoelasticity (i.e. stiffness and viscosity), which is a primary indicator of the development of tissue pathology. Advancing medical imaging technology means it is now possible to reliably non-invasively measure tissue stiffness *in-vivo* through the use of Magnetic Resonance Elastography (MRE). Muscle pathology is traditionally assessed in the clinic through measurement of muscle morphology and function (e.g. Maximum Voluntary Contraction [MVC]). However, MRE has been shown to be an effective method to study muscle pathology and may offer novel biomechanical insight into, for example, muscle engagement, injury and recovery, which cannot be obtained through conventional testing. The aim of this thesis is to perform a series of exploratory investigations to determine the precision, sensitivity and reliability of the muscle MRE technique for studying the relationships between muscle mechanical properties and morphology. This is especially relevant to the clinical application of the technique which is investigated in two pilot studies. Specific interests are to investigate whether muscle MRE offers reliable insight regarding muscle ageing, injury and loading and has potential clinical application such as in monitoring recovery after time in Critical Care and the effects of Total Knee Replacement (TKR) in patients with osteoarthritis of the knee.

This thesis begins with a review of musculoskeletal biomechanics, Magnetic Resonance Imaging (MRI) and MRE research to date. A limited number of clinical musculoskeletal elastography research studies were identified and which motivated several investigations conducted in this thesis. A musculoskeletal MRE analysis pipeline was developed to accurately acquire and analyse MRE data and consists of image co-registration, quantification of muscle mechanical (i.e. stiffness) and morphological properties (i.e. muscle cross-sectional area and a shape measure referred to as circularity), which may be related to clinical measures and relevant functional indices such as MVC. The pipeline includes quality control procedures to detect image artefacts and provides results which can be potentially reliably compared with those of other research groups.

The first two investigations to be reported concern the study of changes in the mechanical properties of muscles that have occurred passively. In particular, the effects of ageing are studied together with the effect of time spent in Critical Care and subsequent rehabilitation. The effect of ageing was primarily evident in the quadriceps muscle group which decreased significantly in cross-sectional area and significantly increased in stiffness. The effects produced by

immobilisation were also predominantly in the quadriceps but here a significant decrease in muscle cross-sectional area was associated with a decrease in muscle stiffness.

The next three exploratory studies all involve an intervention or manipulation in terms of an eccentric exercise protocol which produces muscle injury as well as muscle loading. The former was based on a re-analysis of previously published work with the aim of determining whether there was a significant difference in muscle stiffness in subjects in whom injury was shown to be associated with muscle oedema on T2-weighted MR images. Here the new pixel-wise analysis of the data showed that although the two groups of subjects performed a similar workload, subjects who developed oedema may have used a different combination of muscles to perform the task, and especially may have additionally recruited medial muscles rather than efficiently co-contracting the quadriceps and hamstrings. A loading study revealed a significant relationship between the stiffness and shape (i.e. circularity) of especially rectus femoris and first steps were taken to investigate whether this relationship may show insight into the recovery of patients following TKR surgery.

Taken together these exploratory investigations demonstrate the precision, sensitivity and viability of the muscle MRE technique and its promise for potential clinical application.

Lay Summary

Measuring the stiffness of the body through palpation (i.e. touch) is a practical way to measure the health of tissues and inflammation (i.e. tissue swelling), for example, has been found to produce an increase in muscle stiffness. However, palpation has limitations in that it is generally only performed on the skin. With the development of medical imaging techniques such as Magnetic Resonance Imaging (MRI) it is possible to produce detailed pictures of inside the body and the recent development of an MRI technique known as Magnetic Resonance Elastography (MRE) has made it possible to not only visualise but also measure the mechanical properties of organs and muscles deep in the body. In other words, MRE is a non-invasive method of imaging palpation. Changes in the stiffness of the tissues presented in the form of an image known as an elastogram are a potentially sensitive measure of tissue pathology. They may also provide new insights regarding function (i.e. how the body works). The musculoskeletal system comprises 840 functional muscles and 206 structural bones working together through opposing forces to typically extend and flex joints. So far there have been only a few studies of the clinical application of MRE studies of muscle.

The aim of this thesis is to apply muscle MRE in combination with conventional MRI studies of tissue morphology (i.e. size and shape) to obtain a better understanding of muscle ageing, injury, and loading, with potential clinical applications such as in monitoring recovery after time in so-called Critical Care (i.e. Intensive Care Unit [ICU]), and the effects of Total Knee Replacement (TKR) in patients with osteoarthritis of the knee.

This thesis begins with a review of muscle anatomy, a description of MR imaging, and a review of previous studies of the stiffness of muscles using MRE which motivated the exploratory investigations that will be reported. The first experimental work was to develop a so-called MRE Pipeline (i.e. integrated procedures for acquiring and analysing MRE data) to provide reliable measures of muscle stiffness.

The first application of the pipeline was to study the effect of ageing which was found to be associated with a decrease in size and increase in stiffness of muscles, especially in the quadriceps muscles which play a key role in weight bearing during standing and walking. On the other hand, time in ICU also led to a decrease in size, but there was a decrease in the stiffness of muscles and function, which did not fully recover even after 6 months. Next, a detailed re-

analysis was performed of MRE images obtained for subjects before and after they performed an experimental protocol designed in the Department of Sports Science to produce a transient muscle injury lasting 3-4 days. Results suggested that whether or not the subjects developed oedema (i.e. muscle inflammation) was dependent on the combination of muscles that participants recruited to perform the task. Finally, MRE, and MRI, were applied to measure the change in muscle stiffness, muscle size, and muscle shape, during muscle loading produced by applying relatively small weights to the leg of volunteer subjects lying in the MR scanner. The changes that this produced in muscle stiffness and shape were readily detected and revealed a close relationship to each other for the so-called rectus femoris muscle which was principally recruited to bear the loads. Preliminary investigations were performed to assess the potential clinical application of this assessment to monitor recovery of patients after TKR surgery.

MRE provides unique information on the stiffness of muscles throughout the whole cross-section of the leg and shows significant promise for routine clinical application in the future.

Acknowledgements

I want to thank my supervisors Edwin J. R. van Beek, Neil Roberts, and David Griffith for their guidance during the last three years, and for the numerous international opportunities that I have had during my doctorate. Also, I want to thank Colin Brown and the Mentholatum R&D team for their enthusiasm for funding my musculoskeletal MRE research.

I also want to thank members of the Edinburgh Imaging Facility for offering all their expertise to ensure the application of MRE within the musculoskeletal system was viable. Of course, none of this could have been done without the patience of the radiographers: Annette Cooper, Barbara Allen, Rosie Speed, Aimee Littlejohn, Mairi MacFarlane, Danielle Richardson, Kenneth Dolan, and Carol Ross. Furthermore, I want to thank the insight that Scott Semple, Lucy Kershaw, David Morris, and Gillian Macnaught offered for MR physics, as well as Calum Gray for image analysis techniques. I also want to thank Karen Colvin, Anne Grant, Irene McCulloch, Karen McCurdy, Clair Young, and Patrick Hadoke for ensuring everything was kept on track.

I have been incredibly lucky to pursue a doctorate with other insightful PhD students. First, I want to thank Paul Kennedy and Lyam Hollis for teaching me the fundamentals of MRE. Secondly, I want to thank Eric Barnhill for teaching me several analysis techniques which have formed a basis of my doctorate, and for the continued support even after leaving Edinburgh. Significant gratitude also goes to Lucy Hiscox, who has been a great mentor and friend. A great deal of collaboration was conducted with Michiel Simons, where I was able to learn the key fundamentals of biomechanics and orthopaedic surgery. I also want to wish my friends and recently appointed colleagues, Helen Marshall and Jason Perry, the best of luck for their doctorates.

The data presented in Chapters Two (Inter-rater reliability in Section 2.4), Three (including the loading equipment which is currently under patent review) and Seven (examination of patients following surgical intervention) were in collaboration with a team involving clinical, surgical, and imaging scientists, which will also be components in Mr Michiel R Simons' PhD thesis that will submitted at a later date.

Finally, I want to thank my family and friends for their endless support, belief, and encouragement. Without you all, I would have not been able to pursue this doctorate, and for that I cannot thank you enough.

Thesis Contents

List of Figures

Chapter One

Chapter Two

Chapter Three

Chapter Four

Chapter Five

Chapter Six

Chapter Seven

Chapter Eight

List of Tables

Chapter One

List of Symbols

d	Statistical Power
p	Tissue Density
λ	Shear Wavelength
f	Applied Mechanical Frequency
ω	Vibration Frequency
v_s	Shear Wave Speed
μ	Rheological Component of Elasticity
η	Rheological Component of Viscosity
α	Spring-pot Powerlaw Component
G'	Energy Storage
G''	Energy Dissipation
$\|G^*\|$	Magnitude of the Complex Shear Modulus

List of Equations

$1000 \mathrm{kg/m^3}$	Tissue Density
$\mu = p\lambda^2 f^2$	Helmholtz Equation
$G = pv_s^2 = p(\lambda f)^2$	Elastic Shear Modulus
$G^* = \mu^{1\text{-}\alpha}\eta^\alpha(i\omega)^\alpha$	Spring-pot Multi-frequency Model
$G^* = G' + iG''$	Complex Shear Modulus
$\lvert G^* \rvert = \sqrt{G'^2 + G''^2}$	Magnitude of G*
$\phi = arctan\ [G''/\ G']$	Phase Angle of G*

List of Abbreviations

APACHE II	Acute Physiological and Chronic Health Evaluation II
CC	Contractile Component
CI	Confidence Interval
COPD	Chronic Obstructive Pulmonary Disease
CSA	Cross Sectional Area
D	Distribution
DTI	Diffusion Tensor Imaging
EIMD	Exercise Induced Muscle Damage
EMD	Electromechanical Delay
EMG	Electromyography
EPI	Echo Planar Imaging
ESP	Elastography Software Pipeline
FA	Fractional Anisotropy
FCI	Functional Comorbidity Index
FOV	Field of View
HD-EMG	High Density EMG
ICU	Intensive Care Unit
ICU-AW	Intensive Care Unit Acquired Weakness
LUT	Look-up Table
kJ	Kilojoules
kPa	Kilopascals
M	Mean
MD	Mean Diffusivity
MDEV	Multi-Frequency Dual Parameter Elasto-Visco Inversion
MEG	Motion Encoding Gradient
MR	Magnetic Resonance
MRE	Magnetic Resonance Elastography
MRI	Magnetic Resonance Imaging
MRS	Magnetic Resonance Spectroscopy
MRT	Magnetic Resonance Thermography
MTJ	Myotendinous Junction
MVC	Maximum Voluntary Contraction
NHS	National Health Service
Nm	Newton Metre
OA	Osteoarthritis
PCSA	Physiological Cross Sectional Area
pFDR	Positive False Discovery Rate
ROI	Region of Interest
ROM	Range of Movement
SD	Standard Deviation
SEC	Series Elastic Component
TE	Echo Time
TKR	Total Knee Replacement
TMG	Tensiomyography
TR	Repetition Time

Key Thigh Anatomy

Quadriceps

RF	Rectus Femoris
VI	Vastus Intermedius
VL	Vastus Lateralis
VM	Vastus Medialis

Adductors

AL	Adductor Longus
AM	Adductor Magnus

Medial Muscles

G	Gracilis
S	Sartorius

Hamstrings

BLH	Bicep Femoris (Long Head)
BSH	Bicep Femoris (Short Head)
SMB	Semimembranosus
STD	Semitendinosus

Patent

Simons M, Attard A, Perrins M, Tawy G, Riches P, Rowe P, Roberts N, Biant L, van Beek EJR. Bilateral Antagonistic Muscle Loading Device (MR Safe) - Pending

Conference Proceedings

Proceedings directly related to work within this thesis

Simons M, Perrins M, Roberts N, van Beek EJR, Biant L. Thigh Muscle Recruitment following Total Knee Replacement (TKR) surgery using Magnetic Resonance Elastography (MRE). British Orthopaedic Association Centenary Congress, Birmingham 2018

Simons M, Perrins M, Tawy G, Roberts N, van Beek EJR, Biant L. The Effect of Muscle Loading on Muscle Stiffness. 19th EFORT Congress, Barcelona 2018.

Simons M, Perrins M, Attard A, Tawy G, Roberts N, van Beek EJR, Biant L. Change in Mechanical Properties and Cross Sectional Area (CSA) of Thigh Muscles Following Total Knee Replacements (TKR) Surgery. 19th EFORT Congress, Barcelona 2018.

Perrins M, Simons M, Attard A, Brown C, Baint L, van Beek EJR, Roberts N. Morphometric Adaptions of Rectus Femoris to Muscle Strain Revealed Through Magnetic Resonance Elastography. ISMRM, Paris 2018.

Perrins M, Simons M, Kennedy P, Salisbury L, Brown C, Walsh T, van Been EJR, Griffith D, Roberts N. Magnetic Resonance Elastography (MRE) Reveals Muscle Instability in Middle Aged Healthy Adults. ISMRM, Paris 2018.

Simons M, Perrins M, Tawy G, Brown C, Roberts N, van Beek EJR, Biant L. Clinical Application of Dynamic Magnetic Resonance Elastography (DMRE) Shows Reduced Muscle Strain Following Total Knee Replacement (TKR). ISMRM, Paris 2018.

Simons M, Perrins M, Attard A, Brown C, Roberts, van Beek EJR, N. Biant L. Identification of Muscle Recruitment from Increased Muscle Strain through Dynamic Magnetic Resonance Elastography (DMRE). ISMRM, Paris 2018.

Perrins M, Kennedy P, Simons M, Marshall H, Hiscox L, MacGregor L, Hunter A, Brown C, van Beek EJR, Roberts N. "It's Not What You Do, But The Way That You Do It!" – Magnetic Resonance Elastography (MRE) Reveals Muscle Damage Severity Dependent On Muscle Engagement Strategy. Edinburgh Imaging Expo 2017.

Perrins M, Marshall H, Simons M, Kennedy P, Hiscox L, MacGregor L, Hunter A, Brown C, van Beek EJR, Roberts N. Evidence from MRE that Muscle Engagement Strategy Influences Occurrence of Oedema Following an Exercise Induced Muscle Damage (EIMD) Protocol. 1st International MRE Workshop, Berlin 2017

Perrins M, Simons M, Marshall H, Hiscox L, Gray C, Semple S, Cooper A, Barclay L, Kirkbride R, Salisbury L, Brown C, Walsh T, van Beek EJR, Roberts N, Griffith D. MRE Study of Muscle Recovery Following Time Spent in an Intensive Care Unit (ICU). 1st International MRE Workshop, Berlin 2017

Simons M, Perrins M, Tawy G, Marshall H, Brown C, van Beek EJR, Roberts N, Biant L. Change in Mechanical Properties and Cross-Sectional Area (CSA) of Thigh Muscles Following Total Knee Replacement (TKR) Surgery. 1st International MRE Workshop, Berlin 2017

Simons M, Perrins M, Attard A, Marshall H, Semple S, Cooper A, Brown C, Biant L, van Beek EJR, Roberts N. The Effect of Muscle Loading on Muscle Stiffness. 1st International MRE Workshop, Berlin 2017

Perrins M, Hiscox L, Gray C, Semple S, Barclay L, Kirkbride R, Salisbury L, Brown C, Walsh T, van Beek EJR, Roberts N, Griffith D. Muscle

Change Associated with Time in Intensive Care Unit (ICU). ISMRM, Hawaii 2017

Perrins M, Barnhill E, Kennedy P, Braun J, Sack I, Macgregor L, Hunter A, Brown C, van Beek EJR, Roberts N. Applications of Deep Heat Following Exercise Induced Muscle Damage (EIMD). ESMRMB Vienna 2016.

Perrins M, Barnhill E, Braun J, Sack I, Hunter A, Brown C, van Beek EJR, Roberts N. Super-Resolution Magnetic Resonance Elastography (SR-MRE) of Exercise Induced Muscle Damage (EIMD). ISMRM, Singapore 2016.

Proceedings not directly related to work within this thesis

Marshall H, Hiscox L, Perrins M, Barnhill E, Sack I, Braun J, Hermann T, Bernarding J, van Beek EJR, Roberts N. Comparison of Magnetic Resonance Elastography (MRE) Inversion Reproducibility using MDEV and MREdge in the Brain for the Same Subjects at 1.5, 3 and 7 Tesla. ISMRM, Paris 2018.

Marshall H, Hiscox L, Perrins M, Barnhill E, Sack I, Braun J, Hermann T, Bernarding J, van Beek EJR, Roberts N. Magnetic Resonance Elastography (MRE) Reproducibility Study in the Same Participants at Field Strengths of 1.5, 3 and 7 Tesla. Edinburgh Imaging Expo 2017

Marshall H, Hiscox L, Perrins M, Barnhill E, Sack I, Braun J, Hermann T, Bernarding J, van Beek EJR, Roberts N. Magnetic Resonance Elastography (MRE) Reproducibility Study in the Same Participants at Field Strengths of 1.5, 3 and 7 Tesla. 1st International MRE Workshop, Berlin 2017

Hiscox L, Perrins M, Johnson C, McGarry M, Barnhill E, Huston J, Sack I, Brain J, van Beek EJR, Starr J, Roberts N. Reproducibility Study of Direct and Non-Linear Inversion High-Resolution Magnetic Resonance Elastography (MRE) of the Hippocampus. ISMRM Hawaii 2017.

Hiscox L, Perrins M, Puertollano M, Johnson C, McGarry M, Brown C, van Beek EJR, Starr J, Roberts N. Magnetic Resonance Elastography (MRE) and Diffusion Tensor Imaging (DTI) in a Multi-Modal Brain Tissue Integrity Characterization Pipeline. CCACE Research Day, September 2016

Li X, Roberts N, Perrins M, Vingerhoets V. Measurement of Brain Asymmetry on 3D Magnetic Resonance (MR) Images Obtained for 16 Subjects with Situs Inversus. ISMRM, Singapore 2016.

Barnhill E, Guo J, Dittman F, Perrins M, Hiscox L, Hermann T, Bernarding J, Roberts N, Braun J, Sack I. Impact of Field Strength and Image Resolution on MR Elastography (MRE) Stiffness Estimation. ISMRM, Singapore, 2016.

Awards

Best Research Poster Presentation

European Federation of National Associations of Orthopaedics and Traumatology (EFORT) 2018

Simons M, Perrins M, Tawy G, Roberts N, van Beek EJR, Biant L. The Effect of Muscle Loading on Muscle Stiffness. 19th EFORT Congress, Barcelona 2018.

Publications

Publications directly related to work within this thesis

Perrins M, Simons M, Marshall, H, Biant L, van Beek EJR, Roberts N. Morphometric adaptions of Rectus Femoris over Vasti Muscles to increasing muscle stiffness. (In Preparation).

Perrins M, Kennedy P, Brown C, van Beek EJR, Roberts N. Mapping knee extensor muscle damage through a localised increased stiffness differential between oedemic injury groups. (In Preparation).

Perrins (2018a), CMOcean LUT for ImageJ. GitHub repository, https://github.com/mikeperrins/cmocean-LUT-ImageJ.

Perrins (2018b), Musculoskeletal MRE Template. GitHub repository, https://github.com/mikeperrins/MSK-MRE-Template.

Hollis L, Barnhill E, Perrins M, Kennedy P, Conlisk N, Brown C, Hoskins PR, Pankaj P, Roberts N. Finite element analysis to investigate variability of MR elastography in the human thigh. Magnetic Resonance Imaging. 2017; 43:27-36.

Kennedy P, Macgregor LJ, Barnhill E, Johnson CL, Perrins M, Hunter A, Brown C, Beek EJR, Roberts N. Application of magnetic resonance elastography (MRE) to measure the effect of warm-up using deep heat rub on muscle stiffness following exercise induced muscle damage (EIMD). Journal of Magnetic Resonance Imaging 2017; 46:1115-1127.

Publications not directly related to work within this thesis

Hiscox L, Johnson C, McGarry M, Perrins M, Littlejohn A, van Beek EJR, Roberts N, Starr J. High-resolution MR Elastography (MRE) reveals differences in Subcortical Gray Matter Viscoelasticity between Young and Healthy Older Adults. Neurobiology of Ageing. 2018; 65:158-167.

Chapter One

Introduction

Preface

Chapter One starts with an overview of musculoskeletal epidemiology and the significant impact that this has on the UK National Health Service (NHS), a fundamental reasoning why this thesis is focussing on the musculoskeletal system. This is followed by an overview of musculoskeletal physiology including architecture (or anatomical organisation), function, and muscle engagement methods (i.e. types of muscle contraction). It is important to have an appreciation of muscle architecture as this is closely linked with function, something which is key for manipulation during experimentation. Current musculoskeletal pathophysiological methods which measure muscle function include muscle biopsy, electromyography (EMG) and ultrasound (US), which are explored regarding their strengths and weaknesses. Following this, clinical imaging modalities are discussed including Magnetic Resonance Imaging (MRI), a gold standard in physical properties of tissue, as well as a recent development of the technique known as Magnetic Resonance Elastography (MRE). MRE offers the ability to acquire data of mechanical properties of soft tissue, and also addresses many of the limitations for current musculoskeletal (patho-) physiological measures. A subsequent review of the MRE literature showed that there is a rich supply of clinical applications in static tissues such as the kidney, liver, and the brain, however the application remains limited within the musculoskeletal system. By the close of this chapter, the organisation, aims, and possible contributions of this thesis are outlined, to address the question of whether MRE may offer new clinical insight into musculoskeletal pathophysiology.

1.1 Musculoskeletal Epidemiology

Musculoskeletal conditions are the third largest NHS expenditure, costing the NHS £10.2 billion a year, with this expected to cost £118.6 billion over the next decade (York Health Economics, 2017). This is a result of almost a third of the UK population living with a musculoskeletal condition (17.8 million, 28.9%), and one in five people consulting a GP in reference to musculoskeletal difficulties each year (Arthritis Research UK, 2009). As a result, 8.2% of all admissions requiring consultant care in England were as a result of musculoskeletal conditions.

Musculoskeletal conditions (both acute and long term) are more prevalent with age (Arthritis Research UK, 2016), with 51% of individuals aged between 35 to 64 reportedly have a musculoskeletal condition (Global Burden of Disease Collaborative Network, 2017). For instance, within a year: 10 million people had sought treatment for persistent back pain (Arthritis Research UK, 2015), 8.75 million people aged 45 and above had sought treatment for osteoarthritis (Arthritis Research UK, 2013), 2.8 million for fibromyalgia (Jones et al., 2010), 400,000 for rheumatoid arthritis (Arthritis Research UK, 2015), and 300,000 for fractures (British Orthopaedic Association, 2007). There is also an increasing prevalence of osteoarthritis consultation with age (Arthritis Research UK, 2013). The physical activity of an individual is a risk factor associated with developing a musculoskeletal condition, and with age there is an associated decrease in activity. On average, 21-32% of adults are active for less than 30 minutes per week (16-19 The Scottish Government, 2017; StatsWales, 2017; Department of Health Statistics and Research, 2017; NHS Digital, 2017), this is increased to 40% for adults above 65 years of age (U.C.L. NatCen, 2017). Consequently, half of adult social care expenditure is spent on those over the age of 65 due to musculoskeletal conditions (The King's Fund, 2014). Yet physical activity can reduce pain associated with musculoskeletal conditions and also reduce further comorbidities (Choi et al., 2010; Arthritis Research UK, 2017).

Every £1 invested in musculoskeletal research results in a 25p return each year to the NHS (Wellcome Trust, 2017), so a greater investment in musculoskeletal research is required. The objective of this thesis is to contribute towards the area of clinical musculoskeletal research in an attempt to obtain novel musculoskeletal imaging methods in reference to muscle pathophysiological.

1.2 Muscle Architecture

There are three types of muscles: smooth muscle, cardiac muscle, and skeletal muscle, each having key functional differences (Mackenzie, 1918). Smooth muscle is in hollow structures and organs and is controlled through the autonomous nervous system. Cardiac muscle, which has a striated structure (striped in appearance under a microscope), is also controlled through the autonomous nervous system as well as through humoral factors and internal rhythm control. Contrary to the previous muscle types, skeletal muscle, which is also striated, is controlled by voluntary nervous control, and so can be readily manipulated. Skeletal muscle is connected to the skeletal system through tendons, allowing for movement or locomotion (Fukungaga et al., 2001). Skeletal muscle architecture, or organisation, is hierarchically organized in size (Figure 1.1) from sarcomeres, muscle fibres, and finally the muscle belly.

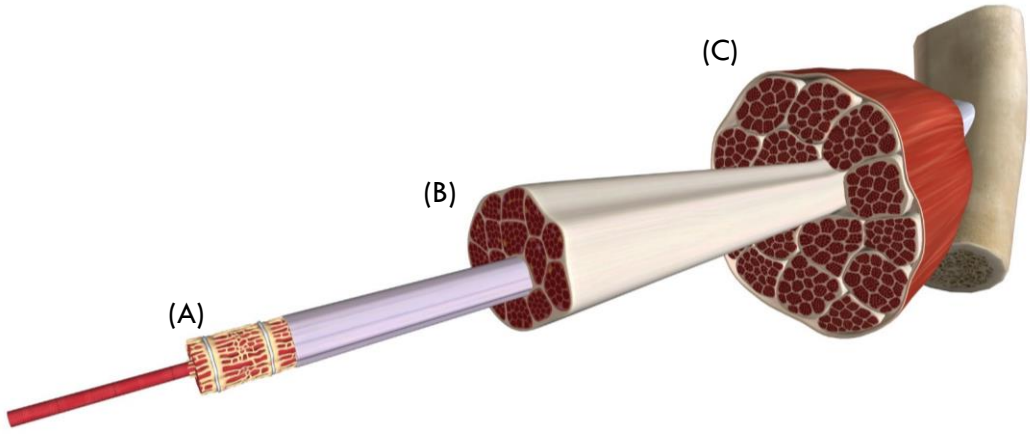

Figure 1.1. Skeletal muscle hierarchical organization including sarcomeres (A), muscle fibres (B) and the muscle belly (C), connected to the skeletal system. Obtained from BioDigitial.com

1.2.1 Sarcomeres

The sliding filament theory describes the physiological mechanism leading to muscle contraction (Huxley et al., 1954, 2004; Anderson et al., 2004). During muscle contraction, multiple muscle fibres act in unison: a sarcomere shortens (Figure 1.2), due to thin filaments (actin) sliding closer together within a thicker filament (myosin) (Huxley et al., 1954). For this to occur, the protein actomyosin is formed. Actomyosin bridges the actin filament to the myosin head (Wood et al., 2012), which is known as the cross-bridge theory.

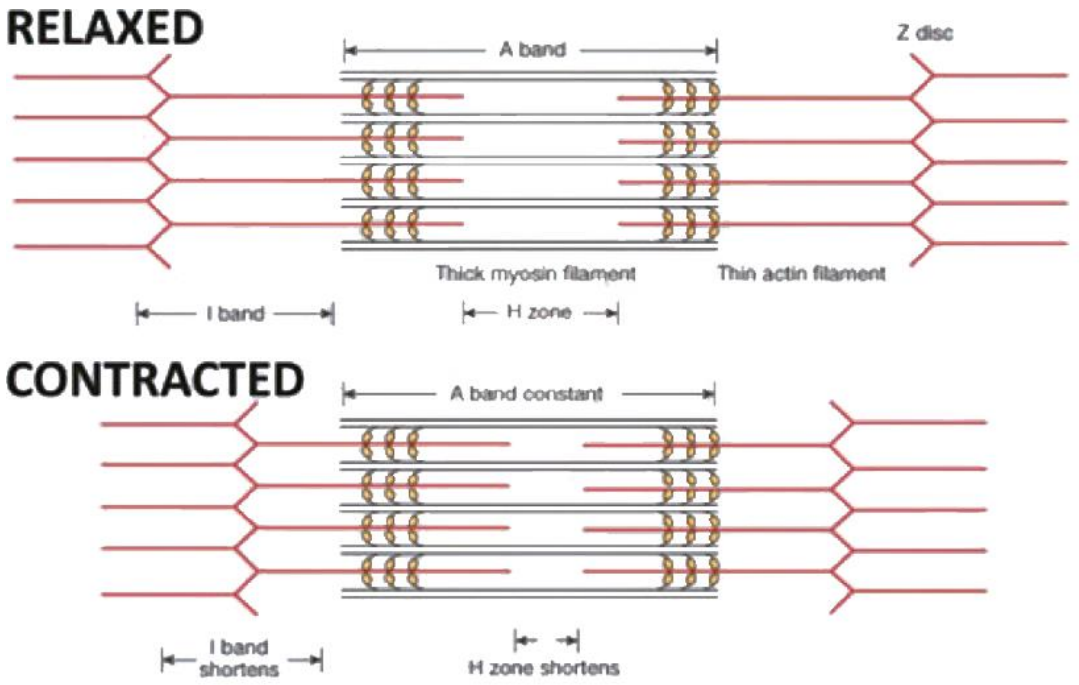

Figure 1.2. Schematic of relaxed and contracted sarcomeres, showing Actin in red (Krans et al., 2010).

Electrical impulses from the central nervous system are a pre-requisite to initiate the sliding of sarcomeres. The neuromuscular junction is a synapse between a motor neuron and a muscle fibre (Levitan et al., 2015). When the motor neuron initiates an action potential releasing Ca^{2+}, it is this release of Ca^{2+} which initiates the sliding of filaments. Actin filaments contain myosin binding sites covered by a protein known as tropomyosin. At the ends of each

tropomyosin is troponin, a Ca^{2+} sensitive complex. Troponin binds to the released Ca^{2+}, opening the myosin binding sites, resulting in a contraction.

1.2.2 Muscle Fibres

The mammalian musculoskeletal system has been shown to include two main fibre types including Type I ('fast twitch') and Type II ('slow twitch') muscles (Hess 1970; Close 1972), with a differential between their Ca^{2+} activation requirements (Stephenson et al., 1981). Temperature has also been shown to impact these fibre types differently for activation (Cullingham et al., 1960; Truong et al., 1964; Isaacson et al., 1970) as the sensitivity of fast fibres to Ca^{2+} significantly rises with increases in temperature, however slow twitch fibres are not as greatly affected by temperature. Fast twitch fibres have a contraction speed greater by a factor of 3 in comparison to slow twitch fibres (Close, 1972).

Muscle fibre organization is a pre-determinant of muscle function (Burkholder et al., 1994). Muscle torque, or speed of contraction, has been shown to be greater with a higher amount of fast twitch fibres (Thorstensson et al., 1976; Coyle et al., 1979; Suter et al. 1993), particularly within the Vastus Lateralis (Froese and Houston, 1985), part of the quadriceps muscle group. However, research has shown that muscle torque was not solely dependent on muscle fibre types, but that muscle cross-sectional area, or size, was also an important factor (Ikai et al., 1968; Tesch et al., 1978; Schantz et al. 1983; Maughan et al., 1983, 1984; Lieber et al., 1988). Further, Lieber et al. (1993) showed that sarcomeres differ in length between muscles, suggesting specialized muscle architecture.

Muscles may have specific roles, which are highly dependent on their architecture (Lieber et al., 1989, 1990, 1992, 2011), with similar muscle architecture being present across a species (Sacks et al., 1982; Wickiewicz et al., 1983; Roy et al., 1984; Lieber et al., 1989; Burkholder et al., 1994; Eng et al., 2008). Muscle function can be understood through a mixture of

architectural features (Figure 1.3) consisting of a combination of physiological cross-sectional area (PCSA; proportionate to muscle force) and fibre length (proportionate to muscle excursion, or maximum length of movement). Lieber et al. (1989) investigated mammalian architecture of thigh muscles and demonstrated that there are discriminatory characteristics of muscles within the same group. Quadriceps are designed for force production in part due to their large muscle fibre angle. However, the hamstrings are designed to allow for muscle excursion due to a large fibre length and the small muscle fibre pennation angles.

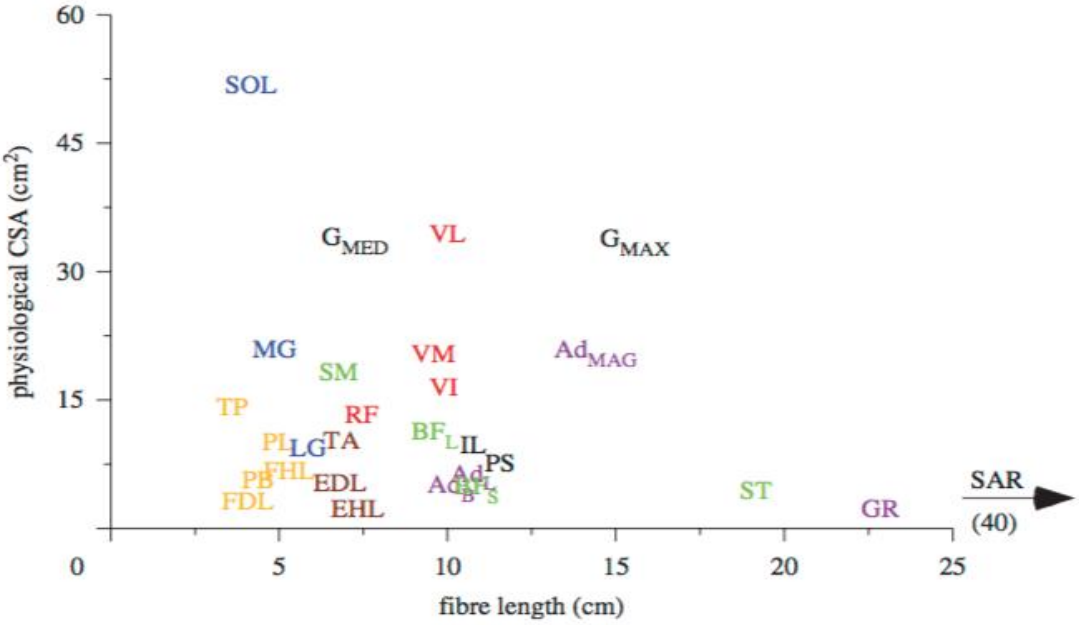

Figure 1.3. PCSA and fibre length of each muscle in the lower leg, with muscles with similar functions identified by the same colours. For the muscles in the thigh: Quadriceps in red, Hamstrings in green, and Adductors / Medial muscles in purple (Lieber et al., 2011).

1.2.3 Muscle Belly

The upper leg, or thigh, can be segmented into different muscle groups based on function: quadriceps, hamstrings, and adductors with medial rotators. The Quadriceps muscle group (Figure 1.4A) consist of the rectus femoris (RF), vastus lateralis (VL), vastus medialis (VM) and vastus intermedius (VI). The rectus femoris is connected from the tibia to the pelvis, which makes it a bi-articular muscle as it connects across the hip and knee joints. The hamstrings

(Figure 1.4B) also consist of four muscles: semimembranosus (SMB), semitendinosus (STD) and the biceps femoris, which splits into the biceps long head (BLH) and biceps short head (BSH). All the hamstring muscles are bi-articular across hip and knee joints, apart from the short head of the bicep femoris. Finally, the adductors (Figure 1.4C) - adductor longus (AL), adductor magnus (AM) and adductor brevis (AB) - are connected to the upper femur and to the pelvis in a fan shaped structure. Lastly, two muscles medially which act predominantly as rotators, gracilis (G) and sartorius (S), are bi-articular and thin.

1.3 Muscle Physiology

In order for movement to occur, there needs to be muscle contraction. Muscle contraction leads to a tension increase of muscle tissue during use. Three types of contractions may occur, depending on the load being exerted (Lieber et al., 2011). When muscle force is greater than the muscle load then this results in a concentric contraction, where the muscle will shorten (Widmaier et al., 2010). However, if the load being applied to a muscle is greater than the muscle force, this will result in muscle lengthening, or an eccentric contraction (Lieber et al., 1991). An additional scenario is when the muscle force and load are equal, meaning that the muscle does not change in length, (i.e. when sustaining a load) which is an isometric contraction. In addition to this, the force of a muscle contraction can be determined by the velocity at which a muscle shortens during stimulation (Abbott et al., 1953). To measure the physiology of muscles, there are currently three main methods of analysis including muscle biopsies, electromyography, ultrasound, and tensiomyography. The strengths and limitations of each of these physiological measures are discussed in relation to their uses within an experimental paradigm.

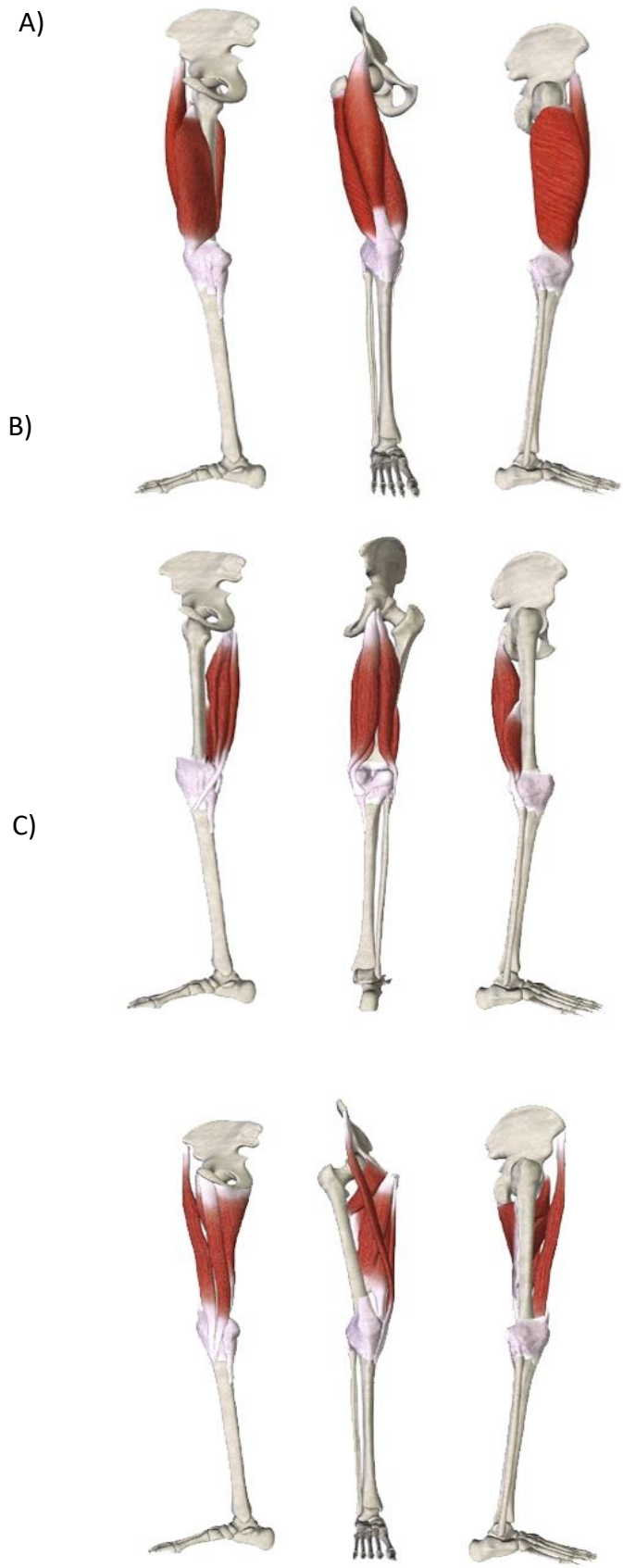

Figure 1.4. Muscle groups segmentation of the thigh. A) Quadriceps, B) Hamstrings, C) Adductors and medial Muscles. Adapted from BioDigitial.com

1.3.1 Muscle Biopsy

A biopsy is a procedure where a small section of tissue is removed and viewed under a microscope. This procedure can incur significant discomfort for patients, however can also offer detailed insight into the pathophysiology of muscle tissue. Muscle biopsies have been shown to be effective in studying muscle pathophysiology of muscle, especially in muscle oxygenation following exercise (Fielding et al., 1993; Amelin et al., 2005). A significant insight this modality can offer is identification of muscle fibre types within muscles, with biopsies being utilised to reveal changes in the composition of muscle fibre types following intensive training of lower extremity muscles (Staron et al., 1994). Further, observations of ageing muscle have shown that associated with a decrease in muscle size there is a decrease in muscle strength due to a composition change of Type I to Type II fibres (Frontera et al., 2000). However, there are also many limitations to biopsy work. Firstly, biopsies are taken from a single point within the muscle, where a myopathy may not be homogeneous. If researchers were to address this and perform several biopsies within a muscle, then this has a significant impact on the tissue, comparable to eccentric muscle stress (Malm et al., 2000), questioning the validity of the readings. In addition to this, the accuracy of biopsy readings has been scrutinised suggesting that due to a high variability of readings, there are limited meaningful results acquired by this technique (Wendling et al., 1996).

1.3.2 Electromyography

Electromyography (EMG) is a non-invasive method to study muscle physiology. It measures muscle activation through electric signals. One significant insight surface EMG can offer is the measurement of Maximum Voluntary Contraction (MVC), which shows the muscle force output. An example of EMG being used in research is in studying the impact of training, showing that MVC increased within the quadriceps following a period of resistance training (Aagaard et al., 2002). An additional measure EMG offers is the electromechanical delay (EMD), the time between the EMG reading and the movement from the muscle (Cavanagh et al., 1979). Comparing three

different contraction methods (eccentric, concentric, isometric), the use of EMG revealed that eccentric contractions incurred the least EMD between signal and movement, contributing to a greater force being generated. One explanation for this may have been the differential positions of the contractile components (muscle fibres; CC) and subsequent stretching of the elastic components (energy storage components such as tendons; SEC) between the contraction types. Whilst the insight EMG may offer is significant into muscle function, the technique has some limitations. Firstly, the placing of the recording electrodes are integral to the readings, with Ralston (1961) highlighting the difficulty of performing EMG on smaller muscles – which is why the quadriceps are commonly examined. For precise measure of muscle activity through EMG the use of a fine wire insertion may have been traditionally required, which can be painful, disturb the tissue impacting on readings, and cannot be performed on deep tissue (Ringleb et al., 2007). However advanced techniques such as High Density surface EMG (HD-EMG) offers insight into individual muscle co-contractions . Secondly, within a clinical setting it is difficult to obtain a true appreciation of muscle performance under load, as it is often not feasible to incorporate significant controls needed to perform EMG (Ralston, 1961).

1.3.3 Ultrasound

Ultrasound (US) is an imaging technique which uses sound waves to obtain an image of musculature and surrounding tissues. Within the last decade the use of US has increased significantly, establishing it as a diagnostic modality in soft tissues (Manger et al., 1995, 1997; Grassi et al., 1998; Gibbon et al., 1999; Wakefield et al., 1999; Kane et al., 2004). US is a non-invasive and portable technique, allowing for real time assessment of musculature, which has been utilised as an effective method to measure impact and recovery of musculoskeletal disease (Reimers et al., 1997; Bureau et al., 1998, Fornage, 2000). However, a limitation of US is that spatial resolution needs to be sacrificed relative to the size of area being imaged (Backhaus et al., 2001). Whilst US and clinical imaging modalities such as Magnetic Resonance Imaging

(MRI) are both used to measure tissue inflammation, US has advantages in guiding biopsies whereas MRI has been shown to be a more sensitive for offering detailed images of musculoskeletal myopathy and soft tissue characterisation.

1.3.4 Tensiomyography

Tensiomyography (TMG) allows for the measurement of muscle contractile properties by measuring the deformation of the tissue (Macgregor et al., 2018). TMG is performed through the electrical stimulation of a muscle and the change in the length of the muscle. A key quantitative measure of this technique is in recording the time duration of a contraction, which can then be used to characterise fibre composition within a muscle. At this time, the use of tensiomyography in clinical cohorts is limited due to the low level of muscle contraction elicited from the technique (less than 10% MVC; Ditrolio et al., 2011). Whilst the work within this domain is promising, greater validation of the measurements obtained are required in order for this technique to reveal a link to muscle function.

1.4 Clinical Imaging

MRI has become widely used to obtain images of soft tissue. Due to the non-requirement of ionizing radioactive contrasts, MRI has become a gold standard for use in clinical imaging to obtain images of physiological and structural changes (van Beek et al., 2018). MRI is based on the excitation of nuclei of hydrogen atoms. As human tissue is comprised of fat (lipids) and water (Mansfield et al., 1975), both abundant in hydrogen, tissue can be identified depending on the magnitude of hydrogen present. During an MRI scan a radio frequency is emitted which is absorbed by protons (hydrogen atoms). This additional energy puts them into a higher state, which is at odds with the direction of the strong magnetic field. As this energy is lost and the protons align themselves back into the direction of the magnetic field, they emit a radiofrequency signal, which is subsequently detected by radiofrequency coils within the magnet (Callaghan, 1994). The radio frequency pulses can be

manipulated to be sensitive to specific tissue types, resulting in medical images having different image contrasts for tissue depending on the time it takes for the tissue to relax after being excited during scanning. This differential in proton relaxation allows for visualisation of different tissues, and following image processing, tissue health can be ascertained (Figure 1.5).

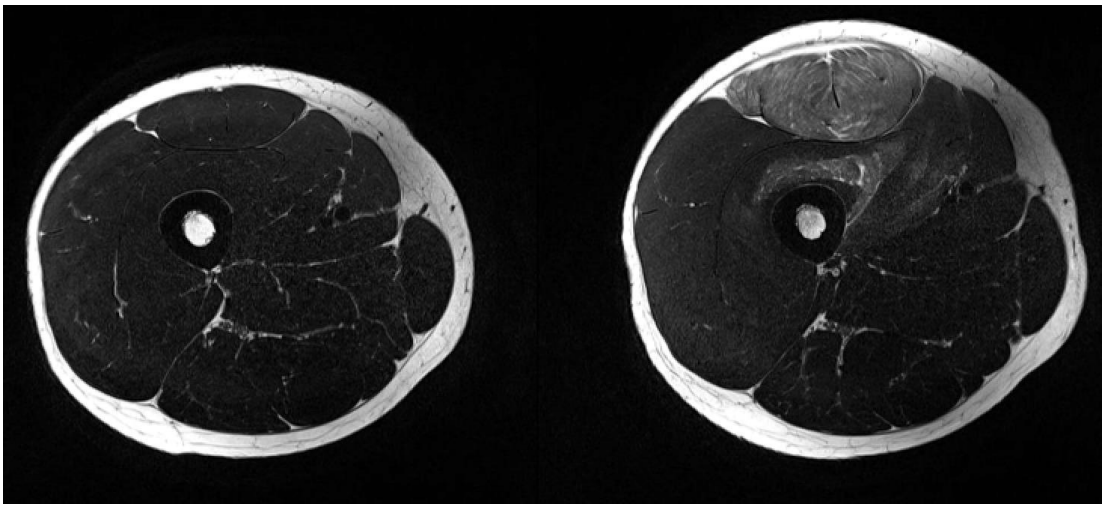

Figure 1.5. Comparison of Healthy thigh (left) and muscle inflammation from oedema following injury (right), demonstrated as higher signal intensity due to increase in proton density. (Chapter Five)

However, whilst MRI can offer good detail into the morphological and physical appearance of tissue, it offers no insight into the mechanical properties (Mariappan et al., 2010), such as the stiffness of a tissue. To obtain a measure of tissue stiffness a medical professional normally carries out a manual assessment of a selected tissue, otherwise known as palpation. Palpation is a commonly used medical practice to measure tissue variety and to feel the presence and consistency of normal and abnormal tissues. Whilst palpation is cheap and easily accessible, there are two key problems: i) it cannot be performed on deep tissue, and ii) this long practised technique remains subjective (Jacob et al., 1994).

1.5 Magnetic Resonance Elastography

Magnetic Resonance Elastography (MRE) was developed at the Mayo Clinic and first published in 1995 (Muthupillai et al., 1995). A variant of conventional MRI, MRE is a non-invasive imaging modality that can calculate tissue viscoelastic properties – which are normally studied through palpation. MRE results in an objective value of stiffness through numeric integers, which can be quantitatively analysed to measure pathophysiology. MRE assesses the elastic modulus of tissue which varies over several magnitudes between tissues, significantly more than previously discussed methods such as MRI or US (Mariappan et al., 2010; Figure 1.6).

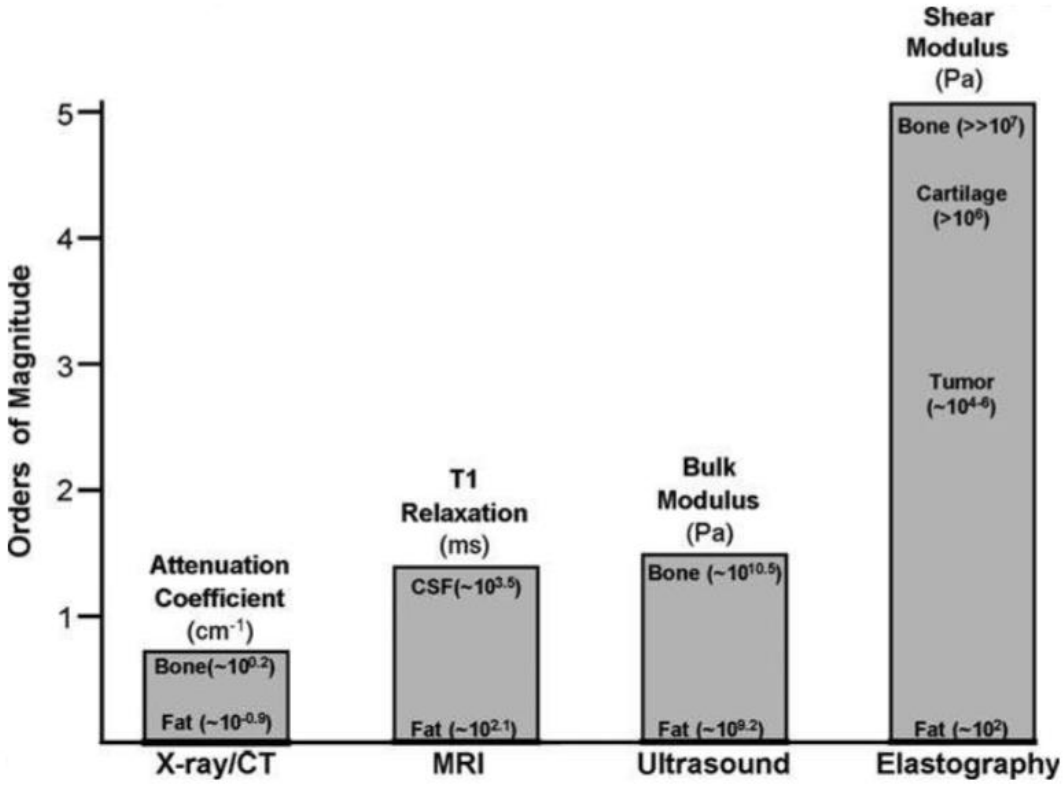

Figure 1.6. Imaging modalities and their contrast mechanisms, showing MRE offers the largest variation across physiological states (Mariappan et al. 2010).

A primary clinical use of MRE is the stiffness mapping of the liver in patients with liver fibrosis. Traditional diagnosis of liver fibrosis includes invasive biopsies. As discussed, the method of biopsy has potential serious adverse events, lack precision due to inhomogeneity of liver disease and therefore

readings lack repeatability (Venkatesh et al., 2013) due to covering a small region of interest (ROI). MRE has been previously used to accurately quantify different stages of liver fibrosis (Yin et al., 2007; Huwart et al., 2008b; Asbach et al., 2010), by showing changes in tissue stiffness (Figure 1.7). Liver fibrosis measurement can be conducted through both ultrasound (Sandrin et al., 2003; Castéra et al., 2005; Ziol et al., 2005) and in conjunction with MRI (Huwart et al., 2006, 2007; Yin et al., 2007). Huwart et al. (2008a) conducted a comparison of the sensitivity between ultrasound and MRE, finding MRE to have the most accurate diagnostic performance (Figure 1.8).

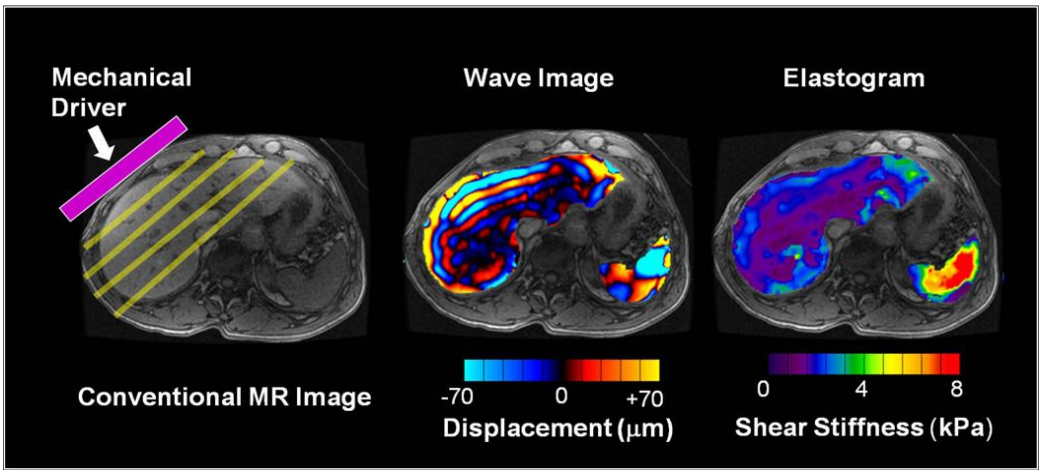

Figure 1.7. Method of liver fibrosis MRE. External actuator applied to the abdomen (Left), Wave displacement images (Middle), shear stiffness elastogram (Right). (Venkatesh et al., 2013).

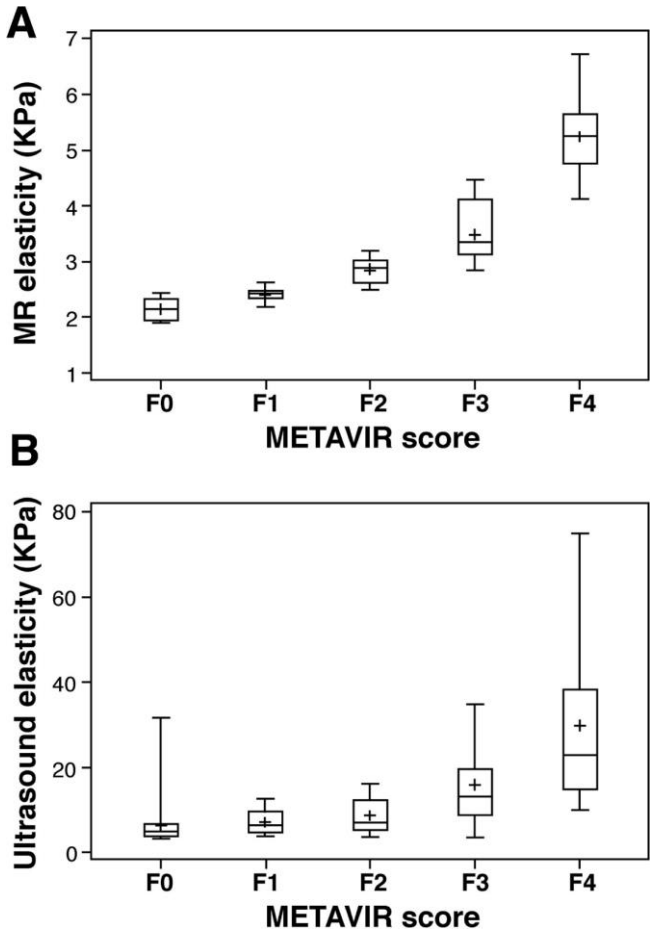

Figure 1.8. Differences in performance of MRE (A) and US (B). (Huwart et al., 2008a)

A recent movement in MRE is towards the study of the brain (Hiscox et al., 2016; 2018). MRE has been used in the brain in order to obtain better understanding of degeneration (Murphy et al., 2011; Hiscox et al., 2018), inflammation (Riek et al., 2012), and also in the aid of tumour detection and delineation (Murphy et al., 2013). It is also important to note that MRE, particularly in the brain, produces reliable measurements for classification of tissue types (Sack et al., 2008; Murphy et al., 2011). MRE is sensitive enough to detect a significant 38% difference in the stiffness of grey (M=5.22 kPa) and white matter (M=13.60 kPa) (Kruse et al., 2008). In addition to this sensitivity, Murphy et al., (2013) showed that in comparison to surgical assessment of brain tumour stiffness, the use of MRE (r=0.65, p=0.023) out

performed traditional MRI measurements (r=0.05, p=0.089), as MRE was significantly correlated with surgical assessment.

As shown here, MRE can offer physiological insight and also address some limitations of currently employed pathophysiological methodologies. Heers et al. (2003) showed a strong correlation between EMG and MRE measurements with regards to leg muscle activity. Such research opens the question of the necessity of MRE, when methodologies such as EMG, which is currently a more established and cheaper option to investigate the musculoskeletal system. However, MRE has several advantages over EMG, in particular the amount of simultaneous data of deep tissue which can be obtained in a short time period. MRE provides an image of the entire muscle and surrounding muscles, which can include deep tissue. MRE also does not require the use of invasive instruments, and only requires an actuator to be placed on the surface of the skin, meaning that both passive and active states of muscle can be measured through MRE (Jenkyn et al., 2003). The application of MRE also has additional advantages over the use of TMG, as it can quantify a much greater level of mechanical change in muscles due to not being limited to a certain level of MVC.

MRE has been used clinically in practice. However, clinical musculoskeletal research using MRE is a relatively unexplored domain. Clinical MRE in tissue such as liver or brain, involves the measurement of disease progression, with the use of MRE to reveal surrogate measures of tissue health. It still remains a limitation that much of the research conducted within MRE is performed on static tissue. However, muscle can be readily manipulated, with the amount of change derived from the manipulation, resulting in a potentially much quicker appreciation of an individual's general health status. This means that instead of a physiologically static image, pathophysiology can also be observed through changes in different levels of tension (i.e. increased stiffness during use), something further explored in Chapters Five and Six). Muscle is fundamentally a tissue which is designed to move and be dynamic. In order to perform MRE it is necessary to first understand musculoskeletal rheology

(tissue deformation), so that the distortion of muscles can be appreciated in terms of mechanical properties.

1.5.1 Musculoskeletal Rheology

Muscle is a viscoelastic tissue, with Hill (1938) describing the relationship between muscle tension and the velocity at which a contraction occurs, finding that the greater the muscle tension the slower a muscle contraction will be. Within viscoelastic tissue there is an elastic and viscous element (Figure 1.9). Elasticity is the storage of energy during deformation, a measure of displacement, whereas viscosity is the dissipation of energy during deformation, or the rate of the displacement. Following from Hill (1938), Boger et al. (1987) showed that a viscoelastic tissue will stiffen quicker as it is progressively loaded. A basis for understanding the dynamic nature of muscle is shown by Mariappan et al. (2010), where increased loading of a soleus muscle (lower leg) resulted in larger wave lengths in distortion images, with the muscle stiffness increasing linearly (Figure 1.12).

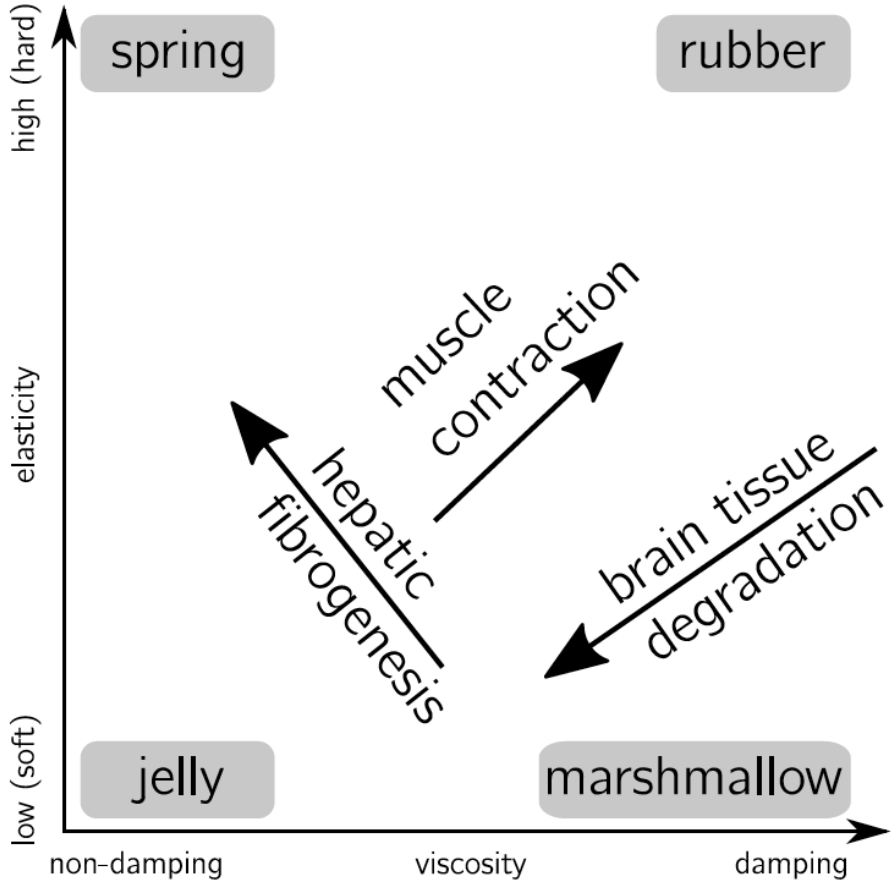

Figure. 1.9. Viscoelastic changes in different soft tissues as well as relative palpation guide. Obtained from Hirsch et al., 2017.

Significant work within musculoskeletal MRE is to model the rheology of the tissue, with the main aim for MRE to quantify the viscoelasticity. MRE measurements of viscoelasticity are in Pascals, due to the quantification of pressure using Young's shear modulus (the relationship between tissue stress and strain, or stiffness) and Hooke's law (linear elasticity). Muscle viscoelasticity is most simply and commonly characterized in the form of the Voigt model (Figure 1.10; Catheline et al., 2004; Debernard et al., 2013), with a spring element representing muscle elasticity (μ [measured in kPa]; Bensamoun et al., 2006), and a dashpot representing viscosity which takes into consideration active muscle fibre friction (η).

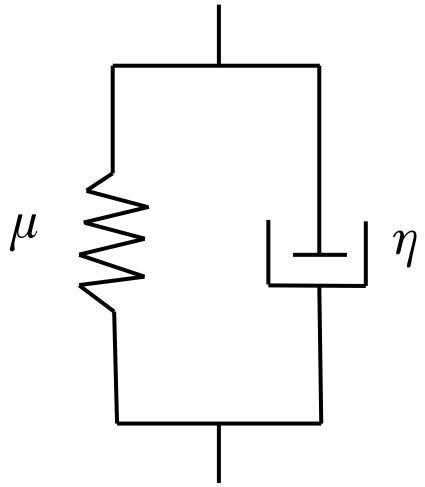

Figure 1.10. Voigt rheological model of muscle viscoelasticity (Debernard et al., 2013).

1.5.2 Imaging Musculoskeletal Rheology

The technical advance which made MRE possible was the introduction of motion encoding gradients (MEG) (Muthupillai et al., 1995; Uffmann et al., 2008) implemented into a typical MRI sequence to capture multiple snapshots of the applied acoustic waves. The MEGs encode the proton spins in addition to the cyclic gradient polarity being switched, which causes a phase shift, with a quantifiable amount of displacement (Muthupillai et al., 1996). Displacement is caused by an external actuator which introduces acoustic waves into the tissue (Figure 1.11).

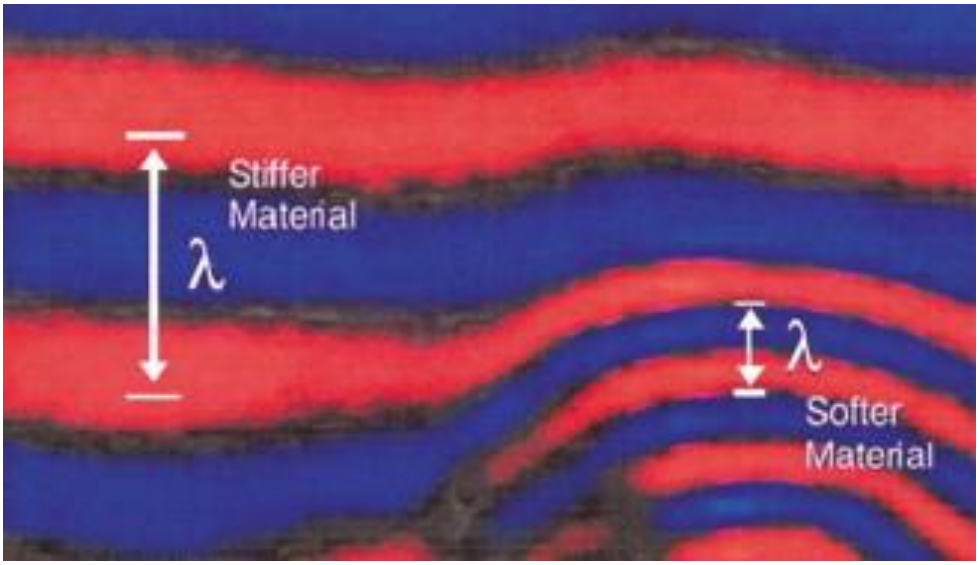

Figure 1.11. Example of acoustic wave propagation through different levels of material stiffness (Basford et al., 2002).

Harmonic low frequency acoustic waves (10Hz-1kHz) displace the tissue in microns. The displacement can be mapped to show the mechanical properties of the tissue, with the amount of displacement relative to the tissue elasticity (or stiffness). The acoustic shear waves can be seen to travel quickly through stiff tissue and slow through soft tissue. As a result, the method of MRE allows researchers to 'virtually' palpate regions of the body previously unreachable, but now also able to quantify tissue stiffness.

Traditionally, quantification of tissue stiffness has been performed by measuring the distance of wavelengths in a specific tissue through virtual callipers, which can then be used to calculate the stiffness of a specific region (Figure 1.12). Wave dissipation can be calculated due to the attenuation of a wave, with a greater tissue viscosity resulting in a greater decrease in wave amplitude. By measuring the distance of the wavelength, one can compute the shear modulus, or elasticity of tissue, using the Helmholtz equation*:* $\mu = p\lambda^2 f^2$ *:* λ being the wavelength, p being approximate tissue density (~1000kg/m^3; Burlew et al., 1980; Debernard et al., 2013), and the applied mechanical frequency (f). Taking this further, one can then measure the elastic shear modulus (G), using the formula: $G = pv_s^2 = p(\lambda f)^2$ – *with* v_s as the shear wave

speed calculated from the wavelength (λ) from the applied mechanical frequency (f).

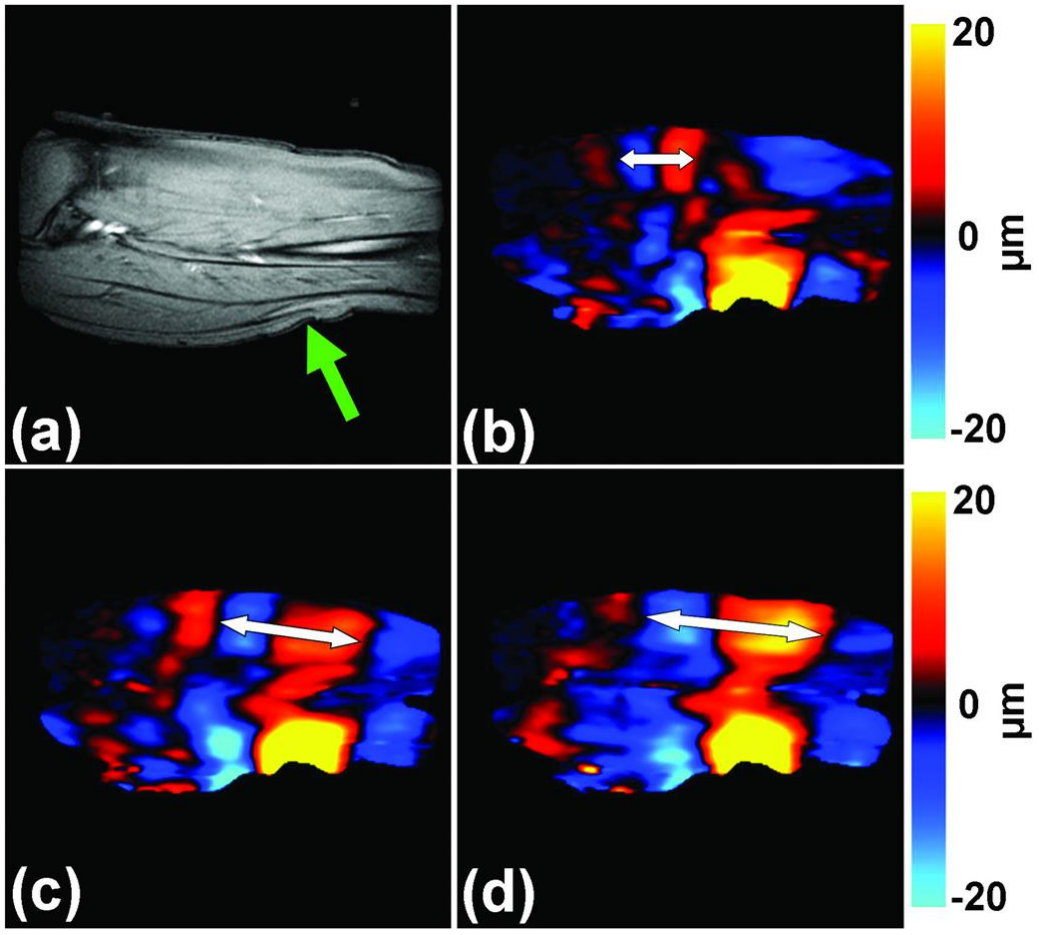

Figure 1.12. Wave lengthens with increased muscle loading, a) anatomical image, b) 0 N/m, c) 5 N/m, d) 10 N/m, from Mariappan et al. (2010).

Advancing technology means we are less dependent on the use of virtual callipers to measure wavelength, and it is now possible to visualise tissue stiffness through the creation of elastograms. Elastograms are images which show the magnitude of stiffness through a scalable colour bar (Barnhill et al., 2013, 2015; Kennedy et al., 2017, Hollis et al., 2017b). This allows for a region of interest (ROI) to be drawn around a tissue to obtain an average muscle stiffness value.

Due to the linearity of muscle elasticity with energy, the higher the frequency of tissue distortion the greater the muscle stiffness measurement. To correct

for this, recent advances within MRE has made it possible to utilise multi-frequency MRE (MMRE; Klatt et al., 2010; Papazoglou et al., 2012). By utilising several frequencies in succession, the resulting elastograms can be concatenated in order to account for frequency bias in measurements. As a result, a multi-frequency dual parameter elasto-visco (MDEV) inversion was developed to account for frequency dependent artefacts and to also increase image resolution and quality (Papazoglou et al., 2012; Braun et al., 2014; Barnhill et al., 2015). Klatt et al. (2010) showed that MMRE can be illustrated through a springpot rheological model (Figure 1.13). This springpot model is comprised of previously discussed elastic and viscous components, as well as a power law behaviour component (α). As a result, the shear complex modulus can be calculated through $G^*=\mu^{1-\alpha}\eta^{\alpha}(i\omega)^{\alpha}$ - with ω representing the excitation pulsation (Debernard et al., 2013).

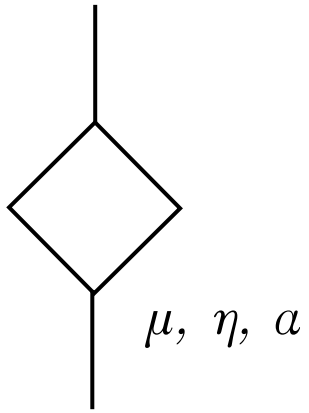

Figure 1.13. Springpot rheological model of multi-frequency muscle viscoelasticity (Debernard et al., 2013).

By calculating the storage of mechanical energy (G') and an imaginary component representing energy dissipation (G") one can calculate the viscoelastic properties of a tissue ($G^*=G'+iG"$), further described in Hiscox et al. (2016). Finally, one can then calculate the 'magnitude of the complex shear modulus' ($|G^*|=\sqrt{G'^2+G''^2}$), and the phase angle of the complex shear modulus ($\phi=\arctan[G''/G']$). $|G^*|$ is a tissue quantification parameter most like that obtained through manual palpation (Sack et al., 2013), as this accounts for tissue displacement (elasticity) and the rate of displacement (viscosity). Hollis et al. (2017a) showed support of using an MDEV inversion to reduce

elastogram artefacts. Further, Hollis et al. (2017b) used finite element analysis (FEA) to model thigh muscle data to measure the reliability of viscoelastic measurements. It was found that the quantification of muscle elasticity (commonly referred to as stiffness) is a highly reliable physiological measure (R^2=0.80) between expected and real-world measurements. In addition to this, Hollis et al. showed that current methods of obtaining measurements of ϕ result in unreliable readings, something which is currently a known difficulty within the domain of MRE, which is why this thesis has focussed on reporting $|G^*|$. Furthermore, the use of the measurement methodology was shown to be strongly in line with real world measurements of stiffness (Barnhill et al., 2013; R^2=0.96).

1.6 Musculoskeletal MRE Research

MRE research has primarily been focussed on physics-based understanding of deforming tissues following application of acoustic waves (Sack et al., 2002; Ringleb et al., 2007). Limited research has been performed on groups of muscles, or functionally similar muscles (Bensamoun et al., 2006; Green et al., 2012, 2013; Barnhill et al., 2013; Guo et al., 2015). A significant amount of musculoskeletal MRE research has focused around investigations of individual muscles, in particular the Biceps Brachii (arm; Dresner et al. 1998, 2001; Sack et al., 2002a; Uffmann et al., 2004; Papazoglou et al., 2005, 2006; Rump et al., 2007), and Vastus Medialis (upper leg; Bensamoun et al., 2007, 2008; Debernard et al., 2011a, 2011b, 2013; Table 1).

Table 1.1. Overview of MRE research investigating the human locomotion system, showing muscles of interest, number of participants and year of publication.

Muscle(s) of Interest	Number of Participants	Research Team	Year	Journal
Gastrocnemius	14	Basford et al.	2002	Archives of Physical Medicine and Rehabilitation
Gastrocnemius	12	Uffman et al.	2004	NMR In Biomedicine
Vastus Lateralis Vastus Medialis Sartorius	14	Bensamoun et al.	2006	Journal of Magnetic Resonance Imaging
Vastus Medialis	5	Bensamoun et al.	2007	Journal of Magnetic Resonance Imaging
Vastus Medialis	6	Bensamoun et al.	2008	Journal of Magnetic Resonance Imaging
Quadriceps	7	Klatt et al.	2010	Physics in Medicine and Biology
Vastus Medialis	26	Debernard et al.	2011	Clinical Biomechanics
Vastus Medialis	13	Debernard et al.	2011	Journal of Biomechanics
Vastus Medialis	9	McCullough et al.	2011	Muscle and Nerve
Gastrocnemius	8	Green et al.	2012	NMR In Biomedicine
Quadriceps Rectus Femoris Vastus Intermedius Vastus Lateralis Vastus Medialis	11	Barnhill et al.	2013	Physiological Measurement
Vastus Medialis	13	Debernard et al.	2013	Journal of Musculoskeletal Research
Gastrocnemius Soleus	10	Green et al.	2013	NMR In Biomedicine
Vastus Intermedius	7	Chakouch et al.	2014	Computer Methods in Biomechanics and Biomedical Engineering
Gastrocnemius Soleus	10	Guo et al.	2015	Magnetic Resonance in Medicine
Rectus Femoris Vastus Intermedius Vastus Lateralis Vastus Medialis Semitendinosus Semimembranosus Bicep Femoris Gracilis Sartorius	29	Chakouch et al.	2015	Public Library of Science One
Vastus Medialis	6	Bensamoun et al.	2015	Innovation and Research in Biomedical Engineering
Whole Thigh	5	Chakouch et al.	2016	Journal of Magnetic Resonance Imaging
Quadriceps	5	Hollis et al.	2017	Magnetic Resonance in Medicine
Quadriceps	15	Kennedy et al.	2018	Journal of Magnetic Resonance Imaging
Gastrocnemius Soleus	9	Tan et al.	2018	NMR In Biomedicine

Muscle stiffness has been shown to increase linearly with tension (Figure 1.8), with the amount of stiffness increase dependent on the magnitude of muscle size (Dresner et al., 2001; Bensamoun et al., 2006; Klatt et al., 2010). This finding suggests that the relationship of muscle size and muscle stiffness may be used as a biomarker for investigating the health of the tissues. MRE has been previously utilised to measure the biceps brachii muscle in vivo for five participants, to model the relationship of muscle function and muscle mechanical properties (Dresner et al., 2001). By applying increasing levels of muscle loading whilst the muscle was contracted it was observed that muscle stiffness increased relative to the amount of weight being lifted (Range of R^2: 0.80–0.99). The relationship between muscle stiffness and load are as a result on muscle tension, volume and cross sectional area (CSA) as shown by Dresner et al. (2001). This model showed that the greater the size of the muscle, the greater the stiffness increase during loading. It is also suggested that the recruitment of more than one muscle may impact the degree to which mechanical properties of a muscle change.

The reasoning behind muscle stiffness increases with use is due to tropomyosin within muscle sarcomeres. By a muscle stretching during use it allows energy to be stored, analogous to that of a spring. Following use, the muscle relaxes, and sarcomeres return to their original length, this process not requiring any additional energy input. As a result, by measuring the degree to which the mechanical properties of a muscle changes allows the use of MRE to quantify the capabilities of a muscle.

It is evident that musculoskeletal soft tissue is viable to measure through MRE, however the application of this technique measuring muscle within medical research has been limited to date (Uffmann et al. 2004). Ringleb et al. (2006) showed that the quantification of muscle mechanical properties shows a significant pathophysiological insight, which cannot be obtained through measuring function alone. Comparing lateral gastrocnemius bilaterally in healthy controls and patients with hemiparesis, they showed that MRE was sensitive enough to show a differential in the bilateral muscle stiffness of the

asymptomatic and symptomatic groups. This showed that MRE is a viable imaging modality to study muscle pathology with the use of muscle stiffness quantification. In addition to this, there is currently only a very limited area of research which employs MRE to investigate the clinical pathophysiology of muscles: Basford et al. (2002) and Ringleb et al. (2006, 2007).

1.6.1 Clinical Musculoskeletal Elastography

Firstly, Basford et al. (2002) set out to investigate whether MRE could offer insight into the effects of neuromuscular dysfunction on the mechanical properties of muscle. It was found that compared to healthy controls, those with muscular dysfunction showed 42% reduction in muscle stiffness ($p<0.001$), and wave lengths increased by 204% when Soleus and Gastrocnemius muscles were loaded ($p<0.001$). This research is particularly interesting as there were inter-muscle differences in the amount of stiffness change with regards to loading and being affected by neuromuscular dysfunction. Basford concluded that the use of MRE measuring the mechanical properties in muscle can result in greater understanding and appreciation for the effects of myopathies in clinical musculoskeletal investigations, especially in measuring the recovery of muscle and the impact of treatment.

Secondly, Ringleb et al. (2006; 2007) applied MRE to noninvasively measure in vivo musculoskeletal tissue and validate it against the model proposed by Dresner et al. (2001), to quantify the effects of muscle pathology. Ringleb et al. showed validation of Dresner's model of muscle due to muscle stiffness increasing linearly with the amount of muscle loading. The conclusion of this paper highlights the importance of applying MRE within clinical investigations of muscle, due to the extensive work to date on examining the effectiveness of MRE within muscle.

In summary, MRE appears to be a clinically useful imaging modality that can provide unique insight into muscle physiology, not available by other more conventional techniques. The conventional use of MVC may show insight into

contraction force but is limited in the spatial appreciation of where the force may be generated. The use of MRE allows for the identification of where the main recruitment of muscle force is taking place, as well as the combination of muscles being used, something further explored in Chapter Five. However, there is a clear lack of research investigating the utility of MRE on the pathophysiology of the musculoskeletal system. Furthermore, the majority of studies on musculoskeletal MRE has focussed on a singular muscle, or muscle group; however, the musculoskeletal system is formed of antagonistic groups operating in opposition. Quantifying changes between muscle groups or muscle types, may provide greater insight into the physiology of the musculoskeletal system, as MRE allows for a unique methodological opportunity to measure both the physical and mechanical properties of muscle. Finally, there have been limited studies that have employed MRE to clinically relevant investigations of muscle injury and recovery. The overall goal of this thesis is to address each of these issues to investigate the clinical utility of musculoskeletal MRE.

1.7 Thesis Objectives

The aim of this thesis is to address the limited physiological research investigating the musculoskeletal system with a series of exploratory investigations whilst performing MRE. In order to achieve these aims, a series of clinically based exploratory musculoskeletal MRE investigations will be performed in order to quantify both muscle morphology (size and shape) and also the mechanical properties.

1.8 Thesis Plan

Chapter One has introduced the relevant topics and clinical research question which this thesis will address in Chapter Two to Eight.

In Chapter Two, I propose a new musculoskeletal analysis pipeline as a methodological basis for this thesis. To quantify musculoskeletal viscoelasticity

an imaging methodology and analysis pipeline are proposed. The key aim of this pipeline is to address several issues surrounding data visualisation within MRE, such as colour maps, registration of images, and presenting group average elastograms. Through the subsequent reliability testing of this pipeline it is shown that the proposed pipeline can result in robust repeatable measurements within and between experiments. The benefit of this analysis pipeline is that is widely available to other research groups and may contribute towards a unified methodological approach to musculoskeletal MRE.

The following chapters are split into two overall sections. Chapters Three and Four explore the passive stiffness and morphological changes in muscle tissues as a result of age and then immobility. Chapters Five, Six, and Seven each involve manipulation of the locomotor muscles through interventions including injury, loading, and surgery.

In Chapter Three, I investigate age related change in size and stiffness, which can result in biomechanical abnormalities, and the overall atrophic effect of age. As discussed in Chapter One, age is a major contributing factor to musculoskeletal conditions. To date, there is a wealth of work investigating the impact of age on muscle size, showing that there is age related atrophy and diminishing strength. However, there is no evidence yet of MRE being employed to study the mechanical changes in muscle as a result of ageing. Musculoskeletal measurements of size and stiffness were obtained for participants ranging in age from 20-55 years old. The aim of this chapter is to explore whether MRE can show added insight into whether certain muscles, or muscle groups, are primarily affected by ageing. The hypothesis for this experiment is that the quadriceps will be predominantly affected by age, evidenced through a decrease in size. It is expected that paired with decreased size there will be an increase in muscle stiffness, due to impairment of anti-gravity muscles supporting the musculoskeletal system. Results such as this could offer significant insight into the ageing musculoskeletal system and help advance geriatric research and preventative methods to keep the ageing population as mobile and independent as possible.

In Chapter Four, I examine whether muscle stiffness and size are sensitive biomarkers to indicate patient health, and a measure of recovery. A cohort of Intensive Care Unit (ICU) patients which have undergone intubation are scanned once at time of ICU discharge and then again following a period of convalescence. Measurements of muscle size and stiffness are compared between scans and also against healthy age matched controls. The aim of this chapter is not only to understand the effects that ICU based immobility has on the mechanical properties of muscles, but to also investigate the recovery of these changes during a period of convalescence. The hypothesis for this study is that the Quadriceps will be primarily affected by immobility, in addition to fat infiltration being evident in additional clinical scanning. It is expected that patients will be significantly impaired in their physical functioning. As discussed, ageing and inactive individuals show signs of musculoskeletal atrophy, whereas patients who are critically ill are immobile and potentially susceptible to systemic inflammatory effects. The use of MRE to investigate the physiological difference between these two states may offer significant pathophysiological insight, obtainable only from MRE.

In Chapter Five, I re-examine previously published data using advances in MRE image analysis techniques to identify why some individuals were prone to oedema induced injury following an Exercise Induced Muscle Damage (EIMD) paradigm. EIMD is a common research area within the musculoskeletal system, due to the significant applications this may have for athletic training. In previous research, participants who took part in an EIMD protocol showed an unexpected differential in presence of oedema following participation. The aim of this chapter was to investigate the reasons behind this, and whether the use of MRE could identify why some individuals were prone to a greater magnitude of damage even though all participants took part in the same protocol. The hypothesis for this experiment is that residual increases in muscle stiffness, because of injury, can be used to distinguish injury severity between two groups of participants. It is expected that those without oedema induced injury will have engaged a more optimal pairings of muscles

compared to individuals who showed a greater magnitude of injury. Those with greater muscle damage will most likely have needed to engage the Quadriceps muscles due to a non-optimal muscle engagement strategy. Findings may be used to aid in the identification of individuals prone to injury whilst also offering new insight into the nature of muscle damage.

In Chapter Six, I explore whether muscle morphology can be an biomarker for muscle strain, and if muscle stiffness can elucidate the magnitude of muscle engagement. As previously discussed, muscle stiffness is related to the amount of loading being applied to the tissue. A custom-made muscle loading apparatus allowed for sustained knee extension and flexion. During a scanning session changes in muscle stiffness, size and shape were examined at incrementally increasing loads: 0kg, 2kg, 4kg, and 8kg. The aim of this chapter is to identify whether there are morphological advantages present in some multiple function muscles, which appear to be less affected by muscle load apparent through morphometric adaptions. The hypothesis for this work being that the rectus femoris will have a greater morphometric change due to loading compared to the vasti muscles during sustained knee extension for this experiment, due to the differential in the connection to the femur between the two muscle types. It is expected that because of loading there will be multiple physiology changes in muscle including: greater muscle stiffness value, lower cross-sectional area and a greater axial circularity of muscles.

In Chapter Seven, I implement the developed analysis methodology to measure the morphometric and mechanical changes in muscles performing a task before and after a surgical intervention. Chapter Four examined patients who were scheduled to undergo total knee replacement (TKR) because of osteoarthritis, who were scanned before and approximately 6 weeks after surgery. During an MRE scan patients performed a knee extension where muscle size, shape and stiffness were examined. The aim of this chapter was to examine whether TKR and participation in physiotherapy would show a decreased change in muscle stiffness changes associated with the task of isometric contractions. It is hypothesized that before TKR surgery, patients will show a significant increase

in muscle stiffness, during sustained knee extension. However, it is expected that following TKR surgery, patients should experience a decreased magnitude of muscle stiffness, especially in the quadriceps, when performing the task.

Finally, Chapter Eight discusses the findings of each chapter and the position that MRE has within clinical musculoskeletal imaging. As a result, this thesis will show that MRE can offer important physiological insight into the health of muscles for a range of clinical applications. With each chapter exploring separate yet complimentary biomechanical examinations of the musculoskeletal system through utility of MRE, the potential contribution to physiological research is explored. As a result, the future direction of musculoskeletal MRE is discussed, as well as the necessity to enhance current work within musculoskeletal reliability and sensitivity of measurements.

Chapter Two

Musculoskeletal Elastography Analysis Pipeline

2.1 Chapter Two Overview

Chapter One outlined the need for future MRE work within musculoskeletal system to obtain a greater appreciation of pathophysiological changes due to injury or myopathy. To do this, Chapter Two outlines the methodological approach employed in this thesis to quantify and visualise muscle mechanical properties. Following this, the reliability of the suggested pipeline is quantified to test the robustness of this pipeline being incorporated. The key questions of Chapter Two is: i) how will images be acquired, processed, analysed, and presented in a robust way? ii) how reliable is the proposed method?

2.2 Proposed Musculoskeletal MRE Methodology

Currently there are several issues within musculoskeletal MRE data visualisation, including ROI segmentation, current use of look-up tables (LUT) within elastograms, and a lack of co-registration templates. The analysis pipeline proposed in this thesis will attempt to resolve these issues to produce anatomically correct elastograms of the musculoskeletal system (Figure 2.1).

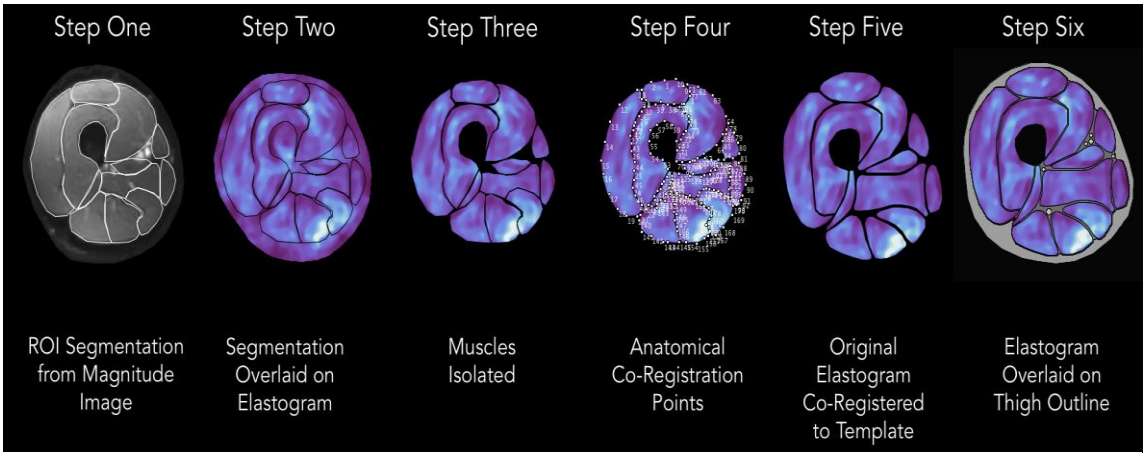

Figure 2.1. Pipeline methodology for musculoskeletal MRE data analysis and data visualisation. Step One: ROI measurements are acquired, Step Two: Post ESP elastogram, Step Three: Muscles segmentation is isolated, Step Four: Co-registration points are applied to data, Step Five: Data is co-registered to template anatomical points, Step Six: Background thigh outline is applied in order to help in data visualisation.

2.2.1 Image Acquisition

MR imaging, including MRE was performed using a 3T Verio MRI system (Siemens Medical Systems, Erlangen, Germany). MRE images were obtained through a modified Cartesian Echo Planar Imaging (EPI) sequence at each of eight phase offsets, with additional motion encoding gradients (Klatt et al., 2010, Barnhill et al., 2013, Kennedy et al., 2017) during multiple frequencies (25Hz, 37.5Hz, 50Hz and 62.5Hz). An actuator cuff was placed anthropometrically (Figure 2.2) around the thigh (Papazoglou et al., 2006), one third of the distance from the patella tendon to the greater trochanter (Bensamoun et al., 2006). A ring-shaped actuator placed around the thigh has been shown to produce axial acoustic waves (Klatt et al., 2010). Imaging parameters: 80 second scan duration consisted of TR = 1600ms, TE = 54ms, FOV = 230mm x 230mm, for five contiguous isometric slices (2.5mm x 2.5mm x 2.5mm^3), which resulted in an image matrix of 93 x 93.

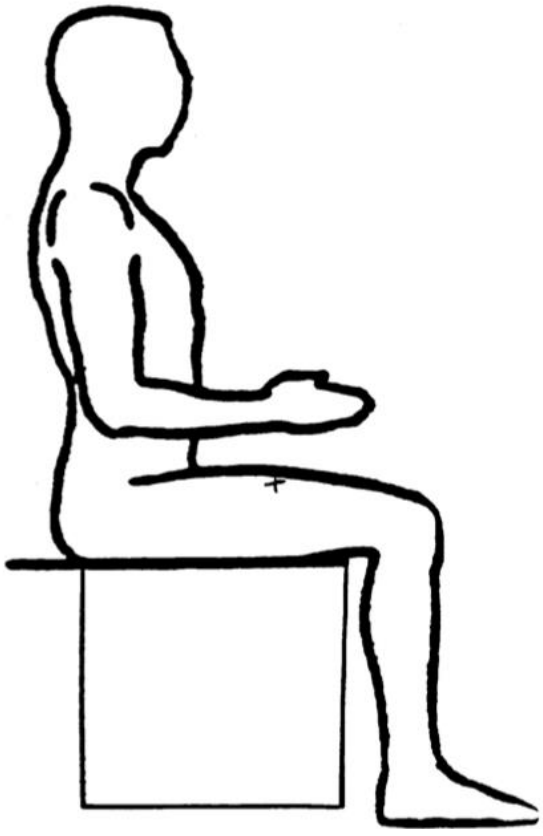

Figure 2.2. Anthropometric placement of MRE actuator cuff for image acquisition, at the midpoint of the thigh as shown by +. (NHANES, 1988).

2.2.2 Image Processing

Images were processed using ESP (Barnhill et al., 2015), running in MATLAB (MathWorks, Natick, MA), with the assumption of muscle being a solid and incompressible homogeneous tissue (Manduca et al., 2001). A Multi-Frequency Dual Parameter Elasto-Visco Inversion (MDEV) was employed to invert three-dimensional displacement data for multiple frequencies. In addition to ESP reducing noise, it also resulted in a greater pixel density for MRE images, increasing the image pixel matrix from 93x93 to 368x368, allowing for detailed ROI segmentation. The use of ESP has been shown to result in elastograms robust to noise and viscoelastic measurements at SNR levels expected within *in vivo* image acquisition (0-10%; Hollis et al., 2017b). Hollis et al. showed that individual muscle coefficient of variance (CoV) of |G*| ranged from 5.29 – 21.90% when there is 2% level of noise evident in the data, with a non-significant linear relationship between size of a muscle and level of variance. A recent meta-analysis of liver MRE research showed a repeatability coefficient of 22% (95% CI [16.1, 28.2]), meaning that changes in MRE readings above this 22% threshold are considered to be real and not due to error (Suraj et al., 2017). However it should be noted that the liver is primarily a static tissue, where as the dynamic nature of muscle may differ between individuals due to factors such as strength or stamina.

2.2.3 ROI Segmentations

Within musculoskeletal MRE there is limited research utilising ROI segmentations of each individual muscle across an axial slice of the thigh. It is more common for a small collection of individual muscles to be segmented (Dresner et al. 1998, 2001; Sack et al., 2002a; Uffmann et al., 2004; Papazoglou et al., 2005, 2006; Rump et al., 2007; Bensamoun et al., 2007, 2008; Debernard et al., 2011a, 2011b, 2013) or an individual muscle group (Barnhill et al., 2013; Kennedy et al., 2017). As discussed in Chapter One, even though muscle groups have functionally similar roles, each muscle has a unique architecture allowing it to perform a specific function. Methodology for this thesis will involve thigh elastograms manually segmented for 12 individual muscles from four muscle

groups visible within the axial slice of the thigh including: quadriceps muscle group (rectus femoris, vastus intermedius, vastus lateralis, and vastus medialis), hamstrings (bicep femoris [long head and short head], semimembranosus, and semitendinosus), adductors (adductor longus and adductor magnus), and the medial rotator muscles (gracilis and sartorius). Region of Interest (ROI) measurements were obtained for muscle stiffness (|G*|, kPa), muscle size (Cross Sectional Area [CSA], cm^2) and muscle circularity (4π[Area/Perimeter^2]). Muscle circularity is quantified as a scale between 0-100%, 0% being an irregular polygon and 100% being a perfect circle. The use of quantifying muscle circularity is to show the axial deformation of the muscle at different levels of tension and paired with the other measures may show new insight into the morphological change in muscle during engagement. As a result, this will allow for the morphological and mechanical composition of each muscle, and also the interaction between one another, something explored in Chapter Six.

2.2.4 Data Visualisation Colour Maps

Current MRE data visualisation largely incorporates the use of the MATLAB default Look-up table (LUT) 'Jet' (as seen in Figure 1.7 and Barnhill et al., 2013). However, Thyng et al. (2016) discusses several issues with this LUT for data visualisation. Firstly, a grey scale LUT represents minimum values as dark and maximum values as light, however the 'Jet' LUT visualises data with minimum and maximum values of hue, as opposed to differing degrees of luminance (Figure 2.3; Stauffer et al., 2015). This is an issue due to hue being cyclical and luminance being linear. Due to there not being clear linear minimum and maximum data points, this can lead to an increased chance of error in analysing data due, particularly when used in clinical research (Borkin et al., 2011). A second way in which the 'Jet' LUT may cause image artefacts is due to the non-monotonic lightness profile of the LUT. Within 'Jet' the lightness of the LUT does not gradually change, unlike a sequential LUT, which Stauffer et al. (2015) outlines as the most suitable LUT for continuous data (such as that seen in the elastograms in this thesis). As a result, the CMOcean

LUT suite (Thyng et al., 2016) was developed in order to offer data scientists more choice in how to accurately display their data (Figure 2.4), with this recently being made available in ImageJ (Rasband, 1997) for clinical image analysis (Perrins, 2018a).

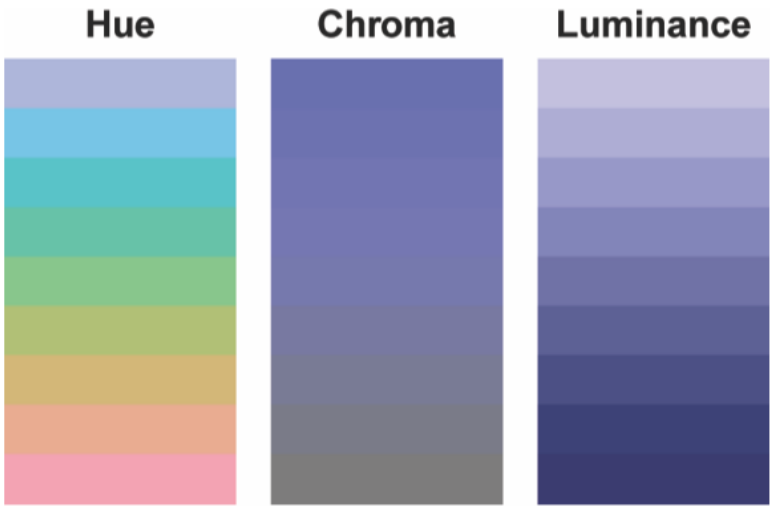

Figure 2.3. HCL Colour system in deciding colour including Hue (Pigment), Chroma (Saturation) and Luminance (Lightness). Obtained from Stauffer et al. (2015).

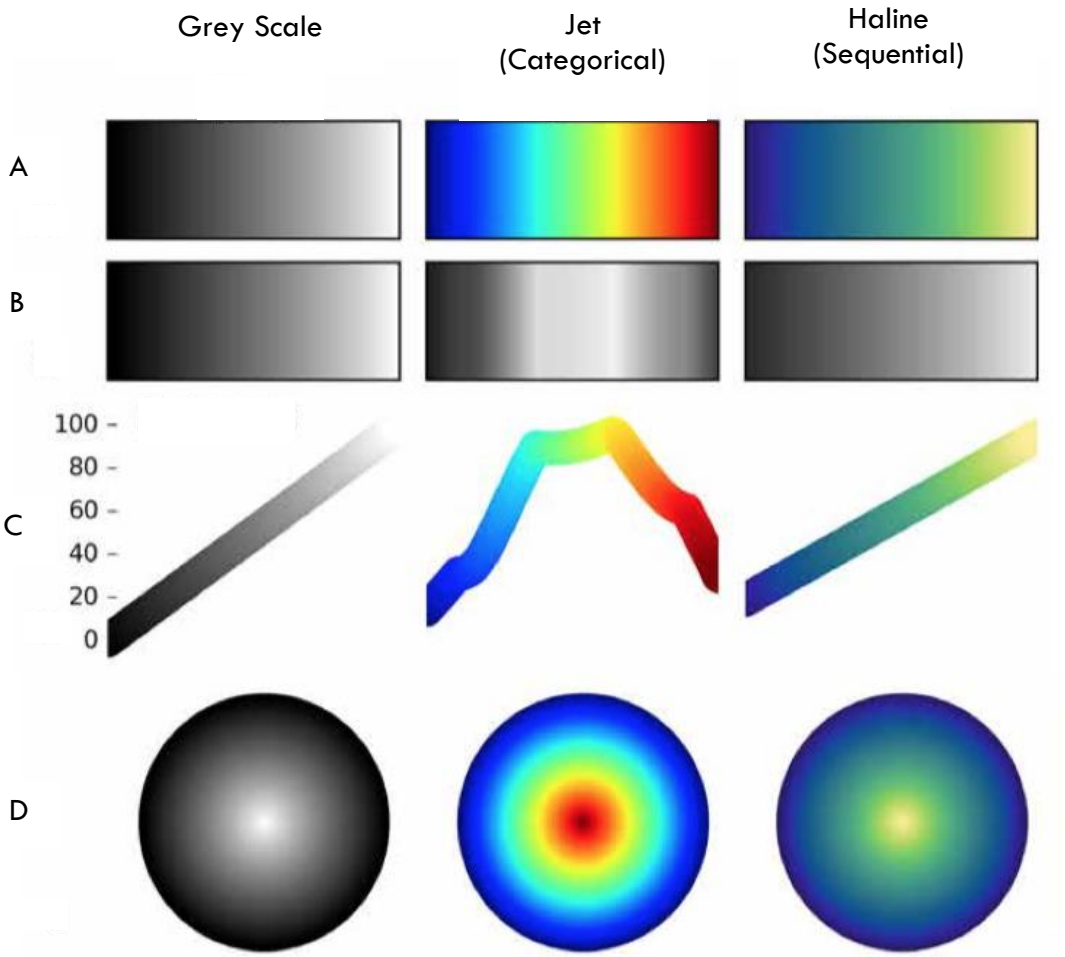

Figure 2.4. Comparison of LUTs displaying data. A: LUTs for Grey Scale, Jet, and Haline. B: Relative grey scale LUT. C: Lightness of LUT. D: Representation of LUT visualising data. Adapted from Thyng et al. (2016).

2.2.5 Musculoskeletal MRE Template

Data visualisation within MRE conventionally uses a single participant as an example for measurements of mechanical properties, or a small selection (Kennedy et al., 2017; Hollis et al., 2017b). A significant problem with this is that there is no opportunity to examine the average differences between participants, with the varied muscle morphology anatomy acting as a confound interfering in appreciating what data is being shown. Previously, Barnhill et al. (2013) showed that a 'Moving Least Squares' algorithm (Schaefer et al., 2006) was a suitable method in which to co-register MRE data, using 125 anatomical landmarks. Taking this methodology further, an idealised thigh was designed (Figure 2.5; Perrins 2018b) in which 180 anatomical points were manually plotted in ImageJ (Figure 2.6). In creating a single template, it avoids possible confounds arising from co-registration of data to a specific elastogram within a cohort to act as a template, as observed in Barnhill et al.

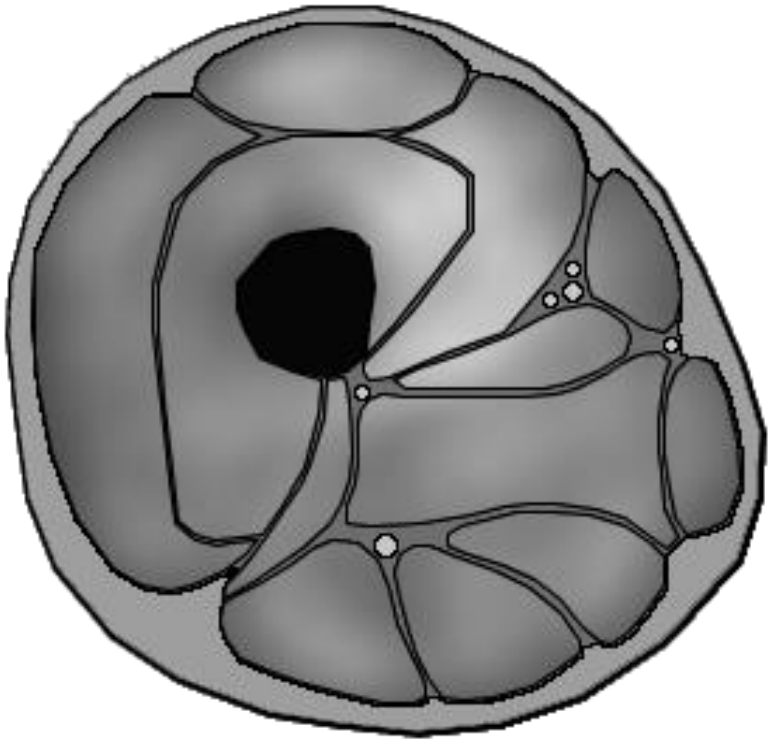

Figure 2.5. Proposed musculoskeletal template for use in co-registering MRE data, based on idealised thigh image for data visualisation (Available from Perrins, 2018b).

By co-registering data to a single template it allows for the appreciation of differentials in location of stiffness within the thigh and makes it easier to appreciate this without navigating the muscular architecture. A consequence with this however is that size changes cannot be visually accounted for following co-registration, and to address this, a zoom factor is applied as a percentage of the change from baseline in elastograms (example in Figure 3.1)

2.3 Summary of Proposed Pipeline

The pipeline which is proposed in this chapter addresses several data visualisation concerns. Firstly, this pipeline will segment an entire axial slice of the thigh, to obtain measurements for changes in the mechanical properties of muscle, as well as morphological. Secondly, by utilising a sequential LUT (as opposed to the conventional 'Jet' LUT used within MRE), the resulting elastograms will be less likely to display visual artefacts, and so will clearly visualise the mechanical properties of individual muscles to both novice and expert researchers. The selection of colours to represent data may appear on the surface arbitrary, yet it is actually a key factor, as a sequential LUT best shows continuous data, and a too large a range of colours may cause visual artefacts. Finally, by co-registering elastograms to a single template it will aid in visual analysis of mechanical properties of muscles without muscle morphology acting as a confound. In conclusion, transforming processed MRE data into a clear template using sequential LUTs assists with analysis of elastograms and is an important stage in data visualisation.

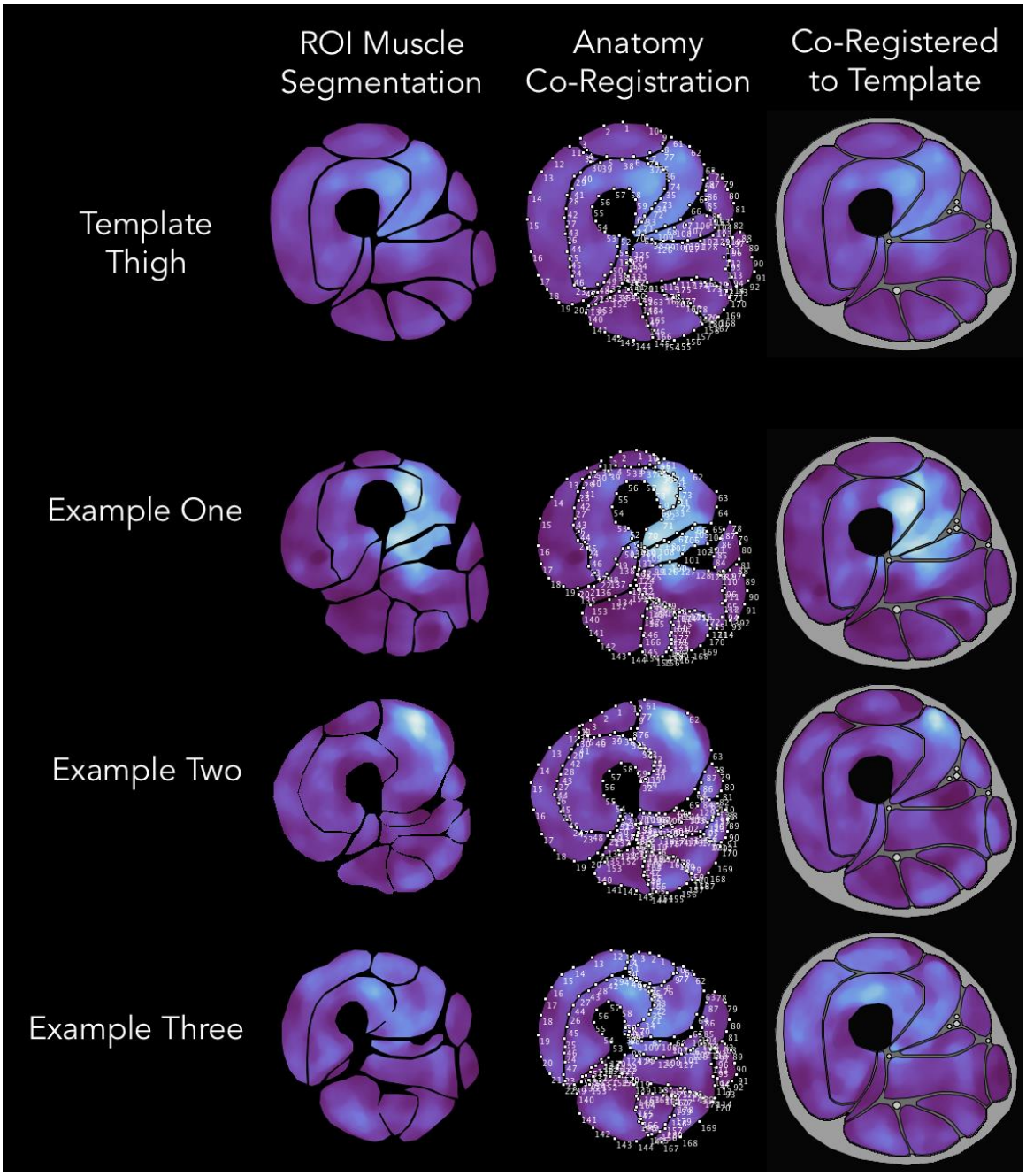

Figure 2.6. Example of co-registration method on three different thigh data towards an average template of the participants. Showing the stages in the pipeline. Firstly with muscle segmentation, followed by the plotting of anatomical points on each example in relation to the template thigh, and finally showing each thigh co-registered to the template whilst keeping individual mechanical data intact.

2.4 Reliability Testing of Proposed MRE Pipeline

To test the reliability of a proposed analysis pipeline and the measurements obtained, a single participant was scanned five times within one hour, with ROI measurements compared within (intra-rater) and between (inter-rater) experimenters (Figure 2.7), with ethical approval being obtained under the development of this pipeline.

2.4.1 Methodological Design

A single participant was scanned five times within a one-hour scanning session with the previously described acquisition protocol (See section 2.2.1). Whilst being scanned multi-frequency MRE was performed (25, 37.5, 50 Hz) taking 4 minutes, this being repeated 5 times. Between each scan the participant stood up from the scanner for 3 minutes and the MRI scanner was reset to original set up. To ensure the scanning position was the same for each scan, the actuator cuff remained on the participant throughout the hour. Analysis consisted of four stages: i) Intra-rater reliability of muscle CSA and $|G^*|$ across the five scans, ii) Inter-rater reliability between CSA and $|G^*|$ measurements, iii) intra-rater reliability of anatomical points plotted on images from each scan, and vi) reliability of $|G^*|$ of co-registered elastograms between scans.

2.4.2 Statistical Analysis

ROI measurements were reported as mean, standard deviation and the coefficient of variance (CV), in order to best show the reliability of ROI measurements. Due to a single participant being measured several times, a Mauchley's test of sphericity was performed to measure the variance for the within-subject analysis for ROI measurements. The assumption that there was equal variance was violated and so a Greenhouse-Geisser correction was used to account for this. Finally, Cronbach's Alpha analysis was performed on intra-rater measures, whilst inter-class correlation was performed on inter-rater measures.

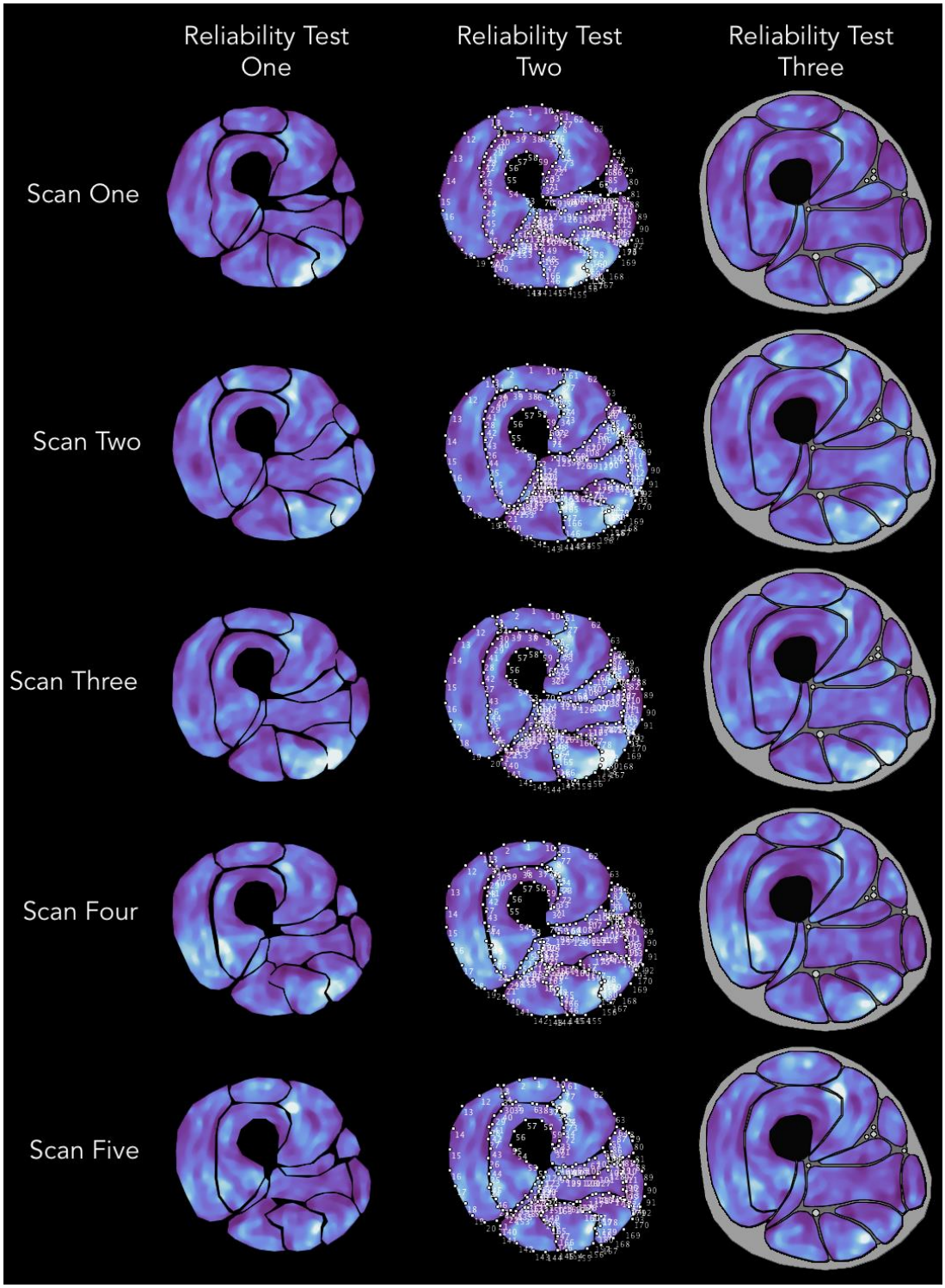

Figure 2.7. Image matrix of repeatability testing. Test one for ROI segmentations (CSA and |G*|), Test two for co-registration points, and Test three for post co-registration |G*| reliability.

2.4.3 Reliability Analysis of ROI Measurements

Firstly, CSA measurements of each muscle were averaged, for scan 1 (M=19.53[±33.14]cm^2, CV=170%), scan 2 (M=19.94[±33.75]cm^2, CV=169%), scan 3 (M=19.43[±32.92]cm^2, CV=169%), scan 4 (M=19.27[±32.56]cm^2, CV=169), and scan 5 (M=18.93[±32.13]cm^2, CV=170). These measurements were analysed using a repeated measures ANOVA, with muscle CSA being the within-subjects factor. A Mauchly's test of sphericity indicated that the assumption of sphericity had been violated ($p<0.001$), resulting in the degrees of freedom being corrected using Greenhouse-Geisser estimates ($\varepsilon=0.37$). This analysis showed that there was no significant difference of muscle CSA between scans ($F[1.46, 16.10]=1.58$, $p=0.235$, $\eta_p^2=0.125$). A Cronbach's Alpha revealed an excellent level of intra-rater reliability (5 items; $\alpha=1.00$). An inter class correlation analysis showed that there was also an excellent level of inter-rater reliability between muscle CSA measurements (ICC=0.998).

Secondly, |G*| measurements were also averaged across muscles for each scan including scan 1 (M=1.36[±0.22]kPa, CV= 16%]), scan 2 (M=1.52[±0.19]kPa, CV=13%]), scan 3 (M=1.51[±0.24]kPa, CV=16%]), scan 4 (M=1.47[±0.20]kPa, CV=14%]), and scan 5 (M=1.45[±0.15]kPa, CV=10%]). In addition to the CSA measurements, the |G*| measurements were analysed using a repeated measures ANOVA, with muscle |G*| being the within-subjects factor. A Mauchly's test of sphericity indicated that the assumption of sphericity had also been violated ($p=0.018$), resulting in the degrees of freedom being corrected using Greenhouse-Geisser estimates ($\varepsilon=0.56$). This analysis showed that there was no significant difference for muscle |G*| between scans ($F[2.22, 24.46]=0.672$, $p=0.615$, $\eta_p^2=0.058$). A Cronbach's Alpha revealed an excellent level of intra-rater reliability (5 items; $\alpha=0.831$). An inter class correlation analysis showed that there was also an excellent level of inter-rater reliability between muscle CSA measurements (ICC=0.836).

2.4.4 Reliability of Anatomical plots

The XY co-ordinates for each of the 180 anatomical plots which were mapped per image. This resulted in 5 lots of 180 'X' co-ordinates, and 5 lots of 180 'Y' co-ordinates. An example of co-registration from anatomical plotting is shown through figure 2.7 with the mechanical features (i.e. stiffness) evident in the original elastogram are retained in the template thigh layout. A Cronbach's Alpha revealed an excellent level of intra-rater reliability for placement of anatomical plots (10 items; α=0.911).

2.4.5 Reliability of Co-Registered Elastograms

Due to the high level of intra-rater reliability in both |G*| and anatomical mapping, the final measurements analysed were those on co-registered elastograms. |G*| measurements for each co-registered elastogram were obtained for scan 1 (M=1.36[±0.24]kPa, CV=16%]), scan 2 (M=1.51[±0.18]kPa, CV=12%]), scan 3 (M=1.48[±0.20]kPa, CV=14%]), scan 4 (M=1.43[±0.18]kPa, CV=13%]), and scan 5 (M=1.43[±0.16]kPa, CV=11%]). A Cronbach's Alpha revealed an excellent level of intra-rater reliability (5 items; α=0.836).

2.5 Chapter Summary

The aim of this chapter was to explore the methodological background of musculoskeletal MRE to propose a pipeline to conduct data analysis and to visualise the mechanical properties of muscle. Reviewing the literature highlighted robust methods of image acquisition, processing and analysis, as well as pinpointing some issues with data visualisation. The pipeline proposed in this chapter addresses the concerns raised of conventional MRE data visualisation by incorporating sequential LUT's and template co-registration. The reliability of each stage of the pipeline was also examined, showing excellent levels of intra-rater and inter-rater reliability, suggesting that it is a robust methodology which may be adopted by future researchers investigating musculoskeletal mechanical properties.

Chapter Three

Musculoskeletal Ageing

3.1 Chapter Three Overview

As mentioned in Chapter One, ageing is a significant contributor to musculoskeletal conditions, which then impacts the quality of life for older individuals. It is well known that there are atrophic effects associated with ageing, something not largely examined with MRE. In identifying muscle groups prone to the effects of ageing, particularly changes in the mechanical properties, this research will contribute to aid geriatric physiotherapy. This insight may offer important new insight into the musculoskeletal pathophysiology of the ageing human. The aim of this chapter, and exploratory study, is to examine the physical and mechanical changes in thigh muscles with age. Here it is shown that with age there is an associated increase in muscle stiffness, a decrease in muscle size, and as a result a reduction in muscle CSA in relation to residual muscle stiffness. This change in relationship of morphology and mechanical properties may offer insight into future musculoskeletal research investigating ageing. The question Chapter Three attempts to answer is: What is the impact that ageing has on the mechanical properties of muscle?

3.2 Introduction

The loss of muscle mass is known as sarcopenia and is a leading cause of impairment in older age (Evans, 1995; Morley et al., 2001). Muscle cross-sectional area (CSA) decreases through ageing (Campbell et al., 1973; Grimby et al., 1983; Lexell et al., 1988; Holloszy et al., 1995; Frontera et al., 2000; Roubenoff, 2003) in combination with a loss of muscle force (Faulkner et al., 1995; Holloszy et al., 1995; Harris, 1997; Frontera et al., 2000; Doherty, 2003; Johnson et al., 2004; Goodpaster et al., 2006; Metter et al., 1997, 1999, 2002; Narici et al., 2010). Muscle CSA and muscle force have been shown to be significantly correlated (Bruce et al., 1989), so muscle size is considered an anatomical biomarker for muscle strength (Wickiewicz et al., 1983, 1984).

The loss of muscle strength with age is known as dynapenia (Clark et al., 2008; Manini et al., 2011). Strength changes occur more rapidly in comparison to muscle size changes, suggesting that there is a decline in muscle quality with age (Bruce et al., 1989; Vandervoort et al., 1986, 2002; Goodpaster et al., 2006), as well as a neurological function (Clark et al., 2008). Further, decreased mobility and muscle force of knee extensions has been shown to be associated with poor health in older adults (Laukkanen et al., 1995; Rantanen et al., 2000, 2003). The quadriceps are particularly prone to the effects of ageing, with Maden-Wilkinson et al., (2013) showing the quadriceps decrease in size by one third between the ages of 22–72. Results from Lexell et al. (1988) suggest that vastus lateralis begins to show signs of age-related atrophy at the age of 25, worsening with age, due to the loss of muscle fibres. Recent research has shown that a differential in sarcopenic and pre-sarcopenic muscles is that in addition to the loss of muscle fibres, the size of these fibres are much smaller in those individuals with sarcopenia (Piasecki et al., 2018).

There is limited research on the effects of ageing on muscle stiffness, however, Alnaqeeb et al., (1984) showed evidence that with age there is an increase in the connective tissue of muscles, which results in increased muscle stiffness. Increased connective tissue in muscles is directly correlated with atrophy because of ageing (Lowry et al., 1942; Williams et al., 1984). Increased muscle stiffness has also been shown following muscle strain (Howell et al., 1993; Barnhill et al., 2013), so as muscles decrease in size with age then muscles are increasingly strained to perform tasks with decreased muscle force, resulting in progressive injury.

An additional factor which may affect musculoskeletal mechanical properties is that with decreased size of muscles, there may likely be a residual increase in muscle stiffness because of extra stress being elicited. As the size of muscles decrease with age, there will be a lower ratio of CSA to kPa older individuals, which may be negatively impacting the biomechanics of the thigh, in particular stability.

The aim of this investigation is to measure changes in muscle morphometry and mechanical properties, through Magnetic Resonance Elastography (MRE), to identify certain muscles, or muscle group which are prone to ageing effects. Firstly, we expect the biomarker for ageing effects to be muscle atrophy paired with increased muscle stiffness. As the quadriceps muscle group are the key anti-gravity muscles, it is expected that there will be an increase in muscle stiffness if there is age related atrophy, due to a greater level of muscle strain during engagement. In addition to this, it is expected that older individuals with have a lower ratio of CSA to kPa in muscles compared to younger adults. This investigation will primarily aid in methodological appreciation of mechanical changes associated with age, highlighting the gradual impact that ageing has on the musculoskeletal system.

3.3 Methods

3.3.1 Methodological Overview

Data from healthy individuals from this thesis were analysed to examine the mechanical physiological changes in muscle tissue because of ageing. Analysis covered whole thigh, individual muscle groups and individual muscles, to identify regions which are prone to ageing atrophy. Participants were initially split into two age groups to show simple mean changes between younger and older adults. The analysis is then taken further to examine changes in CSA, $|G^*|$ and the ratio between the two across age as a factor, as opposed to between two age groups.

3.3.2 Participants

Scan data was analysed from 15 participants from Chapters Four and Five from healthy active males (M=80.18kg, 95% CI[73.08, 87.28]) ranging from 20-55 years old (M=35.33 years old, 95% CI[28.00, 42.67]), with ethics allowing for data comparison from these two investigations. Individuals were normally distributed in two age groups based on whether they were younger or older

than the mean age. As a result, there was a Younger group (n=8) with a mean age of 24.43 [±4.31] years and an Older group (n=7) with a mean age of 47.57 [±7.74] years. Participants were all healthy active male adults.

3.3.3 Image Analysis

Region of interest (ROI) measurements were taken for |G*| (kPa) and muscle cross-sectional area (CSA). For visualisation of mean |G*| increases a 'Moving Least Squares' (Schaefer et al., 2006) algorithm was used to co-register each participant to a custom template. Association between participants age, muscle |G*|, and CSA were examined. An additional measure of physiological change was the ratio for CSA per kPa, an attempt to have a greater physiological insight of muscles. The mean ratio of CSA and |G*| was quantified for the thigh overall, and for individual muscles. Due to the difference in data acquisition methods between data, images from Chapter Five being scaled down to match the data of Chapter Four.

3.3.4 Statistical Analysis

Firstly, the mean comparison between age groups was conducted for both the |G*| and CSA of muscles, as well as the ratio of CSA per kPa. All comparative descriptive data was expressed as mean ± standard deviation. To ensure equal distribution of each group and between the two groups were compared. The comparison of the mean group differences were analysed through a one-way ANOVA. Following this, mean changes across age as a factor were examined, through a Pearson correlation and also linear regressions.

3.4 Results

3.4.1 Comparison of Age Groups

Age groups were normally distributed as shown through a Kolmogorov-Smirnov test (Younger age group: D[8]=0.182, p=0.200; Older age group: D[7]=0.288, p=0.082), as well as non-significant variance (F[1,13]=0.85,

p=0.374), and adequate statistical power between groups (d=0.990). There was not a significant difference in weight between groups (F[1,13]=1.06, p=0.322). Between the age groups the CSA, |G*| and subsequent ratio of CSA to kPa was measured. Firstly, a difference was observed for muscle CSA between groups (Younger group: 176.80[±26.60]cm^2 vs Older group: 116.37[±27.62]cm^2), with the older group showing a reduced overall CSA of 34% (F[1,13]=18.83, p<0.001), this also being observed for individual muscle CSA (Younger group: 14.65[±11.18]cm^2 vs Older group: 9.70[±7.17]cm^2). Secondly, muscle |G*| was greater on average for the older age group in comparison to the younger age group (Younger group: 1.33[±0.17]kPa, Older group: 1.43[±0.35]kPa), significantly greater by 7% (F[1,190]=5.35, p=0.022; Figure 3.1). Further, the ratio of muscle CSA per kPa was greater in the younger group (132.01[±22.87]cm^2) compared to the older group (79.34[±13.78]cm^2). The younger age group showed 40% greater overall ratio of CSA to kPa (F[1,13]=28.05, p<0.001; Figure 3.2).

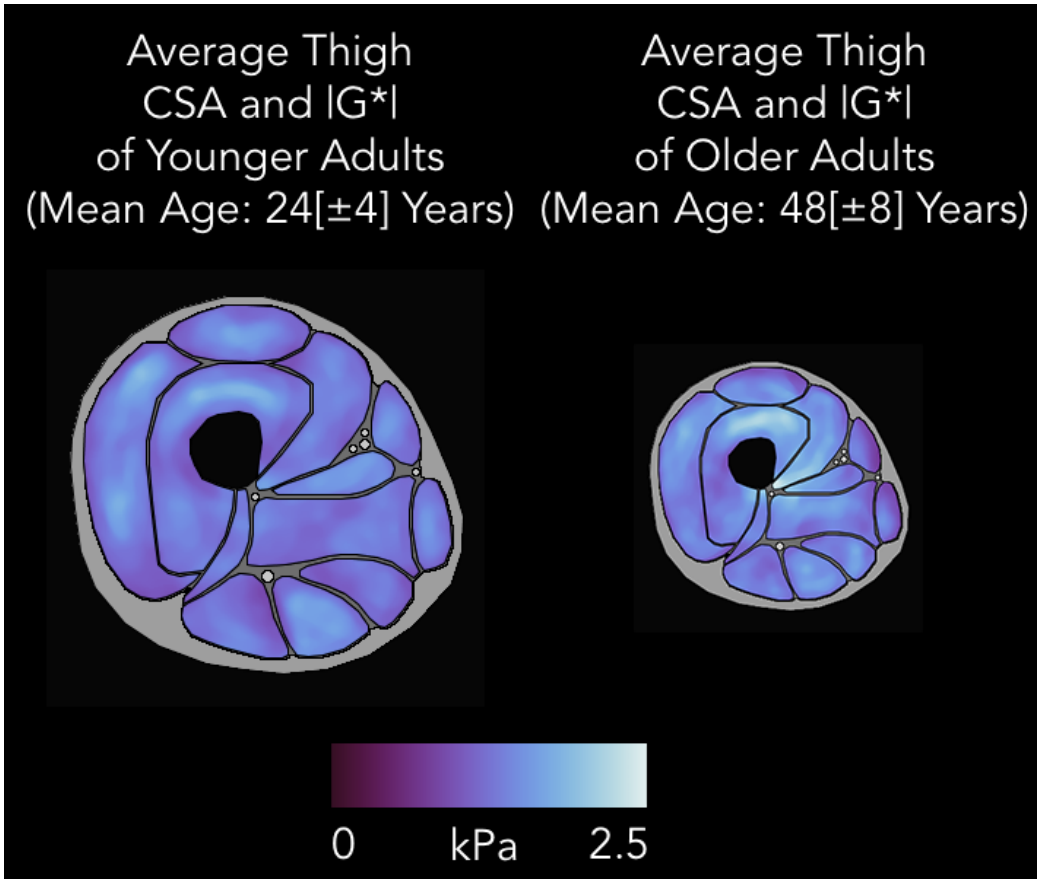

Figure 3.1. Average |G*| for each age group, with the decreases overall CSA of the older group represented with a decreased zoom factor.

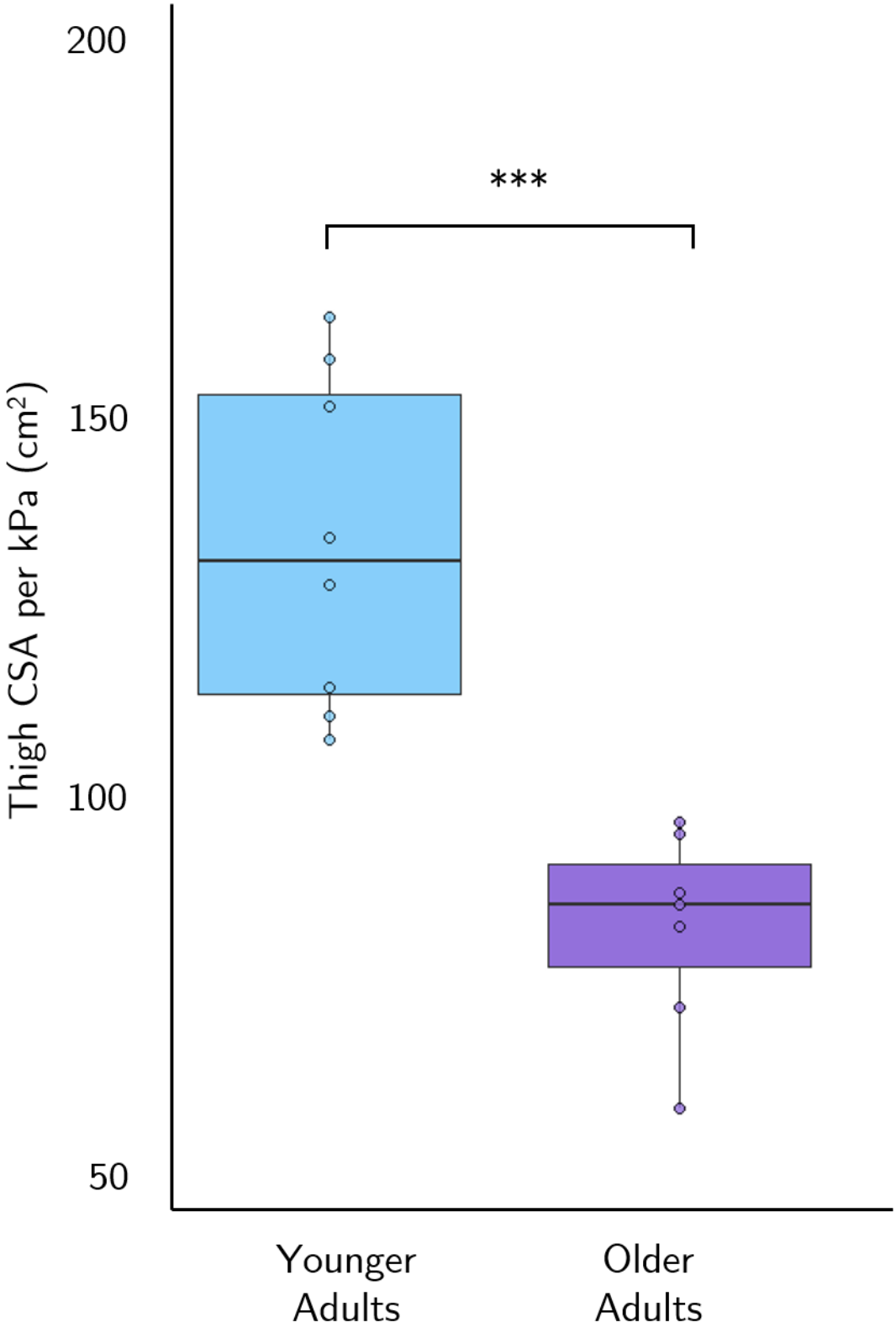

Figure 3.2. The ratio between the amount of CSA per kPa with each age group, showing a significantly lower CSA per kPa in the older group. '***' ≤ 0.001, '**' ≤ 0.01,'*' ≤ 0.05.

3.4.2 Biomechanical Changes Correlated with Age

Data was normally distributed across age as shown through a Kolmogorov-Smirnov test (D[15]=0.167, p=0.200). Changes in muscle tissue were correlated with age whilst separating the groups. Age was correlated with CSA and |G*| changes, showing a moderate negative correlation with for CSA (r[14]=-0.66, p=0.007) and moderate positive correlation with |G*| (r[14]=0.53, p=0.040). However, age was not significantly correlated with weight (r[14]=0.42, p=0.116). Following this, the ratio of CSA to kPa was correlated with age, with a strong negative correlation being observed (r[14]=-0.77, p=0.001). A linear regression analysis showed that there was an increase of 6Pa in muscle per year of age (R^2=0.23, F[1,14]=5.18, p=0.040), a decrease in muscle CSA by 2.03cm^2 per year of age (R^2=0.40, F[1,14]=10.20, p=0.007) and a -1.9cm^2 loss in CSA to kPa per one year of age (R^2=0.55, F[1,14]=18.33, p=0.001). As a result, anthropometry measurements (i.e. age and weight) were examined as a predictor for the ratio of muscle CSA to kPa, with this being found as strong predictor (R^2=0.72, F[3,11]=12.94, p=0.001).

3.4.3 Muscle Groups Prone to Ageing Atrophy

Examining the physiology change with age was then focussed on individual muscle groups. Correlations with age for CSA and |G*| were observed for quadriceps (CSA: r[14]=-0.66, p=0.006; |G*|: r[14]=0.57, p=0.020). Whilst only CSA was correlated with age in the adductors (r[14]=-0.61, p=0.013) and medial muscles (r[14]=-0.76, p=0.001). The hamstrings showed no significant correlation of anatomical change with age (CSA: r[14]=-0.34, p=0.192; |G*|: r[14]=0.40, p=0.124). Furthers, quadriceps CSA and age were observed as significant predictors for Quadriceps |G*| (R^2=0.55, F[3,12]=7.02, p=0.006). Next, the ratio of CSA to kPa was correlated with age between muscle groups (Figure 6.3), with the CSA to kPa ratio being highly correlated with age in quadriceps (r[14]=-0.77, p<0.001; Figure 3.3), medials (r[14]=-0.77, p=0.001), and adductors (r[14]=-0.65, p=0.006), and the hamstrings showing a non-significant association between atrophy with age (r[14]=-0.49, p=0.052). A linear regression analysis showed that there was a loss of 0.98cm^2 CSA to kPa

per year in the quadriceps (R^2=0.57, F[1,14]=20.69. p<0.001), a loss of 0.11cm^2 per year in the medial muscles (R^2=0.56, F[1,14]=20.04, p=0.001), and also a loss of 0.51cm^2 per year in the adductor muscles (R^2=0.39, F[1,14]=10.38, p=0.006).

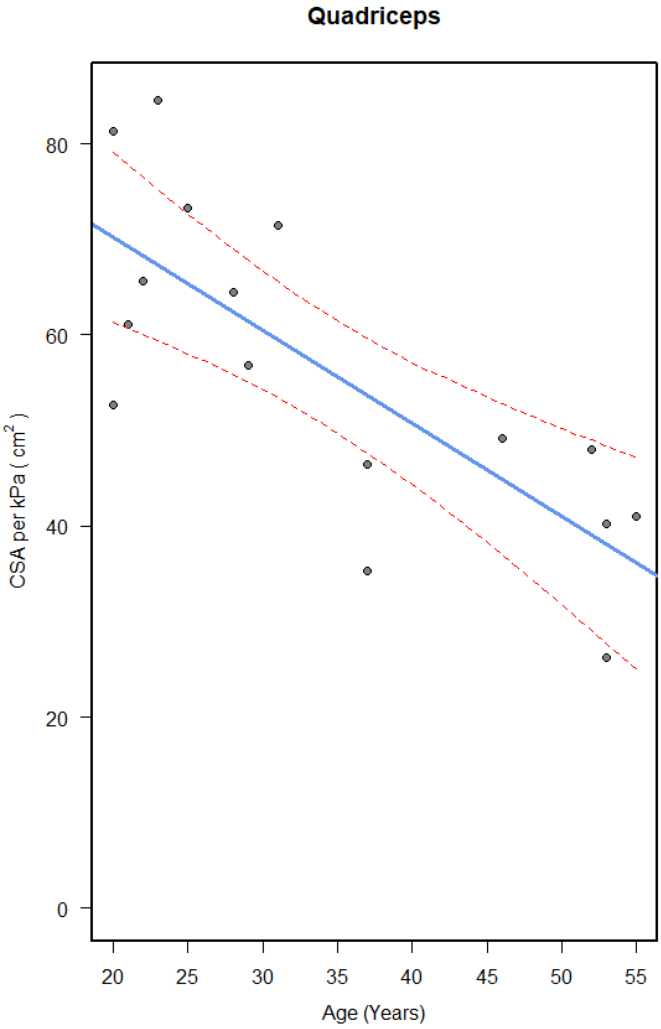

Figure 3.3 The changes in CSA to kPa observed within the quadriceps muscle group correlated with age. Dashed red lines representing the 95% confidence interval.

3.4.4 Changes in Individual Muscles from Ageing

Finally, individual muscles which were prone to changes in |G*| were identified. Of the 12 muscles segmented it was only vastus medialis that showed an individual significant change in |G*| associated with increasing age (r[14]=0.58, p=0.018), with a linear regression showing an increase in 13Pa for every year

of age (R^2=0.29, F[1,14]=7.19, p=0.018). When the CSA of vastus medialis was taken into consideration, the strength of the linear regression increased (R^2=0.86, F[3,12]=31.35, p<0.001). Interestingly, the vastus medialis did not show any significant age related atrophy (r[14]=0.09, p=0.733).

The CSA to kPa for individual muscles were then measured. All the quadriceps muscles, apart from vastus medialis, showed a significant loss of CSA per kPa as a result of ageing, including rectus femoris (r[14]=-0.69, p=0.003), vastus intermedius (r[14]=-0.62, p=0.010), and particularly vastus lateralis (r[14]=-0.74, p=0.001). Both the adductor muscles showed significant correlation with age and CSA to kPa (Adductor Longus: r[14]=-0.54, p=0.029; Adductor Magnus: r[14]=-0.65, p=0.006). Only the semitendinosus showed significant loss of CSA to kPa associated with age within the hamstrings (r[14]=-0.69, p=0.003), with gracilis being the only medial muscle showing a similar loss of CSA to kPa (r[14]=-0.85, p<0.001).

3.5 Discussion

The aim of this study set out to investigate whether certain muscles could be identified as being prone to ageing effects. The hypothesis for this investigation was that in addition to atrophic effects of ageing, there will be likely increases in muscle |G*|. As expected, muscle |G*| increased with age, as well as the quadriceps muscle group being primarily affected by age-related atrophy, supporting previous research (Lexell et al., 1988; Narici et al., 2008; Maden-Wilkinson et al., 2013). This may be due the quadriceps being primarily anti-gravity and weight bearing muscles, so age-related atrophy may have resulted in increased level of strain, as muscle CSA is correlated to muscle force (Lieber et al., 2011). It should be noted that whilst the size of muscle can impact the strength output of muscles, there is also a neurological basis to muscle output. A further finding to support this explanation was evidence of a significant relationship between the age of an individual and the size of the quadriceps in predicting mechanical properties. Further, the age of an individual and the size

of the vastus medialis was shown to be a particularly strong predictor for |G*| (R^2=0.89).

The findings of this study support previous research, which found that the quadriceps were primarily affected by ageing-effects (Lexell et al., 1988; Trappe et al., 2001). The quadriceps did not atrophy uniformly, with the greatest decrease observed in vastus lateralis, and the vastus medialis not showing significant atrophy due to age. Traditionally, the method of measuring muscle quality is to assess the lean muscle (N/g). However, from investigating the effects of ageing and muscle size on |G*|, this study showed that the largest muscle groups of quadriceps and adductors were primarily compromised by ageing, with the medial muscles slightly less affected and hamstrings muscles not appearing to be significantly affected by increasing age.

The current literature on this topic with Grosset et al. (2007) showing that young children (7-11 year old) have a lower muscle stiffness than adults (21 years old). Further, Hortobágyi et al. (2000) showed that there was increased muscle stiffness in older participants (69 years old) compared to younger adults (20 years old). Hortobágyi determined that during a stepping protocol, there was increased stiffness (and muscle co-activation) in older participants in order to increase stability, as a result of decreased neuromotor functions. Eby et al., (2015) investigated stiffness of the biceps brachii of adults aged between 21-94 years old, finding that muscle stiffness increased with age, particularly above the age of 60, where overall muscle strength has been shown to significantly decrease. Decrease in muscle strength can be somewhat explained through age related decreases in muscle size (Aniansson et al., 1981; Lexell et al., 1983, 1988; Essén-Gustaysson et al., 1986; Evans et al., 1992; Porter et al., 1995). Maden-Wilkinson et al. (2013) also showed a 30% decrease in quadriceps size in older adults (72 years old) compared to younger adults (22 years old). Finally, Jones, Rikli and Beam (1999) showed that with increasing age, there was an associated decrease in lower body strength, supporting our findings that increased muscle stiffness was associated with age (Larsson et al., 1978; Viitasalo et al., 1986; Narici et al., 1991; Häkkinen et al., 1996, 1998). The

result of this chapter is important as the ageing population increasingly requires supportive measures to enable people to remain at home as long as possible. The findings here may give insight into how best to enable physiotherapy and muscle strengthening measures, as it offers a quantitative method to study the effects of exercises aimed at muscle strengthening.

The present study, which demonstrated differential differences in muscle CSA and muscle |G*| for each muscle group provides new insight into better understanding age related changes of muscle mechanical properties as a possible biomarker for quality of muscle, through application of the variable |G*|. Though the results of this investigation support the hypothesis, there are limitations to the conclusions of this analysis. Even though there is a normal distribution of age, there are a limited number of participants, with a possible variety in activity levels, where the younger adults may have been more active than the older adults. Health of participants across ages is a particularly difficult to control for, in particular the level of habitual exercise as this may impact residual muscle stiffness, and so there may be more than just age contributing to the mechanical properties and CSA of muscles. However, this chapter does show that in addition to the previously observed size changes in muscle with age, there are also mechanical changes with age. These results should be treated as pilot data, to offer a first step in using MRE to measure ageing effects in muscle, as there are currently no published results on using MRE to study musculoskeletal ageing.

This chapter has shown that as a result of the decreased muscle size, there was an increase in the stiffness of muscles. This result suggests that with age there is a greater degree of residual stiffness, potentially due to a lower muscle size – a conventional measure of muscle strength. Increased muscle stiffness has previously been shown to be related to increased levels of connective tissue as a sign of atrophy. These findings support previous research showing that age resulted in an increase in overall muscle stiffness (Alnaqeeb et al., 1984). Increased muscle stiffness could be a sign of decreased muscle quality, or effectiveness in performing tasks, as previously suggested by Bruce et al., (1989)

and Goodpaster et al., (2006). To further add to the possible measure of muscle quality, the ratio between CSA and kPa has been shown here to be a valuable method in distinguishing individuals between groups, which should be continued in future research.

In summary, by using MRE, age related changes can be detected in muscles through the quantification of muscle morphology and mechanical properties. From the findings of this pilot work that there is a distinction in the ratio of size of muscles to stiffness of muscles between younger and older adults. In addition to this, it was also apparent that with the decreasing size of muscles there was a relative increase in the stiffness of muscles, something which would be of interest to further pursue in future muscle ageing work. The use of MRE in this pilot study has shown that MRE may be used to quantify passive (as opposed to active changes such as muscle engagement) physiological changes in muscle. Further research may be able to offer insight into musculoskeletal stability of geriatric patients by incorporating measurements of muscle mechanical properties in patients.

Chapter Four

Impact and Recovery from Critical Care

4.1 Chapter Four Overview

In the previous chapter, there was a native change in muscle mechanical properties through ageing, this static change in muscle mechanical properties is further explored in this chapter which explores the impact of immobility. The impact that immobility has on muscle stiffness has not been previously explored within MRE. It is well known that a short period of time in an Intensive Care Unit (ICU) can result in muscle atrophy, however by using MRE in this pilot study insight can be gathered on mechanical changes. Examining patients at time of ICU discharge and return allowed for a rare opportunity to contribute to the limited imaging research on post-ICU musculoskeletal recovery. As a result of this contribution, future ICU-Acquired Weakness (ICU-AW) recovery plans could be assessed through the use of MRE to measure changes in muscle morphology and mechanical properties. Here it is shown that stiffness and size of a muscle decreases when we expect a person to be weaker and increases when we expect them to be stronger – this is also explored in the EIMD work (see Chapter Five). The questions being answered by Chapter Four are: i) What impact does time in ICU have on the size and mechanical properties of muscle? ii) Are these negative effects recovered after a period of convalescence?

4.2 Introduction

Patients requiring admission to an Intensive Care Unit (ICU) during a critical illness often require mechanical ventilation. This often leads to immobility and subsequent associated muscle weakness (Herridge, 2009; Herridge et al., 2011; Puthucheary et al., 2013), inactivity muscle atrophy (Plank et al., 2000; Reid et al., 2004; Gruther et al., 2008;), and micro-structural changes (Griffiths et al., 1995; Helliwell et al., 1998; Burnham et al., 2005). Skeletal muscle accounts for 40% of body mass, a reserve relied upon whilst critically ill, as patients can lose 1-4% of body mass per day (Griffiths, 1996, Finn et al., 1996), resulting in severe muscle wastage (Helliwell et al., 1991). ICU-acquired weakness (ICU-AW) from non-use of muscles has been shown to negatively affect muscle

morphology, function and strength (Tabary et al., 1972; Tomanek et al., 1973, 1974; Duchateau et al., 1987; Gibson et al., 1987; Kortebein et al., 2008; Puthucheary et al., 2010), with possible long term effects (Latronico et al., 1996; Coakley et al., 1998; Griffiths et al., 1999; De Seze et al., 2000; Herridge, 2002; Fletcher et al., 2003; Garnacho-Montero et al., 2001; De Jonghe et al., 2007; Stevens et al., 2007; Guarneri et al., 2008; Puthucheary et al., 2010). Muscle immobilization primarily affects anti-gravity muscles (i.e. the Quadriceps), leading to atrophy (Edgerton et al., 1975; Maier et al., 1976; Booth et al., 1982; Spector et al., 1982; Witzman et al., 1982; Musacchia et al., 1983), and as muscle size is directly correlated with force output (Burkholder et al., 1994; Lieber et al. 2001, 2011), ICU patients tend to show muscle weakness at discharge. Additionally, it is possible to measure the fatty infiltration of muscles, i.e. how much of a muscle consists of fat (Doro et al., 2009). Further, it has been shown that critical illness may result in an increase in intramuscular lipids, or increased muscle fat fraction associated with muscle wastage (Caesar et al., 2013). This decrease in muscle quality may impact functional ability. Dirks et al. (2014) showed the preservation of anatomical features does not necessarily preserve function, due to neuro-muscular degeneration being associated with immobility. As a result, it is important to take into consideration both anatomical and functional abilities of patients following ICU in order to study patient recovery.

Recovering ICU patients may require a lengthy rehabilitation process, yet some muscles tend to be resistant to increased rehabilitation (Griffith et al., 2016). Walsh et al. (2015) showed that increasing levels of post-ICU rehabilitation did not improve the physical recovery of patients but did improve patient satisfaction. However, pre-immobilization activity was shown to negate immobility based weakness (Appell et al.,1986). A factor which impacts the length of recovery is a systemic inflammatory process, (Griffith et al., 2016), interrupting the pathophysiological process of muscle recovery in the first three months following discharge. An additional factor which impacts post-ICU recovery is unplanned early hospital readmission (Donaghy et al., 2018). Up to

25% of patients required rehospitalisation following ICU (Lone et al., 2016), making the study of healthy ICU recovery challenging.

Muscle contractures, or muscle shortening, is another potential consequence of periods of immobility (Dittmer et al., 1993; Mollinger et al., 1993; Souren et al., 1995; Trudel et al., 2000; James et al., 2001; Herridge et al., 2003; Laneuville et al., 2007; Winkelman et al., 2007) which can limit muscle function. Sinkjaer et al. (1988) suggested that reduced muscle range could also increase muscle stiffness. Clavet et al (2008) showed that due to prolonged immobility of ICU patients, joint contractures prevalence was 34%. Souren et al., (1995) reported that muscle contracture showed a highly correlated occurrence with functional impairment ($r=0.70$; $p<0.001$). The reduction in muscle length and decreased muscle strength may result in further muscle damage during forced lengthening (Lieber et al., 1993).

ICU-AW affects more than half of ICU patients and is therefore of great clinical interest (Vincent et al., 2009). Magnetic Resonance Imaging and Magnetic Resonance Elastography (MRE), enabled us to study the pathophysiology of thigh muscles in patients following ICU admission. This study aimed to obtain images of muscle cross-sectional area (CSA) and muscle stiffness (kPa) of ICU patients at discharge and following a recovery period of convalescence, in addition to functional ability and muscle fat fraction. We hypothesize that both muscle size and stiffness will decrease following time in ICU, primarily in anti-gravity Quadriceps muscle group. It is also expected that there will be an increase in muscle size and partially in stiffness following convalescence, however function may still be limited due to potential neuromuscular degeneration.

4.3 Methods

4.3.1 Methodological Overview

Scan data was compared between healthy individuals and patients at the time of discharge from ICU. Scan data allowed for quantification of muscle CSA and |G*|, to measure the effects of immobility during time in critical care. An important aspect of this methodology was also to measure the degree of recovery after convalescence, with the comparison of scan data at discharge and following recovery time.

4.3.2 Participants

Ethical approval for this study was obtained from the South East Scotland Research Ethics Committee (Reference: 165265). Data was obtained for 9 ICU patients (Age: 47.56 [±14.77] years; Mass: 82.78 [±19.45] kg) who had been mechanically ventilated for 48 hours or more and had a Rivermead Mobility Index of 14 or above and were due to be discharged. Five ICU patients (47.00 [±12.29] years; 82.40 [±22.21] kg) were also imaged following a period of convalescence (110 [±15] days) and a home physiotherapy plan (Appendix I), of which four were present for two scans. As a result, there were two time points for scans, one at time of discharge and a second if a patient was able to attend following convalescence. For patients, Acute Physiological and Chronic Health Evaluation II (APACHE II) was performed, with additional measures of Functional Comorbidity Index (FCI) and number of days in ICU. All patients gave written informed consent. In addition to this, data was obtained for 10 age and mass matched healthy controls (47.90 [±14.04] years; 85.01 [±14.58] kg).

4.3.3 Data Acquisition, Processing, and Image Analysis

Methods of image acquisition and processing were previously outlined in section 2.4.1. Imaging parameters for an 80 second scan duration consisted of TR = 1600ms, TE = 54ms, FOV = 230mm x 230mm, for five contiguous 2.5mm x 2.5mm x 2.5mm^3 isometric slices, which resulted in an image matrix of 93 x

93. Data processed through ESP consisted of reduced noise in the individual MRE images and the combination of information from several actuation frequencies is used as a basis for presenting the resulting elastograms with an increased pixel density from 93 x 93 to 368 x 368. Region of interest (ROI) measurements were taken for |G*| (kPa) and muscle cross-sectional area (CSA). For data visualisation of participant group images, a 'Moving Least Squares' (Schaefer et al., 2006) algorithm was used to co-register each participant to a template image in ImageJ (Rasband, 1997). Functional measures were also obtained from patients, these including a shuttle walk test and a hand grip strength test. The shuttle walk test involves walking between two points, each 10 metres apart, with a decreasing amount of time allowed to reach each end.

4.3.4 Statistical Analysis

Statistical comparison of ROI measurements was analysed using a one-way ANOVA between healthy controls and discharged ICU patients, with a post-hoc analysis used to identify muscles groups most prone to atrophy. A repeated measures analysis was performed for patients who were able to attend both an initial and second scan. All comparative descriptive data was expressed as mean ± standard deviation. Individual elastograms for individual controls and patients found in Appendix II.

4.4 Results

4.4.1 Immobility Pathophysiology

Normal distributions were observed for patient age and mass as shown through a non-significant Kolmogorov-Smirnov test (Age: p=0.200; Mass: p=0200). Muscle |G*| (M=1.40 kPa, 95% CI[1.19, 1.61]) and muscle CSA (Overall: M=104.97cm^2, 95% CI[93.77, 116.17; Individual: M=8.76cm^2, 95% CI[7.92, 9.60]) were measured with age (M=47.74 years old, 95% CI[41.00, 54.48]) and

mass (M=83.95 kg, 95% CI[75.95, 91.96]) between groups of discharged ICU patients and healthy controls (Figure 4.1).

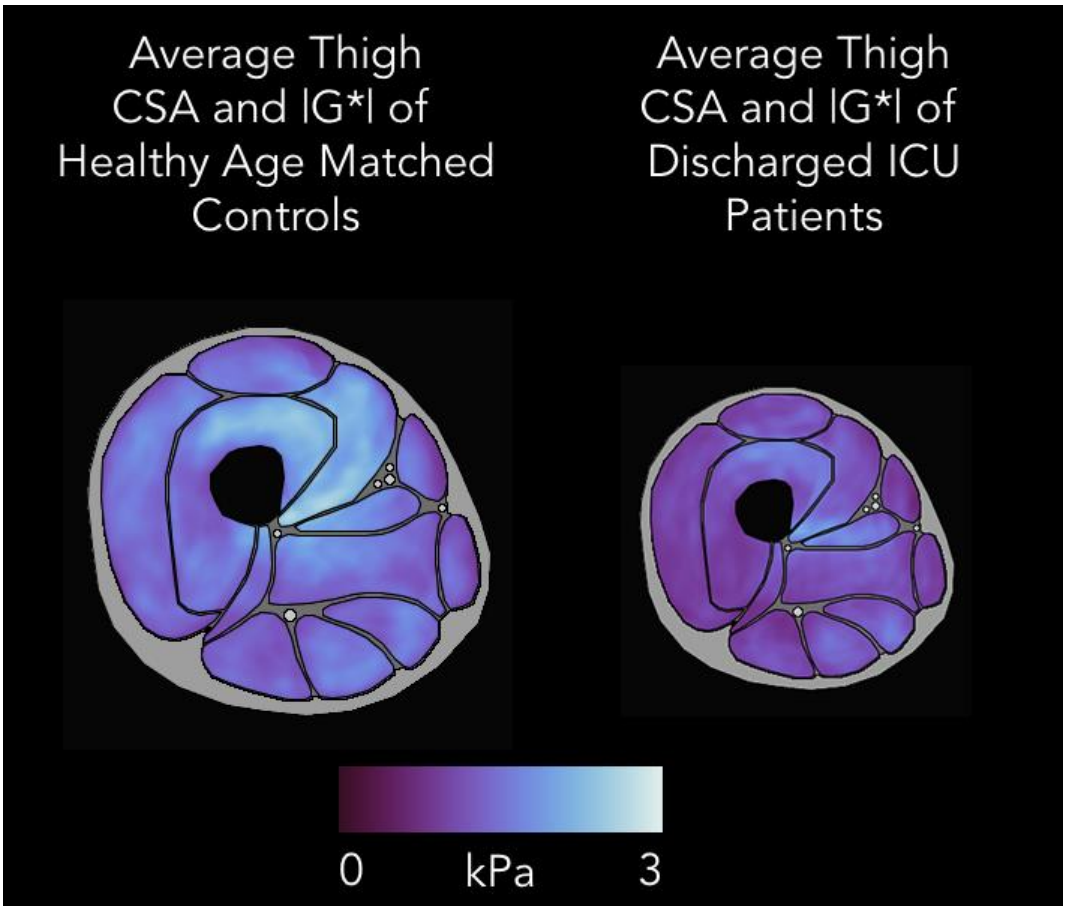

Figure 4.1. Differential in muscle |G*| between the two groups, with CSA of discharged patients visualised by a change in zoom factor based on overall CSA in comparison to healthy controls.

Discharged ICU patients showed a significantly lower thigh muscle CSA in comparison to healthy controls (91.53 [±14.73] cm^2 vs 117.07 [±23.33] cm^2; 22%; p=0.012; Figure 4.2). There was also a significant difference in the size of muscle groups between the participant groups (F[3,68]=6.10, p<0.001). A Tukey post-hoc test identified the quadriceps as the most atrophic muscle group between healthy controls and discharged patients (64.26 [13.63] cm^2 vs 46.46 [±7.86] cm^2; -28%; p<0.001). A further Tukey post-hoc of the quadriceps identified the vastus lateralis (Controls: 21.70 [±5.43] cm^2 vs 15.56 [±4.81] cm^2; -29%; p<0.001) and vastus medialis (Controls: 18.09 cm^2 vs 11.93 cm^2; -34%; p=0.001) as the most atrophied individual muscles in ICU patients.

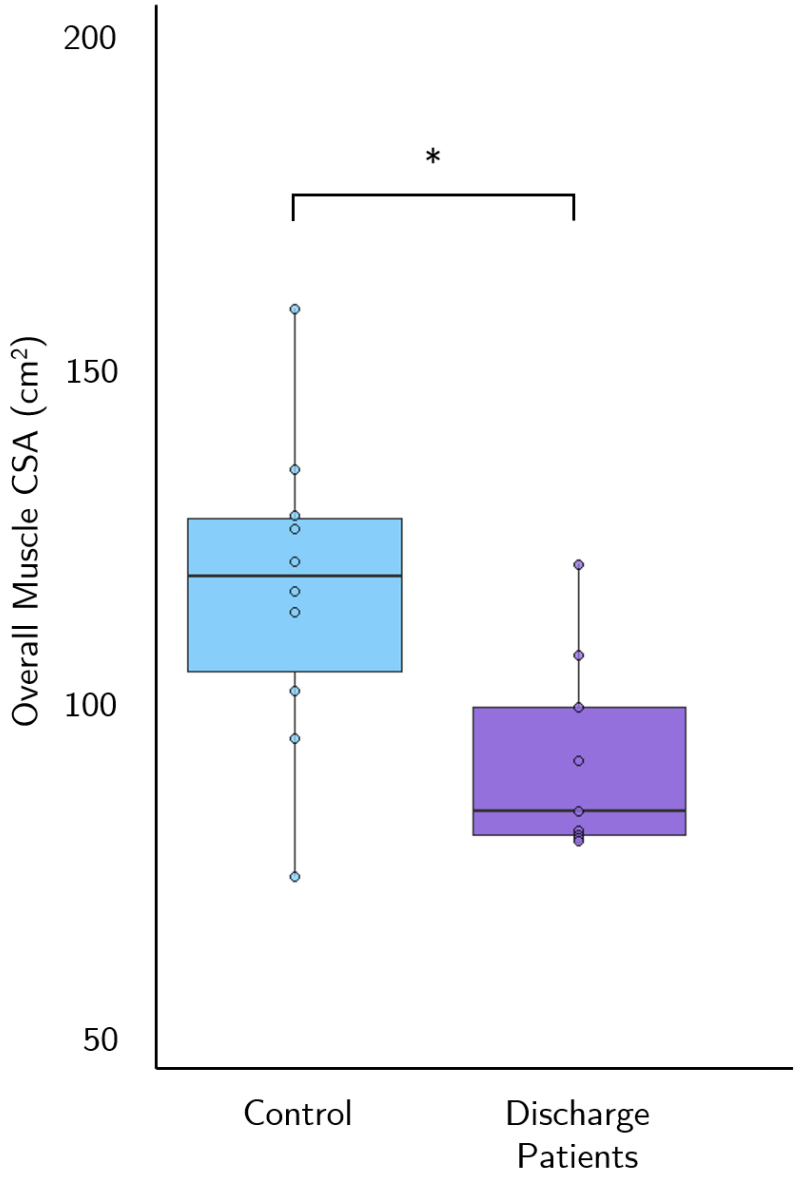

Figure 4.2 Thigh CSA differences between healthy controls and discharged ICU patients. '***' ≤ 0.001, '**' ≤ 0.01, '*' ≤ 0.05

Similarly, |G*| was examined between groups to identify muscles prone to change in the mechanical properties of muscle following immobility (Figure 4.3). Overall muscle |G*| observed as lower in discharged ICU patients in comparison to healthy controls (1.15 ±[±0.25] kPa vs 1.63 [±0.45] kPa; F[1,17]=7.92, p=0.012). The quadriceps muscle group showed significantly decreased |G*| in comparison to healthy controls (1.12 [±0.29] kPa vs 1.73 [±0.54] kPa, p=0.039). The discharged patients (1.15 [±0.37] kPa) showed a -26% lower average muscle |G*| than controls (1.56 [±0.56] kPa), with this being a significant difference in average muscle |G*| (F[1,226]=42.02, p<0.001). A Tukey post-hoc test identified the |G*| of vastus medialis as particularly decreased (-39%; p=0.022) in ICU patients (1.29 [±0.31] kPa).

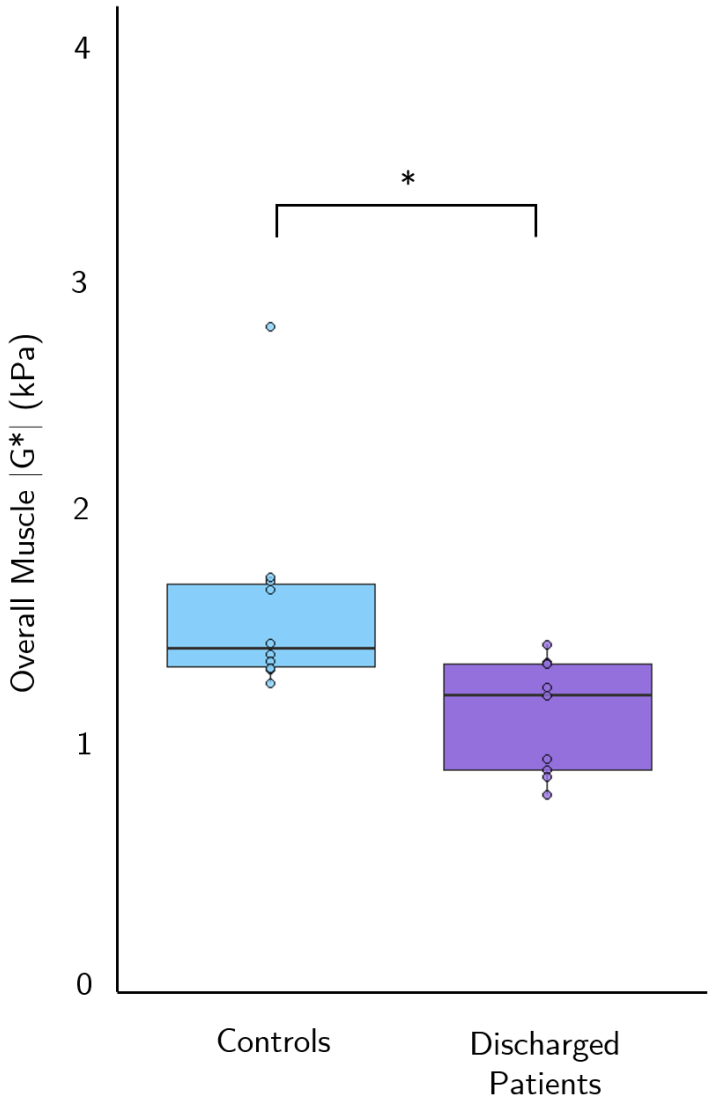

Figure 4.3 Average muscle |G*| differences between healthy controls and discharged ICU patients. '***' ≤ 0.001, '**' ≤ 0.01, '*' ≤ 0.05

Following this, exploratory analysis revealed a difference in the relationship between the mechanical properties and morphology of the vastus medialis between groups. |G*| and CSA were strongly correlated in healthy controls (r[8]=0.76, p=0.011; Figure 4.4) whereas this association was not observed in discharged ICU patients, (r[7]=-0.38, p=0.312).

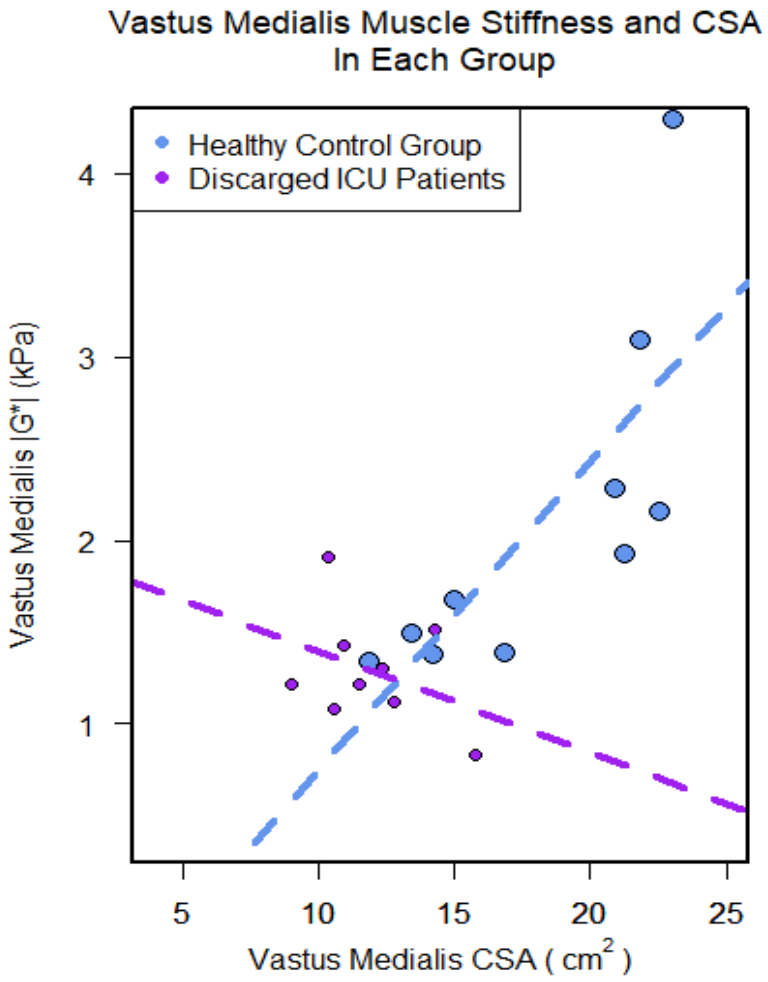

Figure 4.4. Vastus Medialis relationship between CSA and |G*|, with a significant correlation in healthy controls (r=0.76; p=0.011) and a non-significant in ICU patients (r=-0.38; p=0.312).

4.4.2 Muscle Fat Fraction

Quadriceps fat fractions were also obtained for discharged ICU patients and healthy controls. The quadriceps showed significantly greater percentage of fat infiltration for discharged patients in comparison to healthy controls (3.49% vs 1.97%, Mean difference: 1.52%, 95% CI[0.60, 2.44]; p=0.004), with this also being the case for individual muscles including vastus intermedius (3.01% vs 1.97%; Mean difference: 1.05, 95% CI[0.24, 1.85]; p=0.010), vastus lateralis (4.35% vs 2.10%; Mean difference: 2.25, 95% CI[0.61, 3.89]; p=0.010), and vastus medialis (3.41% vs 2.03%; Mean difference: 1.37, 95% CI[0.33, 2.41]; p=0.010). There was no significant difference between groups for rectus femoris fat fraction (p=0.110).

4.4.3 Physical Functions at ICU Discharge

Physical functionality was also quantified, with comparison of hand grip strength and shuttle walk distance between discharged ICU patients and healthy controls. The hand grip strength was significantly lower in discharged ICU patients in comparison to healthy controls (21.8kg vs 41.2kg, Mean difference -19.4kg, 95% CI[-23.9,14.8]; p<0.001), with this also being the case for the shuttle walk test (120m vs 842m, Mean difference: -721m 95% CI[-1070, -373]; p<0.001). Further, muscle fat fraction was negatively correlated with the shuttle walk distance (r=-0.61, 95% CI[-0.82, 0.27], p=0.002).

4.4.4. ICU Recovery Case-Studies

As previously highlighted, measuring the recovery from ICU can be difficult. This is exemplified with only 4 of the discharged patients being able to return for a second scanning session following convalescence. Of the returning patients, physical functionality, mass, age, muscle CSA, and |G*| will be described.

Patient One was between the ages of 50-59 years of age and a BMI of 31.1 at the time of ICU discharge (Figure 4.5). A diagnosis of respiratory infection was recorded, with an APACHE II score of 16 and an FCI score of 3. FCI

comorbidities included depression, hearing impairment and obesity. As a result, Patient One was in ICU for 11 days. Alongside this, overall thigh muscle CSA was measured at 81.01cm^2 (individual muscles 6.76 [±4.53] cm^2), with average muscle |G*| measured at 1.03 [±0.13] kPa. Following 96 days of convalescence Patient One returned for a second scan where mass had decreased to 87kg. However, overall thigh muscle CSA had increased by 62% to 130.86cm^2 (Individual muscles: 10.88 [±8.08] cm^2), and |G*| increased by 27% to 1.31 [±0.27] kPa.

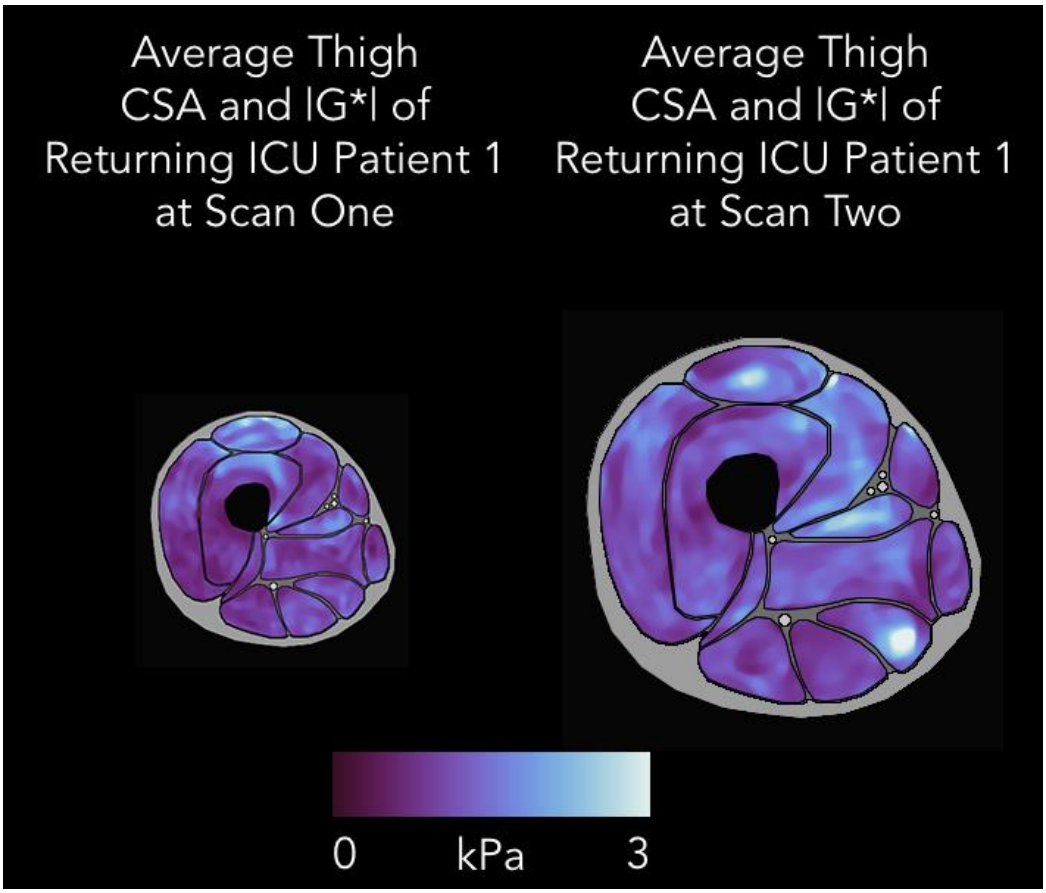

Figure 4.5. Change in |G*| and CSA in Patient One between time of discharged and second scan following convalescence.

Patient Two was in the age range of 40-49 and a BMI of 19.9 at the time of ICU discharge (Figure 4.6). An APACHE II diagnosis of sepsis was recorded, with an APACHE II score of 26, and an FCI score of 1. Patient Two showed a single comorbidity of asthma. Overall thigh CSA was 80.35cm^2 (Individual

muscles 6.72 [±4.29]cm^2), with an average muscle |G*| of 0.86 [±0.18] kPa. Patient Two required slightly longer in convalescence, with the second scanning session being 119 days after the first. On return mass had increased to 70kg, as well as a 21% increase in overall muscle CSA (97.51 cm^2; Individual muscles 8.12 [±5.45]cm^2) and 45% increase in average muscle |G*| (1.25 [±0.32] kPa).

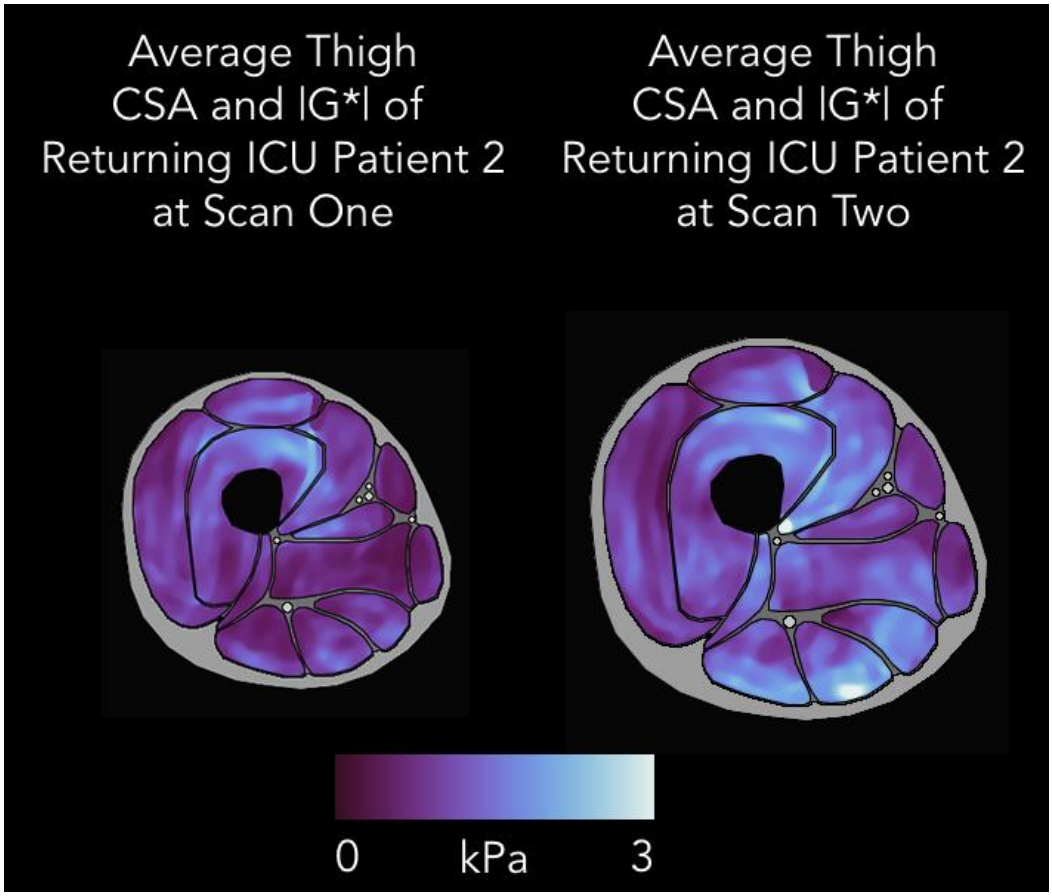

Figure 4.6. Change in |G*| and CSA in Patient Two between time of discharged and second scan following convalescence.

Patient Three was between the age range of 50-59 and a BMI of 21.8 at the time of the first scan (Figure 4.7). A diagnosis of cardiogenic shock was recorded, with an APACHE II score of 17 and no comorbidities. For Patient Three the whole thigh CSA was 80.06cm^2 (Individual muscles: 6.69 [±4.42] cm^2) with an average |G*| of 1.25 [±0.33] kPa. Following convalescence of 98 days, mass had increased by 2.9kg to 80kg. In addition to this, whole thigh

CSA had increased by 69% to 135.46cm^2 (individual muscles 11.29[±8.28] cm^2), and average |G*| had increased by 25% to 1.56 [±0.25] kPa.

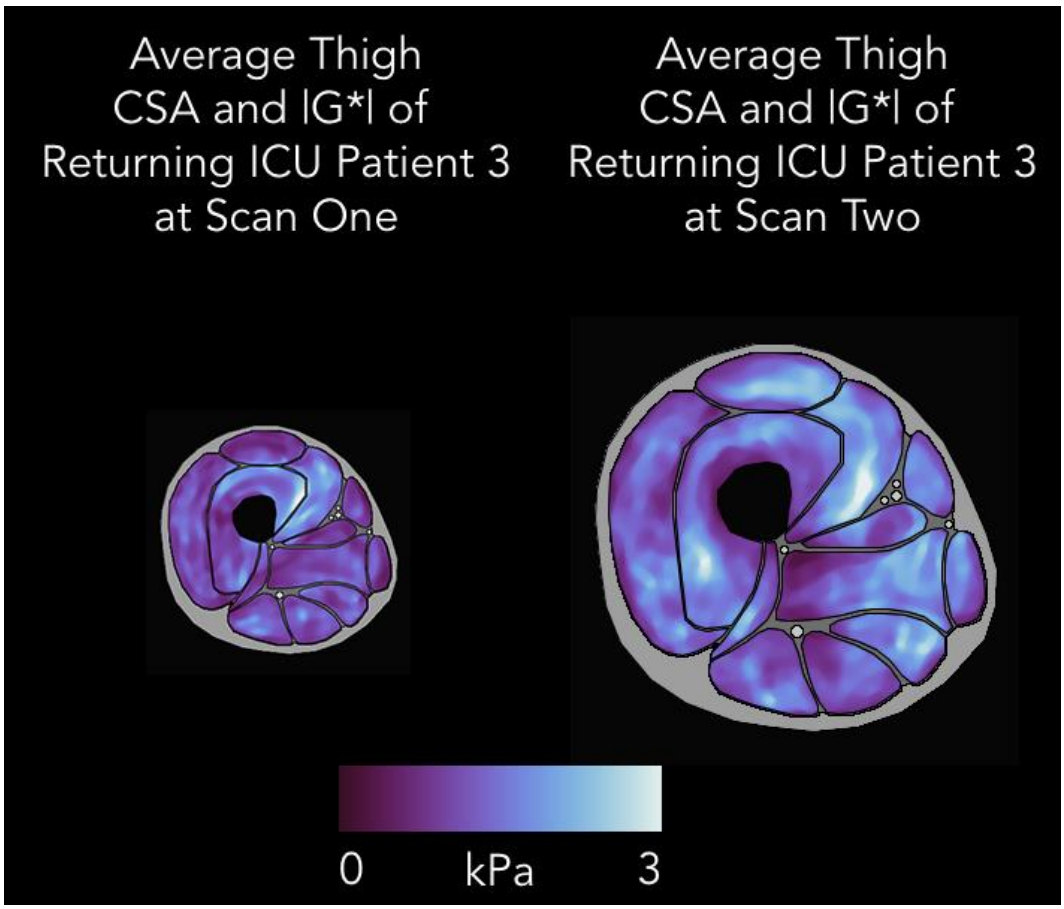

Figure 4.7. Change in |G*| and CSA in Patient Three between time of discharged and second scan following convalescence.

The final patient, Patient Four was aged between 50-59 and had a BMI of 35.7 at time of discharge (Figure 4.8). A diagnosis of Asthma was recorded, with an APACHE II score of 17 and an FCI of 3. Additional comorbidities included Asthma, an anxiety disorder and obesity. Patient Four required the longest time for convalescence, totalling 125 days. At discharge of a weight of 100kg, Patient Four initially showed an overall thigh CSA of 107.18cm^2 (Individual muscles: 8.94 [±5.54] cm^2), and an average |G*| of 1.27 [±0.24] kPa. Following convalescence, weight had increased to 117kg, the greatest increase in mass also. Overall thigh muscle CSA increased by 29% to 138.67cm^2 (Individual

muscles: 11.56 [±7.00] cm^2) and muscle |G*| increased by 96%, the greatest of all returning patients to 2.49 [±0.80] kPa.

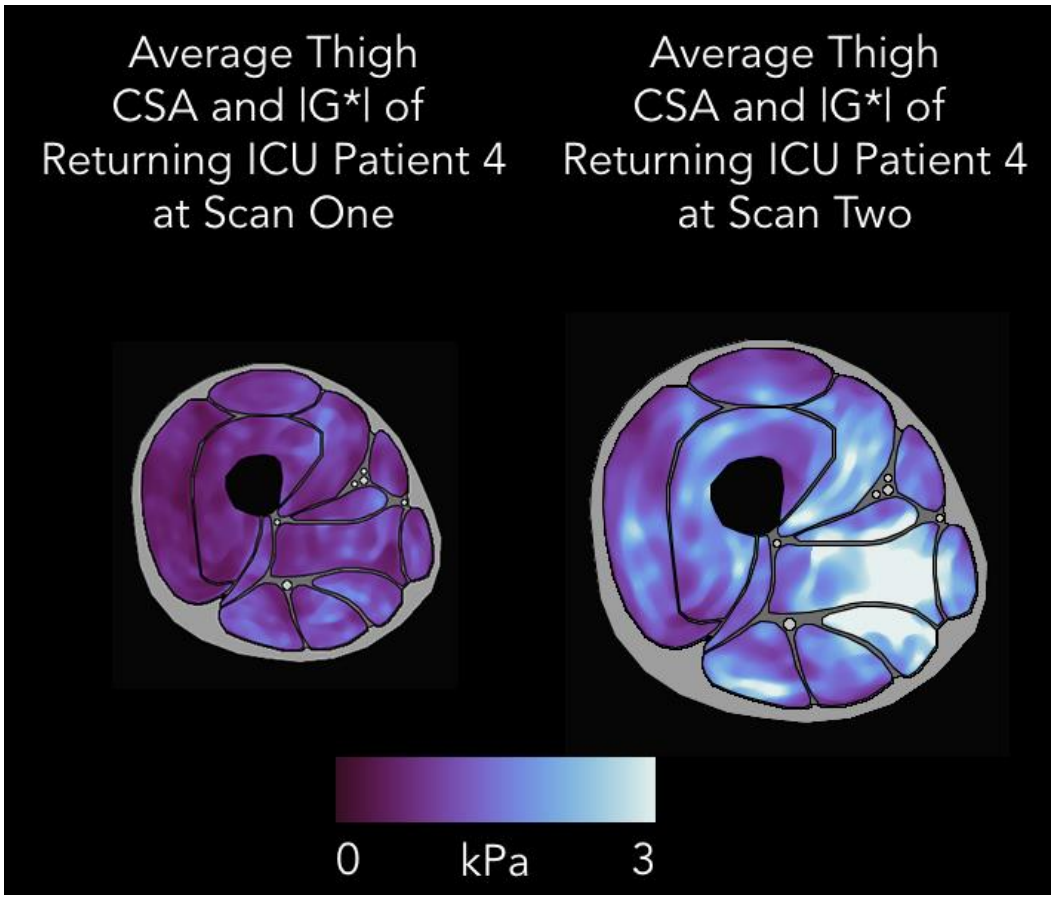

Figure 4.8. Change in |G*| and CSA in Patient Four between time of discharged and second scan following convalescence.

4.4.5 Recovery of Patients

Scan data from the returning patients were then averaged (Figure 4.9). Between scans, average muscle CSA increased significantly ($F[1,47]=30.73$, $p<0.001$), with average muscle CSA being 7.27 [±4.67] cm^2 and increasing by 44% to 10.47 [±7.19] cm^2. Overall thigh CSA in returning ICU patients (n=5) was greater than the group of patients at discharge (Return: 120.48 [±20.08] cm^2 vs Discharge: 91.53 [±14.73]cm^2; Figure 4.10). Likewise, |G*| also increased significantly ($F[1,47]=46.41$, $p<0.001$) by 50% from 1.10 [±0.28] kPa to 1.65 [±0.67] kPa (Figure 4.11). Each muscle group increased significantly in |G*|

including quadriceps (+40%; p<0.001), medials (+46%; p=0.012), hamstrings (+49%; p=0.002) and the adductors increasing the most (+76%; p=0.024). Whereas only the hamstrings (+32%; p=0.004), medials (+35%; p=0.003), and quadriceps (+41%; p=0.001) muscle groups increased significantly in CSA. In addition to this, physical function was examined at the time of scan one and scan two. There was a significant increase in hand grip strength in patients (Mean difference=11.5kg 95% CI[3.5, 19.5]; p=0.010) from scan one (M=20kg) to scan two (M=32kg). However, there was a non-significant change in ability of shuttle walk distance (Scan one: 147m vs Scan two: 123m; Mean difference: -24 95% CI(-212, 164.2), p=0.770).

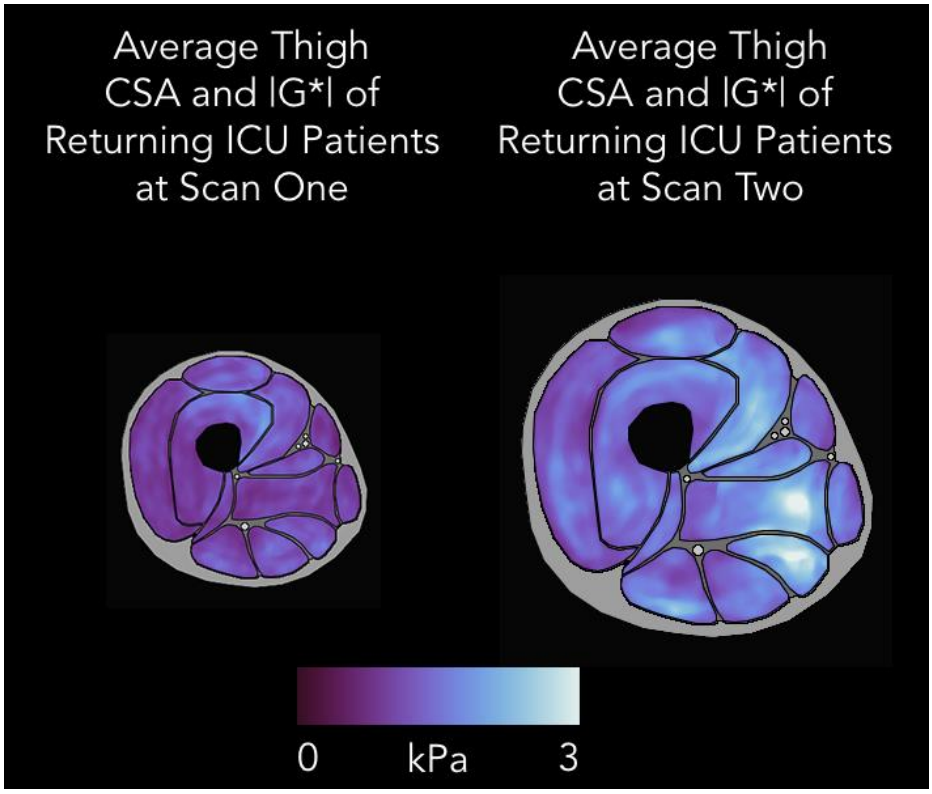

Figure 4.9. Average change in |G*| and CSA in returning patients between time of discharged and second scan following convalescence.

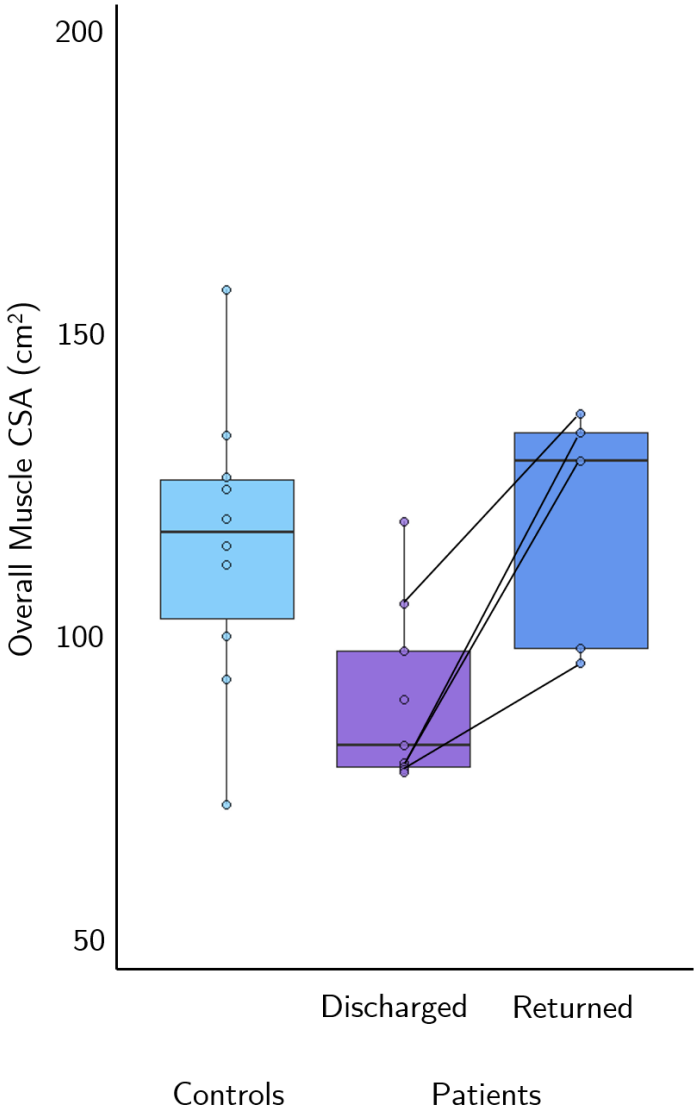

Figure 4.10. Comparison of overall muscle CSA between groups

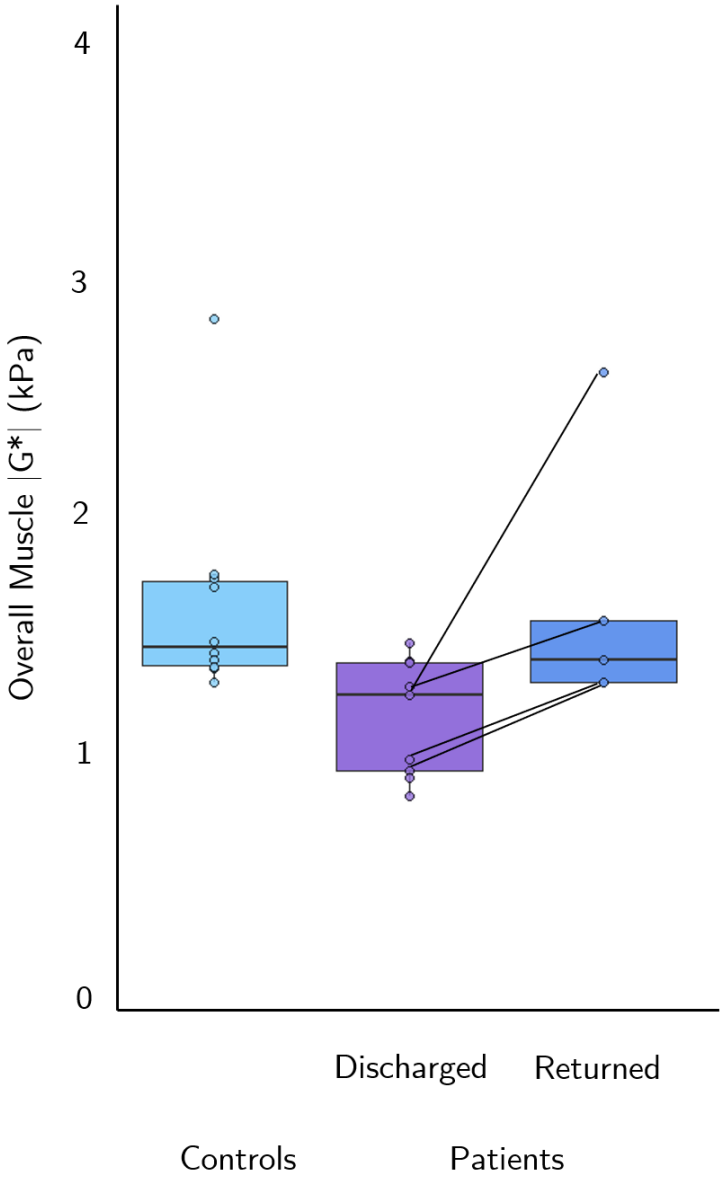

Figure 4.11. Comparison of average muscle |G*| between groups

4.5 Discussion

This study set out to investigate changes in the size and stiffness of thigh muscles of ICU patients at discharge and following recovery and compare this to healthy controls. This chapter showed support for the hypothesis of ICU patients showing a reduced size and stiffness in muscles, with the quadriceps being primarily affected by atrophy. The decrease in both size and stiffness of the quadriceps muscle in ICU patients suggest an anatomical basis for ICU-AW, as muscles with a greater level of force production have a greater magnitude of CSA (Lieber et al., 1989; 2001; 2011). Further, functional impairment was still present for ICU patients and was correlated with the percentage of fat observed within the muscles.

Following convalescence, the adductors had increased in |G*| more than other muscle groups, however there was no significant increase in CSA (as observed with other muscle groups). This is potentially a sign of contracture, as previous research showing ICU patients are prone to muscle contracture (Clavet et al., 2008), however with the current data now including sagittal MRI images, this is a speculative inference of the results. Previous work investigating the effects of time within ICU show that prolonged ICU immobility can alter muscle morphology (Tabary et al., 1972; Seymour et al., 2009), function (Fischabach et al., 1969; Duchateau et al., 1987; Kortebein et al., 2007; Griffiths et al., 2010), and subsequent use (Kortebein et al., 2008). Lieber et al. (1988) showed that immobilized muscles atrophy particularly when immobilized in a shortened position, with this also negatively impacting force generation. Shortened muscles increases in stiffness due to an increase in epimysial and perimysial connective tissue as a consequence of immobilization (Lieber et al., 1988; Appell et al., 1986; Tabary et al., 1972; Witzmann et al., 1982), which has also been shown to decrease mobility (Gossman et al., 1986). As contracture leads to a greater amount of tissue in a smaller overall volume, tissue mobility is restructured, something which is supported by the lack of improved performance in the shuttle walk test in returning patients. These factors, as well as previously discussed neuro-muscular degeneration are likely

to have impaired patient physical ability, however further work is required to full support this current speculation.

The vasti muscles within the quadriceps have very similar architecture, with the only discernible difference being the fibre type distribution, and whether they are bi-articular or mono-articular (Lieber et al., 1988, Wickiewicz et al., 1983, Powell et al., 1984). Lieber et al. (1988) suggests that atrophy prone muscles are those that fit the criteria of: i) anti-gravity muscle, ii) mono-articular, iii) large number of type I fibres. The individual muscles that atrophied most in this present study were vastus medialis and vastus lateralis, supporting previous animal research by Lieber et al. (1988) and human research by Edgerton et al. (1975). Vastus medialis has equal amounts of type I (slow contractile properties) and type II (fast contractile properties) muscle fibres (Armstrong et al., 1982; Snow et al., 1982; Aagaard et al., 2004), with vastus medialis being a vital anti-gravity muscle (Jolesz et al., 1981; Pette et al., 1985; Salmons et al., 1981). However, research has shown that exercise can negate the effects of immobility-based atrophy (Kawakami et al., 2001). However, recovery of muscles following immobilization can be impaired due to age (Zarzhevsky et al., 2001).

This investigation is the first of its kind to utilise MRE to study the impact that ICU has on the musculoskeletal system in terms of physical, mechanical and functional attributes. Whilst there is only a limited number of patients, this research offers key clinical insight into the recovery of patients. The study was limited in the coverage to an axial slice and not of muscles from origin to insertion. This is largely a problem due to the length of the thigh in relation to available radio frequency coils, which would require multiple table positions. Newer hardware and software solutions could enable future MRE investigations to cover the entire muscle system of the thigh. Further, a confound impacting the results is the clinical rational for why individuals were in ICU. In the case of sepsis, a common comorbidity for ICU patients which can take a significant time for recovery (Hodgson et al., 2018), there may be varying lengths for recovery periods in comparison to respiratory difficulties, which may have also

been impacted by the age of the patients. It is also important to note that the patients which returned for a second scan had differing APACHE II diagnoses, highlighting the complexity of conducting recovery research within ICU. Finally, further research should also incorporate the measurement of MVC for patients, the range of motion (ROM), as well as more time points during the measurement of recovery.

In conclusion, we have shown that the quadriceps are particularly prone to the atrophic effects of immobility, with the anatomical consequences of ICU subsequently impairing physical function. The use of MRE showed that at discharge muscle |G*| and size were lower than healthy individuals, and that after a period function had not recovered to healthy levels. These findings are the first time MRE has been implemented to study to impact and recovery from ICU and show that imaging muscle stiffness may offer greater pathophysiological insight of muscles than imaging muscle size alone.

Chapter Five

Identification of Muscle Damage Through Mapping of Localised Residual Stiffness Following Injury

5.1 Chapter Five Overview

So far Chapters Three and Four have provided pilot work to explore the passive mechanical change of muscle through age and disease. Contrary to exploring the lack of muscle use resulting in decreases muscle stiffness in the previous chapter, this chapter examines the changes in muscle stiffness when muscles are used to the extent of injury. This chapter investigates the changes in the mechanical properties of tissue as a result of injury, and whether there are resulting residual increases in muscle stiffness. Data from a previous study is re-analysed to elucidate why some individuals were more prone to injury than others. It is shown here that the method of pixel-wise mapping reveals a localised differential in muscle stiffness increase as a result of muscle damage between two injury groups. As a whole, this chapter shows that MRE can be used to visualise changes in muscle stiffness following muscle injury in order to identify regions of increased stiffness which may be used to explain injury severity. Chapter Five explores the question: i) Can localised residual muscle stiffness increases following injury offer insight into why some individuals more prone to injury than others? ii) Is there an observable relationship between muscle function (i.e. MVC) and anatomical features (i.e. CSA and |G*|)?

5.2 Introduction

The MRE study reported here is an extension of work previously published by Kennedy et al. (2017) in which MRE was used to measure changes in muscle stiffness produced by an experimental Exercise Induced Muscle Damage (EIMD) protocol. Participants completed a personally tailored protocol comprising repetitive eccentric extension of the lower leg against a restraining force produced by an isokinetic dynamometer (System 3, Biodex Medical Systems, New York, USA). The EIMD protocol was designed to produce EIMD in the quadriceps, with |G*| measurements analysed with a Region of Interest (ROI) analysis revealing a significant increase in stiffness. Furthermore, in approximately half of subjects, oedema was present in the quadriceps, which

was interpreted as resulting from a build-up of water in tissue (McMahon et al., 2010), due to production of free calcium (Ca^{2+}), a consequence of muscle fibre strain (Lieber et al., 1993; Lieber et al, 1999).

Due to having a biarticular connection across two joints (i.e. hip and thigh) the rectus femoris is particularly vulnerable to damage caused by forced flexion of the lower leg (Lieber et al., 1991; Allen et al., 2005) during eccentric knee extensions of the EIMD protocol. The cause of half of the participants incurring a more significant degree of injury is still to be addressed. It is important from a clinical perspective to explore biomechanics of quadriceps muscles as they have an integral role in movement, and are primarily affected by activity, or lack of, as shown by the next chapter.

Barnhill et al., (2013) performed pixel-by-pixel statistical mapping of MRE elastograms before and after knee extension, a technique analogous to fMRI studies within the brain. This technique revealed a significant increase in stiffness of the quadriceps and identified muscles which were predominantly engaged. Using this technique, Barnhill et al. showed specific regions of increased muscles stiffness and was able to map these results on an elastogram of the thigh. This technique may be useful in the measurement of residual stiffness following injury in specific regions of muscles, compared to the changes observed by Barnhill et al. (2013). By identifying sights of residual increased stiffness may offer validation in the use of MRE to measure muscle damage. The objective of the new analysis reported here is to utilize pixel-wise statistical mapping to determine the significant changes in residual muscle stiffness (increased static muscle stiffness following injury) as a proxy to reveal the sites of muscle damage following the EIMD protocol. We hypothesise that those with increased injury (observed with oedema) will have had a greater loss of contraction strength (MVC) following the EIMD protocol. It is expected that the differential pattern of stiffness increases will inform on a potentially different muscle engagement strategy being used by the two groups of participants.

5.3 Methods

5.3.1 Methodological Overview

Healthy active young adults were initially recruited to participate in an EIMD task, elicited through repeated knee extensions against an overwhelming downward force. MVC was measured before and immediately after the protocol, with CSA and |G*| of muscles being measured before and three days after the protocol. Registering scan data to the same template allowed for pixel-wise analysis of |G*| changes between scan one and scan two, identifying regions of increased residual stiffness because of the task. The presence of oedema on a T2 MRI scan determined grouping of participants and resulting in comparison of localised |G*| differences between injury groups for elastograms.

5.3.2 Participants

Twenty healthy male subjects participated in the original study (Kennedy et al., 2017) following informed consent and ethical approval for the study. However, five participants were removed from the analysis, one participant due to incidental finding and four as they did not elicit EIMD as measured by reduction in MVC. As a result, there is considerable doubt as to whether they properly engaged in the protocol. Of the 15 remaining participants (M=24.79 [±4.00] years), seven participants formed the no-oedema group. The eight participants which has unexpectedly showed presence of oedema (Figure 5.1) in the quadriceps were assigned to the oedema injury group.

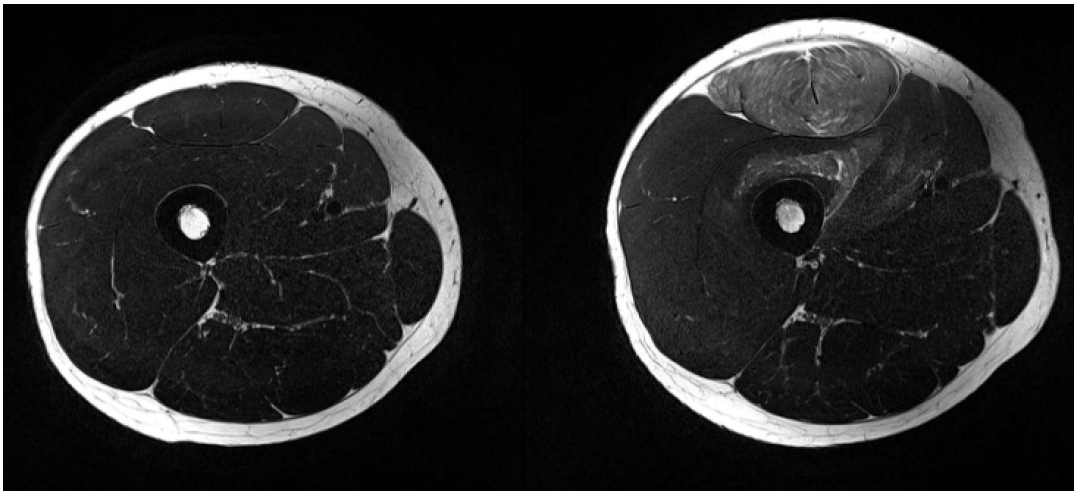

Figure 5.1. T2-weighted MRI scans obtained before (left) and 2 days after (right) the EIMD protocol in a participant who developed Oedema in the Rectus Femoris and Vastus Intermedius muscles of the Quadriceps.

5.3.3 Exercise Induced Muscle Damage (EIMD) Protocol

An Isokinetic Dynamometer (Biodex Medical Systems, USA) was used for the EIMD protocol and a full description of the experimental protocol is given in Kennedy et al (2017). Briefly, individual work targets were set based on the magnitude of the average of three maximal voluntary contractions (MVC) extrapolated to 120%. Participants were securely seated in the Dynamometer (hip angle 90°; Figure 5.2) and resistance started when the Dynamometer arm was at 20° below the horizontal (taken as 0°).

The aim was to resist the downward force of the Dynamometer by performing knee extensions. To perform knee extensions, it is primarily the Quadriceps muscle group which need to be contracted. Gradually the Dynamometer arm overcame the resistance of the participant and moved downwards until it passed 90° (i.e. lower leg vertical) and reached an angle of 110°. This produced a particular forced lengthening of contracted muscles, which may be referred to as eccentric contraction. Once the force of the Dynamometer arm had flexed the leg to 110° the machine reset, with a 10 second rest. The completed EIMD protocol comprised 12 sets of repetitions, in which participants tried to reach their work target in the least number of repetitions possible per set.

Physiological measurements of workload (kJ), number of repetitions, and percentage change in MVC (Nm) were measured.

5.3.4 Image Acquisition

Subjects were scanned using a 3T Verio MRI system (Siemens Medical Systems, Erlangren, Germany) before and two days after the EIMD protocol. On each occasion T2-weighted images were obtained together with MRE images as described in Kennedy et al., (2017). Acquisition parameters included: TE 96msec, TR 4430msec, FOV 200mm x 200mm, voxel size 0.4 x 0.4 x 3mm^3. For MRE images, an actuator cuff was placed anthropometrically (NHANES, 1988) around the thigh (Papazoglou et al., 2006), one third of the distance from the patella tendon to the greater trochanter (Bensamoun et al., 2006). Images were obtained at each of eight phase offsets for vibration frequencies of 25Hz, 37.5Hz, 50Hz and 62.5Hz using a modified Cartesian Echo Planar Imaging (EPI) sequence with additional motion encoding gradients (Klatt et al., 2010, Barnhill et al., 2013). Imaging parameters for five contiguous 2mm x 2mm x 2mm^3 isotropic slices with an FOV of 224mm x 224mm (Kennedy et al., 2017).

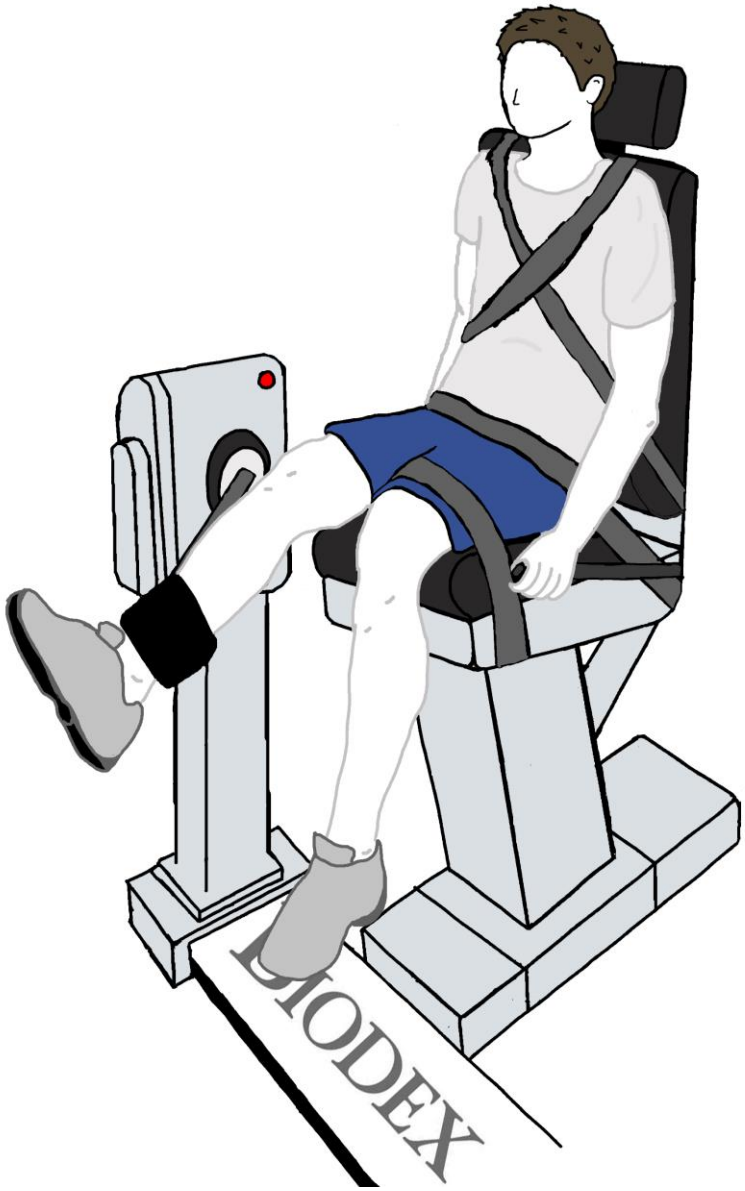

Figure 5.2. Participant experimental set up on Dynamometer.

5.3.5 Image Processing and Analysis

Images were processed through ESP which resulted in the reduction of noise in the individual MRE images and combination of information from several actuation frequencies is used as a basis for presenting the resulting elastograms with an increased pixel spatial resolution of 0.5mm compared to the resolution of 2mm. Of the 15 participants where axial slices were obtained, additional sagittal images were obtained for only 11 participants for rectus femoris (4 no-oedema, 7 oedema), due to the size of rectus femoris and the quality of the

image obtained. A 'Moving Least Squares' (Barnhill et al., 2013; Schaefer et al., 2006) algorithm was used to co-register each participant to a template image corresponding to a single participant in ImageJ (Rasband 1997). This registration was based on a total of 180 anatomically defined points manually plotted on the images for each participant. Scan data was then group and compared on a pixel level in order to identify regions of statistically difference |G*| differences between scans and injury groups.

5.3.6 Statistical Analysis

Firstly, an ROI analysis was performed in order to primarily reveal size and stiffness changes of the thighs through a 2-way ANOVA, followed by Tukey post-hoc testing the different muscle groups. Also, Pearson correlations and linear regressions were performed in order to obtain new insight into the anatomical and mechanical features of muscle. Following this, elastograms before and after injury were then created for individuals of each group, with the pixels within the elastograms being compared statistically. To control for false positives due to multiple comparisons, a 'positive False Discovery Rate' (pFDR) (Storey, 2003; Barnhill et al., 2013) algorithm was performed to identify pixels with statistically significant |G*| increases ($q \leq 25$, $p \leq 0.05$; Ullah et al., 2012). By performing this additional analysis of pixel-wise analysis, in addition to ROI analysis, may offer more precise changes in |G*| changes. Measurements of peak pixel intensity changes as well as average |G*| changes for a significantly highlighted region. Following this, images were compared between the two groups to reveal the impact that injury had on the mechanical properties of the thigh. Individual elastograms for participants in Chapter Five are found in Appendix III.

5.4 Results

5.4.1 ROI Analysis of Muscle Morphology

ROI measurements of muscle CSA were examined between groups, with a Levene's test showing no variance between groups for CSA (F[3,26]=0.26, p=0.851). A one way ANOVA showed there was no difference between whole thigh CSA between injury groups at scan one (p=0.373) or scan two (p=0.297). When comparing average quadriceps CSA, there was no difference in muscle size at scan one between injury groups (No oedema: 12.27 [±5.08]cm^2, Oedema: 12.20 [±5.15]cm^2; p=0.955), however at the time of the second scan, the average thigh of the oedema group was 15% larger than the no-oedema group (No oedema: 19.76 [±11.44]cm^2, Oedema: 23.31 [±11.95]cm^2; p=0.035), and a 91% increase in the oedema group from the first scan.

5.4.2 ROI Analysis of Muscle Mechanical Properties

ROI measurements of |G*| were examined between groups, with a Levene's test showing no variance between groups for |G*| (F[3,26]=0.68, p=0.570). |G*| for the no-oedema group showed an overall decrease between scan one (1.40 [±0.24] kPa) and scan two (1.32 [±0.17] kPa). However, the oedema group showed an increase in |G*| between scans (1.38 [±0.28] kPa vs 1.41 [0.21] kPa]). A multi-variate ANOVA between individual muscle |G*|, time of scans and injury group revealed a significant difference in |G*| between the injury groups and scanning sessions (F[1,356]=5.92, p=0.016). A Tukey post-hoc test revealed that there was a significant difference in average muscle |G*| between groups at scan two (No-oedema: 1.32 [±0.17] kPa vs oedema: 1.41 [±0.21] kPa; p=0.040).

5.4.3 MVC, Workload and Extension Repetitions

The no-oedema group performed an average of 221 [±21] reps resulting in a workload of 4.52 [±1.25] kJ, with the oedema group having performed an average of 276 [±19] reps and a workload of 4.89 [±0.68] kJ. There was a tendency for change between the two injury groups for reps (F[1,28]=4.02,

p=0.055) and no difference for workload (F[1,28]=1.01, p=0.323). The no-oedema group showed a reduction of 24% in MVC following the protocol (Pre: 232 [±53] Nm vs Post 177 [±50]; p<0.001), whilst the oedema group showed a 36% decline in MVC as a result of the protocol (Pre: 294 [±74] vs Post: 188 [±72]; p<0.001). There was also no significant difference between injury groups for pre-EIMD MVC (F[1,13]=3.34, p=0.090) or post-EIMD MVC (F[1,13]=0.12, p=0.731).

5.4.4 Relationship Between Anatomy and Function

The relationship between MVC (M=224 Nm, 95% CI[195, 253]), CSA (Overall M=184.55cm^2, 95% CI[175.66 193.44]; Individual muscle M=16.60cm^2, 95% CI[14.17, 16.60]), and |G*| (M=1.40 kPa, 95% CI [1.35, 1.45]) was examined to investigate the relationship between function, size and stiffness before injury. There were moderate positive correlations with MVC for both CSA (r[13]=0.69; p=0.005) and |G*| (r[13]=0.52; p=0.047; Figure 5.3) of the quadriceps. The combination of both quadriceps CSA and |G*| were strong predictors for participant MVC (R^2=0.70, F[2,12]=13.83, p<0.001).

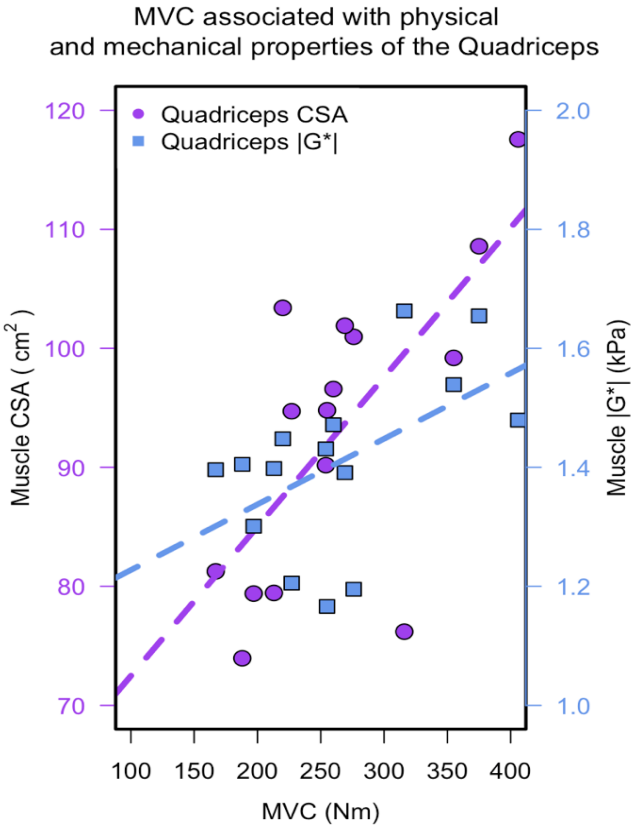

Figure 5.3 Association between function (MVC) and both the muscle size and muscle stiffness. A positive correlation was observed between MVC and muscles CSA (r=0.69; p=0.005), as well as function and muscle |G*| (r=0.52; p=0.047).

5.4.5 Pixel-wise Comparisons of Residual Muscle |G*|

Pixel-wise mapping was performed to identify muscle regions with significantly increased |G*|, for both the axial and sagittal scans. Firstly, within the axial scans, a significant area of effect (regions with significantly increased |G*| at the time of the second scan) of 0.82% for the whole thigh was identified in the no-oedema group. Within the significant pixels, |G*| was 21% greater at the second scan, with a peak pixel increase of +35% identified within the semimembranosus (Figure 5.4). Within the oedema group, a significant area of effect of 3% for the whole thigh was identified. On average there was a 25% increase in |G*| for the oedema group, with a peak pixel value of +58% identified within the rectus femoris. Visual inspection of the locations of significant pixels revealed a differential between injury groups. The no-oedema group showing increased |G*| notably within rectus femoris, Adductor magnus, and semimembranosus, whereas in the oedema groups increased |G*| was identified within rectus femoris, the vasti muscles, adductor magnus, bicep femoris and gracilis.

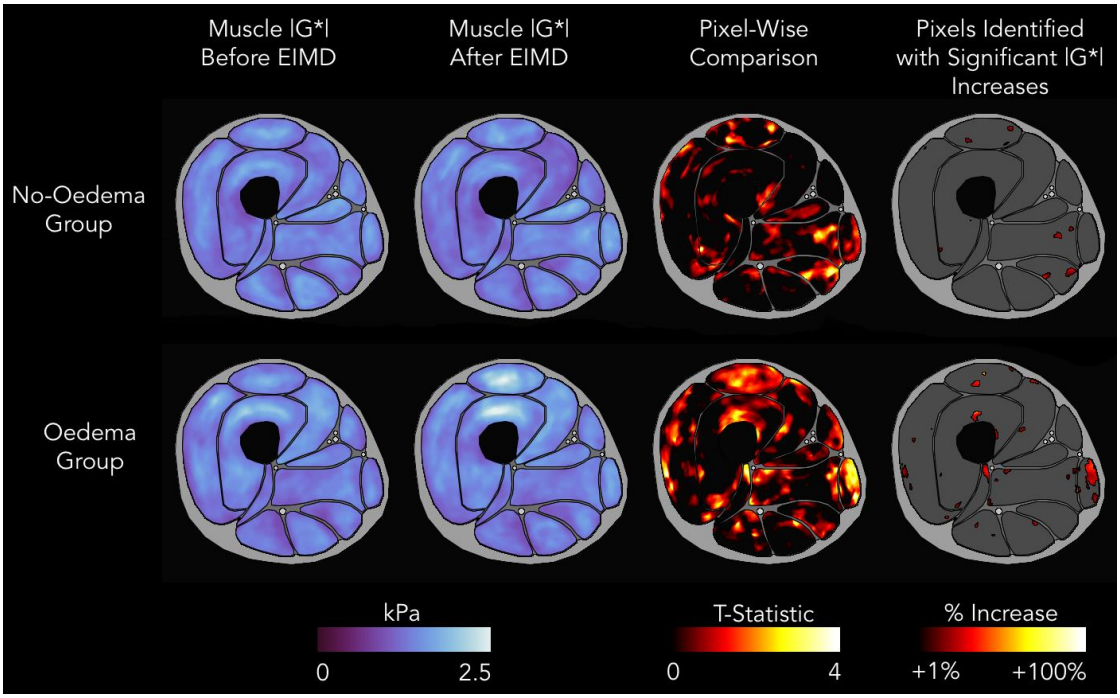

Figure 5.4 Pixel-wise |G*| differences between group averages. Top row showing the no-oedema and the bottom row showing the oedema group. First column showing pre-EIMD, second column the post-EIMD, third column showing the T-Statistic, and finally pixels identified with a significant |G*| increase whilst also showing percentage change.

Following this, post-EIMD muscle |G*| was compared between groups, to identify regions of greater |G*| between the oedema group and no-oedema group. Through this comparison, the oedema group showed a 48% greater |G*| on average, localised to the quadriceps muscles, with a peak pixel |G*| increase of 82% identified within the rectus femoris. Of the muscles identified with greater |G*| in the oedema group, it was the rectus femoris and vastus medialis that showed the greatest differential between groups (Figure 5.5).

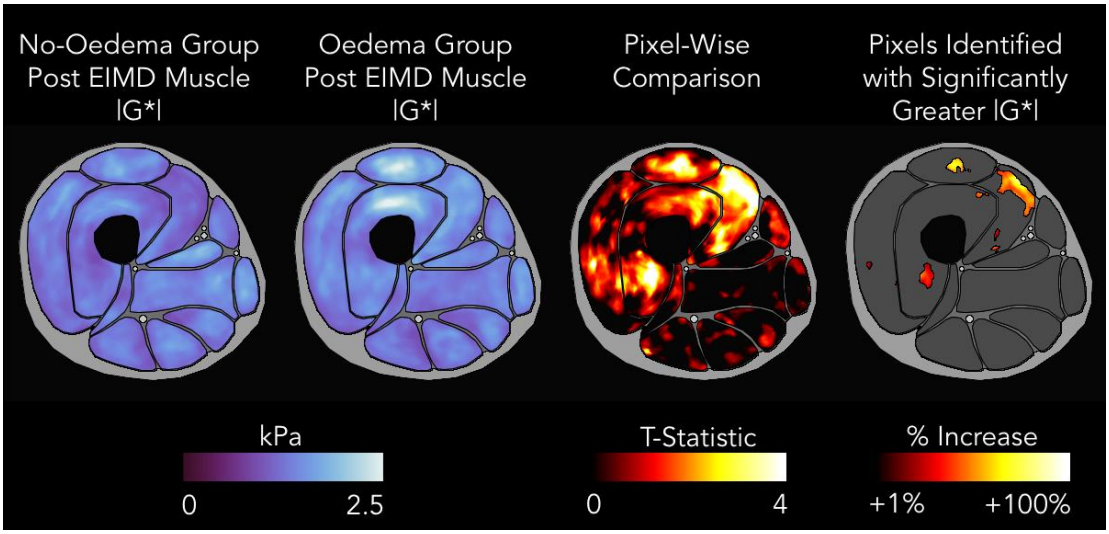

Figure 5.5 Pixel-wise |G*| differences for post-EIMD between group averages. First column showing no-oedema post-EIMD, second column showing oedema post-EIMD, third column showing the T-Statistic, and finally pixels identified with a significant |G*| increase whilst also showing percentage change.

Secondly, regions of significantly increased |G*| were compared between groups for the sagittal slices (Figure 5.6), focussed on the rectus femoris. For the no-oedema group an average |G*| increase of 43% was identified for 8% of the rectus femoris, with a peak pixel increase of 64%, located towards the proximal area of the muscle. However, the oedema groups showed an average |G*| increase of 50%, with a 93% peak pixel intensity located towards the distal part of the muscle. When comparing between injury groups, it appeared that the oedema group had significantly greater damage (average: 33%; peak pixel intensity: 90%) towards the distal musculotendinous junction (MTJ; Figure 5.7).

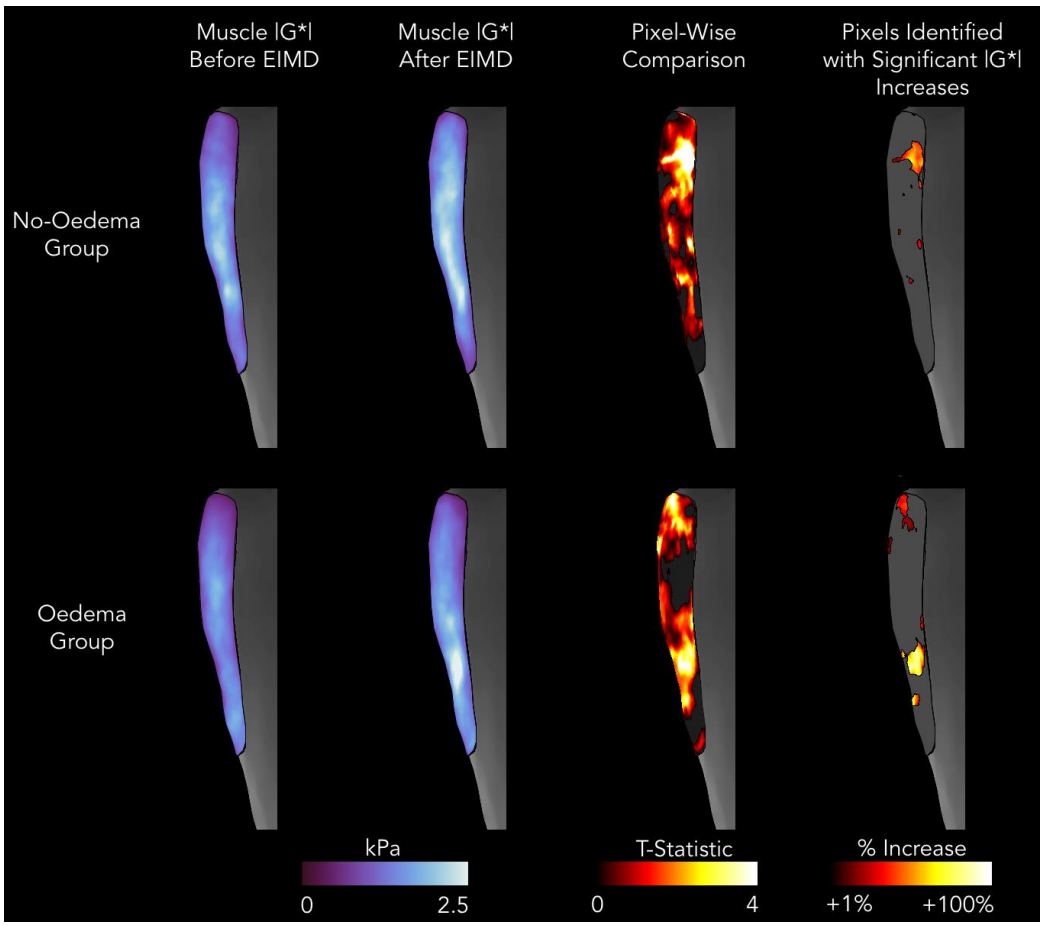

Figure 5.6 Sagittal pixel-wise |G*| differences between group averages. Top row showing the no-oedema and the bottom row showing the oedema group. First column showing pre-EIMD, second column the post-EIMD, third column showing the T-Statistic, and finally pixels identified with a significant |G*| increase whilst also showing percentage change.

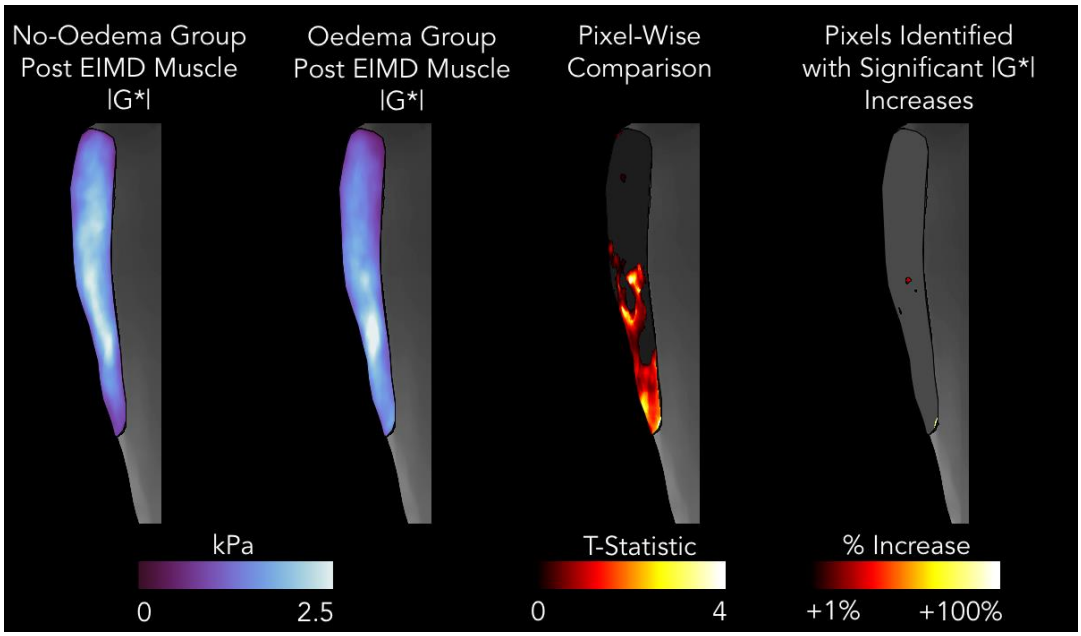

Figure 5.7. Sagittal pixel-wise |G*| differences for post-EIMD between group averages. First column showing no-oedema post-EIMD, second column showing oedema post-EIMD, third column showing the T-Statistic, and finally pixels identified with a significant |G*| increase whilst also showing percentage change.

5.5 Discussion

The key interest of this current chapter was to examine whether injury during knee extension would result in differential in inter-muscle mechanical properties (i.e. residual increase in muscle stiffness between groups) which could then be used to identify muscle engagement strategies. The hypothesis of this study was that the presence of oedema following injury was dependent on muscle engagement strategy, which is supported by the results shown here. To some degree, the use of the newly developed pipeline in Chapter Two which was employed to re-analyse the work of Kennedy et al. (2017), has revealed some possible explanations for why some individuals were more prone to injury than others, something not previously explored.

MRE was utilised in this study to show that the there is an anatomical and mechanical basis for muscle strength. Both the CSA and the |G*| of the quadriceps were strong predictors for the amount of force which was recorded for the knee extensor task. This supports previous anatomical work showing muscle function having a basis in muscle architecture (Wickiewicz et al., 1983; 1984). This shows support for the use of MRE as a proxy for measuring the strength of an individual without the dependence of additional physiological measures.

By incorporating pixelwise mapping to re-analyse the initial data it is able to visualise on elastograms particular areas of increased stiffness down to the pixel level, as opposed to generalising to a specific muscle through ROI analysis. Whilst a large magnitude of research will be aiming to identify key changes in specific muscles, this chapter has shown that it is also possible to identify regions within specific muscles which may show changes in muscle stiffness. A key finding was observed within the sagittal rectus femoris where there was a differential in the focus of |G*| change depending on the magnitude of injury, something not possible through conventional ROI. This methodology of pixel-wise mapping may then be best suited to single muscle investigations.

In addition to this, the oedema group showed a greater residual |G*| increase in the quadriceps following EIMD in comparison to the no-oedema group, suggesting a greater degree of quadricep engagement in the oedema group. Further, sagittal scans of rectus femoris showed increased |G*| of the recuts femoris towards the MTJ of the oedema group, a radiological sign of significant muscle strain (McMahon et al., 2001). Paschalis et al (2005) showed that rectus femoris was prone to damage during eccentric exercised when seated (90°) in comparison to a prone position (180°), due to being stretched to a greater extend due to flexion of the knee and hip during the seated position.

It appears from the result of the current investigation that those within the oedema group encountered greater stiffness increases in producing a knee extension. The reason to why these individuals had greater difficulty in eliciting a knee extension is potentially evident through the differential of muscle engagement between the groups, observable between residual increases in |G*|, however future research is required to further support these suggestions.

The muscle group intended to be most affected by the EIMD protocol was the quadriceps, which play a primary role in knee extension, this being the main task. The no-oedema group showed localised stiffness increase in semimembranosus, a muscle which is the most medial of the hamstrings, and typically is involved in both knee flexion and hip extension. Through co-contraction with the quadriceps, semimembranosus can support knee extension and may stabilize the knee joint during knee extension in order to avoid muscle strain (Faulkner et al., 2003; Baratta et al., 1988; Garrett et al., 1990; Nakajima et al., 2003). Stanton et al (1989) suggested that a greater magnitude of muscle co-activation results in greater muscle force being produced. The co-contraction of the hamstring muscle may be a factor in reducing the muscle damage observed in the no-oedema group. Hamstring muscle group recruitment during knee extension, has been shown to reduce the requirement for injury recovery (Aagaard et al., 2000). As a result, the increased stiffness of the hamstring muscle in the no-oedema group may have been as a result of co-contraction. Contrary to the no-oedema group, the oedema group showed

increased stiffness in the gracilis, which is primarily involved in thigh adduction and in hip flexion (Landin et al., 2016). Thus, it would appear that participants showed a differential in the localisation of muscle stiffness increases and this may suggest that participants performed the protocol quite differently in terms of the muscles that were recruited.

The no-oedema group showed increased stiffness for the quadriceps and Semimembranosus would have produced posterior – anterior knee extension, as expected. However, the oedema group showed increased stiffness in the quadriceps and gracilis, which may have resulted in a medial deviation in the posterior – anterior knee extension (Li et al., 1999), and this movement away from the axis of muscle force generation (Lieber et al., 2001) resulting in greater strain to the muscles.

Musculoskeletal investigations of animals (Lieber et al., 2001, 2011) and humans (Maughan et al., 1983; Jones et al., 1987; Scott et al., 1993; Abe et al., 2000; Aagaard et al., 2001; Kermarrec et al., 2010) suggest a potential rationale for the importance in the differential in location for residual stiffness increases, a proxy for locating damaged muscle following engagement. Muscle fibre length and fibre orientation (pennation) (Burkholder et al., 1994; Lieber et al., 2011) are architectural factors that determine muscle function. Angled muscle fibre pennation can allow for a greater number of fibres to be stacked in order to produce greater force, as seen in the quadriceps (Aagaard et al., 2001). Semimembranosus is characterised by short and angled fibres, paired with a moderate cross-sectional area, whereas gracilis has long non-angled muscle fibres and the smallest cross-sectional area of any muscle in the thigh. In addition to this, muscle fibres which are in line with the force generation axis would have been able to produce more force (Lieber et al., 2001). Both the gracilis and semimembranosus have unipennate muscle fibres, yet as the gracilis is further from the force generation axis the production of muscle force may have been hindered. The greater the angle of muscle fibre to the axis of force generation results in only a portion of the muscle force being transmitted (Lieber et al., 2011).

The engagement of either semimembranosus (no-oedema group) or gracilis (oedema group) may have contributed different levels of force during the protocol according to the muscle architecture. Apparent use of semimembranosus by the no-oedema group may have meant that a greater force was produced whilst also keeping the quadriceps in line with the axis of muscle force generation, resulting in less strain and subsequent damage – further work is required to support this speculative description. On the other hand, the co-contraction of the gracilis by the oedema group may have resulted in a reduced level of muscle force, compared to semimembranosus, which may in turn have resulted in greater dependency on the quadriceps to produce the force. As a result, the technique of mapping muscle damage through pixels has shown a promising method in localising key area of muscle damage. Further testing of this technique may offer future applications to rehabilitation. However, whilst the use of MRE has been shown to be academically insightful, the clinical cost of performing MRE over conventional methodologies may be a limited factor in applying this technique to be applied in physiotherapy based research.

A significant limitation of this study is that researchers were not able to fully control the amount of activity that each individual performed during the EIMD protocol, even though this was controlled for to the best of ability. Secondly, the use of pixel-wise mapping is prone to effects of image manipulation, where conventional ROI measurements are potentially more robust. However, for data visualisation alone, the use of pixel-wise mapping has shown a key physiological insight can be obtained in tandem with MRE elastograms. The ability to map specific areas of muscles which are injured, or prone to injury is possible through the use of MRE, where physical appearance may not appear abnormal, and may be a useful methodological tool in future muscle engagement research.

In conclusion, MRE has shown that severe injury in the form of oedema following EIMD, was not due to the amount of work performed by the participants in completing the EIMD protocol, but rather points towards a

differential in the engagement of muscles to perform the task. Thus, the analysis reported here is likely to be helpful in guiding experiments with respect to developing new protocols using the EIMD protocol and which may include new instructions and potentially also video monitoring. The study also demonstrates the important role that MRE is likely to find in studies of muscle in human movement paradigms. One possible limitation of the study is that the analysis refers to a single axial slice through the thigh and in future work it would be of considerable interest to obtain MRE data covering the whole thigh.

Chapter Six

Morphological Adaptions of Rectus Femoris over Vasti Muscles to Increasing Muscle Tension

6.1 Chapter Six Overview

Results of the previous EIMD chapter suggested muscle stiffness increases as a result of engagement, resulting in the identification of muscle damage. Chapter Six plans to expand on these results and the findings currently in the literature, to explore the morphological adaptions associated with increased muscle stiffness. By incrementally increasing load during an isometric contraction knee extension and knee flexion task, it will result in morphometric (i.e. size and shape) and mechanical measurement of muscle tissue. This work will be the first of its kind to explore the axial deformation of muscles during engagement, in order to identify a novel biomarker for muscle engagement. The question which Chapter Six addresses is: Are there morphological adaptions observable in muscle associated with a change in mechanical properties under load?

6.2 Introduction

The method of MRE has been used to show increased muscle stiffness following muscle damage (Kennedy et al., 2017), knee extension (Barnhill et al., 2013) and muscle myopathies (Basford et al., 2002). Furthermore, MRE allows muscle tension to be computed and can provide insight regarding physiological changes under muscle loading (Basford et al., 2002; Bensamoun et al., 2006; Ringleb et al., 2006). Muscle loading can offer biomechanical insight of muscle tissue as it can be readily manipulated (Dresner et al., 2001). Within the thigh there are muscles which extend across two active joints (bi-articular) and others over a single joint (mono-articular). Bi-articular muscles allow for increased range of movement (van Ingen Shenau et al., 1987), however are prone to injury particularly during eccentric contractions (Prior et al., 2001). Jacobs et al. (1996) showed that bi-articular muscles are primarily engaged in order to produce a significant magnitude of muscle force, with additional research showing mono-articular muscles greatly contribute to movement stability (Doorenbosch et al., 1994; Osu et al., 1999). Van Ingen Schenau (1995) highlighted that the relationship between bi-articular and mono-articular muscles remains relatively unclear in the literature, however

concluded that fundamentally the two muscle types have different roles in extension tasks.

Muscle stiffness and morphological changes from muscle loading could have important clinical applications in predicting peak muscle performance and enhance understanding of muscle co-contraction engagement. Measuring muscle morphology and mechanical properties at different levels of loading allows for a greater appreciation of muscle physiology. By applying different loads, it becomes feasible to evaluate the muscles adaptation to increasing muscle tension and can be used to evaluate changes in muscle mechanical properties in relation to the task (Häkkinen et al., 1998).

Previous MRE work has shown that during contraction of the quadriceps there is a relative increase in muscle stiffness (Barnhill et al., 2013). It is known that with increased tension on a structure there is a change in the morphology (Filon, 1902). Recent work (Tan et al., 2018) investigated the deformation of the triceps surae during plantarflexion, in order to evaluate the efficacy of using MRE to measure physiology of muscle strain and mobility. By measuring the morphological deformation of muscle, it may offer additional insight into the shape changes the muscle undergoes in performing a task in addition to the mechanical and size changes. By varying the degree of muscle strain during an MRE scanning session, it was found that the degree of tissue deformation determined the muscle mechanical properties and supported previous work with an inverse relationship between muscle length and elastic properties (Fung, 1993; Nordez et al., 2008).

The aim of this exploratory study is to examine the relationship between muscle stiffness and morphology. Based on the results shown by Filon (1902), Barnhill et al. (2013), and Tan et al. (2018), it is hypothesised that if increasing load is applied to a muscle, there will be a correlated relationship to muscle stiffness increases (a proxy for muscle engagement), there will be an observable axial deformation in the form of increased in circularity and decreased CSA. It is also expected that the rectus femoris will have a greater magnitude of

morphological adaption to muscle stiffness in comparison to the vasti muscles, due to a lack of attachment to the femur.

6.3 Methods

6.3.1 Method Overview

Participants took part in a sustained knee extension and knee flexion task to obtain a pool of data. By utilising an incremental increase in muscle load during isometric contractions, it allows for the relationship between muscle stiffness and morphology to be investigated. Participants were scanned in an MRI scanner, where MRE was performed, resulting in the quantification of muscle mechanical properties (|G*|) and morphology (size and shape) from ROI segmentation of individual muscles.

6.3.2 Participants

Four healthy adults (33.00 [±9.06] years) participated in this preliminary study (Research Ethics Committee number: 15/SS/0058), with limited time and fund for participant recruitment. The experimental design was explained to participants and consent to take part in the study was obtained, after answering any questions from the participants.

6.3.3 Protocol Design

A custom designed muscle loading apparatus allowed for loading of the Quadriceps and Hamstrings. Participants were asked to perform knee extensions and knee flexions while loads were applied at increasing intervals of 2kg, 4kg and 8kg (Figure 6.1). During knee extension (Figure 6.2), knees were initially flexed at 50°, and then during knee extension partially extended to 20° (with 0° being a full knee extension). For knee flexion (Figure 6.3), participants began with a knee angle of 20° and flexed their knee to 50°. Between muscle

contractions, participants would rest for 1 minute. The loading equipment limited lower leg movement between these two angles, which ensured participants performed isometric contractions and enabled sustained loading during image acquisition.

6.3.4 Image Acquisition, Processing, and Image Analysis

Images were acquired through the previously mentioned imaging protocol in section 2.3.1, with a minor amendment to the number of frequencies. Multi-frequency MRE (Papazoglou et al., 2006) was performed at three vibration frequencies (25, 37.5 and 50Hz) at eight phase offsets, through a modified Cartesian Echo Planar Imaging (EPI) sequence with additional motion encoding gradients (Klatt et al., 2010; Barnhill et al., 2013; Kennedy et al., 2017). Imaging parameters for a 80 second scan duration consisted of TR = 1600ms, TE = 54ms, FOV = 230mm x 230mm, for five contiguous 2.5mm x 2.5mm x 2.5mm^3 isometric slices, which resulted in an image matrix of 93 x 93. Use of ESP reduced noise in the individual MRE images and the combination of information from several actuation frequencies is used as a basis for presenting the resulting elastograms, with an image matrix of 368 x 368 pixels. Data was pooled from segmented thigh muscle elastograms for each loading condition (0kg, 2kg, 4kg, and 8kg) and flexion state (Control, knee extension, knee flexion), resulting in 336 physiological observations. Region of Interest (ROI) measurements were obtained for muscle stiffness (|G*|), muscle size (Cross Sectional Area [CSA]) and muscle circularity (4π[CSA/Perimeter^2]).

6.3.5 Statistical Analysis

Firstly, a post-hoc power analysis was performed through G*Power. Secondly, changes in ROI measures of |G*| were statistically analysed through a repeated measures ANOVA. Statistical comparison of ROI measurements was analysed using R-Studio (RStudio, 2015), with p=0.05 defined as statistically significant. Lastly, Pearson correlations and linear regressions were performed between mechanical and anatomical features of muscles during loading. Individual elastograms for participants in Chapter Six are found in Appendix IV.

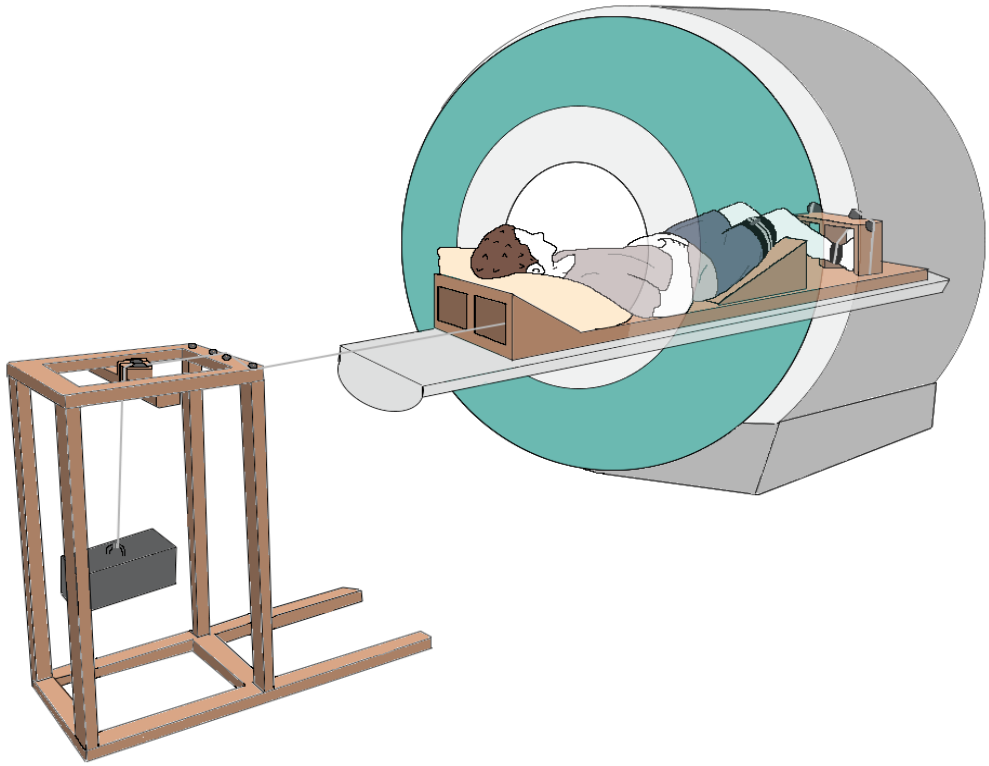

Figure 6.1. Loading equipment set-up

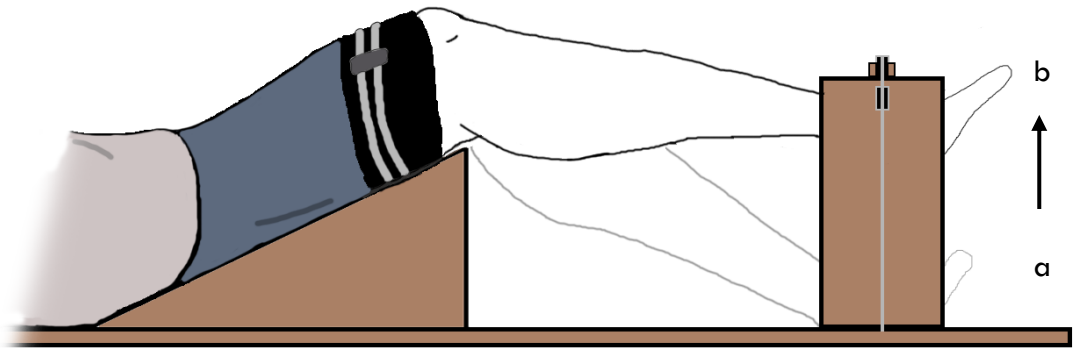

Figure 6.2. Extension loading protocol at rest (a) and extension (b)

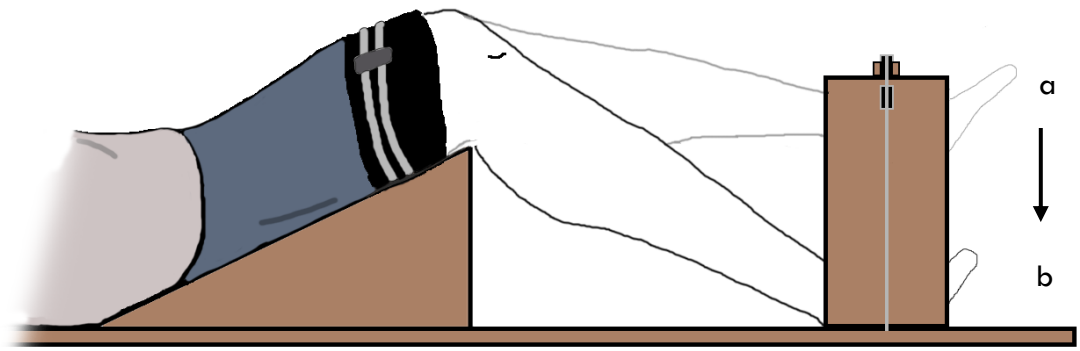

Figure 6.3. Flexion loading protocol at rest (a) and flexion (b)

6.4 Results

6.4.1 Muscle Stiffness with Load

Due to the modest number of participants, statistical power was calculated (d=0.999), with the reported power above the required d=0.8 (Cohen, 1992). At baseline, quadricep muscle group |G*| was 1.91 kPa (95% CI [1.70, 2.10]) with this increasing following additional sustained load (Figure 6.4). When a 2kg load was added to the sustained knee extension task (Figure 6.2) quadricep |G*| increased to 2.56 kPa (95% CI [2.21, 2.90]), to 2.62 kPa (95% CI [2.30, 2.94]) at 4kg of loading, and finally to 2.97 kPa (95% CI [2.66, 3.23]) at 8kg of loading. Further analysis of the quadriceps group showed that Quadriceps |G*| increased significantly with load ($F[3,60]=10.12$, $p<0.001$), with a non-significant change in the hamstrings |G*| during the sustained knee extension task ($F[3,45]=.253$, $p=0.859$). However, during sustained knee flexion, hamstring |G*| increased with load ($F[3,45]=5.24$, $p=0.004$; Figure 6.5).
Within the quadriceps muscle group the rectus femoris was identified as the

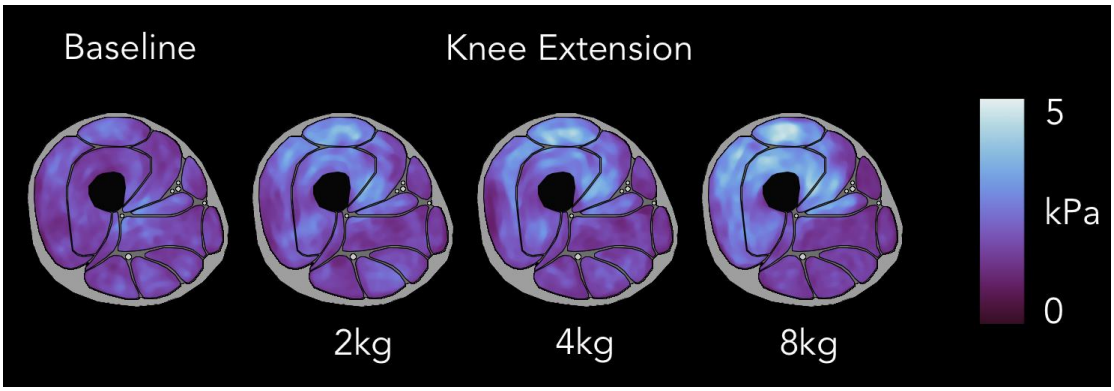

Figure 6.4. Increased muscle |G*| observed within the quadriceps during increased load of isometric knee extension.

muscle with the highest |G*| value (Figure 6.6) at the 8kg load (3.35 [±0.77] kPa), with a 57% increase from baseline, and incremental increases at the 2kg (+43%; 3.07 [±0.85] kPa) and 4kg loads (+50%; 3.22 [±0.73] kPa). The vastus medialis and vastus intermedius were identified as showing the greatest relative change during loading with a 61% (1.94 [±0.40] kPa to 3.11 [±0.72] kPa) and 60% (1.76 [±0.57] to 2.81 [±0.15] kPa) respective increases in |G*| from baseline to 8kg load. However, unlike the rectus femoris there was minimal

change in |G*| at the 2kg and 4kg load points for both the vastus medialis (2kg: 2.77 [±0.60] kPa, +43%; 4kg: 2.78[±0.45] kPa, +43%) and vastus intermedius 2kg: 2.27 [±0.33] kPa, +29% 4kg: 2.23 [±0.29] kPa, +26%). Lastly, the vastus lateralis showed the least incremental change in |G*| from baseline (1.76 [±0.15] kPa) to either 2kg (2.13 [±0.36] kPa, +21%), 4kg (2.25 [±0.30] kPa, +28%) and 8kg (2.60 [±0.40] kPa, +48%) loads.

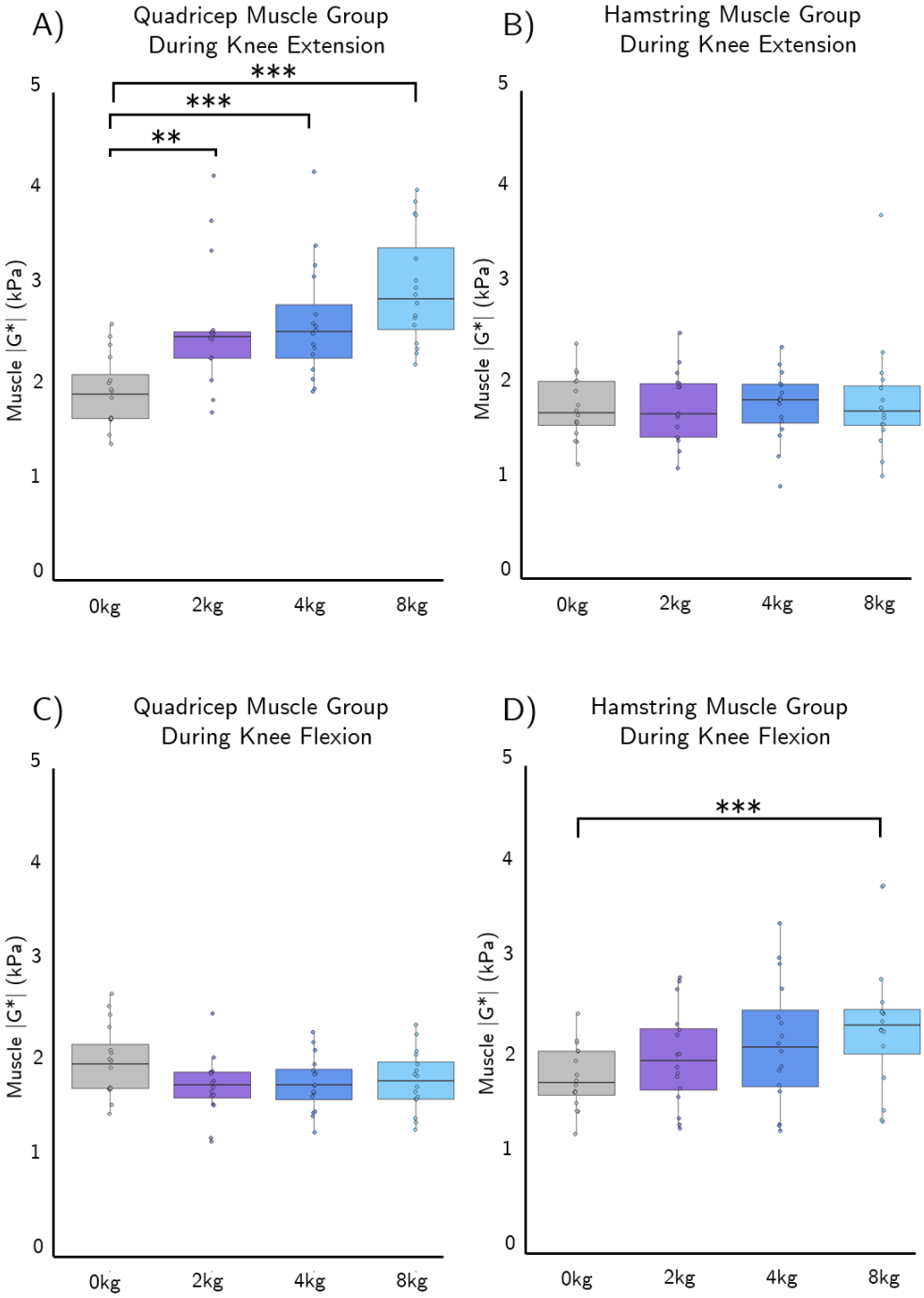

Figure 6.5. |G*| changes in quadriceps and hamstrings muscle groups during loaded knee extension and flexion. '***' ≤ 0.001, '**' ≤ 0.01,'*' ≤ 0.05.

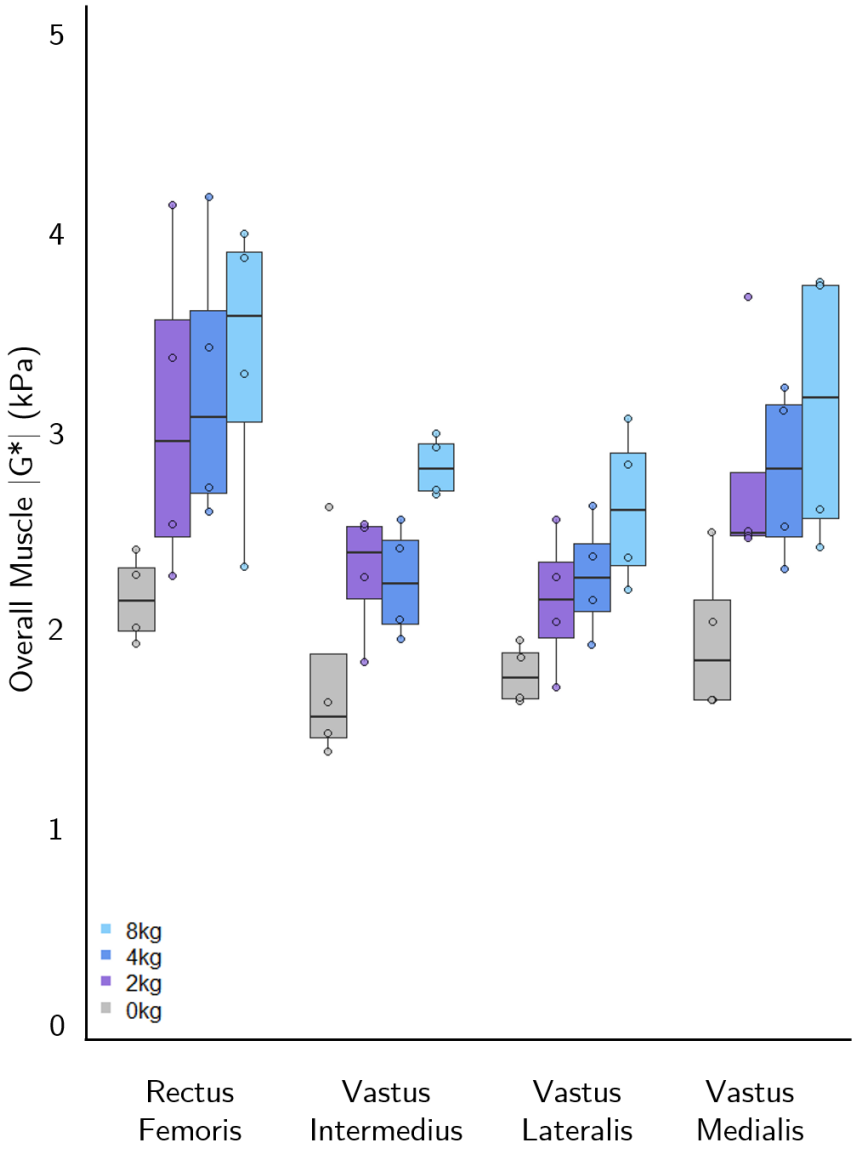

Figure 6.6. Average |G*| changes in quadriceps muscle during sustained knee extension, revealing the recuts femoris as primarily engaged at each load, with minimal recruitment of vastus intermedius and vastus lateralis at 2kg and 4kg load.

6.4.2 Muscle Mechanical Properties Predicted by Morphology

The overall relationships between |G*| (M=1.95 kPa, 95% CI [1.89, 2.02]), CSA (M=12.27, 95% CI [11.33, 13.21]) and muscle circularity (M=60%, 95% CI [58%, 61%]) were examined incorporating all flexion and loading conditions. Significant correlations were observed between average muscle |G*| and CSA (r[334]=0.14, p=0.010), |G*| and circularity (r[334]=0.26, p<0.001), as well as CSA and circularity (r[334]=-0.21, p<0.001). Using a multiple linear regression,

it was revealed that average muscle morphology (i.e. CSA and circularity) was a significant predictor for average |G*| (R^2=0.10, F[3,332]=13.57, p<0.001). Additionally, both muscle |G*| and muscle CSA were shown to be significant predictors for circularity (R^2=0.12, F[3,332]=16.53, p<0.001).

6.4.3 Biarticular and Monoarticular Muscle Morphology

Additionally, this relationship was examined between the bi-articular (n=6) and mono-articular (n=6) muscles in the thigh, with pooled data from loaded knee extensions. For bi-articular muscles, there was a significant association between |G*| and CSA (r[94]=0.44, p<0.001), |G*| and circularity (r[94]=0.45, p<0.001), and also CSA and circularity (r[94]=0.49, p<0.001). As a result, biarticular muscle morphology was a significant predictor for biarticular muscle |G*| (R^2=0.26, F[3,92]=12.16, p<0.001). Mono-articular muscles did not show the same relationships as observed in the bi-articular muscles. There was a non-significant association between |G*| and CSA (r[94]=-0.11, p=0.300) or CSA and circularity (r[94]=0.22, p=0.035), yet there was a significant association between |G*| and circularity (r[94]=0.45, p<0.001). Examining the relationship between the three factors, morphology was not a significant predictor for mono-articular muscles (R^2=0.04, F[3,92]=2.28, p=0.084).

6.4.4 Quadriceps Mechanical Properties and Morphology

The relationship between quadriceps muscle |G*| in relationship to morphology were next examined with data obtained during knee extension (Figure 6.7). A repeated measures ANOVA was used to analyse |G*| increase in the quadriceps during loaded knee extensions, showing a significant increase in muscle |G*| with load (F[3,45]=26.60, p<0.001). Following this, the association between |G*| and morphology was examined for the quadriceps muscles (Figure 6.8). Axial muscle circularity increased significantly with load during knee extension, becoming 8% more circular from baseline to 8kg knee extension (48[±16]% vs 56[±20]%; p=0.001), however circularity of the quadriceps did not change significantly during knee flexion (p=0.534). Overall there was a significant positive correlation between |G*| and average muscle circularity (r[62]=0.47,

p<0.001), with negative correlations between CSA and |G*| (r[62]=-0.25, p=0.047), as well as CSA and muscle circularity (r[62]=-0.59, p<0.001). A comparison of between the rectus femoris and the vasti muscles was performed in relation to their mechanical properties and morphology during knee extension. There was a strong correlation for rectus femoris between |G*| and circularity (r[14]=0.65, p=0.006; Figure 6.9), yet no observable association for the vasti muscles (r[46]=0.21, p=0.147). As a result, the morphology of rectus femoris was a strong predictor for its |G*| (R^2=0.76, F[3,12]=17.05, p<0.001).

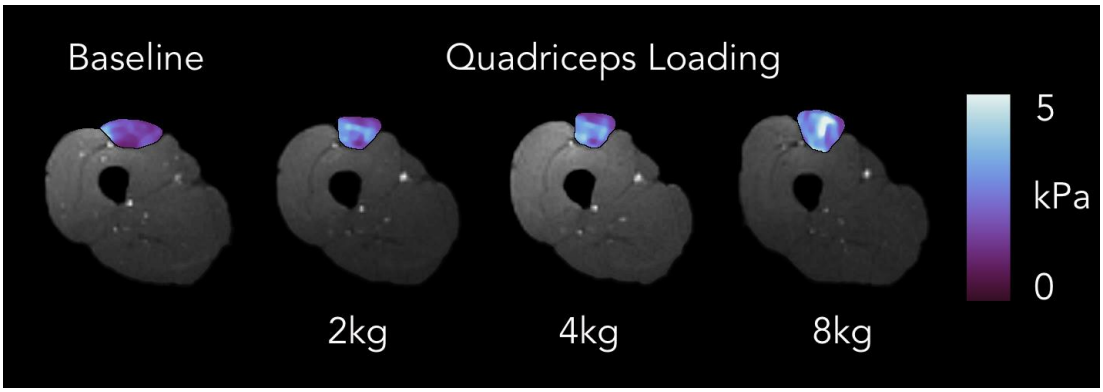

Figure 6.7. Increasing circularity and stiffness of rectus femoris with increasing load.

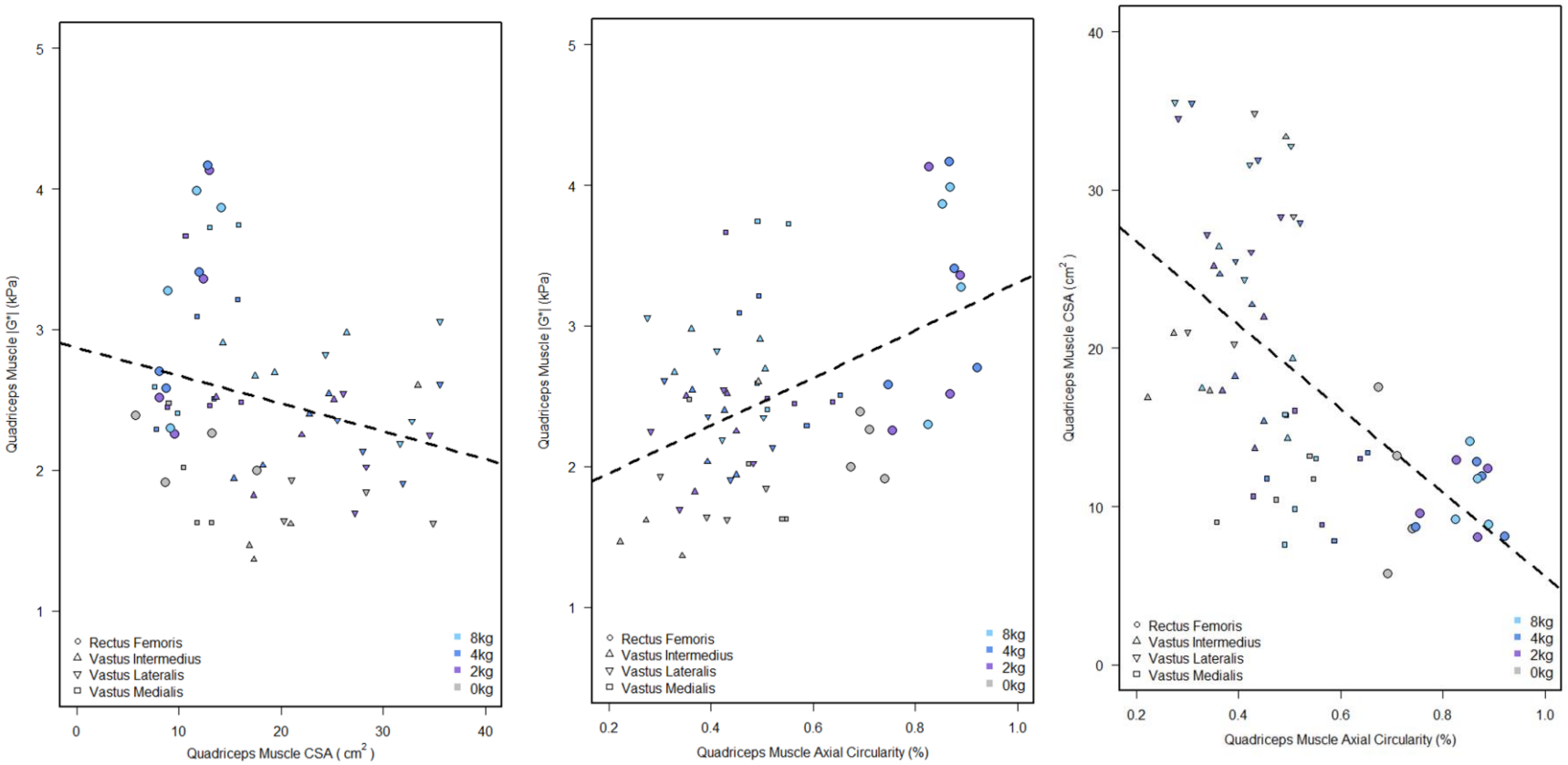

Figure 6.8. Inter-correlations between muscle |G*|, CSA, and circularity for all quadriceps muscles within an axial slice. Identifying the rectus femoris as having a different morphological physiology to the vasti muscles

6.5 Discussion

The aim of this exploratory investigation was to examine the relationship between muscle morphology and mechanical properties. This study showed that muscle stiffness increased during loading of the isometric contractions. Secondly, a greater morphological change was observed within the bi-articular rectus femoris in relation to increasing muscle stiffness, when comparing to the mono-articular vasti muscles. As expected, the quadriceps showed increased |G*| during incrementally increasing load during the isometric knee extension, which supports previous MRE research (Dresner et al., 2001; Barnhill et al., 2013). The results of this investigation suggest that size and shape of muscles are associated with |G*| measurements. This new finding within MRE may aid future analysis of muscle engagement investigations, as the quantification of both the morphological and mechanical properties have been shown here change depending on the extent of load, or muscle tension elicited from a sustained movement.

By demonstrating the relationship between muscle stiffness and morphology changes with increasing load, particularly in the prime mover rectus femoris, it would appear that the quantification of this relationship could be a useful methodology in measuring *in-vivo* muscle tension. The relationship between muscle loading and morphology was most pronounced in rectus femoris. The likely reason that the rectus femoris was most prone to morphological change during increased loading, was due to both a lack of attachments to the femur and the considerable length which this muscle stretches. Bi-articular muscles are primarily engaged to perform a movement (Jacobs et al., 1996), possibly due to bi-articular and mono-articular muscles fatiguing at different rates (Ebenbichler et al., 1998). As rectus femoris is the only bi-articular muscle of the quadriceps, this is likely the reason why the greatest increase in stiffness (a biomarker for muscle engagement) is observed in this quadriceps muscle, due to more engagement and possible fatigue. The vasti muscles all have connections to the femur, so the extent that these muscles can adapt their morphology to greater loading is limited. However, the rectus femoris does not

have any connections to the femur, showing the greatest magnitude of morphometric change to loading. As circularity of the muscle increases, the CSA decreases, with increases in |G*|, as suggested in materials by Filon (1902), showing a close relationship between morphology and mechanical properties of muscles.

Both bi-articular and mono-articular muscles are required to ensure stable movement (Osu et al., 1999). It should be noted that in this present study, during knee extension, bi-articular muscles showed a greater correlation between morphology and muscle stiffness, where-as during knee flexion, mono-articular muscles showed a greater correlation between these physiological measures. The Quadriceps muscle group is the primary muscle group responsible for production of muscle force, and as a result stability is ensure due to a ratio of 3:1 for mono-articular to bi-articular muscles. On the other hand, the Hamstring muscle group is primarily involved with knee excursion and so has a lower ratio of mono-articular to bi-articular muscles (1:3), due to a lack of required stability from explosive muscle force production.

Whilst there are limited participants within this study (n=4), there is adequate statistical power, and also adequate statistical comparison due to the loading methodology. However, recent research found large variety in the morphological changes in muscles during engagement (Tan et al., 2018), something also found in this study, most likely due to inter-participant anatomical biomechanics, strength, and flexibility. This in an important factor to bear in mind especially when investigating fundamentally dynamic tissue, as activity and fitness levels vary between individuals. Future considerations to avoid an issue such as this could be from acquiring a cohort of participants from a specific sport, as regular training of specific tasks may overcome individual differences, such as fatigue (Hunter et al., 2004).

This study is the first of its kind incorporating axial deformation in ROI measurements of MRE elastograms to measure shape changes in muscle. This investigation also introduces the importance of incorporating the shape of

muscle, as opposed to just the size. As observed here, the quantification of axial circularity resulted in an observed differential between the mono-articular and bi-articular quadriceps muscles. By using objective load measurements, it allowed for an effect specific to an amount of loading to be measured, contrary to previous muscle loading tasks which incorporate a percentage of maximum voluntary contraction (MVC). Measurements of MVC output are useful as this may account for differences in individual strength, however it is difficult for individuals to specifically use an arbitrary percentile of their maximum muscle force. By asking participants to lift a specific load allows participants to lift without psychologically limiting themselves to certain methodological constraints on MVC. Further testing should be carried out with the methodology employed in this chapter to investigate whether specific loads or MVC dependent output are best for studying the biomechanics of muscle loading.

In summary, this study has shown that through engagement of muscles, the stiffness of muscle tissue increases. In addition to these tissue stiffness increases there was also an observed morphological deformation in both the size and shape of the muscles. The antagonistic relationship of bi-articular/mono-articular muscle and quadriceps/hamstrings muscle groups highlights the architectural complexity of the musculoskeletal system, ensuring reliable locomotion. The use of muscle loaded MRE here has resulted in the identification of the relationship between muscle mechanical properties and morphology. As the load placed on a muscle increased, as did the muscle stiffness and axial morphological deformation (both in CSA and circularity), most notably in the prime mover rectus femoris. This methodology may have potential applications in future musculoskeletal investigations by measuring the amount of muscle tension (through changes in $|G^*|$, CSA, and circularity) elicited by a movement before and after intervention.

Chapter Seven

Muscle Pathophysiology following Orthopaedic Surgery

7.1 Chapter Seven Overview

In the previous chapter it was shown that with increasing load there was an associated increase in muscle stiffness, as well as a morphological change particularly in the rectus femoris during knee extension. This chapter takes these results further in order to measure the impact that total knee replacement (TKR) has on muscle biomechanics. By employing the use of MRE to measure the change in muscle stiffness in this pilot study it is showed that as a result of TKR there is a decrease in the amount of muscle tension elicited from a knee extension, in comparison to muscle stiffness measure pre-TKR. The use of MRE within this setting shows that the quantification of mechanical properties of the muscle can be used to show a change in muscle tension brought on by a movement, and more importantly the change in muscle tension as a result of a clinical intervention. Chapter Seven explores the question: Do the mechanical and morphological changes in muscles performing a task, before and after clinical intervention, offer pathophysiological insight?

7.2 Introduction

The knee is the most common site for Osteoarthritis (OA), hence many patients require Total Knee Replacement (TKR) surgery each year (Felson et al., 2000). The role of TKR is to alleviate the impaired biomechanics of the deformed knee joint (Felson et al., 2004, 2013; Hinman et al., 2010), such as those brought on by OA, which can result in painful limited range of movement (ROM). In addition to the knee joint itself, the patella is also of interest as this bone increases the leaver arm of the knee joint, aiding in the efficiency of knee extension. Forces on the knee extensor muscles have been shown to be reduced by 30% following TKR (Shenoy et al., 2013), whilst also increasing movement stability, due to re-alignment of the knee joint and balancing of soft tissue forces. Successful TKR is largely driven by meticulous technique, and the Maquet's line (Maquet, 1972) which is a primary cut in the preparation of the femoral condyle block to gain accurate coronal alignment. Accurate coronal alignment has been shown to limit the amount of joint loosening following TKR

(Jeffery et al., 1991). Additionally, patient engagement with a rehabilitation program is vital in ensuring short term recovery (Artz et al., 2015), with Mizner et al. (2005) showing that Quadriceps strength recovery was highly correlated with improved functionality. Unfortunately, home rehabilitation plans have been shown to have a low adherence rate (Mclean et al., 2010).

In Chapter Six it was shown that MRE was sensitive enough to show a difference in the mechanical properties in muscle during increasing load of knee extension. This chapter takes this finding and further investigates this in order to measure the biomechanics of muscles before and after TKR. The aim of this study is to investigate whether MRE is sensitive enough to show a difference in stiffness increases during sustained knee extension following a clinical intervention. It is expected that the surgical intervention and home physiotherapy will result in a reduction of quadricep muscle tension during engagement for the task. As a result, the hypothesis for this study is that the changes elicited by performing a sustained knee extension (in both muscle |G*| and axial circularity) will be reduced following TKR surgery and physiotherapy in comparison to changes observed pre-TKR.

7.3 Methods

7.3.1 Methodological Overview

Patients were scanned during two scanning sessions, one before surgical intervention, and one following TKR surgery. During each scanning session, images were acquired of patients at rest and during knee extension. CSA, |G*|, and axial circularity were measured, as well as regional |G*| differences in engagement between scans.

7.3.2 Participants

Five patients (65.80 [±10.38] years old) were recruited (with informed consent) from an ongoing orthopaedic study whilst waiting for TKR surgery (Research Ethics Committee number: 15/SS/0058). Patients attended a Magnetic Resonance Elastography (MRE) scanning session pre-operatively and then again following 19.74 (±7.31) weeks, in which time they underwent TKR surgery (with the same surgical consult) and at least 6 weeks of home physiotherapy (Appendix I).

7.3.3 Functional Muscle Data Acquisition

Functional measurements of muscles force were obtained through a custom-built dynamometer, with the hip and knee flexed at 20°. Isometric knee activation was measured with Spike2 software, using a load cell which measures the force output of the knee with probes placed across the quadriceps during extension. Whilst in the fixed position patients were asked to extend their knee rapidly and forcefully as so an MVC could be obtained.

7.3.4 Image Acquisition, Processing, and Image Analysis

Axial images of the thigh were obtained at rest, where the thigh was initially flexed at 50° whilst rested on a foam pad, and then scanned again after extension of the knee to 25° (80sec), with ROM being 25°. MRE was performed with a Resoundant system (Resoundant, Mayo Clinic, Rochester, MN, USA). A non-inflated tourniquet cuff with silicone tubing was placed anthropometrically (NHANES, 1988) around the thigh (Papazoglou et al., 2006), one third of the distance from the patella tendon to the greater trochanter (Bensamoun et al., 2006). All imaging was performed using a 3T Verio MRI system (Siemens Medical Systems, Erlangen, Germany). Multi-frequency MRE (Papazoglou et al., 2006) was performed at three vibration frequencies (25, 37.5 and 50Hz) at eight phase offsets, through a modified Cartesian Echo Planar Imaging (EPI) sequence with additional motion encoding gradients (Klatt et al., 2010, Barnhill et al., 2013, Kennedy et al., 2017). Imaging parameters for an 80 second scan duration consisted of TR =

1600ms, TE = 54ms, FOV =230mm x 230mm, for five contiguous 2.5mm x 2.5mm x 2.5mm isometric slices, which resulted in an image matrix of 93 x 93. MRE images were processed with ESP to reduce noise and increase pixel spatial resolution of 0.39mm^2, resulting in an image matrix of 368 x 368.

7.3.5 Statistical Analysis

Firstly, a post-hoc power analysis was performed through G*Power. To best examine change in mechanical and morphological properties of patients' muscles, mean data was expressed through mean [±SD],to analyse data a repeated measures ANOVA approach was employed. Individual elastograms of patients in Chapter Seven are found in Appendix V.

7.4 Results

7.4.1 Functional Changes in Muscle Following Surgery

MVC measurements were obtained from patients before and after TKR surgery. Mean Pre-TKR MVC was 233Nm (95% CI[89.54, 377.28]) whilst Mean Post-TKR MVC was 17% lower at 194Nm (95% CI[60.21,327]). A pairwise t-test showed this was a significant decrease (t[4]=4.10, p=0.015).

7.4.2 Pre-TKR Muscle Physiology

Due to the limited number of participants, statistical power calculations were conducted, showing a significant amount of power (d=.988). At rest the average thigh CSA pre-TKR was 113.11 cm^2 (95% CI[64.00, 162.21) and average thigh muscle |G*| was 1.74 kPa (95% CI[1.28,2.20]). During knee extension the average thigh CSA was 109.63cm^2 (95% CI[61.55, 157.71]) and average |G*| was 2.15 kPa (95% CI[1.80,2.51]). A repeated measure ANOVA revealed that there was a non-significant increase in |G*| for the thigh as a whole during knee extension (p=0.166). However, there was a localised |G*| increase of +56% observed in the agonist quadriceps muscle group (F[1,34]=82.18, p<0.001) from rest to knee extension (1.51 [±0.42] kPa vs 2.36

[±0.33] kPa). Each of the Quadriceps muscles showed a significant increase in |G*| from rest to knee extension (Figure 7.1), with the greatest increase of 69% observed in the rectus femoris (p=0.012), then 61% in vastus intermedius (p<0.001), as well as 48% in the vastus lateralis (p=0.008) and medialis (p=0.025) equally. In addition to the quadriceps muscles, the antagonist hamstrings muscle was also shown to be engaged during knee extension (Rest: 1.96 [±0.64] kPa vs Knee extension: 2.28 [±0.85] kPa; +16%; p=0.041).

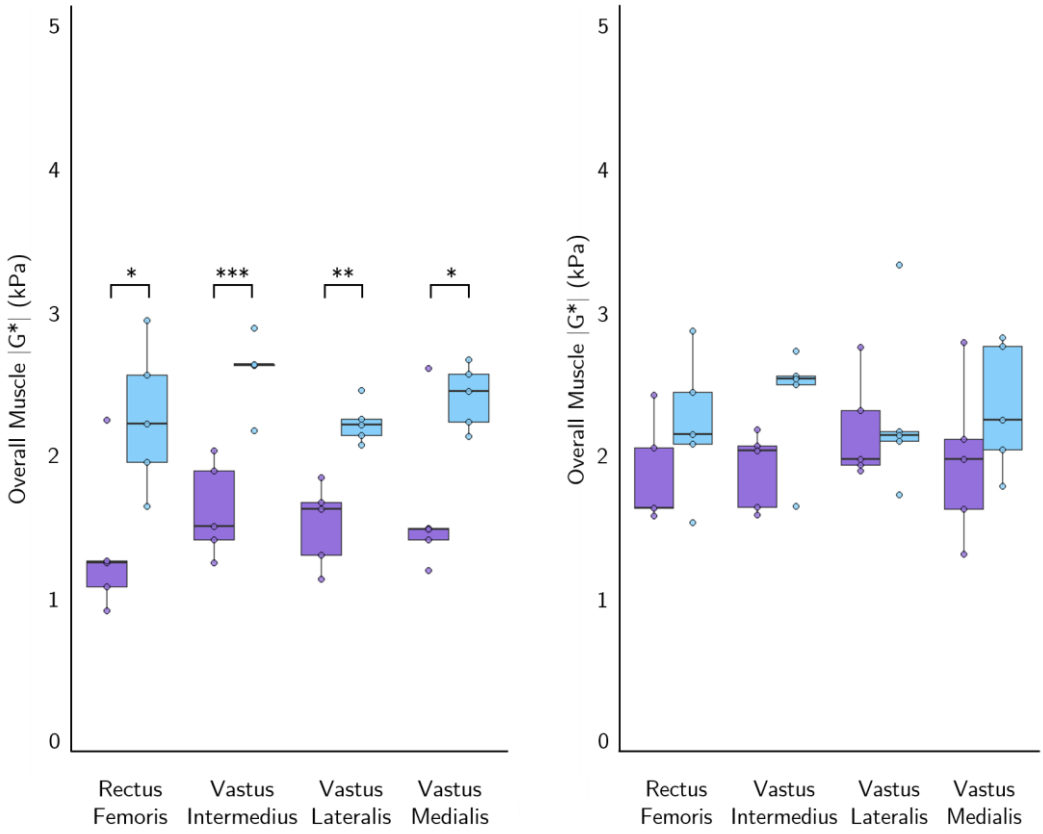

Figure 7.1. Pre-TKR (Left) and Post-TKR (Right) changes in quadricep muscle |G*| during knee extension. '***' ≤ 0.001, '**' ≤ 0.01,'*' ≤ 0.05.

7.4.3 Post TKR Muscle Physiology

At rest, the average thigh CSA post-TKR was 91.29 cm^2 (95% CI[47.42, 135.15) and average thigh muscle |G*| was 2.51 kPa (95% CI[1.65, 3.36]), whereas during knee extension average thigh CSA was 93.24cm^2 (95% CI[40.96, 145.52]) and average |G*| was 2.59 kPa (95% CI[2.02, 3.15]). Following TKR a decrease

of 15% CSA was observed in all muscles at the time of second scan (9.49 [±6.98] cm^2), compared to the first scanning session (8.03 [±6.40] cm^2).

In addition to this, |G*| at rest had significantly increased for all muscles at the time of the second scan (Pre-TKR: 1.69 [±0.56] kPa vs Post-TKR: 2.42 [±1.01] kPa; t[59]=5.00, $p<0.001$). Knee extension post-TKR only elicited a significant |G*| increase in Quadriceps ($p=0.005$), individual quadriceps muscles, such as rectus femoris, did not increase (+19%; $p=0.217$). There was also minimal |G*| change in the vastus Intermedius (+26%), vastus lateralis (+6%), and vastus medialis (+19%) Following TKR there was no observable stiffness change in the hamstring muscle group during knee extension (Baseline: 2.61 [±1.08] kPa vs knee extension 2.67 [±0.87] kPa; p=0.632).

7.4.4 Differential in Regional |G| Changes Before and After TKR Knee Extension*

Co-registration of MRE elastograms allowed for descriptive inspection of regions with an increase in |G*| as a result knee extension and to compare this before and after the TKR intervention (Figure 7.2). Pre-TKR elastograms showed that during knee extension 83% of the whole thigh has been engaged and increased by an average |G*| of 42% (Figure 7.3, C1). Post-TKR elastograms showed that only 62% of the whole thigh was engaged and |G*| increased by only +10% (Figure 7.2, C2)

When inspecting the quadriceps during pre-TKR knee extensions, 95% of the quadriceps muscle group was engaged to perform the movement, resulting in an average |G*| increase of 53%. Following TKR, it was observed that knee extension engaged 77% of the quadriceps muscle group, with an average |G*| increase of 27% from rest. As a result, post-TKR knee extension engaged 17% less of the quadriceps in order to perform a knee extension, with post-TKR

|G*| increase being an average of 26% lower than pre-TKR knee extension (Figure 7.2, C3).

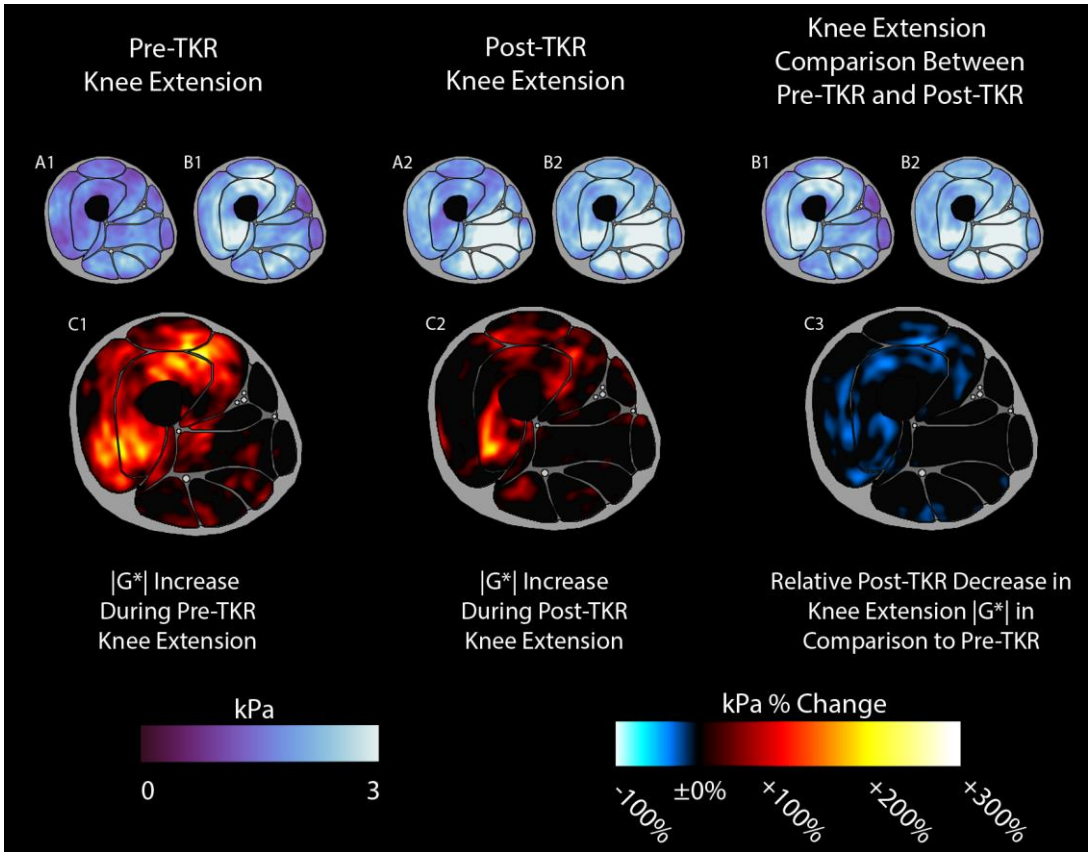

Figure 7.2. Comparison of |G*| increases observed during Pre-TKR and Post-TKR knee extensions. A1: Pre-TKR Rest, B1: Pre-TKR Knee Extension, C1: Percentage increase in |G*| from rest to knee extension Pre-TKR, A2: Post-TKR Rest, B2: Post-TKR Knee Extension, C2: Percentage increase in |G*| from rest to knee extension Post-TKR, C3: Comparison of |G*| increase in Post-TKR relative to Pre-TKR.

7.4.5 Rectus Femoris Biomechanics Following TKR

Rectus Femoris morphology was examined at rest and during knee extension for pre-TKR (M=0.69, CI[0.60, 0.78] CV=10% vs M=0.87, CI[0.78, 0.96], CV=8%) and post-TKR (M=0.65, CI[0.50, 0.80], CV=18% vs M=0.82, CI[0.75, 0.89] CV=7%), finding a no variance between scans (F[3,16]=1.11, p=0.376). Before TKR rectus femoris circularity significantly increased between rest and knee extension by 18% (0.69 [±0.07] vs 0.87 [±0.07]; p=0.022). However, following TKR, Rectus Femoris circularity showed a tendency to change when performing a knee extension (0.65 [±.12] vs 0.82 [±.06]; p=0.053). In addition to this, Rectus Femoris was significantly less

circular (p=0.008) during knee extension post-TKR in comparison to pre-TKR (Figure 7.3).

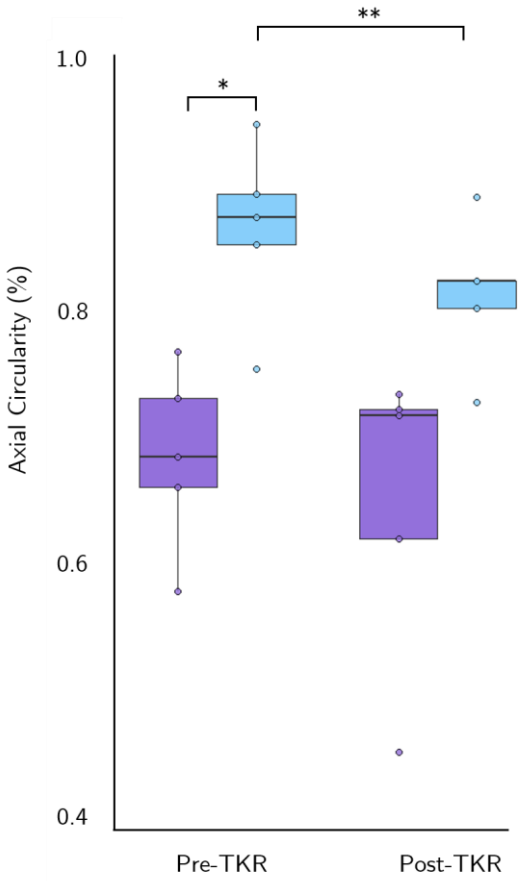

Figure 7.3. Axial circularity of rectus femoris during knee extension before and after TKR surgery. '***' ≤ 0.001, '**' ≤ 0.01,'*' ≤ 0.05.

7.5 Discussion

The aim of this study was to expand on the findings of Chapter Six and examine the changes in muscle physiology during knee extension following TKR and rehabilitation. It was expected that as a result of TKR surgery and physiotherapy there would be a relative decrease in muscle stiffness and morphological changes in quadriceps muscles during the knee extension task. The results of this study showed that following TKR and physiotherapy, the increase in muscle stiffness of quadriceps muscles, which was observed during knee extension previous to TKR, was significantly reduced, with an average

decrease of 26%. In addition to this, the knee extension task following TKR resulted in a reduced morphological change in rectus femoris, suggesting reduced muscle tension. These findings support previous research which discussed TKR surgery reducing muscle stress by 30% (Shenoy et al., 2013).

Additionally, patients with Osteoarthritis (OA) have been shown to recruit a greater magnitude of muscle co-contraction compared to asymptomatic controls (Childs et al., 2004; Lewek et al., 2004; Hubley-Kozey et al., 2006, 2008; Heiden et al. 2009). It is suggested that OA patients exhibit a greater co-contraction method to limit over knee excursion to limit movement related pain. Yoshida et al., (2013) who showed a reduction in Quadriceps recruitment following 3 months after TKR surgery, because of increased patient strength. The findings of this present study are in support of this previous research, as the elastograms for pre-TKR knee extension show a significant co-engagement with the hamstrings, however this muscle group was not significantly engaged following TKR. This shows that following TKR the quadriceps muscle group are able to perform the knee extension task without the need for additional stability. Further, Chapter Six showed that the rectus femoris was prone to changes in the axial circularity during increased muscle tension. This chapter showed that post-TKR surgery circularity of rectus femoris was significantly decreased during knee extension in comparison to before the surgical intervention.

The results here suggest that the Quadriceps are less inhibited following TKR surgery. The quadriceps show a decreased size following TKR, however, functionally the muscles incur less $|G^*|$ increase during knee extension following TKR. By using conventional MRI methods, one may have concluded that patients may have been weaker due to reduced size in addition to the reduced MVC measures. The utility of MRE in this preliminary study has shown that as a result of the clinical intervention, tension elicited by knee extension is reduced. These results may have been due to a combination of the tension relieving TKR surgery and repeated strengthening of the quadriceps due to home physiotherapy.

It is important to note that this is the first exploratory study of its kind to perform MRE on TKR patients before and after surgery. An important methodological aspect of this investigation was the quantification of functional, morphological and mechanical properties of muscles within the thigh. Even though these results offer new insight into the impact of TKR, this study is not without limitations. Firstly, the use of MRE can only show the stiffness changes in a tissue, however to obtain a better appreciation of patient strength, repeated testing throughout recovery would have given a better appreciation of the rate of recovery from surgery. Also, due to the limited number of patients here these results should be used to pursue a follow-on study in order to fully test the hypothesis of this study, even though there are promising results shown here. Finally, there was unfortunately no data gathered on patient pain or progress with physiotherapy. This could have also resulted with useful insight into physiological changes from TKR and whether this may be a confound with regards to task performance.

Future research should look to implement measurement of bone marrow with physical ability. Bone marrow cells have been shown to be a factor in recovery due to their release of systemic cells that are key to healing (Mankin et al., 1982; Orlic et al., 2001; Agung et al., 2006). The role of bone marrow is to provide a continuous resource of cells to fulfil the musculoskeletal demands for oxygenation (Vogler et al., 1988; Sun et al., 2009). To date there is limited research on imaging bone marrow following surgery using Magnetic Resonance Imaging (MRI). However, studying bone marrow in future studies could provide clinicians with an additional diagnostic tool for patient health (Aisen et al., 1986; Steinborn et al., 1999). The present study has highlighted the importance of analysing muscle recruitment strategies, building on work from Chapter Five, as well as measuring morphological changes in muscles which was explored in Chapter Six. Also, this study shows the role which MRE can play in analysing surgical interventions by measuring changes in mechanical properties, morphology, and engagement.

In conclusion, these results show that measurements of muscle stiffness and morphology can deviate between a static position and during function. Following TKR, muscle stiffness was significantly greater than before surgery, suggesting a level of injury. Also, when the muscles were engaged the findings of this pilot study suggest that there is a reduced level of |G*| and axial circularity change when performing a movement. These findings expanded on the work observed in the previous chapters to show that it is important to examine static and functional physiology when measuring musculoskeletal recovery, of which the use of MRE can show insight into pathophysiology.

Chapter Eight

Discussion and Future Work

8.1 Overview of Thesis Results

Each chapter of this thesis has shown novel clinically relevant results in a variety of applications for the measurement of anatomical health, obtained through the implementation of MRE in musculoskeletal research. This present chapter will review the findings of the previous chapters and discuss potential future research which could incorporate additional clinical imaging methodology to further investigate the musculoskeletal system.

Chapter One outlined the fundamental background of musculoskeletal anatomy and function, whilst also detailing the basics of imaging in-vivo tissue. Further, Chapter One briefly reviewed the current literature of musculoskeletal MRE showing that there is limited application of MRE within the musculoskeletal system. In addition to this, it also showed that the majority of research of thigh MRE have limited participant cohorts, as well as limited scope of imaging – with current research focussing primarily on either one muscle or a single group of muscles with a similar function. Finally, Chapter One discusses how MRE may offer significant insight in to musculoskeletal physiology over conventional methodologies including EMG.

Chapter Two highlighted the background understanding of musculoskeletal rheology and current methods of data visualisation. The suggested pipeline in this chapter addressed concerns for the use of conventional colour maps, showing that varying luminance was likely to elicit error is visual analysis of elastograms. In addition to this, a template in which elastograms can be registered to was developed, with this method resulting in |G*| of muscles being examined without the confound of varying muscle morphology. Finally, the pipeline was analysed for inter-rater and intra-rater reliability for each key stage of the pipeline, revealing robust levels of repeatability of measurements between and within experimenters. The use of this pipeline was an initial attempt to show the importance of a unified approach to MRE data visualisation, particularly in musculoskeletal research where muscle morphology can differ greatly between participants. The high level of

repeatability within and between researchers suggests that incorporating such an approach to MRE research may not impede the validity or precision of readings and should result in less error. By developing a promising image analysis pipeline meant that exploratory MRE work was ready to be explored with Chapters Three to Seven, where a wide range of clinically relevant exploratory studies utilised the pipeline outlined in Chapter Two to reveal changes in the mechanical properties of muscle.

Chapter Three examined the changes of the musculoskeletal system during the ageing process from 20-55 years. The hypothesis for this preliminary work was that the Quadriceps would be prone to age related muscle atrophy, and that muscle stiffness would increase due to muscles being impaired due to the decrease in muscle group size. This study showed that the quadriceps were primarily affected by ageing, with the vastus lateralis being prone to muscle atrophy. However, the quadriceps were not equally impacted by ageing as the vastus medialis showed no significant sign of age-related atrophy but did show significant increases in muscle stiffness associated with age. In addition to this, the hamstring muscle group showed a significant level of resistance to the effects of ageing. It must be noted that even though the participants were normally distributed overall and between groups, a greater number of participants would be required to be able to make full conclusions on the impact of ageing. Future musculoskeletal ageing research should look to incorporate a number of participants for incremental age brackets, so that not only the overall impact of ageing can be measured, but also potentially identify ages which are most prone ageing effects. This preliminary work showed that the impact that there is not a universal impact of ageing on the locomotor system and further testing is required in to arrive at comprehensive conclusion of the changes in the mechanical properties of tissue with time.

Chapter Four investigated the effects of immobility within ICU, and whether observed effects recovered after a period of convalescence. The hypothesis of this chapter was that the quadriceps muscles would be primarily affected by immobility, which was supported by the findings of the study. At time of

discharge, both muscle stiffness and muscle size were significantly lower than healthy controls, in addition to significant fat infiltration. In particular, the effects of immobility were prominent in the relationship between size and stiffness of the vastus medialis between groups. Following convalescence, the size and stiffness of muscles had increased in patients, yet there was still an observable inability to perform a walk test to a healthy level. The difficulty with such an investigation is that the cohort being images are particularly weak, so four returning patients is a promising contribution to the area of critical care musculoskeletal immobility. However, a follow-on study should include a full scan of the thigh as to allow the measurement of contracture, and whether this is having an impact on MRE results. A secondary factor to consider may be to incorporate several imaging sessions. This was the first time MRE has been used to measure the impact of ICU on the musculoskeletal system. These results suggest that ICU immobility significantly impact anatomy which can recover, however there appears to be long lasting effects, limiting the function of muscles.

Chapter Five re-investigated previously published data to identify why only certain individuals were prone to injury induced oedema following a repeated knee extension protocol. The hypothesis for this experiment was that residual increases in muscle stiffness, could be used to identify injury severity, and the location of these increases in stiffness could be used to infer the location of damage. The results of this study showed that between two groups of injured participants, there was no significant difference in muscle force output or number of repetitions, yet there was for change in MVC. The use of MRE identified a difference in muscle engagements strategy, by measuring residual increases in muscle stiffness. Those without injury incorporated a balanced anterior and posterior co-contraction, whilst those with oedema incorporated a weaker anterior and medial co-contraction. This was a novel finding for the dataset and in the application of MRE. This exploratory investigation showed the importance of a template to co-register individuals to in order to perform pixel-wise testing. At the moment this technique is currently limited to a single slice, however if future development of this technique were to include full 3D

images, it may result in significant insight into injury. Using this methodology, insight into the dynamics of muscle loading and weight training will assist the development of more balanced and targeted exercise regimens to assist athletes build strength without the risk of inadvertent muscle injury, and perhaps increase performance.

Chapter Six examined morphological and mechanical changes in muscle during incremental loading. The hypothesis for this experiment was that the rectus femoris would have a greater morphometric change to loading compared to the Vasti muscles during sustained knee extension, due to the lack of connection to the Femur. Firstly, muscle group variation was identified during knee extension (through increased quadriceps stiffness) and flexion (through increased hamstrings stiffness). The bi-articular rectus femoris was identified as having a significant linear relationship between muscle morphological and mechanical properties - where increasing axial circularity also resulted in a reduction in axial CSA. By showing that MRE can be used to measure both physical and mechanical properties of tissue may be a useful technique to incorporate in future work within biomechanics. It is understood that with increasing levels of muscle contraction there will be an increase in muscle stiffness. The morphological relationship with muscle stiffness may be used as a biomarker for muscle tension during use – and may have applications in the study of rehabilitation or strength training. This preliminary investigation in the quantification of muscle morphology and mechanical properties are promising, yet further experimental results are required for a better appreciation of this relationship.

Chapter Seven examined the recovery of the musculoskeletal system following Total Knee Replacement (TKR) surgery. It was hypothesized that before TKR surgery, patients would show a significant increase in muscle stiffness during sustained knee extension, and after TKR surgery the same movement would elicit a lower muscle stiffness increase. The findings of Chapter Four are the first time MRE has been used to quantify musculoskeletal recovery from TKR surgery. A key finding for this chapter was that previous to TKR surgery, in

order to extend the knee, the patients engaged 95% of the quadriceps and a significant portion of the hamstrings to perform the movement. Following TKR, a significant drop in muscle tension and co-engagement was observed, yet It is important to note that there was a significant drop in patient MVC following TKR. In addition to this there was a smaller morphological change in muscles performing the task post-TKR in comparison to before the surgery. This finding suggests that it is important to consider the functional, physical and morphological features of muscles when measuring recovery. As a result, the use of the pipeline developed during this thesis visually showed a reduction of muscle engagement following surgery, this method of visual representation of muscle engagement data may be a useful methodological tool in measuring the effectiveness of training or further clinical intervention.

8.2 Summary of Thesis Results

This thesis has covered a wide range of clinical applications for MRE, showing significant and novel findings for each investigation. A recurring theme within each project is the importance of the quadriceps muscles (particularly the vastus medialis) in stability and the sensitivity to change during immobility, ageing, or surgical recovery. An important methodological advancement identified in this thesis is the relationship between muscle tension and morphology of muscles, especially in rectus femoris. By utilizing the unique functionality of this muscle means one can take into consideration mechanical and morphological changes during engagement to obtain a robust understanding of pathophysiology. Overall, the musculoskeletal system is one governed by balance, and as soon as there is significant morphometric (i.e. a decrease in muscle size, as seen in Chapters Three and Four), mechanical (i.e. a change in muscle stiffness, as seen in Chapters Three, Four, Five, and Seven) or functional change (i.e. co-contraction strategy, as seen in Chapters Five and Seven) then this may impact locomotion.

The exploratory work conducted throughout this thesis attempted to address the repeatability, precision and responsiveness of musculoskeletal MRE. Repeatability was initially shown through an review of the literature, as well as a brief reliability comparison for inter-rater and intra-rater reliability of ROI measurements, and also anatomical plotting used for the newly developed pipeline. The precision of MRE was demonstrated through the use of ROI, pixel-wise mapping, and also data visualisation through elastograms, showing that changes in the mechanical properties of muscle can be clearly shown both quantitatively and qualitatively. Finally, the responsiveness of MRE was demonstrated with the comparison of static and active measurements of muscle physical and mechanical properties throughout each chapter.

By clinically applying MRE within the musculoskeletal system this thesis has shown the wealth of additional information which can be obtained for musculoskeletal health, which offers significant clinical insight into musculoskeletal biomechanics and functional anatomy. It is hoped that MRE is employed in future musculoskeletal work to assist those to avoid injury, aid patients in efficient recovery, and to further understanding of this vital system within the human body.

8.3 Musculoskeletal Mechanical Pathophysiology

The goal of this thesis was to explore what the measurement of the mechanical properties of muscle tissue may offer in the quantification of pathophysiology. The application of MRE offers the ability to measure the mechanical properties of muscle as well as the morphological aspects of muscle from conventional MR imaging. Specifically within this thesis the measurement of muscle |G*| in a number of clinical applications has allowed some novel appreciation of the musculoskeletal system in both static and dynamic states. Firstly, the static change in muscle mechanical properties have been shown to be negatively impacted long term through age, as well as lack of use. From the investigation of critical care patient recovery it would appear that the mechanical properties

of the muscle require a greater amount of time to recover compared to the size of the muscles. This new finding offers an important insight into the static mechanical properties of muscle, in that even without the conventional measurement of muscle contraction, the pathophysiology of muscles can be explored through these static images. However, muscle tissue is dynamic, and the main purpose of the tissue is in locomotion. A key finding of this thesis was that MRE can be used to pinpoint (to a high degree of precision) residual stiffness increases in damaged muscle. Previously it was understood that contraction or damage may increase the stiffness of muscle, but this residual stiffness had not been previously used to offer an insight into the severity of muscle damage. Additionally, this thesis also showed that during increasing load, there were morphological deformations of muscle (for both size and shape) in relation to the change in muscle stiffness. By showing a close relationship with both the mechanical and morphological properties of muscle shows the importance in the investigation of both the static and dynamic nature of muscle. As a result, the final experimental chapter put this into practice to study the changes in the musculoskeletal system following surgical intervention. The main experimental finding was that even though it appeared that patients were still in a state of recovery within the static images obtained of the thighs, the analysis of the quadricep muscles during engagement showed that patients were much more able to perform the task – due to a reduced elevation of muscle stiffness during the task. This thesis has focussed primarily on developing an effective pipeline to be utilised in a number of pilot studies, and as such has focussed on relative changes of muscle mechanical properties. However, if MRE is to be taken further, more work is required in order to establish quantifiable range of what muscle |G*| should be for different states of muscle. Once this can be obtained one may be able to further understand why mechanical properties may have deviated from expectations, and more importantly what this may mean for patient pathophysiology.

8.4 Future Work

Future clinical musculoskeletal elastography could benefit greatly from incorporating additional imaging modalities during experimental protocols. Three magnetic resonance imaging methods are discussed as each may offer additional insight into future MRE physiological investigations, including Diffusion Tensor Imaging (DTI) shows insight into tissue microstructure, Magnetic Resonance Spectroscopy (MRS) which offers metabolite quantification, and Magnetic Resonance Thermography (MRT) to show temperature differentials in tissue.

8.4.1 Diffusion Tensor Imaging

Diffusion Tensor Imaging (DTI) is an imaging modality which can characterize the organization of tissue microstructures (Jones et al., 2011; Scheel et al., 2013). The random molecular movements of water are sensitized to the gradient of a magnetic resonance (MR) machine (Stejskal et al., 1965). Depending on the rate of diffusion attenuation, the orientation of the dominant fibres can be determined (Basser et al., 1994), which can then be mapped and colourised to show different fibre directions within a tissue (Pajevic et al., 2000).

DTI allows us to measure several diffusion parameters (Alexander et al., 2007), most notably Mean Diffusivity (MD) and Fractional Anisotropy (FA). Firstly, MD is a measure of molecular motion, without consideration for direction (Cercignani et al., 2001). Secondly, FA is a numerical value representing the anisotropy of diffusion, i.e. the number of directions of diffusion (0 being in all directions, and 1 being in a single direction). The measure of FA can be used to infer fibre density, diameter, alignment, and is one of the most used DTI parameters due to the sensitivity to microstructure changes (Alexander et al., 2007; Soares et al., 2013). It is also possible to map the diffusion of water to show microstructures in a 3D environment (Figure 7.1), known as tractography (Basser et al., 1994, 2000; Jones et al., 1999; Mori et al., 1999; Conturo et al., 1999; Parker et al., 2003).

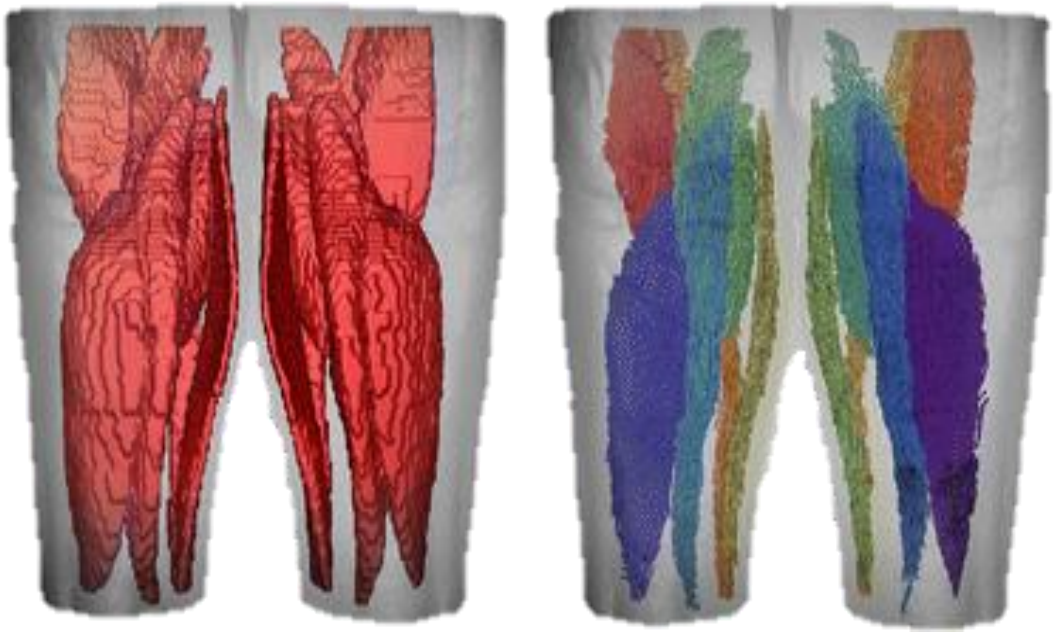

Figure 8.1. Muscle Segmentation (Left) and tractography (Right) of Hamstring muscles, from Froeling et al. (2014).

By combining measurement of MD and FA, it is possible to obtain clinically relevant information on tissue health, particularly within the musculoskeletal system. Following muscle injury, Zaraiskaya et al. (2006) showed a significant increase in diffusivity of calf muscles, supporting previous research suggesting muscle injury impacts muscle microstructure (Hough, 1902; Häggmark et al., 1986). In addition to this, Zaraiskaya et al. (2006) also showed that increased levels of MD may indicate tissue lesions. Further, Froeling et al. (2014) showed that following a period of running there was a significant increase in the MD and FA of Bicep Femoris muscle, something not evident through conventional MR imaging (Figure 7.2).

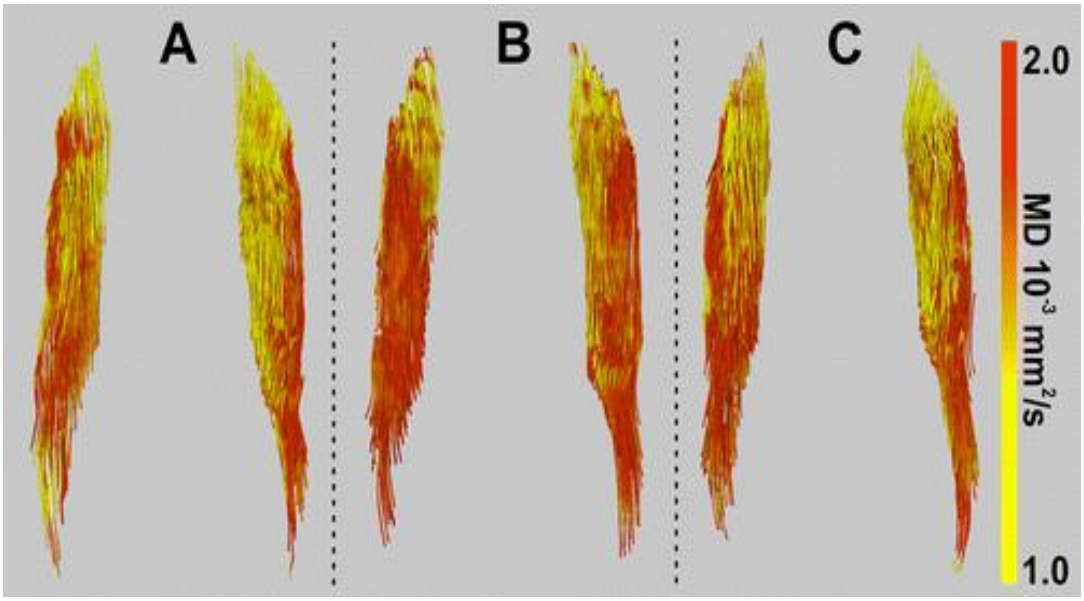

Figure 8.2. Mean Diffusivity of Bicep Femoris one week before (A), two days after (B), and three weeks after (C) a long distance running protocol from Froeling et al. (2014), showing a significantly increased MD ($p<.05$) at time point B.

DTI has also been used to characterize muscle fibre types (Sheel et al., 2013). Comparing biopsy data and FA values, fibre types were able to be characterized, with type 1 fibres showed a higher FA value. In addition to this, DTI has also been used to measure muscle fibre pennation (Lansdown et al., 2007). By being able to utilize a non-invasive imaging modality to obtain highly detailed measurements about muscle structure, previously shown to be linked to muscle force, will mean that future measurements for anatomical biomarkers for muscle force may not only be measured in weaker patients, but also compared to the mechanical properties of muscles.

As shown here, by utilizing future musculoskeletal research with the addition of DTI will allow for measurement of microstructural changes. To date, there has been some work in successfully showing correlations between MRE and DTI measurements of biological tissue (Johnson et al., 2013), with Yin et al. (2016) showing that DTI and MRE data can be obtained simultaneously. By being able to combine both MRE and DTI may result in significantly greater insight into measuring injury recovery.

8.4.2 Magnetic Resonance Spectroscopy

Magnetic Resonance Spectroscopy (MRS) allows for the measures of biochemical changes in pathophysiology, i.e. metabolites including adenosine triphosphate (ATP), an energy generation metabolite (Knowles, 1980). MRS in-vivo is limited to measuring certain nuclei, with phosphorus (31P) being a commonly used clinical application due to the high concentrations in order to result in a strong signal (Gujur et al., 2005).

Park et al. (1994, 1995, 2001, 2005) has shown efficacy of using MRI and MRS in order to obtain clinically relevant data for pathophysiology in myopathies. In particular, Park et al (2001) utilized MRS to obtain data on dermatomyositis (DM; an inflammatory disorder). Within this study, there was a 40% decrease in phosphocreatine (PCr) and 30% decrease in ATP for DM patients in comparison to healthy controls (Figure 8.3). A reduction in these two metabolites (important for the contraction of muscles) showed that DM results in abnormal metabolite with an inefficient use of PCr and ATP during contraction. Massie et al (1987) also found that patients with congestive heart failure (CHF) showed significant musculoskeletal deviations in biochemistry during exercise. Patients were observed as using PCr at a faster rate than healthy controls even though the work rate was less. In addition to this, Petersen et al. (2003) compared ATP between young (18-39 years old) and older (61-84 years old) participants, finding a significant reduction in ATP.

Additional MRS research has investigated metabolic change following the effects of training and fatigue. ATP measurements have been used to study muscle performance and signs of fatigue following exercise (Kent-Braun et al., 1990), with an additional measure of muscle metabolism is the ratio between work production (Pi; inorganic phosphate) and energy cost (PCr). Kent-Braun et al. found an increase in work production to energy cost when comparing a second-time point to an initial testing time point, supporting previous research showing trained muscles have a decreased energy cost for the same relative work production of untrained muscles (Chance et al., 1985; Park et al., 1987). In addition to this, research has suggested that ATP hydrolosis may suggest a measure for muscle fatigue (Takata et al., 1988; Challiss et al., 1987; Dawson et al., 1980; Taylor et al., 1986).

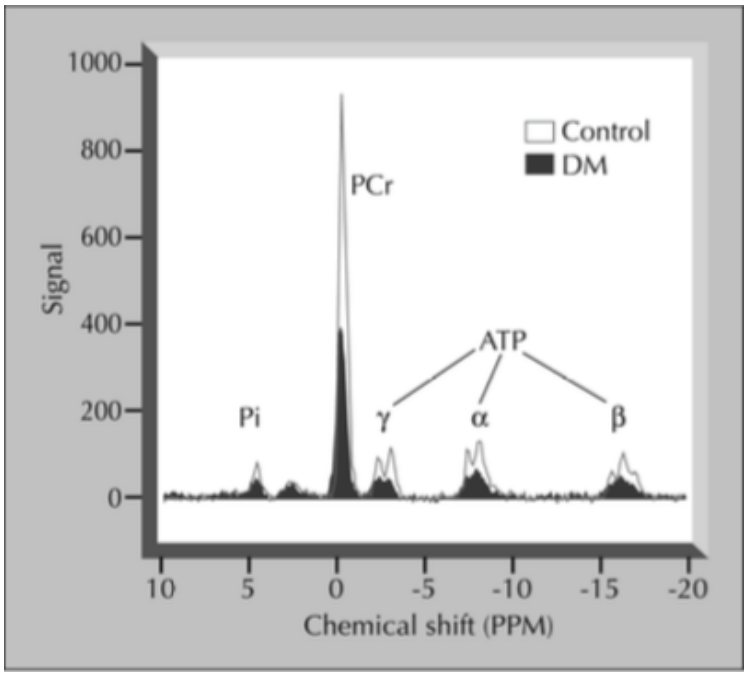

Figure 8.3. Quadriceps muscle MRS spectrum from Park et al. (2001) showing a decreased level of phosphocreatine (PCr) and ATP with a musculoskeletal condition.

MRS has been shown to be an affective measure of muscle biochemistry, particularly in myopathy, muscle contractions and muscle fatigue. By implementing MRS with future MRE research may result in correlations

between muscle stiffness and peaks in metabolites. Previous work has investigated a correlation with MRE and 31P-MRS (Godfrey et al., 2012) for the staging of liver fibrosis. Of the two techniques, MRE was found to be most effective, as fibrosis staging was not found to be correlated with MRS in this study. However, MRS has been shown to be significant measure of fibrosis in other investigations (Corbin et al., 2004; Dezortova et al., 2005), meaning future implementation of MRS and MRE could result in a correlation between changes in the mechanical properties and biochemistry of tissue.

8.4.3 Magnetic Resonance Thermography

As previously discussed, muscle use results in an increase in muscle metabolites (Maughan, 2012; Merla et al., 2010). Krustrup et al (2003) showed that a considerable amount of energy from contractions result in heat production. Heat production in muscles allows for longer periods of exercise whilst also reducing risk of injury (Tucker et al., 2004; Nybo, 2010). As a result of heat production during muscle use, the temperature of the skin increases, from warmed circulatory system near the skin surface (Taylor, 2000), dependent on the magnitude of activity (Akimov et al., 2010; Chudecka and Lubkowska, 2010; de Andrade Fernandes et al., 2014). When the body becomes excessively warm Tucker et al., (2004) found that there is a reduction in muscle recruitment and thus force output, which was determined to be a biophysical adaption in order maintain thermal homeostasis. Thermal maintenance is a vital aspect in sustained muscle contractions as it has been shown that heat related fatigue occurs when core temperature is above 40°C, as this temperature inhibits central nervous system functioning (Gonzalez-Alonso et al., 1999; Nielson et al., 1990; Nybo et al., 2001).

Heat dissipation is possible through exercise related sweating subsequently evaporating, cooling the body (Xu et al., 2013). Interestingly, there is an observable difference in the magnitude of heat produced between trained and untrained individuals (Abate et al., 2013; Formenti et al., 2013). As a result, the measurement of heat production can be used as a physiological measure of

muscle use. Quesada et al., (2015) investigated temperature change in muscles following a cycling exercise protocol finding an inverse relationship between heat production and activation of vastus lateralis, a key muscle force generator (Kautz and Neptune, 2002). Quesada et al also suggested that subcutaneous fat effects heat regulation, due to its role for insulation. In addition to this, it should be noted that subcutaneous fat has been shown to be reduced with higher levels of activity (Johnson et al., 2015).

Measurements of tissue temperature can be obtained through the method known as Magnetic Resonance Thermography (MRT). The method of MRT can be performed on much of the understanding from MRS imaging, and is an anticipated clinical imaging technique (Kuroda, 2005; Lüdemann et al., 2010), as early investigations have shown promising results for the musculoskeletal system (Mietzsch et al., 1998), and also in offering highly detailed non-invasive tissue characterisation through temperature differentials (Stauffer et al., 2009; Gellerman et al., 2006; Figure 8.4).

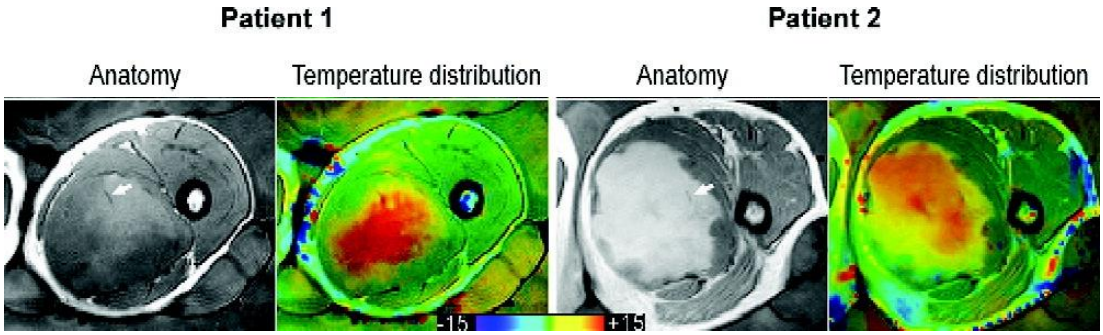

Figure 8.4. Example of image output for MRT, showing anatomical images and relative temperature distributions (Adapted from Gellerman et al., 2006).

Magnetic Resonance Thermography may offer aid to MRE as Kruse et al. (2000) showed that the viscoelastic properties of tissue may change depending on temperature. Future clinical investigations could incorporate the measurements of temperature in order to measure muscle fatigue or muscle strain, as well as differences between heat production before and after clinical interventions.

8.4.4. Summary of Future MR Imaging

The three additional imaging modalities mentioned here, DTI, MRS, and MRT, each offer insight in the pathophysiology of tissue. As shown through this thesis, the combination of physical, mechanical and functional measures of musculoskeletal tissue resulted in new insight into muscle use, injury, and recovery. If future MRE research were to then also include measurements of tissue microstructure through DTI, muscle metabolism through MRS, and the temperature change of muscle from MRT, then this will result in a holistic pathophysiological approach to better understanding the pathophysiology of the musculoskeletal system.

8.5 Thesis Conclusion

In this thesis, the applications of MRE in the musculoskeletal system has been explored through a series of clinical investigations. Applications of MRE consisted of immobility, ageing, muscle injury, muscle morphology and applied muscle morphology following TKR surgery. Within each of the chapters of this thesis the utility of MRE has revealed additional anatomical information, not obtainable through conventional imaging.

Chapters Three and Four both investigate passive changes in the musculoskeletal system. Chapter Three showed that the ageing process significantly impacts the musculoskeletal system, observed through muscle atrophy and increasing muscle stiffness. The Quadriceps muscle group were identified as being particularly affected by the ageing process, with atrophy of the anti-gravity muscle group resulting in muscle stiffness increasing with age. The use of MRE in this investigation showed that increased muscle stiffness can be used as a biomarker for muscle damage. Chapter Four showed that muscle stiffness and size are sensitive biomarkers to the health of a patient, with both decreasing due to immobility, and then increasing with the health of convalesced patients. An additional finding revealed by MRE was that overall muscle size and stiffness increased following convalescence. A key finding in

this study was that there was a differential in healthy controls and ICU patients in the mechanical and morphological relationship within vastus medialis.

Following on from this result, Chapters Five, Six, and Seven examined the changes in the musculoskeletal system following some form of manipulation or intervention. Chapter Five investigated whether residual increase of stiffness of damaged muscles could identify engagement strategy during time of injury. The results of this chapter showed that level of exertion was secondary to muscle engagement for determining injury severity. Those without oedema induced injury engaged a strong combination of muscles with complimentary functions. Analysis of residual muscle stiffness increases revealed a different functional participation in the muscle damage paradigm in individuals who were damaged to a greater severity. Individuals with oedema had incorporated hip flexion as well as knee extension, resulting in greater damage and oedema.

Chapter Six examined changes in muscle morphology and mechanical properties during muscle engagement as a biomarker for muscle stress. Chapter Six showed that in addition to muscle size and muscle stiffness, the axial circularity of a muscle changes with increased loading. During knee extension, rectus femoris showed a very significant correlation between the increase of muscle stiffness with both a decrease in cross sectional area and an increase in axial circularity. This relationship observed in rectus femoris was stronger than that observed in the vasti muscles during knee extension. As a result, MRE revealed that the difference in muscle architecture between bi-articular and mono-articular muscles, as a possible physiological adaption for bi-articular muscles producing more muscle force. Chapter Seven showed that following a surgical intervention of total knee replacement (TKR) in osteoarthrosis (OA) patients revealed a significant decrease in muscle tension. In addition to this, the morphological change in rectus femoris was significantly lower in performing knee extension following TKR.

This thesis has shown that MRE can offer additional physiological insight into the health of muscles for a range of clinical applications, over conventional imaging methods. MRE could be improved significantly by being paired with DTI, MRS, or MRT. By utilising DTI, muscle microstructures could be revealed, such as muscle fibre length, pennation, and density, for a greater appreciation of anatomical strength. MRS may be able to show biochemical changes in the muscle, whilst MRT may be able to show heat production in muscle. By combining these anatomical and physiological features with MRE could allow for a more precise measurement of musculoskeletal healthy following atrophy, use, or injury.

However, there are some questions still unanswered which would aid future musculoskeletal MRE work. The work in this thesis has focussed primarily on relative changes in muscle stiffness through either use, injury or recovery. This has meant that an all-encompassing stiffness level has not been established. As a result, so far there is not a single level of muscle stiffness which would indicate the musculoskeletal health of an individual and in order to do this will require significant further research. If this were developed then this would allow for a much better appreciation of viscoelastic changes in muscle, as opposed to there being a requirement for analysis of relative changes in muscle. Also, future work should look to include reliable quantification of tissue viscosity. It appears that at this time measurements of viscosity alone are not a reliable source of data, however if methods were developed to address this then this may add an even greater appreciation to muscle physiology over just muscle stiffness. Finally, a key problem in MRE is that there is a wide range of methodologies, imaging protocols, and data visualisation techniques. Additionally, MRE would benefit greatly from advances in imaging protocols which allow for a full thigh image acquisition sequence. Future musculoskeletal MRE work should aim to work towards a unifying approach to examine muscle tissue, to aid in comparison between research outcomes. As shown in this thesis, by remaining with a largely single imaging protocol, analysis technique and data visualisation methodology it allows for an appreciation of the results with limited difficulty or the requirement of significant MRE experience.

In conclusion, this thesis has shown that the implementation of Magnetic Resonance Elastography in clinical musculoskeletal investigations results in promising biomechanical insight. A key aspect of this thesis is the identification of muscle engagement strategy through increased muscle stiffness following use and injury, in addition to the relationship between morphology and mechanical properties of muscle. The quantification of changes in muscle mechanical properties during engagement allows for identification of co-contraction patterns, which may offer new biomarkers for characterising individual muscles for potential injury, instability, or weakness. In addition to this, the finding of a potential muscle tension biomarker through the combination of muscle morphology and mechanical properties during use showed physiological insight into the differences in muscles with varying architecture. Work within this thesis has shown that MRE measures are reliable between investigators, able to precisely identify regions of increased injury, and also able to show mechanical changes in both the passive and active states of muscle. As a result, this thesis has shown that the implementation of MRE in musculoskeletal research may offer future musculoskeletal research previously unobtainable insight into physiology. If MRE is paired with additional imaging techniques and functional measures, then this new and non-invasive methodology may be used as a holistic approach to studying musculoskeletal physiology. This approach could be a strong basis in measuring the performance of athletes, the recovery of patients, or potentially used as a biomarker to identify reasoning for those susceptible to musculoskeletal injuries.

References

Aagaard P, Andersen JL, Dyhre-Poulsen P, Leffers AM, Wagner A, Magnusson SP, Halkjær-Kristensen J, Simonsen EB. A mechanism for increased contractile strength of human pennate muscle in response to strength training: changes in muscle architecture. The journal of physiology. 2001 Jul 1;534(2):613-23.

Aagaard P, Andersen JL, Dyhre-Poulsen P, Leffers AM, Wagner A, Magnusson SP, Halkjær-Kristensen J, Simonsen EB. A mechanism for increased contractile strength of human pennate muscle in response to strength training: changes in muscle architecture. The journal of physiology. 2001 Jul 1;534(2):613-23.

Aagaard P, Simonsen EB, Andersen JL, Magnusson P, Dyhre-Poulsen P. Increased rate of force development and neural drive of human skeletal muscle following resistance training. Journal of applied physiology. 2002 Oct 1;93(4):1318-26.

Aagaard P, Simonsen EB, Andersen JL, Magnusson SP, Bojsen-Møller F, Dyhre-Poulsen P. Antagonist muscle coactivation during isokinetic knee extension. Scandinavian journal of medicine & science in sports. 2000 Apr 1;10(2):58-67.

Abate M, Di Carlo L, Di Donato L, Romani GL, Merla A. Comparison of cutaneous thermic response to a standardised warm up in trained and untrained individuals. Journal of Sports Medicine and Physical Fitness. 2013 Apr 1;26(53):18-37.

Abbott BC, Wilkie DR. The relation between velocity of shortening and the tension-length curve of skeletal muscle. The Journal of Physiology. 1953 Apr 28;120(1-2):214-23.

Abe T, Kumagai K, Brechue WF. Fascicle length of leg muscles is greater in sprinters than distance runners. Medicine and science in sports and exercise. 2000 Jun 1;32(6):1125-9.

Agung M, Ochi M, Yanada S, Adachi N, Izuta Y, Yamasaki T, Toda K. Mobilization of bone marrow-derived mesenchymal stem cells into the injured tissues after intraarticular injection and their contribution to tissue regeneration. Knee Surgery, Sports Traumatology, Arthroscopy. 2006 Dec 1;14(12):1307-14.

Aisen AM, Martel W, Braunstein EM, McMillin KI, Phillips WA, Kling TF. MRI and CT evaluation of primary bone and soft-tissue tumors. American journal of Roentgenology. 1986 Apr 1;146(4):749-56.

Akimov EB, Andreev RS, Kalenov YN, Kirdin AA, Son'kin VD, Tonevitsky AG. The human thermal portrait and its relations with aerobic working capacity and the blood lactate level. Human physiology. 2010 Jul 1;36(4):447-56.

Alexander AL, Lee JE, Lazar M, Field AS. Diffusion tensor imaging of the brain. Neurotherapeutics. 2007 Jul 1;4(3):316-29.

Allen DG, Whitehead NP, Yeung EW. Mechanisms of stretch-induced muscle damage in normal and dystrophic muscle: role of ionic changes. The Journal of physiology. 2005 Sep 1;567(3):723-35.

Alnaqeeb MA, Al Zaid NS, Goldspink G. Connective tissue changes and physical properties of developing and ageing skeletal muscle. Journal of Anatomy. 1984 Dec;139(Pt 4):677.

Ameln H, Gustafsson T, Sundberg CJ, Okamoto K, Jansson E, Poellinger L, Makino Y. Physiological activation of hypoxia inducible factor-1 in human skeletal muscle. The FASEB journal. 2005 Jun;19(8):1009-11.

Andersen OS. 50-year anniversary of sliding filament. The Journal of general physiology. 2004 Jun 1;123(6):629-.

Aniansson A, Grimby G, Hedberg M, Krotkiewski M. Muscle morphology, enzyme activity and muscle strength in elderly men and women. Clinical Physiology and Functional Imaging. 1981 Feb 1;1(1):73-86.

Appell HJ. Morphology of immobilized skeletal muscle and the effects of a pre-and postimmobilization training program. International journal of sports medicine. 1986 Feb;7(01):6-12.

Armstrong RB, Saubert C, Seeherman HJ, Taylor CR. Distribution of fiber types in locomotory muscles of dogs. Developmental Dynamics. 1982 Jan 1;163(1):87-98.

Arthritis Research UK National Primary Care Centre, Keele University, "Musculoskeletal Matters: Bulletin 1," 2009.

Arthritis Research UK, "State of Musculoskeletal Health", 2018.

Arthritis Research UK, "Musculoskeletal conditions and multimorbidity,"2017.

Arthritis Research UK, "Osteoarthritis in General Practice," 2013.

Arthritis Research UK, "The Musculoskeletal Calculator," 2015.

Arthritis Research UK, "Working with arthritis," 2016.

Artz N, Elvers KT, Lowe CM, Sackley C, Jepson P, Beswick AD. Effectiveness of physiotherapy exercise following total knee replacement: systematic review and meta-analysis. BMC musculoskeletal disorders. 2015 Dec;16(1):15.

Asbach P, Klatt D, Schlosser B, Biermer M, Muche M, Rieger A, Loddenkemper C, Somasundaram R, Berg T, Hamm B, Braun J. Viscoelasticity-based staging of hepatic fibrosis with multifrequency MR elastography. Radiology. 2010 Oct;257(1):80-6.

B. Choi, J. Verbeek, W. Tam and J. Jiang,"Exercises for prevention of recurrences of lowback pain," The Cochrane Database for Systematic Reviews, vol. 1, 2010.

Backhaus M, Burmester GR, Gerber TH, Grassi W, Machold KP, Swen WA, Wakefield RJ, Manger B. Guidelines for musculoskeletal ultrasound in rheumatology. Annals of the rheumatic diseases. 2001 Jul 1;60(7):641-9.

Baratta R, Solomonow M, Zhou BH, Letson D, Chuinard R, D'ambrosia R. Muscular coactivation: the role of the antagonist musculature in maintaining knee stability. The American journal of sports medicine. 1988 Mar;16(2):113-22.

Barnhill E, Hollis L, Sack I, Braun J, Hoskins PR, Pankaj P, Brown C, van Beek EJ, Roberts N. Nonlinear multiscale regularisation in MR elastography: Towards fine feature mapping. Medical image analysis. 2017 Jan 1;35:133-45.

Barnhill E, Kennedy P, Hammer S, van Beek EJ, Brown C, Roberts N. Statistical mapping of the effect of knee extension on thigh muscle viscoelastic properties using magnetic resonance elastography. Physiological measurement. 2013 Nov 20;34(12):1675.

Barnhill E, Kennedy P, Johnson CL, Mada M, Roberts N. Real-time 4D phase unwrapping applied to magnetic resonance elastography. Magnetic resonance in medicine. 2015 Jun 1;73(6):2321-31.

Basford JR, Jenkyn TR, An KN, Ehman RL, Heers G, Kaufman KR. Evaluation of healthy and diseased muscle with magnetic resonance elastography. Archives of physical medicine and rehabilitation. 2002 Nov 1;83(11):1530-6.

Basser PJ, Mattiello J, LeBihan D. MR diffusion tensor spectroscopy and imaging. Biophysical journal. 1994 Jan 1;66(1):259-67.

Basser PJ, Pajevic S, Pierpaoli C, Duda J, Aldroubi A. In vivo fiber tractography using DT-MRI data. Magnetic resonance in medicine. 2000 Oct 1;44(4):625-32.

Bensamoun SF, Charleux F, Debernard L, Themar-Noel C, Voit T. Elastic properties of skeletal muscle and subcutaneous tissues in Duchenne muscular dystrophy by magnetic resonance elastography (MRE): a feasibility study. Irbm. 2015 Feb 1;36(1):4-9.

Bensamoun SF, Glaser KJ, Ringleb SI, Chen Q, Ehman RL, An KN. Rapid magnetic resonance elastography of muscle using one-dimensional projection. Journal of Magnetic Resonance Imaging. 2008 May 1;27(5):1083-8.

Bensamoun SF, Ringleb SI, Chen Q, Ehman RL, An KN, Brennan M. Thigh muscle stiffness assessed with magnetic resonance elastography in hyperthyroid patients before and after medical treatment. Journal of Magnetic Resonance Imaging. 2007 Sep 1;26(3):708-13.

Bensamoun SF, Ringleb SI, Littrell L, Chen Q, Brennan M, Ehman RL, An KN. Determination of thigh muscle stiffness using magnetic resonance elastography. Journal of Magnetic Resonance Imaging. 2006 Feb 1;23(2):242-7.

Boger DV. Viscoelastic flows through contractions. Annual review of fluid mechanics. 1987 Jan;19(1):157-82.

Booth FW. Effect of limb immobilization on skeletal muscle. Journal of applied physiology. 1982 May 1;52(5):1113-8.

Borkin M, Gajos K, Peters A, Mitsouras D, Melchionna S, Rybicki F, Feldman C, Pfister H. Evaluation of artery visualizations for heart disease diagnosis. IEEE transactions on visualization and computer graphics. 2011 Dec;17(12):2479-88.

British Orthopaedic Association, "The Care of Patients with Fragility Fractures", British Orthopaedic Association, 2007.

Bruce SA, Newton D, Woledge RC. Effect of Age on Voluntary Force and Cross-Sectional Area of Human Adductor Pollicis Muscle. Experimental Physiology. 1989 May 16;74(3):359-62.

Bureau NJ, Cardinal E, Chhem RK. Ultrasound of soft tissue masses. Semin Musculoskelet Radiol 1998;2:283–298.

Burkholder TJ, Fingado B, Baron S, Lieber RL. Relationship between muscle fiber types and sizes and muscle architectural properties in the mouse hindlimb. Journal of morphology. 1994 Aug 1;221(2):177-90.

Burlew MM, Madsen EL, Zagzebski JA, Banjavic RA, Sum SW. A new ultrasound tissue-equivalent material. Radiology. 1980 Feb;134(2):517-20.

Burnham EL, Moss M, Ziegler TR. Myopathies in critical illness: characterization and nutritional aspects. The Journal of nutrition. 2005 Jul 1;135(7):1818S-23S.

Callaghan PT. Principles of nuclear magnetic resonance microscopy. Oxford University Press on Demand; 1993.

Campbell MJ, McComas AJ, Petito F. Physiological changes in ageing muscles. Journal of Neurology, Neurosurgery & Psychiatry. 1973 Apr 1;36(2):174-82.

Casaer MP, Langouche L, Coudyzer W, Vanbeckevoort D, De Dobbelaer B, Güiza FG, Wouters PJ, Mesotten D, Van den Berghe G. Impact of early parenteral nutrition on muscle and adipose tissue compartments during critical illness. Critical care medicine. 2013 Oct 1;41(10):2298-309.

Castéra L, Vergniol J, Foucher J, Le Bail B, Chanteloup E, Haaser M, Darriet M, Couzigou P, de Lédinghen V. Prospective comparison of transient elastography, Fibrotest, APRI, and liver biopsy for the assessment of fibrosis in chronic hepatitis C. Gastroenterology. 2005 Feb 1;128(2):343-50.

Catheline S, Gennisson JL, Delon G, Fink M, Sinkus R, Abouelkaram S, Culioli J. Measurement of viscoelastic properties of homogeneous soft solid using transient elastography: An inverse problem approach. J Acoust Soc Am 116: 3734, 2004.

Cavanagh PR, Komi PV. Electromechanical delay in human skeletal muscle under concentric and eccentric contractions. European journal of applied physiology and occupational physiology. 1979 Nov 1;42(3):159-63.

Cercignani M, Inglese M, Pagani E, Comi G, Filippi M. Mean diffusivity and fractional anisotropy histograms of patients with multiple sclerosis. American Journal of Neuroradiology. 2001 May 1;22(5):952-8.

Chakouch MK, Charleux F, Bensamoun SF. New magnetic resonance elastography protocols to characterise deep back and thigh muscles.

Computer methods in biomechanics and biomedical engineering. 2014 Aug 6;17(sup1):32-3.

Challiss RA, Hayes DJ, Radda GK. A 31P-nmr study of the acute effects of β-blockade on the bioenergetics of skeletal muscle during contraction. Biochemical Journal. 1987 Aug 15;246(1):163-72.

Chance B, Leigh JS, Clark BJ, Maris J, Kent J, Nioka S, Smith D. Control of oxidative metabolism and oxygen delivery in human skeletal muscle: a steady-state analysis of the work/energy cost transfer function. Proceedings of the National Academy of Sciences. 1985 Dec 1;82(24):8384-8.

Childs JD, Sparto PJ, Fitzgerald GK, Bizzini M, Irrgang JJ. Alterations in lower extremity movement and muscle activation patterns in individuals with knee osteoarthritis. Clinical biomechanics. 2004 Jan 1;19(1):44-9.

Chudecka M, Lubkowska A. The use of thermal imaging to evaluate body temperature changes of athletes during training and a study on the impact of physiological and morphological factors on skin temperature. Human Movement. 2012 Mar 1;13(1):33-9.

Clark BC, Manini TM. Sarcopenia≠ dynapenia. The Journals of Gerontology Series A: Biological Sciences and Medical Sciences. 2008 Aug 1;63(8):829-34.

Clavet H, Hébert PC, Fergusson D, Doucette S, Trudel G. Joint contracture following prolonged stay in the intensive care unit. Canadian Medical Association Journal. 2008 Mar 11;178(6):691-7.

Close RI. Dynamic properties of mammalian skeletal muscles. Physiological reviews. 1972 Jan;52(1):129-97.

Coakley JH, Nagendran K, Yarwood GD, Honavar M, Hinds CJ. Patterns of neurophysiological abnormality in prolonged critical illness. Intensive care medicine. 1998 Aug 1;24(8):801-7.

Conturo TE, Lori NF, Cull TS, Akbudak E, Snyder AZ, Shimony JS, McKinstry RC, Burton H, Raichle ME. Tracking neuronal fiber pathways in the living human brain. Proceedings of the National Academy of Sciences. 1999 Aug 31;96(18):10422-7.

Corbin IR, Ryner LN, Singh H, Minuk GY. Quantitative hepatic phosphorus-31 magnetic resonance spectroscopy in compensated and decompensated cirrhosis. American Journal of Physiology-Gastrointestinal and Liver Physiology. 2004 Aug 1;287(2):G379-84.

Coyle EF, Costill DL, Lesmes GR. Leg extension power and muscle fiber composition. Med Sci Sports. 1979 Jan 1;11(1):12-5.

Cullingham PJ, Lind AR, Morton RJ. The maximal isometric tetanic tensions developed by mammalian muscle, in situ, at different temperatures. Experimental Physiology. 1960 Apr 7;45(2):142-56.

Dawson MJ, Gadian DG. Studies of the biochemistry of contracting and relaxing muscle by the use of 31P nmr in conjunction with other techniques. Phil. Trans. R. Soc. Lond. B. 1980 Jun 25;289(1037):445-55

de Andrade Fernandes A, dos Santos Amorim PR, Brito CJ, de Moura AG, Moreira DG, Costa CM, Sillero-Quintana M, Marins JC. Measuring skin temperature before, during and after exercise: a comparison of thermocouples and infrared thermography. Physiological measurement. 2014 Jan 7;35(2):189.

De Jonghe B, Lacherade JC, Durand MC, Sharshar T. Critical illness neuromuscular syndromes. Critical care clinics. 2006 Oct 1;22(4):805-18.

De Seze M, Petit H, Wiart L, Cardinaud JP, Gaujard E, Joseph PA, Mazaux JM, Barat M. Critical illness polyneuropathy. European neurology. 2000;43(2):61-9.

Debernard L, Leclerc GE, Robert L, Charleux F, Bensamoun SF. In vivo characterization of the muscle viscoelasticity in passive and active conditions using multifrequency MR elastography. Journal of Musculoskeletal Research. 2013 Jun;16(02):1350008.

Debernard L, Leclerc GE, Robert L, Charleux F, Bensamoun SF. In vivo characterization of the muscle viscoelasticity in passive and active conditions using multifrequency MR elastography. Journal of Musculoskeletal Research. 2013 Jun;16(02):1350008.

Debernard L, Robert L, Charleux F, Bensamoun SF. Analysis of thigh muscle stiffness from childhood to adulthood using magnetic resonance elastography (MRE) technique. Clinical biomechanics. 2011b Oct 1;26(8):836-40.

Debernard L, Robert L, Charleux F, Bensamoun SF. Characterization of muscle architecture in children and adults using magnetic resonance elastography and ultrasound techniques. Journal of biomechanics. 2011a Feb 3;44(3):397-401.

Department of Health Statistics and Research, "Health Survey Northern Ireland 2016-17: Trend Tables," 2017.

Dezortova M, Taimr P, Skoch A, Spicak J, Hajek M. Etiology and functional status of liver cirrhosis by 31P MR spectroscopy. World journal of gastroenterology. 2005 Nov 28;11(44):6926.

Dirks ML, Wall BT, Snijders T, Ottenbros CL, Verdijk LB, Loon LJ. Neuromuscular electrical stimulation prevents muscle disuse atrophy during leg immobilization in humans. Acta physiologica. 2014 Mar 1;210(3):628-41.

Ditroilo M, Hunter AM, Haslam S, De Vito G. The effectiveness of two novel techniques in establishing the mechanical and contractile responses of biceps femoris. Physiol Meas. 2011;32(8):1315–26

Dittmer DK, Teasell RC. Complications of immobilization and bed rest. Part 1: Musculoskeletal and cardiovascular complications. Canadian Family Physician. 1993 Jun;39:1428.

Doherty TJ. Invited review: aging and sarcopenia. Journal of applied physiology. 2003 Oct 1;95(4):1717-27.

Domire ZJ, McCullough MB, Chen Q, An KN. Wave attenuation as a measure of muscle quality as measured by magnetic resonance elastography: Initial results. J Biomech 42: 537540, 2009.

Donaghy E, Salisbury L, Lone NI, Lee R, Ramsey P, Rattray JE, Walsh TS. Unplanned early hospital readmission among critical care survivors: a mixed methods study of patients and carers. BMJ Qual Saf. 2018 May 25:bmjqs-2017.

Doorenbosch CA, Harlaar J, Roebroeck ME, Lankhorst GJ. Two strategies of transferring from sit-to-stand; the activation of monoarticular and biarticular muscles. Journal of biomechanics. 1994 Nov 1;27(11):1299-307.

Doro LC, Ladd B, Hughes RE, Chenevert TL. Validation of an adapted MRI pulse sequence for quantification of fatty infiltration in muscle. Magnetic resonance imaging. 2009 Jul 1;27(6):823-7.

Dresner MA, Rose GH, Rossman PJ, Muthupillai R, Manduca A, Ehman RL. Magnetic resonance elastography of skeletal muscle. Journal of Magnetic Resonance Imaging. 2001 Feb 1;13(2):269-76.

Dresner MA, Rose GH, Rossman PJ, Smith JA, Muthupillai R, Ehman RL. Functional MR elastography of human skeletal muscle. InProc. of the 6th Conf. of the Intl. Soc. Magn. Reson. Med 1998 (Vol. 463).

Duchateau J, Hainaut K. Electrical and mechanical changes in immobilized human muscle. Journal of Applied Physiology. 1987 Jun 1;62(6):2168-73.

Ebenbichler G, Kollmitzer J, Quittan M, Uhl F, Kirtley C, Fialka V. EMG fatigue patterns accompanying isometric fatiguing knee-extensions are different in mono-and bi-articular muscles. Electroencephalography and Clinical Neurophysiology/Electromyography and Motor Control. 1998 Jun 1;109(3):256-62.

Eby SF, Cloud BA, Brandenburg JE, Giambini H, Song P, Chen S, LeBrasseur NK, An KN. Shear wave elastography of passive skeletal muscle stiffness: influences of sex and age throughout adulthood. Clinical biomechanics. 2015 Jan 1;30(1):22-7.

Edgerton VR, Barnard RJ, Peter JB, Maier A, Simpson DR. Properties of immobilized hind-limb muscles of the Galago senegalensis. Experimental neurology. 1975 Jan 1;46(1):115-31.

Eng CM, Smallwood LH, Rainiero MP, Lahey M, Ward SR, Lieber RL. Scaling of muscle architecture and fiber types in the rat hindlimb. Journal of Experimental Biology. 2008 Jul 15;211(14):2336-45.

Essén-Gustavsson B, Borges O. Histochemical and metabolic characteristics of human skeletal muscle in relation to age. Acta Physiologica. 1986 Jan 1;126(1):107-14.

Evans WJ, Lexell J. Human aging, muscle mass, and fiber type composition. The Journals of Gerontology Series A: Biological Sciences and Medical Sciences. 1995 Nov 1;50(Special_Issue):11-6.

Evans WJ. Sarcopenia: the age-related loss in skeletal muscle mass. InMusculoskeletal soft-tissue aging: impact on mobility. Colorado Springs, CO: American Academy of Orthopaedic Surgeons Symposium 1992 (pp. 217-227).

Evans WJ. What is sarcopenia?. The Journals of Gerontology Series A: Biological Sciences and Medical Sciences. 1995 Nov 1;50(Special_Issue):5-8.

Faulkner JA. Terminology for contractions of muscles during shortening, while isometric, and during lengthening. Journal of Applied Physiology. 2003 Aug;95(2):455-9.

Felson DT, Lawrence RC, Dieppe PA, Hirsch R, Helmick CG, Jordan JM, Kington RS, Lane NE, Nevitt MC, Zhang Y, Sowers M. Osteoarthritis: new insights. Part 1: the disease and its risk factors. Annals of internal medicine. 2000 Oct 17;133(8):635-46.

Felson DT. An update on the pathogenesis and epidemiology of osteoarthritis. Radiologic Clinics. 2004 Jan 1;42(1):1-9.

Felson DT. Osteoarthritis as a disease of mechanics. Osteoarthritis and cartilage. 2013 Jan 1;21(1):10-5.

Fielding RA, Manfredi TJ, Ding WE, Fiatarone MA, Evans WJ, Cannon JG. Acute phase response in exercise. III. Neutrophil and IL-1 beta accumulation in skeletal muscle. American Journal of Physiology-

Regulatory, Integrative and Comparative Physiology. 1993 Jul 1;265(1):R166-72.

Filon LN. On the elastic equilibrium of circular cylinders under certain practical systems of load. Proceedings of the Royal Society of London. 1901 Sep 1;68(442-450):353-8.

Finn PJ, Plank LD, Clark MA, Connolly AB, Hill GL. Progressive cellular dehydration and proteolysis in critically ill patients. The Lancet. 1996 Mar 9;347(9002):654-6.

Fischbach GD, Robbins N. Changes in contractile properties of disused soleus muscles. The Journal of physiology. 1969 Apr 1;201(2):305-20.

Fletcher SN, Kennedy DD, Ghosh IR, Misra VP, Kiff K, Coakley JH, Hinds CJ. Persistent neuromuscular and neurophysiologic abnormalities in long-term survivors of prolonged critical illness. Critical care medicine. 2003 Apr 1;31(4):1012-6.

Formenti D, Ludwig N, Gargano M, Gondola M, Dellerma N, Caumo A, Alberti G. Thermal imaging of exercise-associated skin temperature changes in trained and untrained female subjects. Annals of biomedical engineering. 2013 Apr 1;41(4):863-71.

Fornage BD. The case for ultrasound of muscles and tendons. Semin. Musculoskelet Radiol 2000;4:375–91.

Friden J, Lieber RL. Eccentric exercise-induced injuries to contractile and cytoskeletal muscle fibre components. Acta Physiologica. 2001 Mar 1;171(3):321-6.

Froeling M, Oudeman J, Strijkers GJ, Maas M, Drost MR, Nicolay K, Nederveen AJ. Muscle changes detected with diffusion-tensor imaging after long-distance running. Radiology. 2014 Oct 3;274(2):548-62.

Froese EA, Houston ME. Torque-velocity characteristics and muscle fiber type in human vastus lateralis. Journal of Applied Physiology. 1985 Aug 1;59(2):309-14.

Frontera WR, Hughes VA, Fielding RA, Fiatarone MA, Evans WJ, Roubenoff R. Aging of skeletal muscle: a 12-yr longitudinal study. Journal of applied physiology. 2000 Apr 1;88(4):1321-6.

Frontera WR, Hughes VA, Fielding RA, Fiatarone MA, Evans WJ, Roubenoff R. Aging of skeletal muscle: a 12-yr longitudinal study. Journal of applied physiology. 2000 Apr 1;88(4):1321-6.

Fung YC (Ed). Biomechanics, Mechanical Properties of Living Tissues. 2nd ed. New York: Springer-Verlag; 1993.

G. Jones, F. Atzeni, M. Beasley, E. Flus, P. Sarzi-Puttini and G. Macfarlane, "The prevalence of fibromyalgia in the general population: a comparison of the American College of Rheumatology 1990, 2010, and modified 2010 classification criteria," Arthritis & Rheumatology, vol. 67, no. 2, pp. 568-675, 2015.

Garnacho-Montero J, Madrazo-Osuna J, Garcia-Garmendia JL, Ortiz-Leyba C, Jiménez-Jiménez F, Barrero-Almodovar A, Garnacho-Montero M, Moyano-Del-Estad M. Critical illness polyneuropathy: risk factors and clinical consequences. A cohort study in septic patients. Intensive care medicine. 2001 Aug 1;27(8):1288-96.

Garrett JW. Muscle strain injuries: clinical and basic aspects. Medicine and Science in Sports and exercise. 1990 Aug;22(4):436-43.

Gellermann J, Hildebrandt B, Issels R, Ganter H, Wlodarczyk W, Budach V, Felix R, Tunn PU, Reichardt P, Wust P. Noninvasive magnetic resonance thermography of soft tissue sarcomas during regional

hyperthermia: correlation with response and direct thermometry. Cancer. 2006 Sep 15;107(6):1373-82.

Gibbon WW, Wakefield RJ. Ultrasound in inflammatory disease. Radiol Clin North Am 1999;37:633–51.

Gibson JN, Halliday D, Morrison WL, Stoward PJ, Hornsby GA, Watt PW, Murdoch G, Rennie MJ. Decrease in human quadriceps muscle protein turnover consequent upon leg immobilization. Clinical Science. 1987 Apr 1;72(4):503-9.

Global Burden of Disease Collaborative Network,"Global Burden of Disease Study 2016 (GBD 2016) Results," Institute for Health Metrics and Evaluation (IHME), Seattle, 2017.

Godfrey EM, Patterson AJ, Priest AN, Davies SE, Joubert I, Krishnan AS, Griffin N, Shaw AS, Alexander GJ, Allison ME, Griffiths WJ. A comparison of MR elastography and 31P MR spectroscopy with histological staging of liver fibrosis. European radiology. 2012 Dec 1;22(12):2790-7.

González-Alonso J, Teller C, Andersen SL, Jensen FB, Hyldig T, Nielsen B. Influence of body temperature on the development of fatigue during prolonged exercise in the heat. Journal of applied physiology. 1999 Mar 1;86(3):1032-9.

Goodpaster BH, Park SW, Harris TB, Kritchevsky SB, Nevitt M, Schwartz AV, Simonsick EM, Tylavsky FA, Visser M, Newman AB. The loss of skeletal muscle strength, mass, and quality in older adults: the health, aging and body composition study. The Journals of Gerontology Series A: Biological Sciences and Medical Sciences. 2006 Oct 1;61(10):1059-64.

Goss BC, McGee KP, Ehman EC, Manduca A, Ehman RL. Magnetic resonance elastography of the lung: technical feasibility. Magnetic resonance in medicine. 2006 Nov 1;56(5):1060-6.

Goss BC, McGee KP, Grimm RC, Rossman PJ, Ehman RL. Thermally Polarized 3He Magnetic Resonance Elastography: Initial Feasibility. In Proceeding of the 13th Annual Meeting of ISMRM 2005.

Gossman MR, Rose SJ, Sahrmann SA, Katholi CR. Length and circumference measurements in one-joint and multijoint muscles in rabbits after immobilization. Physical therapy. 1986 Apr 1;66(4):516-20.

Grassi W, Cervini C. Ultrasonography in rheumatology: an evolving technique. Ann Rheum Dis 1998;57:268–71.

Green MA, Geng G, Qin E, Sinkus R, Gandevia SC, Bilston LE. Measuring anisotropic muscle stiffness properties using elastography. NMR in Biomedicine. 2013 Nov 1;26(11):1387-94.

Green MA, Sinkus R, Gandevia SC, Herbert RD, Bilston LE. Measuring changes in muscle stiffness after eccentric exercise using elastography. NMR in Biomedicine. 2012 Jun;25(6):852-8.

Griffith DM, Lewis S, Rossi AG, Rennie J, Salisbury L, Merriweather JL, Templeton K, Walsh TS. Systemic inflammation after critical illness: relationship with physical recovery and exploration of potential mechanisms. Thorax. 2016 Apr 26.

Griffiths RD, Hall JB. Intensive care unit-acquired weakness. Critical care medicine. 2010 Mar 1;38(3):779-87.

Griffiths RD, Jones C. ABC of intensive care: recovery from intensive care. BMJ: British Medical Journal. 1999 Aug 14;319(7207):427.

Griffiths RD, Palmer TE, Helliwell T, Maclennan P, MacMillan RR. Effect of passive stretching on the wasting of muscle in the critically ill. Nutrition (Burbank, Los Angeles County, Calif.). 1995;11(5):428-32.

Griffiths RD. Muscle mass, survival, and the elderly ICU patient. Nutrition. 1996 Jun 1;12(6):456-8.

Grimby G, Saltin B. The ageing muscle. Clinical Physiology and Functional Imaging. 1983 Jun 1;3(3):209-18.

Grosset JF, Mora I, Lambertz D, Pérot C. Changes in stretch reflexes and muscle stiffness with age in prepubescent children. Journal of applied physiology. 2007 Jun;102(6):2352-60.

Gruther W, Benesch T, Zorn C, Paternostro-Sluga T, Quittan M, Fialka-Moser V, Spiss C, Kainberger F, Crevenna R. Muscle wasting in intensive care patients: ultrasound observation of the M. quadriceps femoris muscle layer. Journal of Rehabilitation Medicine. 2008 Mar 5;40(3):185-9.

Guarneri B, Bertolini G, Latronico N. Long-term outcome in patients with critical illness myopathy or neuropathy: the Italian multicentre CRIMYNE study. Journal of Neurology, Neurosurgery & Psychiatry. 2008 Jul 1;79(7):838-41.

Gujar SK, Maheshwari S, Björkman-Burtscher I, Sundgren PC. Magnetic resonance spectroscopy. Journal of neuro-ophthalmology. 2005 Sep 1;25(3):217-26.

Guo J, Hirsch S, Scheel M, Braun J, Sack I. Three-parameter shear wave inversion in MR elastography of incompressible transverse isotropic media: Application to in vivo lower leg muscles. Magnetic resonance in medicine. 2016 Apr 1;75(4):1537-45.

Häggmark T, Eriksson E, Jansson E. Muscle fiber type changes in human skeletal muscle after injuries and immobilization. Orthopedics. 1986 Feb 1;9(2):181-5.

Häkkinen K, Kraemer WJ, Kallinen M, Linnamo V, Pastinen UM, Newton RU. Bilateral and unilateral neuromuscular function and muscle cross-sectional area in middle-aged and elderly men and women. The Journals of Gerontology Series A: Biological Sciences and Medical Sciences. 1996 Jan 1;51(1):B21-9.

Häkkinen K, Newton RU, Gordon SE, McCormick M, Volek JS, Nindl BC, Gotshalk LA, Campbell WW, Evans WJ, Häkkinen A, Humphries BJ. Changes in muscle morphology, electromyographic activity, and force production characteristics during progressive strength training in young and older men. The Journals of Gerontology Series A: Biological Sciences and Medical Sciences. 1998 Nov 1;53(6):B415-23.

Harris T. Muscle mass and strength: relation to function in population studies. The Journal of nutrition. 1997 May 1;127(5):1004S-6S.

Heers G, Jenkyn T, Dresner MA, Klein MO, Basford JR, Kaufman KR, Ehman RL, An KN. Measurement of muscle activity with magnetic resonance elastography. Clinical Biomechanics. 2003 Jul 1;18(6):537-42.

Heiden TL, Lloyd DG, Ackland TR. Knee joint kinematics, kinetics and muscle co-contraction in knee osteoarthritis patient gait. Clinical biomechanics. 2009 Dec 1;24(10):833-41.

Helliwell TR, Coakley JH, Wagenmakers AJ, Griffiths RD, Campbell IT, Green CJ, McClelland P, Bone JM. Necrotizing myopathy in critically-ill patients. The Journal of pathology. 1991 Aug 1;164(4):307-14.

Helliwell TR, Wilkinson A, Griffiths RD, McClelland P, Palmer TE, Bone IM. Muscle fibre atrophy in critically ill patients is associated with the loss of myosin filaments and the presence of lysosomal enzymes and ubiquitin. Neuropathology and applied neurobiology. 1998 Dec 1;24(6):507-17.

Herridge MS, Cheung AM, Tansey CM, Matte-Martyn A. az-Granados N, Al-Saidi F, Cooper AB, Guest CB, Mazer CD, Mehta S, Stewart TE, Barr A, Cook D, Slutsky AS: One-year outcomes in survivors of the acute respiratory distress syndrome. N Engl J Med. 2003;348:683-93.

Herridge MS, Tansey CM, Matté A, Tomlinson G, Diaz-Granados N, Cooper A, Guest CB, Mazer CD, Mehta S, Stewart TE, Kudlow P. Functional disability 5 years after acute respiratory distress syndrome. New England Journal of Medicine. 2011 Apr 7;364(14):1293-304.pp.592-602.

Herridge MS. Legacy of intensive care unit-acquired weakness. Critical care medicine. 2009 Oct 1;37(10):S457-61.

Herridge MS. Long-term outcomes after critical illness. Current opinion in critical care. 2002 Aug 1;8(4):331-6.

Hess AR. Vertebrate slow muscle fibers. Physiological Reviews. 1970 Jan;50(1):40-62.

Hill AV. The heat of shortening and the dynamic constants of muscle. InProc. R. Soc. Lond. B 1938 Oct 10 (Vol. 126, No. 843, pp. 136-195). The Royal Society.

Hinman RS, Hunt MA, Creaby MW, Wrigley TV, McManus FJ, Bennell KL. Hip muscle weakness in individuals with medial knee osteoarthritis. Arthritis care & research. 2010 Aug 1;62(8):1190-3.

Hirsch S, Sack I, Braun J. Magnetic resonance elastography: physical background and medical applications. John Wiley & Sons; 2017 Mar 20.

Hiscox LV, Johnson CL, Barnhill E, McGarry MD, Huston 3rd J, Van Beek EJ, Starr JM, Roberts N. Magnetic resonance elastography (MRE) of the human brain: technique, findings and clinical applications. Physics in Medicine & Biology. 2016 Nov 15;61(24):R401.

Hiscox LV, Johnson CL, McGarry MD, Perrins M, Littlejohn A, van Beek EJR, Roberts N, Starr JM. High-resolution magnetic resonance elastography reveals differences in subcortical gray matter viscoelasticity between young and healthy older adults. Neurobiology of aging. 2018 May 1;65:158-67.

Hodgson CL, Walsh TS, Lone N. The long road home: are outcomes different for patients with sepsis?. Intensive care medicine. 2018 Jul 18.

Hollis L, Barnhill E, Conlisk N, Thomas-Seale LE, Roberts N, Pankaj P, Hoskins PR. Finite element analysis to compare the accuracy of the direct and MDEV inversion algorithms in MR elastography. IAENG Int J Comput Sci. 2016 May 1;43(2):137-46.

Hollis L, Barnhill E, Perrins M, Kennedy P, Conlisk N, Brown C, Hoskins PR, Pankaj P, Roberts N. Finite element analysis to investigate variability of MR elastography in the human thigh. Magnetic Resonance Imaging. 2017 Nov 1;43:27-36.

Holloszy JO, Faulkner JA, Brooks SV, Zerba E. Muscle atrophy and weakness with aging: contraction-induced injury as an underlying mechanism. The Journals of Gerontology Series A: Biological Sciences and Medical Sciences. 1995 Nov 1;50(Special Issue):124-9.

Holmberg S, Thelin A, Thelin N. Knee osteoarthritis and body mass index: a population-based case–control study. Scandinavian journal of rheumatology. 2005 Feb 1;34(1):59-64.

Hortobágyi T, DeVita P. Muscle pre-and coactivity during downward stepping are associated with leg stiffness in aging. Journal of Electromyography and Kinesiology. 2000 Apr 1;10(2):117-26.

Hough T. Ergographic studies in muscular soreness. American Physical Education Review. 1902 Mar 1;7(1):1-7.

Howell JN, Chleboun G, Conatser R. Muscle stiffness, strength loss, swelling and soreness following exercise-induced injury in humans. The Journal of physiology. 1993 May 1;464(1):183-96.

Hubley-Kozey C, Deluzio K, Dunbar M. Muscle co-activation patterns during walking in those with severe knee osteoarthritis. Clinical biomechanics. 2008 Jan 1;23(1):71-80.

Hubley-Kozey CL, Deluzio KJ, Landry SC, McNutt JS, Stanish WD. Neuromuscular alterations during walking in persons with moderate knee osteoarthritis. Journal of Electromyography and Kinesiology. 2006 Aug 1;16(4):365-78.

Hunter SK, Duchateau J, Enoka RM. Muscle fatigue and the mechanisms of task failure. Exercise and sport sciences reviews. 2004 Apr;32(2):44-9.

Huwart L, Salameh N, Ter Beek L, Vicaut E, Peeters F, Sinkus R, Van Beers BE. MR elastography of liver fibrosis: preliminary results comparing spin-echo and echo-planar imaging. European radiology. 2008b Nov 1;18(11):2535-41.

Huwart L, Sempoux C, Vicaut E, Salameh N, Annet L, Danse E, Peeters F, ter Beek LC, Rahier J, Sinkus R, Horsmans Y. Magnetic resonance

elastography for the noninvasive staging of liver fibrosis.Gastroenterology. 2008a Jul 1;135(1):32-40.

Huxley AF, Niedergerke R. Structural changes in muscle during contraction: interference microscopy of living muscle fibres. Nature. 1954 May;173(4412):971.

Huxley HE. Fifty years of muscle and the sliding filament hypothesis. The FEBS Journal. 2004 Apr 1;271(8):1403-15.

Ikai M, Fukunaga T. Calculation of muscle strength per unit cross-sectional area of human muscle by means of ultrasonic measurement. Internationale Zeitschrift für Angewandte Physiologie Einschliesslich Arbeitsphysiologie. 1968 Mar 1;26(1):26-32.

Isaacson AL, Hinkes MJ, Taylor SR. Contracture and twitch potentiation of fast and slow muscles of the rat at 20 and 37 C. American Journal of Physiology-Legacy Content. 1970 Jan 1;218(1):33-41.

J Braun, J Guo, R Lutzkendorf, J Stadler, S Papazoglou, S Hirsch, I Sack, and J Bernarding. "High-resolution mechanical imaging of the human brain by three-dimensional multifrequency magnetic resonance elastography at 7T." Neuroimage, vol. 90, pp. 308-314, 2014.

Jacob TC, Penn NE, Giebink J, Bastien R. A comparison of breast self-examination and clinical examination. Journal of the National Medical Association. 1994 Jan;86(1):40.

Jacobs R, Bobbert MF, van Ingen Schenau GJ. Mechanical output from individual muscles during explosive leg extensions: the role of biarticular muscles. Journal of biomechanics. 1996 Apr 1;29(4):513-23.

James SF. Contractures in orthopaedic and neurological conditions: a review of causes and treatment. Disability and rehabilitation. 2001 Jan 1;23(13):549-58.

Jeffery RS, Morris RW, Denham RA. Coronal alignment after total knee replacement. Bone & Joint Journal. 1991 Sep 1;73(5):709-14.

Jenkyn TR, Ehman RL, An KN. Noninvasive muscle tension measurement using the novel technique of magnetic resonance elastography (MRE). Journal of biomechanics. 2003 Dec 1;36(12):1917-21.

Johnson CL, McGarry MD, Gharibans AA, Weaver JB, Paulsen KD, Wang H, Olivero WC, Sutton BP, Georgiadis JG. Local mechanical properties of white matter structures in the human brain. Neuroimage. 2013 Oct 1;79:145-52.

Johnson MA, Polgar J, Weightman D, Appleton D. Data on the distribution of fibre types in thirty-six human muscles: an autopsy study. Journal of the neurological sciences. 1973 Jan 1;18(1):111-29.

Johnson W, de Ruiter I, Kyvik KO, Murray AL, Sørensen TI. Genetic and environmental transactions underlying the association between physical fitness/physical exercise and body composition. Behavior genetics. 2015 Jan 1;45(1):84-105.

Jolesz F, Sreter FA. Development, innervation, and activity-pattern induced changes in skeletal muscle. Annual Review of Physiology. 1981 Mar;43(1):531-52.

Jones CJ, Rikli RE, Beam WC. A 30-s chair-stand test as a measure of lower body strength in community-residing older adults. Research quarterly for exercise and sport. 1999 Jun 1;70(2):113-9.

Jones DA, Rutherford OM. Human muscle strength training: the effects of three different regimens and the nature of the resultant changes. The Journal of physiology. 1987 Oct 1;391(1):1-1.

Jones DK, Leemans A. Diffusion tensor imaging. InMagnetic resonance neuroimaging 2011 (pp. 127-144). Humana Press.

Jones DK, Simmons A, Williams SC, Horsfield MA. Non-invasive assessment of axonal fiber connectivity in the human brain via diffusion tensor MRI. Magnetic Resonance in Medicine. 1999 Jul 1;42(1):37-41.

Kane D, Grassi W, Sturrock R, Balint PV. Musculoskeletal ultrasound—a state of the art review in rheumatology. Part 2: clinical indications for musculoskeletal ultrasound in rheumatology. Rheumatology. 2004 May 25;43(7):829-38.

Kautz SA, Neptune RR. Biomechanical determinants of pedaling energetics: internal and external work are not independent. Exercise and sport sciences reviews. 2002 Oct 1;30(4):159-65.

Kawakami Y, Akima H, Kubo K, Muraoka Y, Hasegawa H, Kouzaki M, Imai M, Suzuki Y, Gunji A, Kanehisa H, Fukunaga T. Changes in muscle size, architecture, and neural activation after 20 days of bed rest with and without resistance exercise. European journal of applied physiology. 2001 Feb 1;84(1-2):7-12.

Kennedy P, Macgregor LJ, Barnhill E, Johnson CL, Perrins M, Hunter A, Brown C, Beek EJR, Roberts N. Application of magnetic resonance elastography (MRE) to measure the effect of warm-up using deep heat rub on muscle stiffness following exercise induced muscle damage (EIMD). Journal of Magnetic Resonance Imaging. 2017 Oct 1;46(4):1115-27.

Kent-Braun JA, McCully KK, Chance B. Metabolic effects of training in humans: a 31P-MRS study. Journal of Applied Physiology. 1990 Sep 1;69(3):1165-70.

Kermarrec E, Budzik JF, Khalil C, Le Thuc V, Hancart-Destee C, Cotten A. In vivo diffusion tensor imaging and tractography of human thigh muscles in healthy subjects. American Journal of Roentgenology. 2010 Nov;195(5):W352-6.

Klatt D, Friedrich C, Korth Y, Vogt R, Braun J, Sack I. 55 Viscoelastic properties of liver measured by oscillatory rheometry and multifrequency magnetic resonance elastography. Biorheology 47: 133141, 2010.

Klatt D, Papazoglou S, Braun J, Sack I. Viscoelasticity-based MR elastography of skeletal muscle. Physics in Medicine & Biology. 2010 Oct 15;55(21):6445.

Knowles JR. Enzyme-catalyzed phosphoryl transfer reactions. Annual review of biochemistry. 1980 Jul;49(1):877-919.

Kortebein P, Ferrando A, Lombeida J, Wolfe R, Evans WJ. Effect of 10 days of bed rest on skeletal muscle in healthy older adults. Jama. 2007 Apr 25;297(16):1769-74.

Kortebein P, Symons TB, Ferrando A, Paddon-Jones D, Ronsen O, Protas E, Conger S, Lombeida J, Wolfe R, Evans WJ. Functional impact of 10 days of bed rest in healthy older adults. The Journals of Gerontology Series A: Biological Sciences and Medical Sciences. 2008 Oct 1;63(10):1076-81.

Krans JL. The sliding filament theory of muscle contraction. Nature Education. 2010;3(9):66.

Kruse SA, Rose GH, Glaser KJ, Manduca A, Felmlee JP, Jack Jr CR, Ehman RL. Magnetic resonance elastography of the brain. Neuroimage. 2008 Jan 1;39(1):231-7.

Kruse SA, Smith JA, Lawrence AJ, Dresner MA, Manduca AJ, Greenleaf JF, Ehman RL. Tissue characterization using magnetic resonance elastography: preliminary results. Physics in Medicine & Biology. 2000 Jun;45(6):1579.

Kruse SA, Smith JA, Lawrence AJ, Dresner MA, Manduca AJ, Greenleaf JF, Ehman RL. Tissue characterization using magnetic resonance elastography: preliminary results. Physics in Medicine & Biology. 2000 Jun;45(6):1579.

Krustrup P, Ferguson RA, Kjær M, Bangsbo J. ATP and heat production in human skeletal muscle during dynamic exercise: higher efficiency of anaerobic than aerobic ATP resynthesis. The Journal of physiology. 2003 May 1;549(1):255-69.

Kuroda K. Non-invasive MR thermography using the water proton chemical shift. International Journal of Hyperthermia. 2005 Sep 1;21(6):547-60.

Landin D, Thompson M, Reid M. Actions of Two Bi-Articular Muscles of the Lower Extremity: A Review. Journal of clinical medicine research. 2016 Jul;8(7):489.

Laneuville O, Zhou J, Uhthoff HK, Trudel G. Genetic influences on joint contractures secondary to immobilization. Clinical Orthopaedics and Related Research. 2007 Mar 1;456:36-41.

Lansdown DA, Ding Z, Wadington M, Hornberger JL, Damon BM. Quantitative diffusion tensor MRI-based fiber tracking of human

skeletal muscle. Journal of Applied Physiology. 2007 Aug;103(2):673-81.

Larsson L. Morphological and functional characteristics of the aging skeletal muscle in man. Acta Physiol. Scand. Suppl. 1978;457:1-36.

Latronico N, Recupero D, Candiani A, Guarneri B, De Maria G, Antonini L, Fenzi F, Tomelleri G, Tonin P, Rizzuto N. Critical illness myopathy and neuropathy. The Lancet. 1996 Jun 8;347(9015):1579-82.

Laughton CA, Slavin M, Katdare K, Nolan L, Bean JF, Kerrigan DC, Phillips E, Lipsitz LA, Collins JJ. Aging, muscle activity, and balance control: physiologic changes associated with balance impairment. Gait & posture. 2003 Oct 1;18(2):101-8.

Laukkanen PI, Heikkinen E, Kauppinen M. Muscle strength and mobility as predictors of survival in 75–84-year-old people. Age and Ageing. 1995 Nov 1;24(6):468-73.

Levitan IB, Kaczmarek LK. The neuron: cell and molecular biology. Oxford University Press, USA; 2015.pp. 153–328.

Lewek MD, Rudolph KS, Snyder-Mackler L. Control of frontal plane knee laxity during gait in patients with medial compartment knee osteoarthritis. Osteoarthritis and Cartilage. 2004 Sep 1;12(9):745-51.

Lexell J, Henriksson-Larsén K, Winblad B, Sjöström M. Distribution of different fiber types in human skeletal muscles: effects of aging studied in whole muscle cross sections. Muscle & nerve. 1983 Oct 1;6(8):588-95.

Lexell J, Taylor CC, Sjöström M. What is the cause of the ageing atrophy?: Total number, size and proportion of different fiber types studied in

whole vastus lateralis muscle from 15-to 83-year-old men. Journal of the neurological sciences. 1988 Apr 1;84(2-3):275-94.

Li G, Rudy TW, Sakane M, Kanamori A, Ma CB, Woo SY. The importance of quadriceps and hamstring muscle loading on knee kinematics and in-situ forces in the ACL. Journal of biomechanics. 1999 Apr 1;32(4):395-400.

Lieber RL, Blevins FT. Skeletal muscle architecture of the rabbit hindlimb: functional implications of muscle design. Journal of morphology. 1989 Jan 1;199(1):93-101.

Lieber RL, Boakes JL. Muscle force and moment arm contributions to torque production in frog hindlimb. American Journal of Physiology-Cell Physiology. 1988 Jun 1;254(6):C769-72.

Lieber RL, Brown CG. Sarcomere length-joint angle relationships of seven frog hindlimb muscles. Cells Tissues Organs. 1992;145(4):289-95.

Lieber RL, Fazeli BM, Botte MJ. Architecture of selected wrist flexor and extensor muscles. Journal of Hand Surgery. 1990 Mar 1;15(2):244-50.

Lieber RL, Fridëan JO, Hargens AR, Danzig LA, Gershuni DH. Differential response of the dog quadriceps muscle to external skeletal fixation of the knee. Muscle & nerve. 1988 Mar 1;11(3):193-201.

Lieber RL, Fridén J. Clinical significance of skeletal muscle architecture. Clinical orthopaedics and related research. 2001 Feb 1;383:140-51.

Lieber RL, Friden J. Functional and clinical significance of skeletal muscle architecture. Muscle and Nerve. 2000;23(11):1647-66.

Lieber RL, Fridén J. Mechanisms of muscle injury after eccentric contraction. Journal of Science and Medicine in Sport. 1999 Oct 1;2(3):253-65.

Lieber RL, Friden J. Muscle damage is not a function of muscle force but active muscle strain. Journal of Applied Physiology. 1993 Feb 1;74(2):520-6.

Lieber RL, Jacobson MD, Fazeli BM, Abrams RA, Botte MJ. Architecture of selected muscles of the arm and forearm: anatomy and implications for tendon transfer. Journal of Hand Surgery. 1992 Sep 1;17(5):787-98.

Lieber RL, Ward SR. Skeletal muscle design to meet functional demands. Philosophical Transactions of the Royal Society of London B: Biological Sciences. 2011 May 27;366(1570):1466-76.

Lieber RL, Woodburn TM, Friden J. Muscle damage induced by eccentric contractions of 25% strain. Journal of Applied Physiology. 1991 Jun 1;70(6):2498-507.

Lone NI, Gillies MA, Haddow C, Dobbie R, Rowan KM, Wild SH, Murray GD, Walsh TS. Five-year mortality and hospital costs associated with surviving intensive care. American journal of respiratory and critical care medicine. 2016 Jul 15;194(2):198-208.

Lowry OH, Hastings AB. Histochemical changes associated with aging I. methods and calculations. Journal of Biological Chemistry. 1942 Mar 1;143(1):257-69.

Lüdemann L, Wlodarczyk W, Nadobny J, Weihrauch M, Gellermann J, Wust P. Non-invasive magnetic resonance thermography during regional hyperthermia. International Journal of Hyperthermia. 2010 Jan 1;26(3):273-82.

Macgregor LJ, Hunter AM, Orizio C, Fairweather MM, Ditroilo M. Assessment of skeletal muscle contractile properties by radial

displacement: the case for tensiomyography. Sports Medicine. 2018 Jul 1:1-4.

Mackenzie C. The Action of Muscles: Including Muscle Rest and Muscle Re-education. PB Hoeber; 1918.

Maden-Wilkinson T, Degens H, Jones DA, McPhee JS. Comparison of MRI and DXA to measure muscle size and age-related atrophy in thigh muscles. Journal of musculoskeletal & neuronal interactions. 2013 Sep 1;13(3):320-8.

Magnusson SP. Passive properties of human skeletal muscle during stretch maneuvers. Scandinavian journal of medicine & science in sports. 1998 Apr 1;8(2):65-77.

Malm C, Nyberg P, Engström M, Sjödin B, Lenkei R, Ekblom B, Lundberg I. Immunological changes in human skeletal muscle and blood after eccentric exercise and multiple biopsies. The Journal of physiology. 2000 Nov;529(1):243-62.

Manduca A, Oliphant TE, Dresner MA, Mahowald JL, Kruse SA, Amromin E, Felmlee JP, Greenleaf JF, Ehman RL. Magnetic resonance elastography: non-invasive mapping of tissue elasticity. Medical image analysis. 2001 Dec 1;5(4):237-54.

Manger B, Backhaus M. [Ultrasound diagnosis of rheumatic/inflammatory joint diseases.] Z Arztl Fortbild Qualitatssich 1997;91:341–5

Manger B, Kalden JR. Joint and connective tissue ultrasonography—a rheumatologic bedside procedure? A German experience. Arthritis Rheum 1995;38:736–42.

Manini TM, Clark BC. Dynapenia and aging: an update. Journals of Gerontology Series A: Biomedical Sciences and Medical Sciences. 2011 Mar 28;67(1):28-40.

Mankin HJ. The response of articular cartilage to mechanical injury. JBJS. 1982 Mar 1;64(3):460-6.

Mansfield P, Grannell PK. " Diffraction" and microscopy in solids and liquids by NMR. Physical Review B. 1975 Nov 1;12(9):3618.

Maquet P. Biomecanique de la gonarthrose. Acta Orthop Belg. 1972; 38: Suppl.I:S33-S54

Mariappan YK, Glaser KJ, Ehman RL. Magnetic resonance elastography: a review. Clinical anatomy. 2010 Jul 1;23(5):497-511.

Massie BM, Conway M, Yonge R, Frostick S, Sleight P, Ledingham J, Radda G, Rajagopalan B. 31P nuclear magnetic resonance evidence of abnormal skeletal muscle metabolism in patients with congestive heart failure. The American journal of cardiology. 1987 Aug 1;60(4):309-15.

Maughan RJ, Nimmo MA. The influence of variations in muscle fibre composition on muscle strength and cross-sectional area in untrained males. The Journal of physiology. 1984 Jun 1;351(1):299-311.

Maughan RJ, Watson JS, Weir J. Strength and cross-sectional area of human skeletal muscle. The Journal of physiology. 1983 May 1;338(1):37-49.

Maughan RJ. Thermoregulatory aspects of performance. Experimental physiology. 2012 Mar 1;97(3):325-6.

McCullough MB, Domire ZJ, Reed AM, Amin S, Ytterberg SR, Chen Q, An KN. Evaluation of muscles affected by myositis using magnetic resonance elastography. Muscle & nerve. 2011 Apr;43(4):585-90.

McLean SM, Burton M, Bradley L, Littlewood C. Interventions for enhancing adherence with physiotherapy: a systematic review. Manual therapy. 2010 Dec 1;15(6):514-21.

McMahon CJ, Wu JS, Eisenberg RL. Muscle edema. American Journal of Roentgenology. 2010 Apr;194(4):W284-92.

McNair PJ, Stanley SN. Effect of passive stretching and jogging on the series elastic muscle stiffness and range of motion of the ankle joint. British journal of sports medicine. 1996 Dec 1;30(4):313-7.

Merla A, Mattei PA, Di Donato L, Romani GL. Thermal imaging of cutaneous temperature modifications in runners during graded exercise. Annals of biomedical engineering. 2010 Jan 1;38(1):158-63.

Metter EJ, Conwit R, Tobin J, Fozard JL. Age-associated loss of power and strength in the upper extremities in women and men. The Journals of Gerontology Series A: Biological Sciences and Medical Sciences. 1997 Sep 1;52(5):B267-76.

Metter EJ, Lynch N, Conwit R, Lindle R, Tobin J, Hurley B. Muscle quality and age: cross-sectional and longitudinal comparisons. Journals of Gerontology Series A: Biomedical Sciences and Medical Sciences. 1999 May 1;54(5):B207-18.

Metter EJ, Talbot LA, Schrager M, Conwit R. Skeletal muscle strength as a predictor of all-cause mortality in healthy men. The Journals of Gerontology Series A: Biological Sciences and Medical Sciences. 2002 Oct 1;57(10):B359-65.

Mietzsch E, Koch M, Schaldach M, Werner J, Bellenberg B, Wentz KU. Non-invasive temperature imaging of muscles with magnetic resonance imaging using spin-echo sequences. Medical and Biological Engineering and Computing. 1998 Nov 1;36(6):673-8.

Mizner RL, Petterson SC, Snyder-Mackler L. Quadriceps strength and the time course of functional recovery after total knee arthroplasty.

Journal of Orthopaedic & Sports Physical Therapy. 2005 Jul;35(7):424-36.

Mollinger LA, Steffen TM. Knee flexion contractures in institutionalized elderly: prevalence, severity, stability, and related variables. Physical therapy. 1993 Jul 1;73(7):437-44.

Mori S, Crain BJ, Chacko VP, Van Zijl P. Three-dimensional tracking of axonal projections in the brain by magnetic resonance imaging. Annals of neurology. 1999 Feb 1;45(2):265-9.

Morley JE, Baumgartner RN, Roubenoff R, Mayer J, Nair KS. Sarcopenia. Journal of Laboratory and Clinical Medicine. 2001 Apr 1;137(4):231-43.

Murphy MC, Huston III J, Glaser KJ, Manduca A, Meyer FB, Lanzino G, Morris JM, Felmlee JP, Ehman RL. Preoperative assessment of meningioma stiffness using magnetic resonance elastography. Journal of neurosurgery. 2013 Mar;118(3):643-8.

Murphy MC, Huston J, Jack CR, Glaser KJ, Manduca A, Felmlee JP, Ehman RL. Decreased brain stiffness in Alzheimer's disease determined by magnetic resonance elastography. Journal of magnetic resonance imaging. 2011 Sep 1;34(3):494-8.

Musacchia XJ, Steffen JM, Deavers DR. Rat hindlimb muscle responses to suspension hypokinesia/hypodynamia. Aviation, space, and environmental medicine. 1983 Nov;54(11):1015-20.

Muthupillai R, Ehman RL. Magnetic resonance elastography. Nature medicine. 1996a May;2(5):601.

Muthupillai R, Lomas DJ, Rossman PJ, Greenleaf JF, Manduca A, Ehman RL. Magnetic resonance elastography by direct visualization of

propagating acoustic strain waves. Science. 1995 Sep 29;269(5232):1854-7.

Muthupillai R, Lomas DJ, Rossman PJ, Greenleaf JF, Manduca A, Ehman RL. Magnetic resonance elastography by direct visualization of propagating acoustic strain waves. Science. 1995 Sep 29;269(5232):1854-7.

Muthupillai R, Rossman PJ, Lomas DJ, Greenleaf JF, Riederer SJ, Ehman RL. Magnetic resonance imaging of transverse acoustic strain waves. Magnetic Resonance in Medicine. 1996b Aug 1;36(2):266-74.

Nakajima M, Kawamura K, Takeda I. Electromyographic analysis of a modified maneuver for quadriceps femoris muscle setting with co-contraction of the hamstrings. Journal of orthopaedic research. 2003 Jan 1;21(3):559-64.

Narici MV, Bordini M, Cerretelli P. Effect of aging on human adductor pollicis muscle function. Journal of Applied Physiology. 1991 Oct 1;71(4):1277-81.

Narici MV, Maffulli N, Maganaris CN. Ageing of human muscles and tendons. Disability and rehabilitation. 2008 Jan 1;30(20-22):1548-54.

Narici MV, Maffulli N. Sarcopenia: characteristics, mechanisms and functional significance. British medical bulletin. 2010 Mar 2;95(1):139-59.

National Health and Nutrition Examination Survey III (NHANES), Centers for Disease Control and Prevention (CDC), National Center for Health Statistics (NCHS). Body Measurements (Anthropometry). 1988.

NHS Digital, "Health Survey for England 2016 Excel Tables," Health and Social Information Centre, 2017.

Nielsen B, Savard G, Richter EA, Hargreaves M, Saltin B. Muscle blood flow and muscle metabolism during exercise and heat stress. Journal of applied physiology. 1990 Sep 1;69(3):1040-6.

Nordez A, Gennisson JL, Casari P, Catheline S, Cornu C. Characterization of muscle belly elastic properties during passive stretching using transient elastography. J Biomech. 2008;41(10):2305-2311.

Nybo L, Nielsen B. Hyperthermia and central fatigue during prolonged exercise in humans. Journal of applied physiology. 2001 Sep 1;91(3):1055-60.

Nybo L. Cycling in the heat: performance perspectives and cerebral challenges. Scandinavian journal of medicine & science in sports. 2010 Oct 1;20(s3):71-9.

Orlic D, Kajstura J, Chimenti S, Limana F, Jakoniuk I, Quaini F, Nadal-Ginard B, Bodine DM, Leri A, Anversa P. Mobilized bone marrow cells repair the infarcted heart, improving function and survival. Proceedings of the National Academy of Sciences. 2001 Aug 28;98(18):10344-9.

Osu R, Gomi H. Multijoint muscle regulation mechanisms examined by measured human arm stiffness and EMG signals. Journal of neurophysiology. 1999 Apr 1;81(4):1458-68.

Pajevic S, Pierpaoli C. Color schemes to represent the orientation of anisotropic tissues from diffusion tensor data: application to white matter fiber tract mapping in the human brain. Magnetic resonance in medicine. 1999 Sep 1;42(3):526-40.

Papazoglou S, Braun J, Hamhaber U, Sack I. Two-dimensional waveform analysis in MR elastography of skeletal muscles. Physics in Medicine & Biology. 2005 Mar 2;50(6):1313.

Papazoglou S, Hirsch S, Braun J, Sack I. Multifrequency inversion in magnetic resonance elastography. Physics in Medicine & Biology. 2012 Mar 30;57(8):2329.

Papazoglou S, Rump J, Braun J, Sack I. Shear wave group velocity inversion in MR elastography of human skeletal muscle. Magnetic resonance in medicine. 2006 Sep 1;56(3):489-97.

Park JH, Brown RL, Park CR, McCully K, Cohn M, Haselgrove J, Chance B. Functional pools of oxidative and glycolytic fibers in human muscle observed by 31P magnetic resonance spectroscopy during exercise. Proceedings of the National Academy of Sciences. 1987 Dec 1;84(24):8976-80.

Park JH, Olsen NJ, Vital T, Buse R, Kari S, Schulman MH, Price RR. Use of magnetic resonance imaging and P-31 magnetic resonance spectroscopy to detect and quantify muscle dysfunction in the amyopathic and myopathic variants of dermatomyositis. Arthritis & Rheumatology. 1995 Jan 1;38(1):68-77.

Park JH, Olsen NJ. Utility of magnetic resonance imaging in the evaluation of patients with inflammatory myopathies. Current rheumatology reports. 2001 Aug 1;3(4):334-45.

Park JH, Vital TL, Ryder NM, Hernanz-Schulman M, Leon Partain C, Price RR, Olsen NJ. Magnetic resonance imaging and P-31 magnetic resonance spectroscopy provide unique quantitative data useful in the longitudinal management of patients with dermatomyositis. Arthritis & Rheumatology. 1994 May 1;37(5):736-46.

Parker GJ, Haroon HA, Wheeler-Kingshott CA. A framework for a streamline-based probabilistic index of connectivity (PICo) using a

structural interpretation of MRI diffusion measurements. Journal of Magnetic Resonance Imaging. 2003 Aug 1;18(2):242-54.

Paschalis V, Koutedakis Y, Baltzopoulos V, Mougios V, Jamurtas AZ, Giakas G. Short vs. long length of rectus femoris during eccentric exercise in relation to muscle damage in healthy males. Clinical Biomechanics. 2005 Jul 1;20(6):617-22.

Perrins (2018a), CMOcean LUT for ImageJ. GitHub repository, https://github.com/mikeperrins/cmocean-LUT-ImageJ.

Perrins (2018b), Musculoskeletal MRE Template. GitHub repository, https://github.com/mikeperrins/MSK-MRE-Template.

Petersen KF, Befroy D, Dufour S, Dziura J, Ariyan C, Rothman DL, DiPietro L, Cline GW, Shulman GI. Mitochondrial dysfunction in the elderly: possible role in insulin resistance. Science. 2003 May 16;300(5622):1140-2.

Pette D, Vrbová G. Invited review: neural control of phenotypic expression in mammalian muscle fibers. Muscle & nerve. 1985 Oct 1;8(8):676-89.

Piasecki M, Ireland A, Piasecki J, Stashuk DW, Swiecicka A, Rutter MK, Jones DA, McPhee JS. Failure to expand the motor unit size to compensate for declining motor unit numbers distinguishes sarcopenic from non-sarcopenic older men. The Journal of physiology. 2018 May 1;596(9):1627-37.

Plank LD, Hill GL. Similarity of changes in body composition in intensive care patients following severe sepsis or major blunt injury. Annals of the New York Academy of Sciences. 2000 May 1;904(1):592-602.

Porter MM, Vandervoort AA, Lexell J. Aging of human muscle: structure, function and adaptability. Scandinavian journal of medicine & science in sports. 1995 Jun 1;5(3):129-42.

Powell PL, Roy RR, Kanim PA, Bello MA, Edgerton VR. Predictability of skeletal muscle tension from architectural determinations in guinea pig hindlimbs. Journal of Applied Physiology. 1984 Dec 1;57(6):1715-21.

Puthucheary Z, Harridge S, Hart N. Skeletal muscle dysfunction in critical care: wasting, weakness, and rehabilitation strategies. Critical care medicine. 2010 Oct 1;38(10):S676-82.

Puthucheary ZA, Rawal J, McPhail M, Connolly B, Ratnayake G, Chan P, Hopkinson NS, Phadke R, Dew T, Sidhu PS, Velloso C. Acute skeletal muscle wasting in critical illness. Jama. 2013 Oct 16;310(15):1591-600.

Quesada JI, Carpes FP, Bini RR, Palmer RS, Pérez-Soriano P, de Anda RM. Relationship between skin temperature and muscle activation during incremental cycle exercise. Journal of thermal biology. 2015 Feb 28;48:28-35.

Ralston HJ. Uses and limitations of electromyography in the quantitative study of skeletal muscle function. American Journal of Orthodontics. 1961 Jul 1;47(7):521-30.

Rantanen T, Harris T, Leveille SG, Visser M, Foley D, Masaki K, Guralnik JM. Muscle strength and body mass index as long-term predictors of mortality in initially healthy men. The Journals of Gerontology Series A: Biological Sciences and Medical Sciences. 2000 Mar 1;55(3):M168-73.

Rantanen T, Volpato S, Ferrucci L, Heikkinen E, Fried LP, Guralnik JM. Handgrip strength and cause-specific and total mortality in older disabled women: exploring the mechanism. Journal of the American Geriatrics Society. 2003 May 1;51(5):636-41.

Rasband WS. ImageJ. US National Institutes of Health, Bethesda, MD, USA. 1997.

Reid CL, Campbell IT, Little RA. Muscle wasting and energy balance in critical illness. Clinical Nutrition. 2004 Apr 1;23(2):273-80.

Reimers CD, Finkenstaedt M. Muscle imaging in inflammatory myopathies. Curr Opin Rheumatol 1997;9:475–85.

Riek K, Millward JM, Hamann I, Mueller S, Pfueller CF, Paul F, Braun J, Infante-Duarte C, Sack I. Magnetic resonance elastography reveals altered brain viscoelasticity in experimental autoimmune encephalomyelitis. NeuroImage: Clinical. 2012 Jan 1;1(1):81-90.

Ringleb SI, Bensamoun SF, Chen Q, Manduca A, An KN, Ehman RL. Applications of magnetic resonance elastography to healthy and pathologic skeletal muscle. Journal of Magnetic Resonance Imaging. 2007 Feb 1;25(2):301-9.

Ringleb SI, Kaufman KR, Basford JR, Coleman-Wood K, Chen Q, Ehman RL, An KN. Magnetic resonance elastography: A non-invasive method to differentiate between healthy and pathologic muscle stiffness. In30th Annual Meeting of the American Society of Biomechanics 2006.

Roubenoff R. Sarcopenia: effects on body composition and function. The Journals of Gerontology Series A: Biological Sciences and Medical Sciences. 2003 Nov 1;58(11):M1012-7.

Roy RR, Powell PL, Kanim P, Simpson DR. Architectural and histochemical analysis of the semitendinousus muscle in mice, rats, guinea pigs, and rabbits. Journal of morphology. 1984 Aug 1;181(2):155-60.

RStudio Team. RStudio: Integrated Development for R. RStudio, Inc., Boston, MA. 2015. URL http://www.rstudio.com/.

Rump J, Klatt D, Braun J, Warmuth C, Sack I. Fractional encoding of harmonic motions in MR elastography. Magnetic resonance in medicine. 2007 Feb 1;57(2):388-95.

Sack I, Beierbach B, Hamhaber U, Klatt D, Braun J. Non-invasive measurement of brain viscoelasticity using magnetic resonance elastography. NMR in Biomedicine. 2008 Apr 1;21(3):265-71.

Sack I, Bernarding J, Braun J. Analysis of wave patterns in MR elastography of skeletal muscle using coupled harmonic oscillator simulations. Magnetic resonance imaging. 2002a Jan 1;20(1):95-104.

Sack I, Jöhrens K, Würfel J, Braun J. Structure-sensitive elastography: on the viscoelastic powerlaw behavior of in vivo human tissue in health and disease. Soft Matter. 2013;9(24):5672-80.

Sack I, Rump J, Elgeti T, Samani A, Braun J. MR elastography of the human heart: noninvasive assessment of myocardial elasticity changes by shear wave amplitude variations. Magnetic resonance in medicine. 2009 Mar 1;61(3):668-77.

Sack I, Tolxdorff J, Bernarding T, Braun J. Simulation of MR elastography wave images measured in the biceps brachii. InProc Intl Soc Magn Reson Med 2002b (Vol. 10).

Sacks RD, Roy RR. Architecture of the hind limb muscles of cats: functional significance. Journal of Morphology. 1982 Aug 1;173(2):185-95.

Salmons S, Henriksson J. The adaptive response of skeletal muscle to increased use. Muscle & nerve. 1981 Mar 1;4(2):94-105.

Sandrin L, Fourquet B, Hasquenoph JM, Yon S, Fournier C, Mal F, Christidis C, Ziol M, Poulet B, Kazemi F, Beaugrand M. Transient elastography: a new noninvasive method for assessment of hepatic fibrosis. Ultrasound in Medicine and Biology. 2003 Dec 1;29(12):1705-13.

Schaefer S, McPhail T, Warren J. Image deformation using moving least squares. In ACM transactions on graphics (TOG) 2006 Jul 30 (Vol. 25, No. 3, pp. 533-540). ACM.

Schantz P, Randall-Fox E, Hutchison W, Tyden A, and Astrand PO. Muscle fibre type distribution, muscle cross-sectional area and maximal voluntary strength in humans. Acta Physiologica. 1983 Feb 1;117(2):219-26.

Scheel M, Roth P, Winkler T, Arampatzis A, Prokscha T, Hamm B, Diederichs G. Fiber type characterization in skeletal muscle by diffusion tensor imaging. NMR in Biomedicine. 2013 Oct 1;26(10):1220-4.

Schiessel H, Metzler R, Blumen A, Nonnenmacher TF. Generalized viscoelastic models: their fractional equations with solutions. Journal of physics A: Mathematical and General. 1995 Dec 7;28(23):6567.

Scott SH, Engstrom CM, Loeb GE. Morphometry of human thigh muscles. Determination of fascicle architecture by magnetic resonance imaging. Journal of anatomy. 1993 Apr;182(Pt 2):249.

Segal NA, Yack HJ, Khole P. Weight, rather than obesity distribution, explains peak external knee adduction moment during level gait.

American journal of physical medicine & rehabilitation/Association of Academic Physiatrists. 2009 Mar;88(3):180.

Seraj SD, Obuchowski NA, Venkatesh SK, Sirlin CB, Miller FH, Ashton E, Cole PE, Ehman RL. Repeatability of MR elastography of liver: a meta-analysis. Radiology. 2017 May 22;285(1):92-100.

Seymour JM, Ward K, Sidhu PS, Puthucheary Z, Steier J, Jolley CJ, Rafferty G, Polkey MI, Moxham J. Ultrasound measurement of rectus femoris cross-sectional area and the relationship with quadriceps strength in COPD. Thorax. 2009 May 1;64(5):418-23.

Shenoy R, Pastides PS, Nathwani D. (iii) Biomechanics of the knee and TKR. Orthopaedics and Trauma. 2013 Dec 1;27(6):364-71.

Sinkjaer T, Toft E, Andreassen S, Hornemann BC. Muscle stiffness in human ankle dorsiflexors: intrinsic and reflex components. Journal of neurophysiology. 1988 Sep 1;60(3):1110-21.

Snow DH, Billeter R, Mascarello F, Carpene E, Rowlerson A, Jenny E. No classical type IIB fibres in dog skeletal muscle. Histochemistry. 1982 Mar 1;75(1):53-65.

Soares J, Marques P, Alves V, Sousa N. A hitchhiker's guide to diffusion tensor imaging. Frontiers in neuroscience. 2013 Mar 12;7:31.

Souren LE, Franssen EH, Reisberg B. Contractures and loss of function in patients with Alzheimer's disease. Journal of the American Geriatrics Society. 1995 Jun 1;43(6):650-5.

Spector SA, Simard CP, Fournier M, Sternlicht E, Edgerton VR. Architectural alterations of rat hind-limb skeletal muscles immobilized at different lengths. Experimental neurology. 1982 Apr 1;76(1):94-110.

Stanton P, Purdam C. Hamstring injuries in sprinting—the role of eccentric exercise. Journal of Orthopaedic & Sports Physical Therapy. 1989 Mar;10(9):343-9.

Staron RS, Karapondo DL, Kraemer WJ, Fry AC, Gordon SE, Falkel JE, Hagerman FC, Hikida RS. Skeletal muscle adaptations during early phase of heavy-resistance training in men and women. Journal of applied physiology. 1994 Mar 1;76(3):1247-55.

StatsWales, "National Survey for Wales 2016-17: Results Viewer," Welsh Government, 2017.

Stauffer PR, Craciunescu OI, Maccarini PF, Wyatt C, Arunachalam K, Arabe O, Stakhursky V, Soher B, MacFall JR, Li Z, Joines WT. Clinical utility of magnetic resonance thermal imaging (MRTI) for realtime guidance of deep hyperthermia. InEnergy-based Treatment of Tissue and Assessment V 2009 Feb 25 (Vol. 7181, p. 71810I). International Society for Optics and Photonics.

Stauffer R, Mayr GJ, Dabernig M, Zeileis A. Somewhere over the rainbow: How to make effective use of colors in meteorological visualizations. Bulletin of the American Meteorological Society. 2015 Feb;96(2):203-16.

Steinborn MM, Heuck AF, Tiling R, Bruegel M, Gauger L, Reiser MF. Whole-body bone marrow MRI in patients with metastatic disease to the skeletal system. Journal of computer assisted tomography. 1999 Jan 1;23(1):123-9.

Stejskal EO, Tanner JE. Spin diffusion measurements: spin echoes in the presence of a time-dependent field gradient. The journal of chemical physics. 1965 Jan 1;42(1):288-92.

Stephenson DG, Williams DT. Calcium-activated force responses in fast- and slow-twitch skinned muscle fibres of the rat at different temperatures. The Journal of Physiology. 1981 Aug 1;317(1):281-302.

Stevens RD, Dowdy DW, Michaels RK, Mendez-Tellez PA, Pronovost PJ, Needham DM. Neuromuscular dysfunction acquired in critical illness: a systematic review. Intensive care medicine. 2007 Nov 1;33(11):1876-91.

Storey JD. The positive false discovery rate: a Bayesian interpretation and the q-value. The Annals of Statistics. 2003;31(6):2013-35.

Sun D, Martinez CO, Ochoa O, Ruiz-Willhite L, Bonilla JR, Centonze VE, Waite LL, Michalek JE, McManus LM, Shireman PK. Bone marrow-derived cell regulation of skeletal muscle regeneration. The FASEB Journal. 2009 Feb;23(2):382-95.

Suter ES, Herzog WA, Sokolosky J, Wiley JP, Macintosh BR. Muscle fiber type distribution as estimated by Cybex testing and by muscle biopsy. Medicine and science in sports and exercise. 1993 Mar;25(3):363-70.

Tabary JC, Tabary C, Tardieu C, Tardieu G, Goldspink G. Physiological and structural changes in the cat's soleus muscle due to immobilization at different lengths by plaster casts. The Journal of physiology. 1972 Jul 1;224(1):231-44.

Takata S, Takai H, Ikata T, Miura I. Observation of fatigue unrelated to gross energy reserve of skeletal muscle during tetanic contraction-an application of 31P-MRS. Biochemical and biophysical research communications. 1988 Nov 30;157(1):225-31.

Tan K, Jugé L, Hatt A, Cheng S, Bilston LE. Measurement of large strain properties in calf muscles in vivo using magnetic resonance

elastography and spatial modulation of magnetization. NMR in Biomedicine. 2018 Apr 19:e3925.

Taylor DJ, Styles P, Matthews PM, Arnold DA, Gadian DG, Bore P, Radda GK. Energetics of human muscle: exercise-induced ATP depletion. Magnetic resonance in medicine. 1986 Feb 1;3(1):44-54.

Taylor NA. Principles and practices of heat adaptation. Journal of the Human-Environment System. 2000;4(1):11-22.

Tesch P, Karlsson J. Isometric strength performance and muscle fibre type distribution in man. Acta Physiologica. 1978 May 1;103(1):47-51.

The King's Fund, "Making our health and care," 2014.

The Scottish Government, "Scottish Health Survey 2016: Supplementary Tables," 2017.

Thorstensson A, Grimby GU, Karlsson J. Force-velocity relations and fiber composition in human knee extensor muscles. Journal of applied physiology. 1976 Jan 1;40(1):12-6.

Thyng, K.M., C.A. Greene, R.D. Hetland, H.M. Zimmerle, and S.F. DiMarco. 2016. True colors of oceanography: Guidelines for effective and accu- rate colormap selection. Oceanography 29(3):9–13

Tomanek RJ, Lund DD. Degeneration of different types of skeletal muscle fibres. II. Immobilization. Journal of anatomy. 1974 Dec;118(Pt 3):531.

Tomanek RJ, Lund DD. Degeneration of different types of skeletal muscle fibres. I. Denervation. Journal of anatomy. 1973 Dec;116(Pt 3):395.

Trappe TA, Lindquist DM, Carrithers JA. Muscle-specific atrophy of the quadriceps femoris with aging. Journal of Applied Physiology. 2001 Jun 1;90(6):2070-4.

Travnik L, Pernus F, Erzen I. Histochemical and morphometric characteristics of the normal human vastus medialis longus and vastus medialis obliquus muscles. Journal of Anatomy. 1995 Oct;187(Pt 2):403.

Trudel G, Uhthoff HK. Contractures secondary to immobility: is the restriction articular or muscular? An experimental longitudinal study in the rat knee. Archives of physical medicine and rehabilitation. 2000 Jan 1;81(1):6-13.

Truong XT, Wall BJ, Walker SM. Effects of temperature on isometric contraction of rat muscle. American Journal of Physiology--Legacy Content. 1964 Aug 1;207(2):393-6.

Tucker R, Rauch L, Harley YX, Noakes TD. Impaired exercise performance in the heat is associated with an anticipatory reduction in skeletal muscle recruitment. Pflügers Archiv. 2004 Jul 1;448(4):422-30.

U. C. L. NatCen Social Research and Department of Epidemiology and Public Health, "Health Survey for England, 2015,"UK Data Service, 2017.

Uffmann K, Ladd ME. Actuation systems for MR elastography. IEEE Engineering in medicine and biology magazine. 2008 May;27(3):28-34.

Uffmann K, Maderwald S, Ajaj W, Galban CG, Mateiescu S, Quick HH, Ladd ME. In vivo elasticity measurements of extremity skeletal muscle with MR elastography. NMR in Biomedicine. 2004 Jun 1;17(4):181-90.

Ullah U, Tripathi P, Lahesmaa R, Rao KV. Gene set enrichment analysis identifies LIF as a negative regulator of human Th2 cell differentiation. Scientific reports. 2012 Jun 18;2:464.

van Beek EJ, Kuhl C, Anzai Y, Desmond P, Ehman RL, Gong Q, Gold G, Gulani V, Hall-Craggs M, Leiner T, Lim CT. Value of MRI in medicine: More than just another test?. Journal of Magnetic Resonance Imaging. 2018

van Ingen Schenau GJ, Dorssers WM, Welter TG, Beelen A, De Groot G, Jacobs R. The control of mono-articular muscles in multijoint leg extensions in man. The Journal of physiology. 1995 Apr 1;484(1):247-54.

van Ingen Schenau GV, Bobbert MF, Rozendal RH. The unique action of bi-articular muscles in complex movements. Journal of anatomy. 1987 Dec;155:1.

Vandervoort AA, McComas AJ. Contractile changes in opposing muscles of the human ankle joint with aging. Journal of Applied Physiology. 1986 Jul 1;61(1):361-7.

Vandervoort AA. Aging of the human neuromuscular system. Muscle & nerve. 2002 Jan 1;25(1):17-25.

Venkatesh SK, Yin M, Ehman RL. Magnetic resonance elastography of liver: technique, analysis, and clinical applications. Journal of magnetic resonance imaging. 2013 Mar 1;37(3):544-55.

Viitasalo JT, Era P, Leskinen AL, Heikkinen E. Muscular strength profiles and anthropometry in random samples of men aged 31–35, 51–55 and 71–75 years. Ergonomics. 1985 Nov 1;28(11):1563-74.

Vincent JL, Norrenberg M. Intensive care unit-acquired weakness: framing the topic. Critical care medicine. 2009 Oct 1;37(10):S296-8.

Vogler 3rd JB, Murphy WA. Bone marrow imaging. Radiology. 1988 Sep;168(3):679-93.

Wakefield RJ, Gibbon WW, Emery P. The current status of ultrasonography in rheumatology. Rheumatology (Oxford) 1999;38:195–8.

Walsh TS, Salisbury LG, Merriweather JL, Boyd JA, Griffith DM, Huby G, Kean S, Mackenzie SJ, Krishan A, Lewis SC, Murray GD. Increased hospital-based physical rehabilitation and information provision after intensive care unit discharge: the RECOVER randomized clinical trial. JAMA internal medicine. 2015 Jun 1;175(6):901-10.

Ward SR, Eng CM, Smallwood LH, Lieber RL. Are current measurements of lower extremity muscle architecture accurate?. Clinical orthopaedics and related research. 2009 Apr 1;467(4):1074-82.

Wellcome Trust, "Medical Research: What's it worth? A briefing on the economic benefits of musculoskeletal disease research in the UK," 2017.

Wendling PS, Peters SJ, Heigenhauser GJ, Spriet LL. Variability of triacylglycerol content in human skeletal muscle biopsy samples. Journal of Applied Physiology. 1996 Sep 1;81(3):1150-5.

Wickiewicz TL, Roy RR, Powell PL, Edgerton VR. Muscle architecture of the human lower limb. Clinical orthopaedics and related research. 1983 Oct(179):275-83.

Wickiewicz TL, Roy RR, Powell PL, Perrine JJ, Edgerton VR. Muscle architecture and force-velocity relationships in humans. Journal of Applied Physiology. 1984 Aug 1;57(2):435-43.

Widmaier EP, Raff H, Strang KT. "Muscle". Vander's Human Physiology: The Mechanisms of Body Function (12th ed.). New York, NY: McGraw-Hill. 2010.pp. 250–291.

Williams PE, Goldspink G. Connective tissue changes in immobilised muscle. Journal of Anatomy. 1984 Mar;138(Pt 2):343.

Winkelman C. Inactivity and inflammation in the critically ill patient. Critical care clinics. 2007 Jan 1;23(1):21-34.

Witzmann FA, Kim DH, Fitts RH. Hindlimb immobilization: length-tension and contractile properties of skeletal muscle. Journal of applied physiology. 1982 Aug 1;53(2):335-45.

Wood AW. Physiology, Biophysics, and Biomedical Engineering. Taylor & Francis. 2012. pp. 158–162

Xu X, Karis AJ, Buller MJ, Santee WR. Relationship between core temperature, skin temperature, and heat flux during exercise in heat. European journal of applied physiology. 2013 Sep 1;113(9):2381-9.

Yin M, Talwalkar JA, Glaser KJ, Manduca A, Grimm RC, Rossman PJ, Fidler JL, Ehman RL. Assessment of hepatic fibrosis with magnetic resonance elastography. Clinical Gastroenterology and Hepatology. 2007 Oct 1;5(10):1207-13.

York Health Economics, “The Cost of Arthritis Calculation conducted on behalf of Arthritis Research UK,” Unpublished, 2017.

Yoshida Y, Mizner RL, Snyder-Mackler L. Association between long-term quadriceps weakness and early walking muscle co-contraction after total knee arthroplasty. The Knee. 2013 Dec 1;20(6):426-31.

Zaraiskaya T, Kumbhare D, Noseworthy MD. Diffusion tensor imaging in evaluation of human skeletal muscle injury. Journal of Magnetic Resonance Imaging. 2006 Aug 1;24(2):402-8.

Zarzhevsky N, Carmeli E, Fuchs D, Coleman R, Stein H, Reznick AZ. Recovery of muscles of old rats after hindlimb immobilisation by external fixation is impaired compared with those of young rats. Experimental gerontology. 2001 Jan 1;36(1):125-40.

Ziol M, Handra-Luca A, Kettaneh A, Christidis C, Mal F, Kazemi F, de Lédinghen V, Marcellin P, Dhumeaux D, Trinchet JC, Beaugrand M. Noninvasive assessment of liver fibrosis by measurement of stiffness in patients with chronic hepatitis C. Hepatology. 2005 Jan 1;41(1):48-54.

Appendices

Appendix I. Royal Infirmary Home Exercise Programme offered to patients by the Physiotherapy Department during convalescence.

ROYAL INFIRMARY
HOME EXERCISE PROGRAMME

Little France,Old Dalkeith Rd,Edinburgh EH16 4SU
Tel: 0131-2421940
Fax: 0131-2421942

Provided for : [redacted] — Bed Exercises
Provided by : Physiotherapy Department — Date : 17/01/2007

Lying on your back or sitting.

Bend and straighten your ankles briskly. If you keep your knees straight during the exercise you will stretch your calf muscles.

Repeat 10 times.

This exercise is good for improving movement of the ankles and encouraging blood flow.

Lying on your back with legs straight.

Bend your ankles and push your knees down firmly against the bed. Hold 5 secs. - relax.

Repeat 10 times.

This exercise is good for strengthening the muscles in your legs and for improving blood flow.

Lying on your back. Bend one leg, putting your foot on the bed. Lie your other leg flat on the bed, placing a rolled up towel under the knee.

Exercise your straight leg by pulling your foot and toes up, tightening your thigh muscle and straightening the knee (keep knee on the towel). Hold approx. 3 secs. and slowly relax.

Repeat 10 times with both legs.

This exercise is good for improving your blood flow and strengthing your thigh muscles.

Appendix II. Individual elastograms for data in Chapter Four.

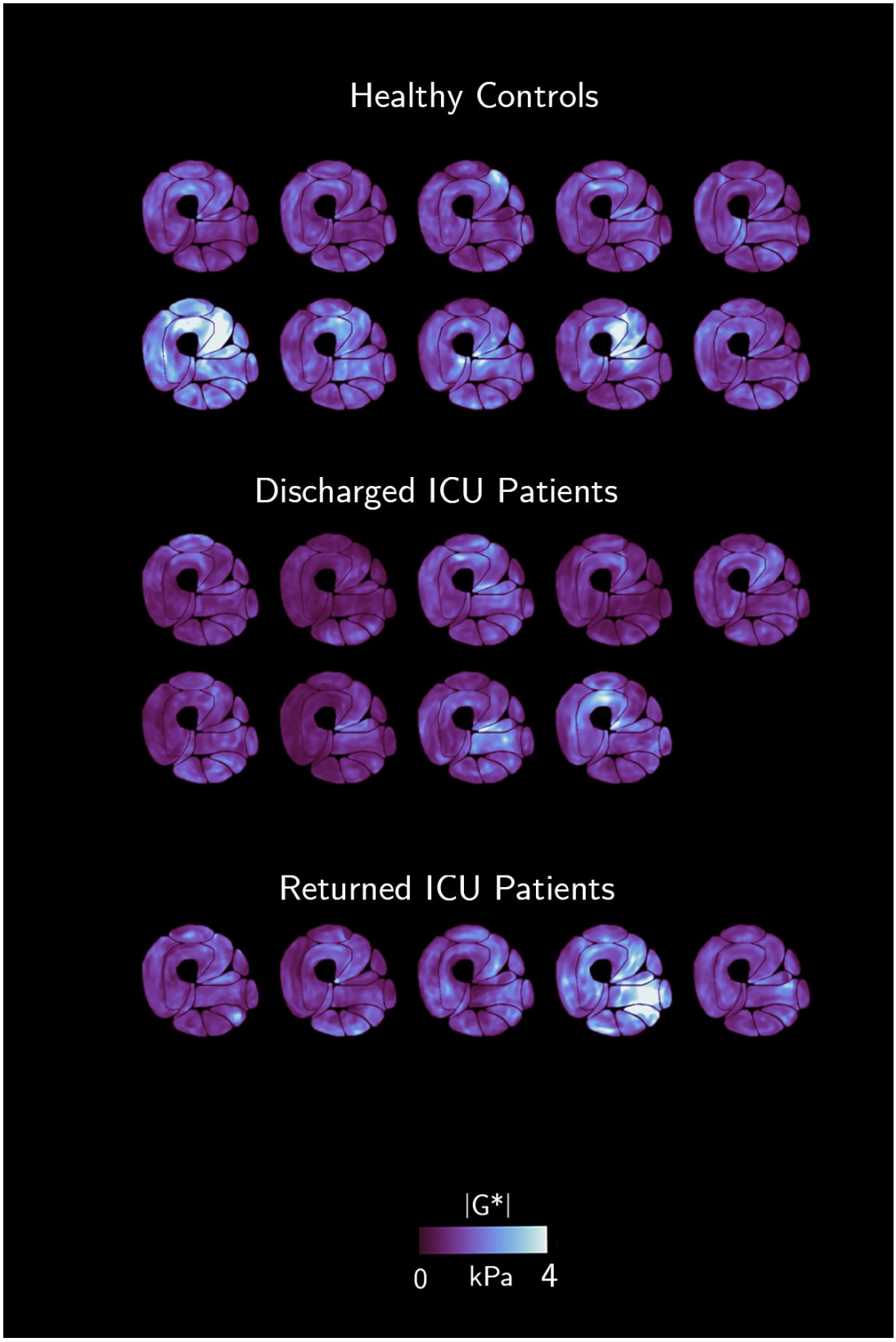

Appendix III. Individual Elastogram Data for Chapter Five.

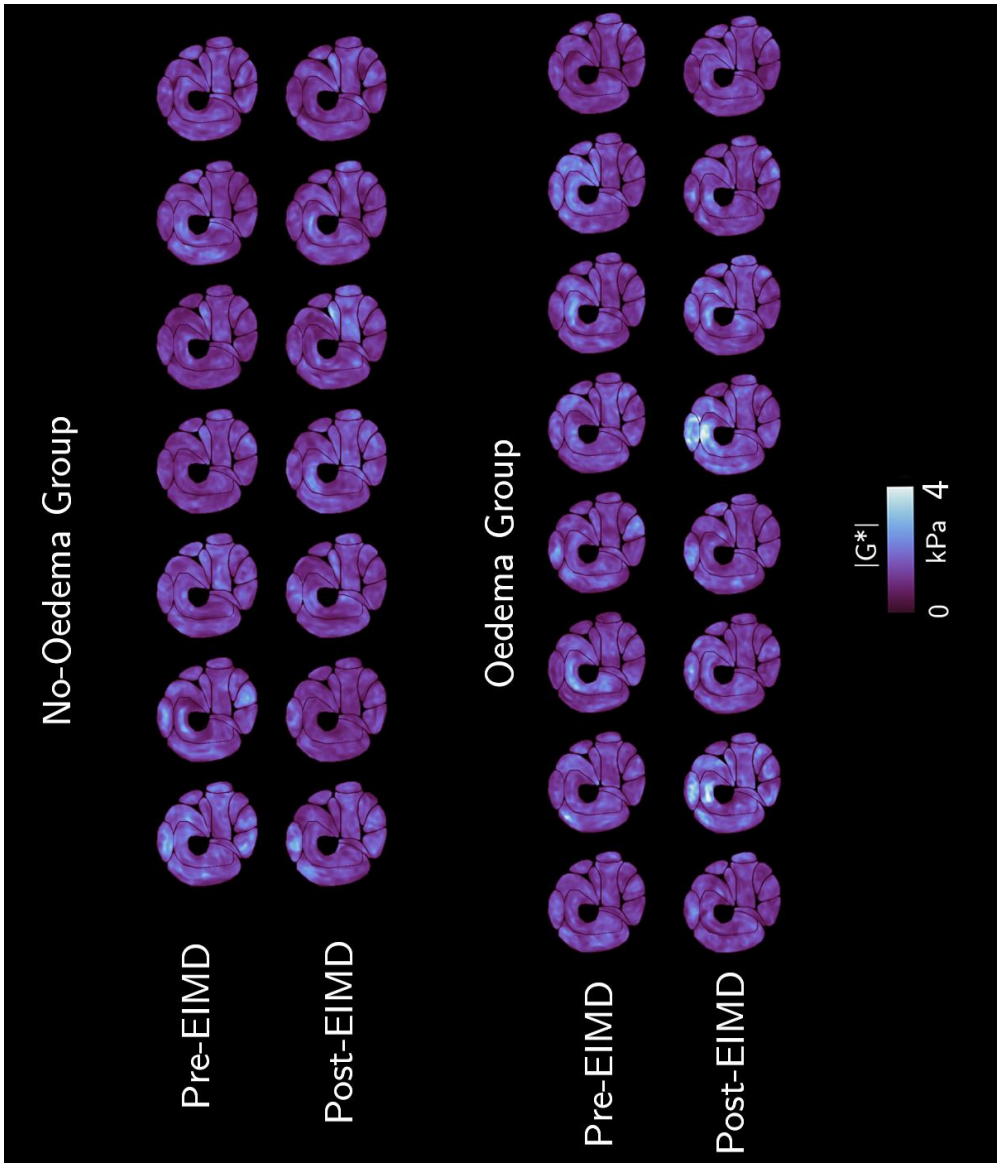

Appendix IV. Individual elastogram data for sustained knee extension for Chapter Six

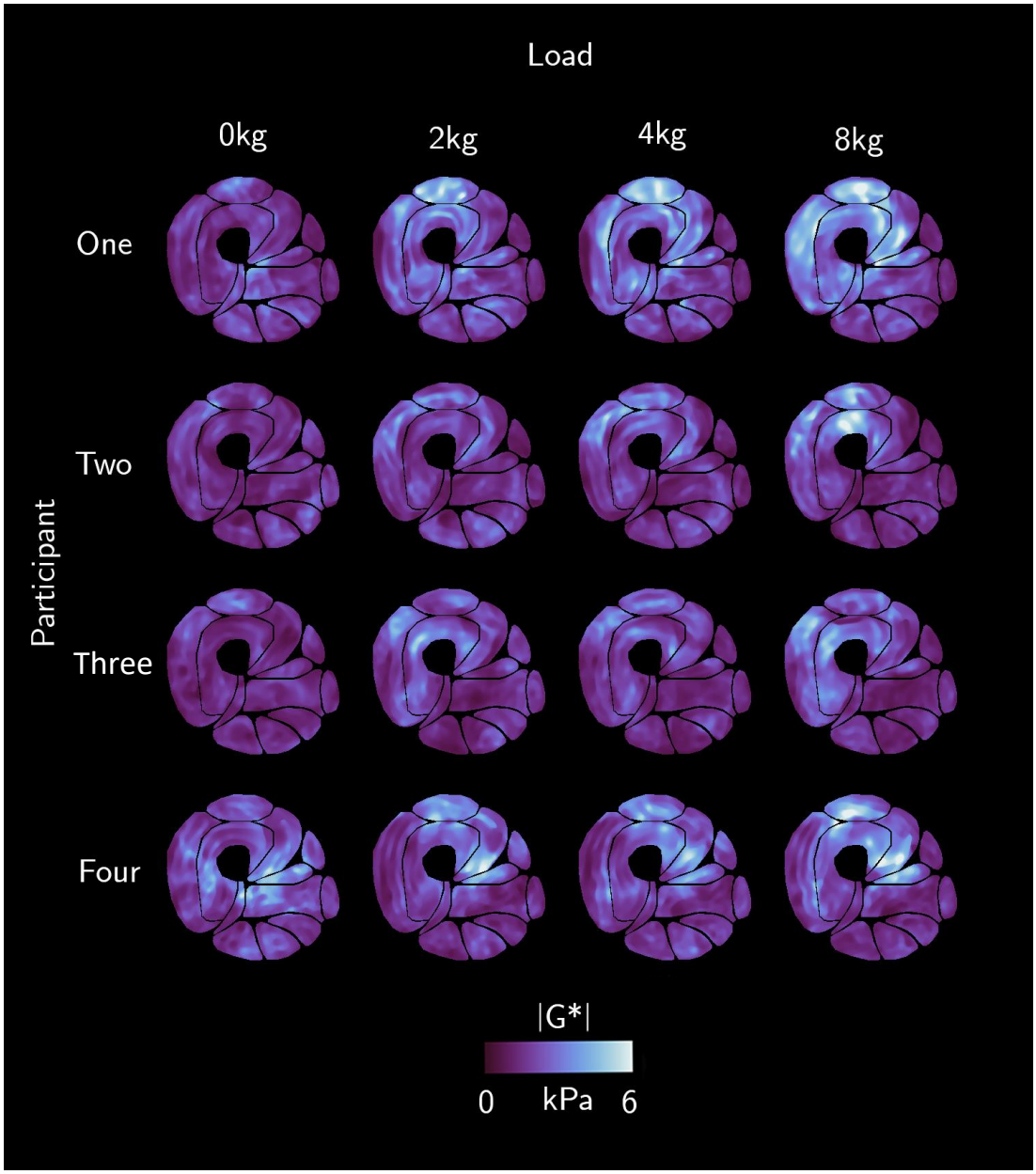

Appendix V. Individual elastogram data for patients in Chapter Seven.